Decoding the Organohalide-Respiration Potential of Aarhus Bay Sediments

Chen Zhang

Propositions

1. Multi'Omics approaches boost our understanding of organohalide respiration in marine sediments.
(this thesis)

2. Experimental studies are essential to validate predictions based on molecular data.
(this thesis)

3. Microbial activity depends on the surrounding environment, which in turn is reshaped.

4. Artificial intelligence (AI) improves the efficiency of work within a given frame but does not enlarge the framework.

5. Ethical rules and principles should be established prior to artificial intelligence (AI) development and application.

6. Hate is the germ of being bad, but thankfully empathy stops its germination.

7. Human history is the process of saving humanity from historical shackles.

Propositions belonging to the thesis, entitled

Decoding the Organohalide-Respiration Potential of Aarhus Bay Sediments

Chen Zhang

Wageningen, 05 July 2023

Decoding the Organohalide-Respiration Potential of Aarhus Bay Sediments

Chen Zhang

Thesis committee

Promotor

Prof. Dr H. Smidt

Personal chair at the Laboratory of Microbiology

Wageningen University & Research

Co-promotors

Dr S. Atashgahi

Applied Microbiologist

AB Mauri, Etten-Leur

Dr T.N.P. Bosma

Research Scientist

Deltares, Utrecht

Guest Researcher at the Laboratory of Microbiology

Wageningen University & Research

Other members

Prof. Dr H.H.M. Rijnaarts, Wageningen University & Research

Dr M. Bekker, Wageningen University & Research

Dr I. Dinkla, Wetsus, Leeuwarden

Dr D Maat, Deltares, Utrecht

This research was conducted under the auspices of the Graduate School for Socio-Economic and Natural Science of the Environment (SENSE).

Decoding the Organohalide-Respiration Potential of Aarhus Bay Sediments

Chen Zhang

Thesis

submitted in fulfilment of the requirements for the degree of doctor

at Wageningen University

by the authority of the Rector Magnificus,

Prof. Dr A.P.J. Mol,

in the presence of the

Thesis Committee appointed by the Academic Board

to be defended in public

on Wednesday 5 July 2023

at 11 a.m. in the Omnia Auditorium.

Chen Zhang

Decoding the Organohalide-Respiration Potential of Aarhus Bay Sediments

218 Pages.

PhD thesis, Wageningen University, Wageningen, the Netherlands (2023)
With references, with summary in English

ISBN: 978-94-6447-717-7
DOI: https://doi.org/10.18174/631318

Table of contents

Chapter 1

General introduction and thesis outline

Organohalide respiration (OHR)

Since the second half of the 20th century, large amounts of halogenated compounds have been widely used and discharged to the environment, which raised increasing public concerns due to the persistence of especially polyhalogenated compounds in oxic environments threatening the health of human beings (Mohn and Tiedje 1992). In contrast, recalcitrant polyhalogenated organohalides were found disappearing in anoxic environments, apparently through biodegradation, and chemical measurements confirmed that the products were the result of reductive dehalogenation via the stepwise removal of halides, rather than the complete mineralization of the compound into carbon dioxide (Bosma*,* et al. 1988, Esaac and Matsumura 1980, Kuhn and Suflita 1989, Tiedje*,* et al. 1987). Subsequent studies revealed that reductive dehalogenation is the key biological process of transformation of halogenated compounds under anoxic conditions (Bosma*, et al.* 1988, DeWeerd*, et al.* 1991, Dolfing 1991, Mikesell and Boyd 1990, Mohn and Tiedje 1990). The mechanisms of reductive dehalogenation utilizing halogenated compounds are well-demonstrated and classified into several processes. The first is hydrogenolysis, in which halides are replaced by hydrogen atoms (Figure 1.1A). The second is dihalo-elimination, also termed as vicinal reduction, in which two halogens from neighboring carbon atoms are removed, with the bond between the two carbon atoms being converted into a double bond after dehalogenation (Figure 1.1B). A third mechanism of reductive dehalogenation is that of thiolytic dehalogenation, which is associated with aerobic microorganisms, rather than anaerobes (Figure 1.1C). Noticeably, the first two processes have been shown to be used as terminal electron accepting processes for anaerobic respiration, conserving the energy for bacterial growth, which was thereafter termed organohalide respiration (OHR). Correspondently, bacteria able to perform OHR are referred to as OHRB (Adrian and Löffler 2016). Further, the key enzyme for OHR is reductive dehalogenase (RDase).

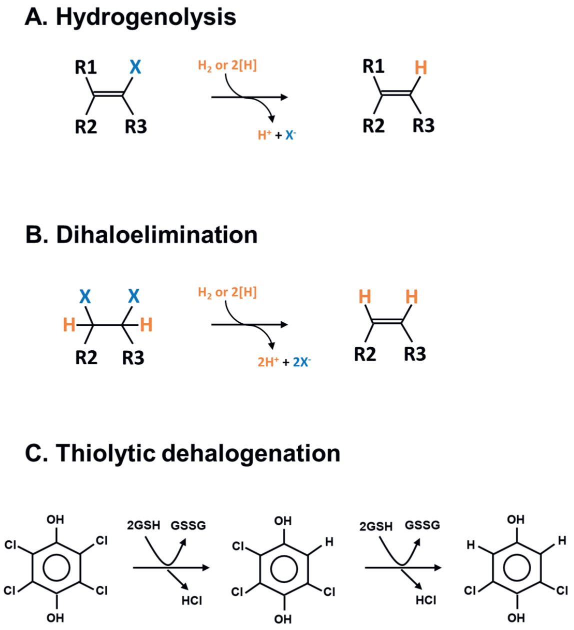
A. Hydrogenolysis

B. Dihaloelimination

C. Thiolytic dehalogenation

Figure 1.1 Reductive dehalogenation can proceed through several different mechanisms: Hydrogenolysis (A) and Dihalo-elimination (B) are typically observed in anaerobic microorganisms. Electron donors can be hydrogen gas or unknown sources for providing 2[H]. A third mechanism, thiolytic dehalogenation (C) is typically found in aerobes instead. “X” in blue represents the halogens, F, Cl, Br or I; “R” represents aliphatic or aromatic groups, but can also be, e.g., additional halogens or hydrogen. GSH: glutathione; GSSG: glutathione disulfide;

Organohalide-respiring Bacteria (OHRB)

In the early days of its discovery, microbial reductive dehalogenation of halogenated organic compounds in most cases was demonstrated in mixed cultures and cell-free systems (Gibson and Suflita, 1986; Apajalahti and Salkinoja-Salonen, 1987; Belay and Daniels, 1987; Bosma et al., 1988), and thus it was difficult to specify the particular bacteria that were responsible for the observed dehalogenating activity. Following the initial discovery, the isolation of OHRB has been of much importance to identify the organisms capable of reductive dehalogenation and corresponding mechanisms. Most of the OHRB are characterized by a versatile metabolism with respect to their ability to oxidise a wide range of electron donors such as, e.g., hydrogen, formate, acetate and other organic compounds (Fincker and Spormann, 2017). Also, availability of OHRB isolates allowed to study the metabolic connection of reductive dehalogenation with other activities, e.g. sulfate reduction. Hitherto, many OHRB were isolated from various environments, and characterized with respect to their physiology, biochemistry and genetics, for example, the well-documented *Dehalococcoides* spp. and *Desulfitobacterium* spp. (Maymo-Gatell et al., 1997; Drzyzga and Gottschal, 2002). In addition, recent studies provided new insight into the evolution of OHR, combining newly-identified genomic assemblies with the genomes of well-documented OHRB, and constructed a curated database of reductive dehalogenases, the key enzymes in reductive dehalogenation (Molenda et al., 2020). This e.g. suggested that the observed synteny of RDase genes for dehalogenating industrial organohalide pollutants most likely has been the result of multiple events of lateral transfer.

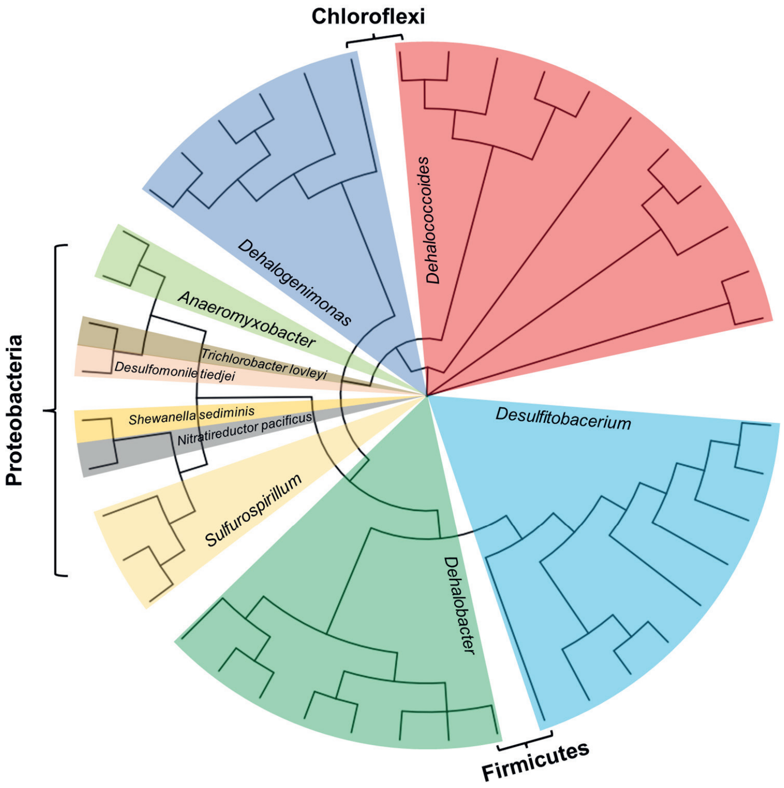

Figure 1.2 Phylogenetic analysis of OHRB based on entries available in the RDase database (https://rdasedb.biozone.utoronto.ca/). GToTree was employed to construct this phylogenetic tree using the concatenated sequences of 74 bacterial marker genes (Lee, 2019). Details regarding the selected OHRB representatives and their genomes are provided in Table 1.1.

Currently known OHRB belong to three phyla, *Chloroflexota*, *Firmicutes*, and *Proteobacteria* (Figure 1.2). Among these OHRB, members of the genera *Dehalococcoides* and *Dehalogenimonas* belonging to the *Chloroflexota*, and *Dehalobacter* belonging to the *Firmicutes* are obligate OHRB, using hydrogen as the only electron donor for reductive dehalogenation as the only terminal electron accepting process. Other OHRB, including e.g. members of the *Proteobacteria*, such as *Sulfurospirillum*, and *Desulfitobacterium* spp. in the *Firmicutes*, are generalists, utilizing various organic compounds as electron donor for OHR, and are generally referred to as facultative OHRB (Adrian and Löffler, 2016).

Table 1.1 Genomic information of OHRB currently included in RDaseDB. Compl: Completeness (%) and Conta: contamination (%), were calculated by checkM as implemented in the GTDB database (Rinke et al., 2021).

Organisms	NCBI_Accession	Genome Size (bp)	GC (%)	Compl (%)	Conta (%)	Number of RDase genes
Anaeromyxobacter dehalogenans 2CP-1	GCA_000022145.1	5,029,329	74.72	99.35	0	2
Anaeromyxobacter sp. K	GCA_000020805.1	5,061,632	74.84	99.35	0	2
Dehalobacter restrictus DSM 9455	GCA_000512895.1	2,943,336	44.56	99.94	0.47	21
Dehalobacter sp. 12DCB1	GCA_004343605.1	2,850,914	44.38	99.94	0.04	43
Dehalobacter sp. 14DCB1	GCA_004343635.1	3,035,609	43.96	100	0.34	37
Dehalobacter sp. CF	GCA_000305815.1	3,092,048	44.31	99.94	0	18
Dehalobacter sp. DCA	GCA_000305775.1	3,069,953	44.61	99.94	0	18
Dehalobacter sp. MCB1	GCA_003590275.1	2,854,199	44.18	99.94	0.04	42
Dehalobacter sp. TeCB1	GCA_001707455.1	3,133,217	44	99.94	0.17	21
Dehalobacter sp. UNSWDHB	GCA_000445165.1	3,201,560	44.88	99.94	0.38	20
Dehalococcoides mccartyi 195	GCA_000011905.1	1,469,720	48.85	99.01	0	17
Dehalococcoides mccartyi BAV1	GCA_000016705.1	1,341,892	47.17	99.01	0	10
Dehalococcoides mccartyi BTF08	GCA_000341695.1	1,452,335	47.28	99.01	0	18
Dehalococcoides mccartyi CBDB1	GCA_000009025.1	1,395,502	47.03	99.01	0	30
Dehalococcoides mccartyi CG1	GCA_000830925.1	1,486,678	46.93	99.01	0	36
Dehalococcoides mccartyi CG4	GCA_000830905.1	1,382,308	48.72	99.01	0.99	13
Dehalococcoides mccartyi CG5	GCA_000830885.1	1,362,151	47.22	99.01	0	25
Dehalococcoides mccartyi DCMB5	GCA_000341655.1	1,431,902	47.07	99.01	0	21
Dehalococcoides mccartyi GT	GCA_000025585.1	1,360,154	47.31	99.01	0	20
Dehalococcoides mccartyi GY50	GCA_000499365.1	1,407,418	47	99.01	0	22
Dehalococcoides mccartyi IBARAKI	GCA_001547795.1	1,451,056	46.99	99.01	0	25
Dehalococcoides mccartyi VS	GCA_000025025.1	1,413,462	47.27	99.01	0	35

Dehalococcoides mccartyi WBC-2	GCA_001761445.1	1,374,583	47.45	99.01	0	13
Dehalogenimonas alkenigignens BRE15M	GCA_003095415.1	1,652,753	56.32	95.21	0	34
Dehalogenimonas alkenigignens IP3-3	GCA_001466665.1	1,851,576	55.88	95.21	0	42
Dehalogenimonas formicexedens	GCA_001953175.1	2,092,789	53.96	95.71	0	26
Dehalogenimonas lykanthroporepellens BC-DL-9	GCA_000143165.1	1,686,510	55.04	97.36	0	21
Dehalogenimonas sp. GP	GCA_014672715.2	2,068,322	51.93	94.39	0	19
Dehalogenimonas sp. WBC-2	GCA_001005265.1	1,725,728	49.19	98.68	0	22
Desulfitobacterium chlororespirans DSM 11544	GCA_900143285.1	5,606,984	47.34	98.98	3.06	1
Desulfitobacterium dehalogenans	GCA_012842225.1	3,960,095	44.85	81.03	2.59	1
Desulfitobacterium dehalogenans ATCC 51507	GCA_000243155.3	4,321,753	44.97	98.72	3.98	1
Desulfitobacterium dichloroeliminans LMG P-21439	GCA_000243135.3	3,624,449	44.22	97.96	1.36	1
Desulfitobacterium hafniense DCB-2	GCA_000021925.1	5,279,134	47.54	98.98	3.32	6
Desulfitobacterium hafniense PCP-1	GCA_000379505.1	5,563,209	47.52	98.98	4.51	2
Desulfitobacterium hafniense Y51	GCA_000010045.1	5,727,534	47.36	98.98	4.08	1
Desulfitobacterium sp. PCE1	GCA_000384015.1	4,220,584	44.98	98.72	3.74	3
Desulfitobacterium hafniense sp. PCE-S	GCA_000944695.1	5,666,696	47.28	98.98	3.15	1
Desulfomonile tiedjei	GCA_000266945.1	6,527,027	50.09	98.39	1.29	1
Geobacter lovleyi SZ	GCA_000020385.1	3,994,874	54.74	99.68	0.65	1
Nitratireductor pacificus pht-3B	GCA_000300335.1	4,466,205	65.51	99.51	0.18	1
Shewanella sediminis HAW-EB3	GCA_000018025.1	5,517,674	46.08	99.84	0	1
Sulfurospirillum halorespirans DSM 13726	GCA_001723605.1	3,029,840	41.32	100	1.04	1
Sulfurospirillum multivorans DSM 12446	GCA_000568815.1	3,175,729	40.9	100	1.04	1
Sulfurospirillum multivorans strain N	GCA_008083195.1	3,181,530	40.9	100	1.04	1

Among the currently known obligate OHRB, *Dehalococcoides* spp. have the smallest genome size (1.2 - 1.5 Mbp), followed by *Dehalogenimonas* (1.5 - 2.0 Mbp) and Dehalobacter (2.7 – 3.1 Mbp). For the versatile OHRB, *Sulfurospirillum* spp. have the smallest genomes (2.9 Mbp to 3.1 Mbp), which are similar in size as those of *Dehalobacter* spp. Interestingly, compared with other OHRB genomes, and particularly those of obligate OHRB, OHRB within the genus *Sulfurospirillum* only have a limited number of different RDase genes and over half of the genomes within the genus don't encode any RDase gene, suggesting that RDase genes were acquired from the environment more recently (Türkowsky et al., 2018). Furthermore, *Dehalobacter* appears in the transitional stage in genome size to maintain a similar number of RDase genes as *Dehalococcoides* and *Dehalogenimonas* potentially using various organohalides for OHR.

Reductive dehalogenases (RDases)

Reductive dehalogenation is catalyzed by the reductive dehalogenase subunit A, normally termed as RdhA or RDase, and a number of RDases have been biochemically and genetically characterized. Overall, RDases exhibit a relatively low identity of less than 30 % in amino acid sequences with each other (Fincker and Spormann, 2017). This is illustrated by the alignment of well-studied representative RDases from *Dehalococcoides mccartyi*, *Dehalobacter restrictus*, *Sulfurospirillum multivorans*, *Dehalogenimonas lykanthroporepellens*, and *Desulfomonile tiedjei* (Figure 1.3). Despite the extensive differences in amino acid sequence between the full-length proteins, these identified RDases share three conserved motifs, including a twin-arginine translocating signal motif (Tat) at the N-terminus and two Fe-S cluster-binding motifs (Fincker and Spormann, 2017; Atashgahi, 2019) Figure 1.3A). Usually, the respiratory RDase is accompanied by a membrane anchor protein B, also described as RdhB. It has been shown that RdhB supports the translocation of RDase to the periplasmatic face to facilitate access to the organohalide substrates and to support the generation of a proton motive force across the cytoplasmatic membrane (Mansfeldt et al., 2014; Fincker and Spormann, 2017).

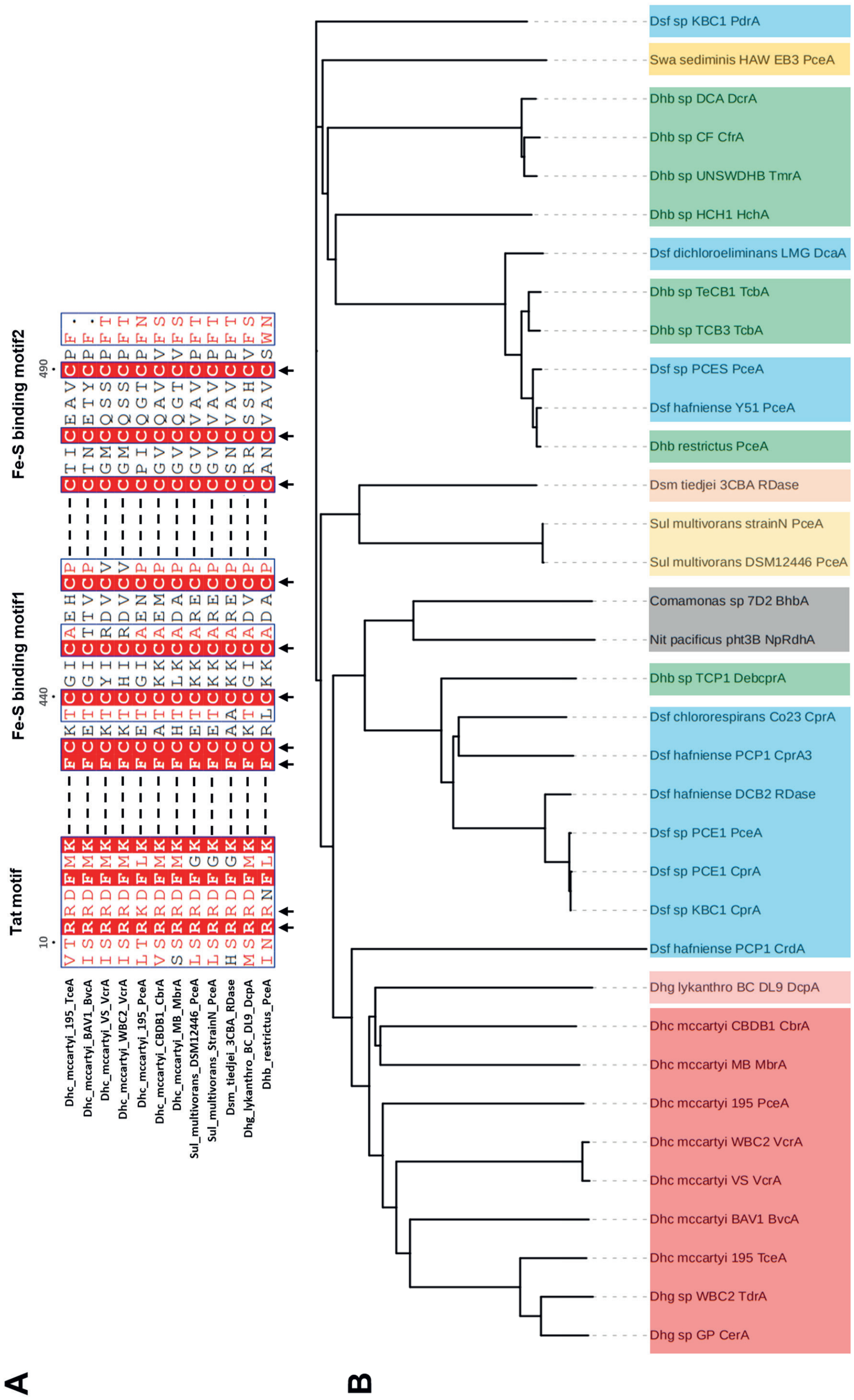
A
B
Tat motif
Fe-S binding motif1
Fe-S binding motif2
10
440
490
Dhc_mccartyi_195_TceA
Dhc_mccartyi_BAV1_BvcA
Dhc_mccartyi_VS_VcrA
Dhc_mccartyi_WBC2_VcrA
Dhc_mccartyi_195_PceA
Dhc_mccartyi_CBDB1_CbrA
Dhc_mccartyi_MB_MbrA
Sul_multivorans_DSM12446_PceA
Sul_multivorans_StrainN_PceA
Dsm_tiedjei_3CBA_RDase
Dhg_lykanthro_BC_DL9_DcpA
Dhb_restrictus_PceA
Dsf sp KBC1 PdrA
Swa sediminis HAW EB3 PceA
Dhb sp DCA DcrA
Dhb sp CF CfrA
Dhb sp UNSWDHB TmrA
Dhb sp HCH1 HchA
Dsf dichloroeliminans LMG DcaA
Dhb sp TeCB1 TcbA
Dhb sp TCB3 TcbA
Dsf sp PCES PceA
Dsf hafniense Y51 PceA
Dhb restrictus PceA
Dsm tiedjei 3CBA RDase
Sul multivorans strainN PceA
Sul multivorans DSM12446 PceA
Comamonas sp 7D2 BhbA
Nit pacificus pht3B NpRdhA
Dhb sp TCP1 DebcprA
Dsf chlororespirans Co23 CprA
Dsf hafniense PCP1 CprA3
Dsf hafniense DCB2 RDase
Dsf sp PCE1 PceA
Dsf sp PCE1 CprA
Dsf sp KBC1 CprA
Dsf hafniense PCP1 CrdA
Dhg lykanthro BC DL9 DcpA
Dhc mccartyi CBDB1 CbrA
Dhc mccartyi MB MbrA
Dhc mccartyi 195 PceA
Dhc mccartyi WBC2 VcrA
Dhc mccartyi VS VcrA
Dhc mccartyi BAV1 BvcA
Dhc mccartyi 195 TceA
Dhg sp WBC2 TdrA
Dhg sp GP CerA

Figure 1.3 Phylogenetic analysis of characterized RDases in RDaseDB that uses a 90 % amino acid pairwise identity cut-off for the identification of different RDases (https://rdasedb.biozone.utoronto.ca/). (A) Multiple sequence alignment of representative RDases. Arrows indicate the conserved residues in the Twin Arginine Translocation (Tat) motif, as well as in two Fe-S cluster binding motifs, FCXXCXXXCP and CXXCXXXCP. (B) Phylogenetic analysis of Rdase sequences. Tips of the phylogenetic tree were colored following the patterns in Figure 1.2. Dhc, *Dehalococcoides*; Dhg, *Dehalogenimonas*; Dsf, *Desulfitobacterium*; Dhb, *Dehalobacter*; Sul, *Sulfurospirillum*; Nit, *Nitratireductor*; Dsm, *Desulfomonile*; Swa, *Shewanella*.

Furthermore, phylogenetic analysis revealed that these RDases remained evolutionarily conserved at genus level, especially for proteins from members of the *Dehalococcoides*. RDases from *Dehalogenimonas* are most closely related to those of *Dehalococcoides* keeping in line with their genomic phylogenies (Figure 1.2 and 1.3B). This and the fact that both are obligatory OHRB suggests their common ancestral origin. Similarly, RDases from *Desulfitobacterium* spp. are most closely related to those of *Dehalobacter*. While isolates within the latter genus belong to the group of obligatory OHRB with more than 15 RDases in each genome (Table 1.1), genomes of the metabolically versatile *Desulfitobacterium* isolates encode a lower number of RDases, with *D. hafniense* DCB-2 harbouring the highest number of six. Both, *Dehalobacter* and *Desulfitobacterium,* belong to the same phylum, *Firmicutes* (Figure 1.2), and their close phylogenomic relationship suggests that they likely originated from a common ancestor. The question whether this difference in RDase gene number is due to gene expansion in *Dehalobacter* spp. or gene loss in *Desulfitobacterium* spp. has not been unequivocally solved, and requires further research.

To date, two RDases have been structurally characterized, including PceA (PDB: 4UR3) from *Sulfurospirillum multivorans* and NpRdhA (PDB: 4RAS) from *Nitratireductor pacificus* pht-3B (Bommer et al., 2014; Payne et al., 2015). Both RDases share common features with respect to cobalamin (vitamin B12) binding and Fe-S clusters, essential features of most RDases

(Figure 1.4), in which the center of the cobalamin is located at the active site, binding directly to the halogenated compound, and the Fe-S clusters being involved in the transfer of the deprived electrons to the active site (van de Pas et al., 1999; Fincker and Spormann, 2017). Several configurational structures of RDases with various halogenated compounds were crystallized and submitted to the PDB protein data bank (https://www.rcsb.org/), including, for example, PceA in a complex with 2,4,6-tribromophenol (PDB ID: 5M2G), which provides a template for accurate homology modeling of newly-discovered RDases.

Distinctively, PceA has been shown to be active as a dimer in contrast to the monomer of NpRdhA (Payne et al., 2015). Furthermore, PceA contains the Tat translocating signal peptide and is neighbored by anchor protein PceB, which indicates its role as a membrane-associated complex. In contrast, NpRdhA lacks these functional features, suggesting that it acts as a soluble cytoplasmic enzyme.

As supported by the structural configurations shown in Figure 1.4, vitamin B12 (B12) was confirmed to be required for reductive dehalogenation. Obligate OHRB, e.g. *Dehalococcoides* and *Dehalogenimonas*, are B12 auxotrophic due to the lack of complete *de novo* B12 biosynthesis pathways, indicating their dehalogenating activity depends on the environmental availability of B12.

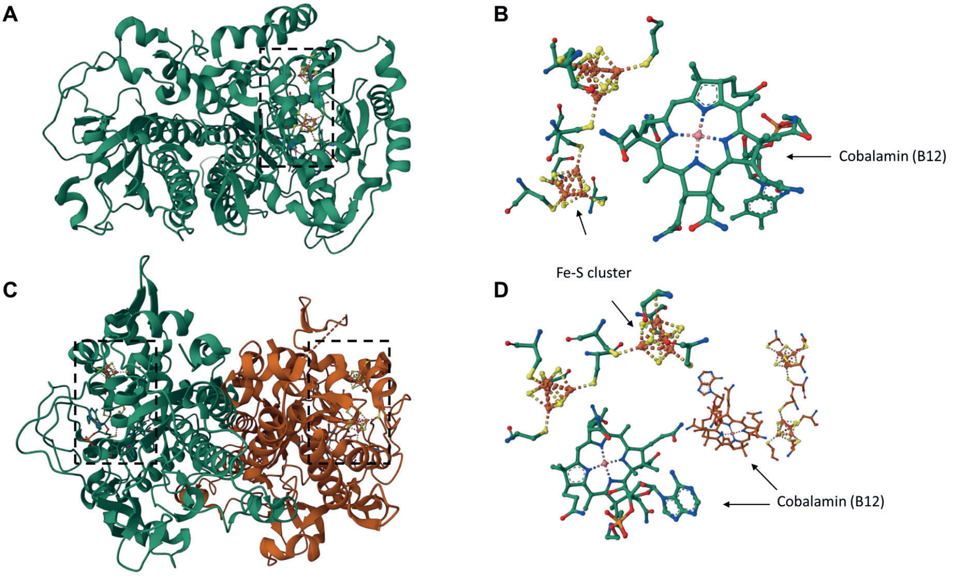

Figure 1.4 Structure of RDase containing cobalamin (vitamin B12) and Iron-Sulfur (Fe-S) clusters in the monomer of NpRdhA (A and B, PDB ID: 4RAS) and dimer of PceA (C and D, PDB ID: 4UR3), respectively.

RDase-associated electron transport chains (ETCs)

Desulfomonile tiedjei was the first identified OHRB to dehalogenate 3-chlorobenzoate coupled to ATP synthesis (Mohn and Tiedje, 1992). Since then, many more OHRB were isolated and characterized, and the mechanisms of RDase-associated ETCs were gradually unveiled and divided into two types according to the dependence of quinones. For *Dehalococcoides* and *Dehalogenimonas*, their genomes lack the pathways needed for *de novo* quinone biosynthesis (Moe et al., 2009; Schipp et al., 2013). Further, the menaquinone inhibitor, 2-n-heptyl-4-hydroxyquinoline N-oxide, HOQNO, cannot block the electron transfer from the hydrogenase to the RDase dechlorinating 1,2,3-trichlorobenzene of *D. mccartyi* CBDB1, which indicated the nonessential role of quinones to OHR (Figure 1.5A) (Jayachandran et al., 2004; Moe et al., 2009; Schipp et al., 2013). The ETC of *D. mccartyi* strain CBDB1 is composed of Hup hydrogenase, CISM (complex iron-sulfur molybdoenzyme), and RDase, in which CISM has been characterized as a well-known protein complex for respiratory redox reactions providing electron relay (Rothery et al., 2008; Kublik et al., 2016). The CISM connects Hup hydrogenase and RDase directly and functions in a similar role as quinones for the transfer of electrons. For many facultative OHRB, such as *Sulfurospirillum* and *Desulfitobacterium*, and some obligatory OHRB, such as *Dehalobacter*, quinones, instead of CISM, play an important role in electron transfer (Figure 1.5B) (Wang et al., 2018). It has, for example, been shown that HOQNO can effectively inhibit the reductive dehalogenation of *D. restrictus* and *D. tiedjei* (Schumacher and Holliger, 1996; Louie and Mohn, 1999). In addition, it was shown that menaquinone is reduced and oxidized by adding H_2 or PCE in *D. restrictus*, respectively (Schumacher and Holliger, 1996).

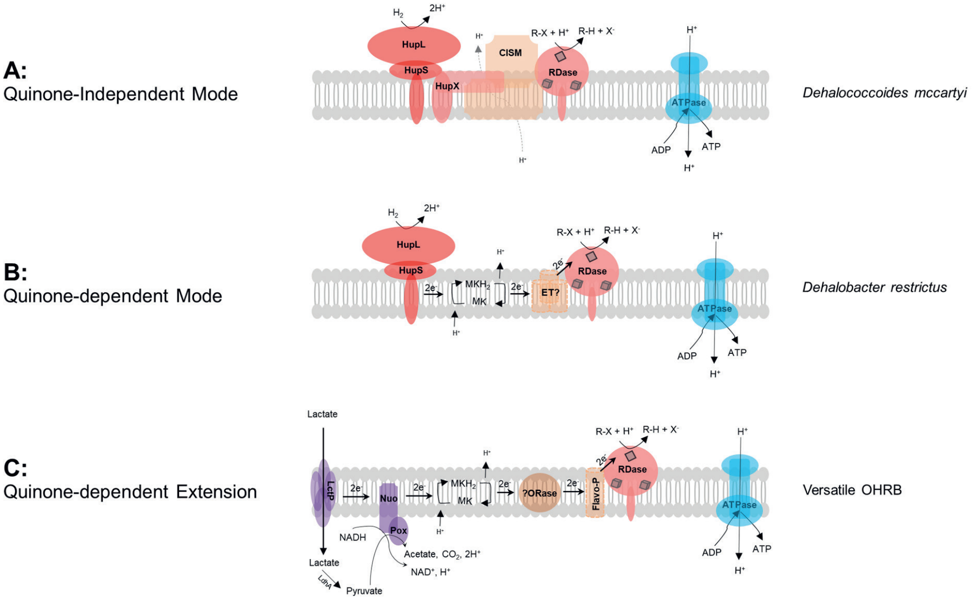

Figure 1.5 Diagrams of electron transport chains in OHRB (in)dependent on quinones. The electron transport chains of *Dehalococcoides mccartyi* (A), *Dehalobacter restrictus* (B) and combined versatile OHRB (C), including *Sulfurospirillum multivorans*, *Desulfitobacterium*

dehalogenans and *Desulfoluna spongiiphila*, for OHR (Luijten et al., 2003; Kruse et al., 2013; Rupakula et al., 2013; Goris et al., 2015b; Goris et al., 2015a; Kruse et al., 2015; Kublik et al., 2016; Peng et al., 2020). Hup: Ni-Fe hydrogen uptake hydrogenase with large (L) and small (S) subunits; CISM: complex iron-sulfur molybdoenzyme; MK/MKH_2: menaquinones; ET?: electron transporter; LctP: lactate permease; Nuo: NADH dehydrogenase; Pox: pyruvate oxidase; ?ORase: oxidoreductase; Flavo-P: flavoprotein; grey cubes in RDase: two Iron-Sulfur clusters; grey rhombus: vitamin B12.

With more versatile OHRB isolated and characterized (Kruse et al., 2013; Goris et al., 2014; Goris et al., 2015a; Peng et al., 2020), the diversity of OHR ECTs was further extended with the integration of diverse electron transporters and electron donors, such as lactate in addition to H_2 as shown in Figure 1.5C. Mostly, these were quinol dehydrogenases that were found encoded in the same gene region as the RDase gene, such as FixABCX in *D. hafniense*. They were found expressed during OHR by transcriptomics and proteomics, suggesting their involvement as the intermediate shuttle in electron flow to the RDase (Prat et al., 2011; Peng et al., 2012). Noticeably, a quinol dehydrogenase complex, NapGH, was critical for nitrate respiration, which was found encoded adjacent to RDase (Kern and Simon, 2008; Goris et al., 2014), indicating shared ECTs for different modes of anaerobic respiration. Henceforth, further studies will be needed to further extend our understanding of ETCs in OHRB.

Aim and outline of this thesis

Marine environments are a large reservoir of natural halogenated compounds, with currently over 5000 compounds being described, some of which have excellent medical potential to cure cancers, bacterial and viral infection, whereas, others, such as polybrominated diphenylethers, are toxic and accumulated over millions of years (Wiseman et al., 2011; Gribble, 2012; Gribble, 2015). Recently, sequencing-based surveys revealed the potential activity of OHR in pristine marine environments of Aarhus Bay, which indicated that marine microbes drive the halogen cycle (Zinke et al., 2017; Jochum et al., 2018). However, the eco-physiological verification of

OHR and identification of the responsible OHRB still remains in its infancy. Henceforth, research described in this thesis aimed to demonstrate OHR of Aarhus Bay marine sediments stepwise. We firstly verified the OHR potential on various halogenated compounds, and then further focused on PCE dechlorinating enrichments by means of metagenomic and -transcriptomic analyses to clarify the diversity and activity of OHRB. The "Dilution-to-extinction" principle guided the isolation of OHRB, and the obtained consortium was found to be capable of reductive dehalogenation that was achieved in an interactive manner by OHRB and non-OHRB. Finally, an OHRB representative strain from a genus not previously affiliated with OHR was further characterized to explore the role of OHR and interconnection with other metabolic pathways.

Chapter 2 firstly validates the reductive dehalogenation in marine sediments from Aarhus Bay on a range of organohalides, including chlorinated, brominated and iodinated compounds. The combination of molecular identification and sequence analysis revealed the responsible OHRB were likely from taxa other than the well-characterized OHRB. Moreover, deiodination of 2,4,6-triiodophenol (2,4,6-TIP) enriched for members of the *Lokiarchaea*.

Chapter 3 focuses on PCE dechlorinating cultures obtained from Aarhus Bay sediments, in which 16 metagenome-assembled genomes (MAGs) were found bearing RDase genes. MAGs were further classified into the class of *Bacilli*, and phyla of *Bacteroidota*, *Synergistota*, and *Spirochaetota*. Members of these taxa were rarely reported to date to catalyze reductive dehalogenation. Intriguingly, one MAG, designated as CH3_bin.26, closest to the genus *Vulcanibacillus*, carried 97 RDase genes, exceeding the RDase complement of *Dehalococcoides*. Thereinto, 84 RDase genes of CH3_bin.26 were found transcribed during PCE dechlorination. Moreover, the RDase-containing operons indicated diverse regulatory mechanisms for the expression of RDase genes. Further studies of these in response to environmental stimuli suggested diverse modes of regulation of RDase genes could be the result of adaptation to challenging environments.

Chapter 4 reports on the isolation of a consortium that was composed of newly-classified OHRB and non-OHRB to catalyze the reductive debromination of 2,6-dibromiphenol (2,6-DBP). Two MAGs, CH4_bin.3 belonging to *Desulfoplanes* codes for two putative RDase genes, and CH4_bin.4 belonging to *Marinifilaceae* has one. Interestingly, CH4_bin.5 belonging to *Desulforhopalus* carries a gene predicted to encode a tetrachloro-*p*-hydroquinone RDase (TPh-RDase) that acts without energy conservation. The expression of all these RDase genes was found induced under debromination conditions. The CH4_bin.5 RDase gene was found most strongly expressed. Acetylene was identified as a specific inhibitor of RDase activity at post-transcriptional level. Furthermore, the predicted metabolic association of the bins found in this enrichment provides more insights into possibilities for optimizing synthetic OHR communities for *in situ* bioremediation.

Chapter 5 describes a representative strain, *Desulforhopalus singaporensis*, which was characterized as a sulfate-reducing formatotroph to catalyze the reductive dehalogenation of brominated compounds. The genome of *D. singaporensis* bears the complete complement of *de novo* B12 biosynthesis genes. Formate, rather than H_2, serves as the electron donor for the Wood-Ljungdahl pathway and OHR simultaneously to support cell growth. The genome analysis of *D. singaporensis* revealed it contains all genes necessary for poly-β-hydroxybutyrate (PHB) production which agrees to previous observations, and suggests a role for the formed PHB that could serve as a long-chain carbon source for the growth of other community members. Further, phylogenomic analysis revealed metabolic differences between two isolates, *D. singaporensis* and *D. vacuolatus*, of which the latter exhibited closer phylogeny to MAG bin.5 (Chapter 4), from the same niche, suggesting that bacterial metabolism is shaped by the local environments, and the RDase could be obtained by gene transfer from the environment.

In **Chapter 6** I provide a general discussion of the results described in this thesis and future perspectives.

References

Adrian L, Löffler FE. *Organohalide-respiring bacteria* volume 85: Springer, 2016.

Apajalahti JH, Salkinoja-Salonen MS. Complete dechlorination of tetrachlorohydroquinone by cell extracts of pentachlorophenol-induced *Rhodococcus chlorophenolicus*. *J Bacteriol* 1987;169: 5125-30.

Atashgahi S. Discovered by genomics: putative reductive dehalogenases with N-terminus transmembrane helixes. *FEMS Microbiol Ecol* 2019;95: fiz048.

Belay N, Daniels L. Production of ethane, ethylene, and acetylene from halogenated hydrocarbons by methanogenic bacteria. *Appl Environ Microbiol* 1987;53: 1604-10.

Bommer M, Kunze C, Fesseler J *et al.* Structural basis for organohalide respiration. *Science* 2014;346: 455-8.

Bosma TN, van der Meer JR, Schraa G *et al.* Reductive dechlorination of all trichloroand dichlorobenzene isomers. *FEMS Microbiol Ecol* 1988;53: 223-9.

DeWeerd K, Concannon F, Suflita JM. Relationship between hydrogen consumption, dehalogenation, and the reduction of sulfur oxyanions by *Desulfomonile tiedjei*. *Appl Environ Microbiol* 1991;57: 1929-34.

Dolfing J, and James M. Tiedje. Influence of substituents on reductive dehalogenation of 3-chlorobenzoate analogs. *Appl Environ Microbiol* 1991;57: 820-4.

Drzyzga O, Gottschal JC. Tetrachloroethene dehalorespiration and growth of *Desulfitobacterium frappieri* TCE1 in strict dependence on the activity of *Desulfovibrio fructosivorans*. *Appl Environ Microbiol* 2002;68: 642-9.

Esaac E, Matsumura F. Metabolism of insecticides by reductive systems. *Pharmacol Ther* 1980;9: 1-26.

Fincker M, Spormann AM. Biochemistry of catabolic reductive dehalogenation. *Annu Rev Biochem* 2017;86: 357-86.

Gibson SA, Suflita JM. Extrapolation of biodegradation results to groundwater aquifers: reductive dehalogenation of aromatic compounds. *Applied and Environmental Microbiology* 1986;52: 681-8.

Goris T, Hornung B, Kruse T *et al.* Draft genome sequence and characterization of Desulfitobacterium hafniense PCE-S. *Standards in genomic sciences* 2015a;15.

Goris T, Schiffmann CL, Gadkari J *et al.* Proteomics of the organohalide-respiring Epsilonproteobacterium *Sulfurospirillum multivorans* adapted to tetrachloroethene and other energy substrates. *Sci Rep* 2015b;5.

Goris T, Schubert T, Gadkari J *et al.* Insights into organohalide respiration and the versatile catabolism of *Sulfurospirillum multivorans* gained from comparative genomics and physiological studies. *Environ Microbiol* 2014;16: 3562-80.

Gribble GW. Recently discovered naturally occurring heterocyclic organohalogen compounds. *Heterocycles* 2012;84: 157-207.

Gribble GW. A recent survey of naturally occurring organohalogen compounds. *Environ Chem* 2015;12: 396-405.

Jayachandran G, Görisch H, Adrian L. Studies on hydrogenase activity and chlorobenzene respiration in *Dehalococcoides* sp. strain CBDB1. *Arch Microbiol* 2004;182: 498-504.

Jochum LM, Schreiber L, Marshall IPG *et al.* Single-cell genomics reveals a diverse metabolic potential of uncultivated *Desulfatiglans*-related Deltaproteobacteria widely distributed in marine sediment. *Front Microbiol* 2018;9: 2038.

Kern M, Simon J. Characterization of the NapGH quinol dehydrogenase complex involved in *Wolinella succinogenes* nitrate respiration. *Mol Microbiol* 2008;69: 1137-52.

Kruse T, Maillard J, Goodwin L *et al.* Complete genome sequence of *Dehalobacter restrictus* PER-K23T. *Stand Genomic Sci* 2013;8: 375-88.

Kruse T, van de Pas BA, Atteia A *et al.* Genomic, proteomic, and biochemical analysis of the organohalide respiratory pathway in *Desulfitobacterium dehalogenans*. *J Bacteriol* 2015;197: 893-904.

Kublik A, Deobald D, Hartwig S *et al.* Identification of a multi-protein reductive dehalogenase complex in *Dehalococcoides mccartyi* strain CBDB1 suggests a protein-dependent respiratory electron transport chain obviating quinone involvement. *Environ Microbiol* 2016;18: 3044-56.

Kuhn EP, Suflita JM. Dehalogenation of pesticides by anaerobic microorganisms in soils and groundwater—a review. *Reactions and movement of organic chemicals in soils Soil Science Society of American and American Society of Agronomy, Madison, Wis* 1989;22: 111-80.

Lee MD. GToTree: a user-friendly workflow for phylogenomics. *Bioinformatics* 2019;35: 4162-4.

Louie TM, Mohn WW. Evidence for a chemiosmotic model of dehalorespiration in *Desulfomonile tiedjei* DCB-1. *Journal of bacteriology* 1999;181: 40-6.

Luijten ML, de Weert J, Smidt H *et al.* Description of *Sulfurospirillum halorespirans* sp. nov., an anaerobic, tetrachloroethene-respiring bacterium, and transfer of *Dehalospirillum multivorans* to the genus *Sulfurospirillum* as *Sulfurospirillum multivorans* comb. nov. *Int J Syst Evol Microbiol* 2003;53: 787-93.

Mansfeldt CB, Rowe AR, Heavner GL *et al.* Meta-analyses of *Dehalococcoides mccartyi* strain 195 transcriptomic profiles identify a respiration rate-related gene expression transition point and interoperon recruitment of a key oxidoreductase subunit. *Appl Environ Microbiol* 2014;80: 6062-72.

Maymo-Gatell X, Chien YT, Gossett JM *et al.* Isolation of a bacterium that reductively dechlorinates tetrachloroethene to ethene. *Science* 1997;276: 1568-71.

McCauley KM, Wilson SR, Van der Donk WA. Characterization of chlorovinylcobalamin, a putative intermediate in reductive degradation of chlorinated ethylenes. *J Am Chem Soc* 2003;125: 4410-1.

Mikesell MD, Boyd SA. Dechlorination of chloroform by *Methanosarcina* strains. *Appl Environ Microbiol* 1990;56: 1198-201.

Moe WM, Yan J, Nobre MF *et al. Dehalogenimonas lykanthroporepellens* gen. nov., sp. nov., a reductively dehalogenating bacterium isolated from chlorinated solvent-contaminated groundwater. *Int J Syst Evol Microbiol* 2009;59: 2692-7.

Mohn WW, Tiedje J. Microbial reductive dehalogenation. *Microbiol Mol Biol Rev* 1992;56: 482-507.

Mohn WW, Tiedje JM. Strain DCB-1 conserves energy for growth from reductive dechlorination coupled to formate oxidation. *Arch Microbiol* 1990;153: 267-71.

Molenda O, Puentes Jacome LA, Cao X *et al.* Insights into origins and function of the unexplored majority of the reductive dehalogenase gene family as a result of genome assembly and ortholog group classification. *Environ Sci Process Impacts* 2020.

Payne KA, Quezada CP, Fisher K *et al.* Reductive dehalogenase structure suggests a mechanism for B12-dependent dehalogenation. *Nature* 2015;517: 513-6.

Peng P, Goris T, Lu Y *et al.* Organohalide-respiring *Desulfoluna* species isolated from marine environments. *ISME J* 2020;14: 815-27.

Peng X, Yamamoto S, Vertès AA *et al.* Global transcriptome analysis of the tetrachloroethene-dechlorinating bacterium *Desulfitobacterium hafniense* Y51 in the presence of various electron donors and terminal electron acceptors. *J Ind Microbiol Biotechnol* 2012;39: 255-68.

Prat L, Maillard J, Grimaud R *et al.* Physiological adaptation of *Desulfitobacterium hafniense* strain TCE1 to tetrachloroethene respiration. *Appl Environ Microbiol* 2011;77: 3853-9.

Rinke C, Chuvochina M, Mussig AJ *et al.* A standardized archaeal taxonomy for the Genome Taxonomy Database. *Nat Microbiol* 2021;6: 946-59.

Rothery RA, Workun GJ, Weiner JH. The prokaryotic complex iron–sulfur molybdoenzyme family. *Biochim Biophys Acta - Biomembr* 2008;1778: 1897-929.

Rupakula A, Kruse T, Boeren S *et al.* The restricted metabolism of the obligate organohalide respiring bacterium *Dehalobacter restrictus*: lessons from tiered functional genomics. *Philos Trans R Soc Lond B Biol Sci* 2013;368: 20120325.

Schipp CJ, Marco-Urrea E, Kublik A *et al.* Organic cofactors in the metabolism of *Dehalococcoides mccartyi* strains. *Philos Trans R Soc Lond B Biol Sci* 2013;368: 20120321.

Schumacher W, Holliger C. The proton/electron ration of the menaquinone-dependent electron transport from dihydrogen to tetrachloroethene in" *Dehalobacter restrictus*". *J Bacteriol* 1996;178: 2328-33.

Tiedje JM, Boyd SA, Fathepure BZ. 13. Anaerobic degradation of chlorinated aromatic hydrocarbons. *Dev Ind Microbiol* 1987;27: 117-27.

Türkowsky D, Jehmlich N, Diekert G *et al.* An integrative overview of genomic, transcriptomic and proteomic analyses in organohalide respiration research. *FEMS Microbiol Ecol* 2018;94: fiy013.

van de Pas BA, Smidt H, Hagen WR *et al.* Purification and molecular characterization of ortho-chlorophenol reductive dehalogenase, a key enzyme of halorespiration in *Desulfitobacterium dehalogenans*. *J Biol Chem* 1999;274: 20287–92.

Wang S, Qiu L, Liu X *et al.* Electron transport chains in organohalide-respiring bacteria and bioremediation implications. *Biotechnol Adv* 2018;36: 1194-206.

Wiseman SB, Wan Y, Chang H *et al.* Polybrominated diphenyl ethers and their hydroxylated/methoxylated analogs: environmental sources, metabolic relationships, and relative toxicities. *Mar Pollut Bull* 2011;63: 179-88.

Zinke LA, Mullis MM, Bird JT *et al.* Thriving or surviving? Evaluating active microbial guilds in Baltic Sea sediment. *Environ Microbiol Rep* 2017;9: 528-36.

Chapter 2

Organohalide respiration potential in marine sediments from Aarhus Bay

Chen Zhang, Siavash Atashgahi, Tom N.P Bosma, Peng Peng, Hauke Smidt

Published in *FEMS Microbiology Ecology*

https://doi.org/10.1093/femsec/fiac073

Abstract

Organohalide respiration (OHR), catalyzed by reductive dehalogenases (RDases), plays an important role in halogen cycling. Natural organohalides and putative RDase-encoding genes have been reported in Aarhus Bay sediments, however, OHR has not been experimentally verified. Here we show that sediments of Aarhus Bay can dehalogenate a range of organohalides, and different organohalides differentially affected microbial community compositions. PCE-dechlorinating cultures were further examined by 16S rRNA gene-targeted quantitative PCR and amplicon sequencing. Known organohalide-respiring bacteria (OHRB) including *Dehalococcoides*, *Dehalobacter* and *Desulfitobacterium* decreased in abundance during transfers and serial dilutions, suggesting the importance of yet uncharacterized OHRB in these cultures. Switching from PCE to 2,6-DBP led to its complete debromination to phenol in cultures with and without sulfate. 2,6-DBP debrominating cultures differed in microbial composition from PCE-dechlorinating cultures. *Desulfobacterota* genera recently verified to include OHRB, including *Desulfovibrio* and *Desulfuromusa*, were enriched in all microcosms, whereas *Halodesulfovibrio* was only enriched in cultures without sulfate. Hydrogen and methane were detected in cultures without sulfate. Hydrogen likely served as electron donor for OHR and methanogenesis. This study shows that OHR can occur in marine environments mediated by yet unknown OHRB, suggesting their role in natural halogen cycling.

Keywords: Aarhus Bay marine sediments; tetrachloroethene (PCE); 2,6-Dibromophenol (2,6-DBP); reductive dehalogenation; organohalide respiring prokaryotes; 16S rRNA gene amplicon sequencing

Introduction

Halogenated organic compounds, also termed organohalides, can be man-made or of natural origin. Over 5000 organohalides with a natural origin have been reported (Gribble 1996, Gribble 2012, Gribble 2015). Marine environments are a large reservoir of natural organohalides, which are produced via biotic and abiotic mechanisms (Gribble 1996, Gribble 2012, Gribble 2015). Marine organisms such as algae, sponges, corals and microorganisms recruit either substrate-specific halogenases or haloperoxidases to catalyse the biotic formation of organohalides (Atashgahi, et al. 2018, Bayer, et al. 2013, Gribble 2015, Gutleben, et al. 2019, Ozturk, et al. 2013, Wagner, et al. 2009, Wever and van der Horst 2013). Abiotic halogenation on the other hand occurs by photochemical reaction, volcanic eruption and Fenton-like mechanisms (Comba, et al. 2015, Leri, et al. 2014, Méndez-Díaz, et al. 2014). Some of these natural organohalides have excellent medical potential to cure cancers, and viral- and bacterial infections (Gribble 2015), whereas some are toxic such as polychlorinated dibenzo-p-dioxin (PCDDs) and polybrominated diphenyl ethers (PBDEs) (Wiseman, et al. 2011). Further, most of the highly halogenated natural organohalides, for example PBDEs, have been found precipitated and buried in marine sediments of millions of years of age (Hashimoto, et al. 1995, Moon, et al. 2007). Accordingly, anaerobic dehalogenation likely occurs in marine sediments as the biggest anoxic environment on Earth, and thus contributing to the detoxification, decomposition and recycling of toxic/persistent organohalides (Ahn, et al. 2003, Häggblom, et al. 2003, Liu, et al. 2017, Peng, et al. 2020a).

Halides are replaced by hydrogen through reductive dehalogenation that often is linked to a specific type of anaerobic respiratory metabolism termed organohalide respiration (OHR). In this process, organohalides serve as the terminal electron acceptors to conserve energy (Dolfing and Tiedje 1987, Mohn and Kennedy 1992, Smidt and De Vos 2004). This process has been documented in bacteria known as organohalide-respiring bacteria (OHRB) (Atashgahi, et al.

2016, Fincker and Spormann 2017, Smidt and De Vos 2004). OHR is mediated by reductive dehalogenase (RDase) enzymes (Adrian and Loeffler, 2016; Agarwal et al., 2017; Fincker and Spormann, 2017). Since the isolation of the first OHRB, *Desulfomonile tiedjei* (Dolfing and Tiedje 1987, Mohn and Tiedje 1990), a broad diversity of OHRB have been isolated, belonging to three phyla: *Chloroflexota*, *Firmicutes*, and *Proteobacteria* (Atashgahi, et al. 2016, Fincker and Spormann 2017, Türkowsky, et al. 2018). Members of the genera *Dehalococcoides* (Dhc) and *Dehalogenimonas* (Dhg) within the *Chloroflexota*, and *Dehalobacter* (Dhb) in the *Firmicutes* are obligate OHRB based on their restriction to OHR as the sole energy metabolism (Fincker and Spormann 2017, Holscher, et al. 2004, Maillard, et al. 2003, Moe, et al. 2009, Molenda, et al. 2016, Muller, et al. 2004). Members of *Desulfitobacterium* (Dsb) in *Firmicutes*, *Sulfurospirillum* (Sul) in *Epsilonproteobacteria* and various *Desulfobacterota* (previously *Deltaproteobacteria*) species including members of *Geobacter* (Geo), *Desulfoluna* and *Desulfovibrio* are considered as facultative OHRB that have a versatile metabolism including but not restricted to OHR (Liu and Haggblom 2018, Maphosa, et al. 2010, Peng, et al. 2020a). Intriguingly, up to 10 % of all available *Desulfobacterota* genomes were found to contain at least one putative RDase gene (Liu and Haggblom 2018). Accordingly, a recent genome-guided study experimentally verified OHR potential in three *Desulfobacterota* isolates (Liu and Haggblom 2018).

Using degenerate primers based on sequences of well-characterized RDase genes, different RDase genes have been reported from subsea sediments of the Pacific Ocean close to Peru, Japan, Oregon (United States) and the eastern equator, that were diverse and phylogenetically distinct from their characterized counterparts from contaminated terrestrial environments (Futagami, et al. 2009, Futagami, et al. 2013). Application of various techniques such as (meta)genomics and (meta)transcriptomics have revealed an enormous diversity of RDase genes in marine sediments (Jochum, et al. 2017, Jochum, et al. 2018, Petro, et al. 2019a, Petro, et al. 2019b, Zinke, et al. 2017). For instance, meta-transcriptomic analysis of deep subsea sediments from site M59, close to Aarhus Bay, in the Baltic sea led to the discovery of a trichloroethene (TCE) reductive dehalogenase (*tceA*)-like gene that was transcribed, indicating the potential for PCE or TCE dechlorination in deep sea sediments as previously described for other environments (Fung, et al. 2007, Magnuson, et al. 1998, Zinke, et al. 2017). Recently, single-cell genomics and metagenomics analyses revealed the presence of RDase genes in sulfate-rich sediments of Aarhus Bay (Fincker, et al. 2020, Jochum, et al. 2018). This begged the question whether there is actual OHR potential in marine sediments of Aarhus Bay that may prevent accumulation of organohalides and contribute to halide and CO2 recycling back to the sea. It is interesting to note that sulfate reduction has been reported to be the predominant bioprocess in near-surface Aarhus Bay marine sediments (Leloup, et al. 2009, Ozuolmez, et al. 2020, Petro, et al. 2019b), in which reductive dehalogenation is likely to be inhibited by the produced and accumulated sulfide according to previous reports (Azizian, et al. 2010b, DeWeerd, et al. 1991, Mao, et al. 2017, Nelson, et al. 2002). Henceforth, taking the presence and absence of sulfate into consideration would add more insights to explore OHR potential in laboratory microcosms.

In this study, we showed that cultures obtained from marine sediments from Aarhus Bay were capable of dechlorinating, debrominating and deiodinating organohalides, further corroborating above-mentioned (meta)genome based studies with respect to the predicted occurrence of OHR in marine sediments. Interestingly, the microbial communities in reductively dechlorinating and debrominating enrichment cultures were divergent, suggesting the coexistence of diverse OHRB. Furthermore, enriched microorganisms did not belong to the well-identified OHRB, suggesting the presence of novel dehalogenators in these pristine marine environments.

Materials and methods

Chemicals

PCE, TCE, cDCE, trans-dichloroethene (tDCE) vinyl chloride (VC), ethene (ETH), 2,4,6-trichlorophenol (2,4,6-TCP), 2,6-dichlorophenol (2,6-DCP), 2,4- dichlorophenol (2,4-DCP), chlorophenol (CP), 2,6-DBP, 3-bromophenol (3-BP), 2-bromophenol (2-BP), 2,4,6-triiodophenol (2,4,6-TIP), 2,6-diiodophenol (2,6-DIP), 2,4-diiodophenol (2,4-DIP), 2-iodophenol (2-IP) and 4-iodophenol (4-IP), phenol, 1,4-dibromobenzene (1,4-DBB), bromobenzene (BB), and benzene were purchased from Sigma-Aldrich. Sulfate (0.5 M) and lactate (0.5 M) stock solutions were prepared by filter sterilization (syringe filter, 0.2 µm, mdimembrane, Ambala Cantt, India). All other (in)organic chemicals were of analytical grade.

Table 2.1 List of halogenated compounds for testing reductive dehalogenation of Aarhus Bay marine sediments.

Aarhus Bay Sediments^a	Station	Halogenated Compounds	Sulfate Addition^b	Products^c
3-35 cm / 36-68 cm	M5	Tetrachloroethane (PCE)	+ / -	Trichloroethene (TCE)^e; Cis-dichloroethene (cDCE)^f;
3-35 cm / 36-68 cm	M5	2,6-Dibromophenol (2,6-DBP)	+ / -	Bromophenol (BP)^e; Phenol^f;
3-35 cm	M5	1,4-Dibromobenzene (1,4-DBB)	+ / -	Bromobenzene (BB)^e; Benzene^f;
3-35 cm	M5	3-Bromophenol (3-BP)	+ / -	Phenol^f;
3-35 cm	M5	2,4,6-Trichlorophenol (2,4,6-TCP)	+ / -	ND^d;
3-35 cm	M5	2,4,6-Triiodorophenol (2,4,6-TIP)	+ / -	4-Iodophenol (4-IP)^g; Phenol^g;

[a] Different depths of Aarhus Bay marine sediments from one core.

[b] Cultures incubated with (+) or without (-) sulfate.

[c] Transformation products detected under both sulfate (+ / -) conditions.

[d] ND means no dehalogenation.

[e] Intermediate metabolites.

[f] Final product after 100 % disappearance of the original compound.

[g] Indicates coexistance of metabolites 4-IP and phenol in a ratio around 1:2.

Sediment collection and enrichment set-up

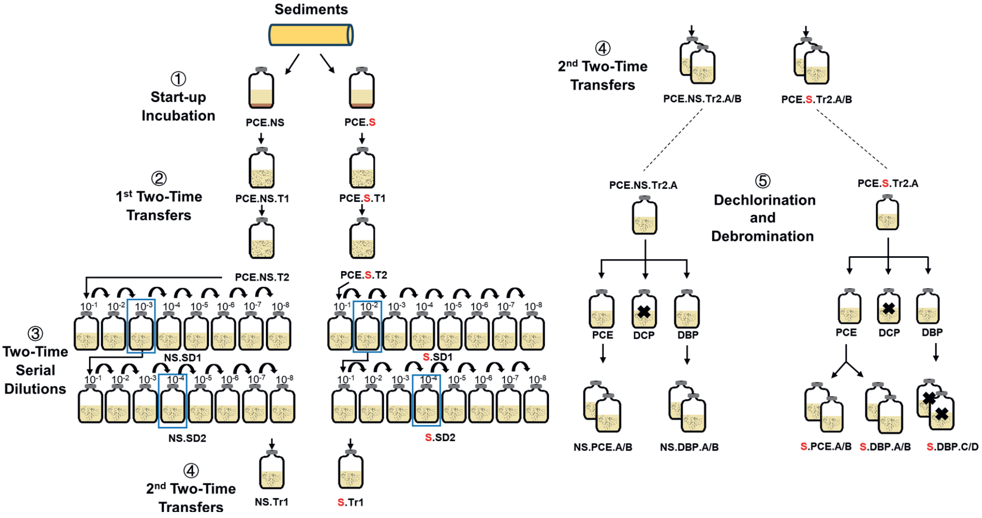

Figure 2.1 Experimental outline of reductive dehalogenation by marine sediments from Aarhus Bay M5 station. This experiment was carried out in 5 steps as labelled by ①, ②, ③, ④ and ⑤. "Sediments" stands for samples from near-surface marine sediments (3-35cm) of Aarhus Bay. Transfer volumes are 10% (v/v) in steps ①, ②, and ③, and 5% (v/v) in steps ④ and ⑤. Curved arrows in step ③ indicate the transfer pattern in 10 fold dilutions. NS: sulfate-free; S in red: sulfate-amended; Blue boxes in serial dilutions indicate the highest dilution at which dechlorination of PCE to cDCE was observed. Consequently, these are also the cultures that were used for the subsequent transfer; Bold cross marks indicate cultures that were unable to dehalogenate DCP or DBP.

Samples were kindly provided by Kasper U. Kjeldsen (Aarhus University). Specifically, samples were collected from a marine sediment core at station M5 in Aarhus Bay (56.103333 N, longitude 10.457833 E), Denmark, and were depth-fractioned into two parts: 3-35 cm and 36-68 cm. Ten grams of sediment from each fraction was transferred into 120 mL serum bottles containing 50 mL anoxic marine medium as previously described (Monserrate and Häggblom 1997, Peng, et al. 2020a). $Na_2S\cdot 9H_2O$ (0.48 g/L, 2 mM) was added as reducing reagent and Resazurin (0.005 g/L) as redox indicator. The bottle headspace was exchanged with N_2 and CO_2

(80 : 20 %, 140 KPa), bottles were sealed with Teflon-coated butyl rubber septa and aluminum crimp caps (GRACE, MD, USA) and incubated statically in the dark at 20 °C. Some organohalides were added to the marine medium separately and tested, including PCE, 2,6-DBP, 1,4-DBB, 3-BP, 2,4,6-TCP, and 2,4,6-TIP with/without additional 5mM sulfate and 5mM lactate as the electron donor. Subsequently, experiments focused first on more detailed characterization of PCE dechlorination. The dechlorinating cultures were spiked with PCE (100 μM) as electron acceptor and lactate (5 mM) serving as the electron donor and carbon source. One set of bottles received sulfate (5 mM) as an additional electron acceptor (designated "S"; bottles with only PCE were designated "NS") (Figure 2.1). Two transfers were set as the initial step to enrich for PCE dechlorinating microorganisms. Cultures were transferred when the PCE was reductively dechlorinated to cDCE. For each transfer, 10 % (v/v) of the mother cultures was transferred to fresh medium (Figure 2.1), with cultures being designated PCE.NS.T1 and PCE.S.T1 for first transfers, and PCE.NS.T2 and PCE.S.T2 indicating the second transfer. Second transfers were subsequently 10-fold serially diluted (SD) according to the dilution-to-extinction principle (NS.SD1, S.SD1; Figure 2.1). Highest dilutions for which dehalogenation was observed (NS.SD13, S.SD12, indicated by blue boxes in Figure 2.1) were used as inocula for a second series of 10-fold serial dilutions (NS.SD2, S.SD2; Figure 2.1). Highest dilutions with active dehalogenation (NS.SD24, S.SD24; Figure 2.1) after four spikes of 250 μM PCE and corresponding chemicals (5 mM lactate in NS, 5 mM lactate and 5 mM sulfate in S cultures) in the second serial dilution were used to inoculate a new set of transfers (NS.Tr1 and S.Tr1, Figure 2.1). These cultures were transferred once more to obtain duplicate sediment-free enrichment cultures (PCE.NS.Tr2.A/B and PCE.S.Tr2.A/B, Figure 2.1). In addition to dechlorination of the aliphatic organohalide PCE, the potential to dehalogenate aromatic organohalides was also investigated. To this end, 2,6-DBP and 2,6-DCP were selected as representative electron acceptors and injected into fresh cultures separately, to which microbes

were transferred from sediment-free PCE dechlorinating enrichments (PCE.NS.Tr2.A and PCE.S.Tr2.A). In order to obtain a comprehensive overview of PCE dechlorination and 2,6-DBP debromination potential under both sulfate-free and sulfate-amended conditions, the test cultures (PCE and DBP) were further transferred to duplicate cultures (NS.PCE.A/B, NS.DBP.A/B, S.PCE.A/B and S.DBP.C/D). Due to the lack of debromination from 2,6-DBP under sulfate-amended conditions (S.DBP.C/D), a new set of duplicate cultures (S.DBP.A/B) was inoculated from the PCE culture (Figure 2.1). During the 5th part of the experiment “Dechlorination and Debromination”, duplicates of dechlorinating cultures were spiked five times with PCE (250 μM) and in the same way, debrominating cultures were also spiked five times with 2,6-DBP (100 μM). For the duplicate 2,6-DBP debrominating cultures, additional lactate (5 mM) and lactate/sulfate (5 mM) were also injected into the cultures from the second spike, based on the assumption that debromination was halted due to depletion of lactate. Before each spike, hydrogen and methane were measured in headspace samples, and 2 ml culture was sampled and centrifuged for 5 min at 8000 g. Supernatants were used for metabolite measurements, whereas pellets were used for DNA extraction.

Chemical analyses

Gas chromatography combined with mass spectrometry (GC-MS) was used to measure PCE, TCE and cDCE using an Rt$^{®}$-Q-BOND column (Retek, PA, USA) and a DSQ MS (Thermo Fisher Scientific). Helium served as carrier gas with a flow rate of 2 ml/min. The split ratio was 30 and the inlet temperature was 100 °C. The temperature program included 40 °C holding for 1 min, followed by an increase by 40 °C/min to 260 °C and a final hold at this temperature for 1.5 min. Hydrogen and methane were detected by a Compact GC (Global Analyzer Solutions, Breda, The Netherlands) with a pulsed discharge ionization detector (GC-PDD). Halogenated phenols, benzenes, benzene and phenol were measured using a Thermo Scientific Accela High-performance liquid chromatography (HPLC) system equipped with an Agilent Poroshell 120

EC-C18 column and a UV/Vis detector (set at 210 nM for aromatic halogenated compounds). Short chain fatty acids were measured using a SHIMADZU LC2030 PLUS coupled with a Shodex SUGAR Series® SH1821 column. Sulfate was analysed by using a Thermo Scientific Dionex™ ICS-2100 Ion Chromatography System (Dionex ICS-2100). Sulfide was measured by a photometric method using methylene blue as described previously (Cline 1969).

Genomic DNA isolation and quantitative PCR (qPCR)

Genomic DNA was isolated from pelleted biomass using the DNeasy PowerSoil Kit (QIAGEN, Hilden, Germany) following manufacturer's instructions. qPCR was used to quantify the copy number of 16S rRNA genes with primers targeting total bacteria (Muyzer, et al. 1993), and well-characterized OHRB, including *Dehalococcoides* (Smits, et al. 2004), *Dehalogenimonas* (Chen, et al. 2013), *Dehalobacter* (Smits, et al. 2004), *Desulfitobacterium* (Smits, et al. 2004), *Geobacter* (Amos, et al. 2007) and *Sulfurospirillum* (Sutton, et al. 2015). Furthermore, primers targeting well-characterized functional RDase genes *tceA*, *vcrA*, and *bvcA* were used as listed in Table S2.1. All reactions were performed in triplicate using a C1000 Thermal Cycler (CFX384 Real-Time system, Bio-Rad Laboratories, Hercules, CA, USA) with iQTM SYBR Green Supermix (Bio-Rad Laboratories, Hercules, CA, USA) as outlined previously (Peng, et al. 2019).

Analysis of microbial composition based on 16S rRNA gene amplicon sequences

Barcoded amplicons of 16S rRNA genes were amplified targeting the V4 region of prokaryotic 16S rRNA genes. The forward primer 515F (5'- GTGCCAGC[AC]GCCGCGGTAA-3') and reverse primer 806R (5'-GGACTAC[ACT][ACG]GGGT[AT]TCTAAT-3') (Caporaso, et al. 2011, Walters, et al. 2016) were amended at the 5'-end with sample-specific barcodes. The PCR mixture (50 μL) was prepared containing 20 μL 5 × HF Green buffer (Thermo Fisher Scientific, the Netherlands), 1 μl (2 U) of Phusion hot start II High-Fidelity DNA polymerase (Thermo

Fisher Scientific), primer mix (500 nM for each forward and reverse primer), and 500 nM dNTP (Promega, USA), 10 ng DNA template and nuclease-free water (Promega, USA). The PCR conditions were: 98 °C, 30 s for pre-denaturation, followed by 25 cycles of 98 °C, 10 s for denaturation, annealing at 50 °C for 10 s, elongation at 72 °C for 10 s, and a final extension at 72 °C for 7 min. Three μL of PCR product was analysed by electrophoresis on a 1 % (w/v) agarose gel. All samples were amplified in duplicate reactions, and duplicate PCR products were pooled and purified using CleanPCR (cleanNA, the Netherlands) according to the manufacturer's instructions. The DNA concentration of the purified amplicons was measured by Qubit (Thermo Fisher Scientific). The purified amplicons were pooled in equimolar amounts, including PCR products prepared from synthetic Mock communities of known composition as positive control and nuclease-free water as negative control, and sent for sequencing by Hiseq2000 (GATC-Biotech GmbH, now part of Eurofins Genomics Germany GmbH, Konstanz, Germany).

Analysis of microbial community diversity

The raw sequence data was analyzed by NG-Tax 2.0 (Poncheewin, et al. 2019, Ramiro-Garcia, et al. 2016), which consists of three core processes: barcode-primer filtering, amplicon sequencing variants (ASV) picking and taxonomic assignment. Only the reads completely pairing with primers and barcodes were retained. A threshold of 0.1 % relative abundance was used on a per-sample basis to prevent the inclusion of spurious ASVs produced by sequencing and PCR errors. Taxonomic assignment was done based on Silva 132 SSU Ref (Edgar 2010, Yilmaz, et al. 2014). The generated BIOM (Biological Observation Matrix) and tree files were further organized to form phyloseq objects (McMurdie and Holmes 2013). Downstream analyses, including alpha and beta diversity, and microbial composition were performed by Microbiome and Phyloseq R packages (Lahti and Shetty 2017, McMurdie and Holmes 2013).

Statistical analysis

Statistical analyses and graphics were performed in R (Team 2013) and the built-in libraries ggplot2, tidyverse, ggpubr and vegan. For microbial diversity analysis, alpha diversity was analysed using Phylogenetic diversity, Observed, Chao1, Shannon and Inverse Simpson indices. Student's t-test was used to assess significance of observed differences in alpha diversity indices. The function adonis as implemented in vegan (Oksanen, et al. 2007) was used for permutational multivariate analysis of variance (PERMANOVA) to assess significance of observed differences in beta diversity based on UniFrac distances (Lozupone and Knight 2005, Lozupone, et al. 2011), in which the number of permutations was set to 999 by default. In addition, permutation tests for significance in CAPSCALE were also applied following the default settings.

Results

Reductive dechlorination of PCE in Aarhus Bay sediments

Samples from a sediment core taken in Aarhus Bay and depth-fractionated were incubated in mineral marine medium with a range of organohalides separately in the presence (S) and absence (NS) of sulfate (Table 2.1). Our results revealed the dehalogenating potential of Aarhus Bay sediments for various chlorinated, brominated and iodinated compounds. The microbial composition of PCE dechlorinating cultures exhibited evident differences to cultures to which other organohalides had been added (Figure S2.1). Considering the discovery of *tceA*-like transcripts in sediments of Aarhus Bay (Zinke, et al. 2017), PCE dechlorination was initially selected for subsequent experiments to demonstrate OHR in Aarhus Bay sediments, followed up by experiments with 2,6-DBP.

Dechlorination of PCE to cDCE was observed with TCE as intermediate, within 15 days after inoculation with sediment obtained from Aarhus Bay (Figure 2.2A). After two transfers and two consecutive serial dilution series, the obtained enrichments still actively dechlorinated PCE to cDCE (Figure 2.2B). Thereinto, the most diluted dechlorinating cultures (the fourth cultures in the second serial dilution (NS/S.SD24)) were selected for two additional transfers aiming to enrich the responsible dechlorinating consortium. In the second transfer, cultures incubated in the presence (S) or absence (NS) of sulfate stably dechlorinated PCE to cDCE after three spikes of PCE (Figure 2.2C). The overall experimental workflow is shown in Figure 2.1, and results of transfers and serial dilutions are provided in Figure S2.2 and Figure S2.3, respectively.

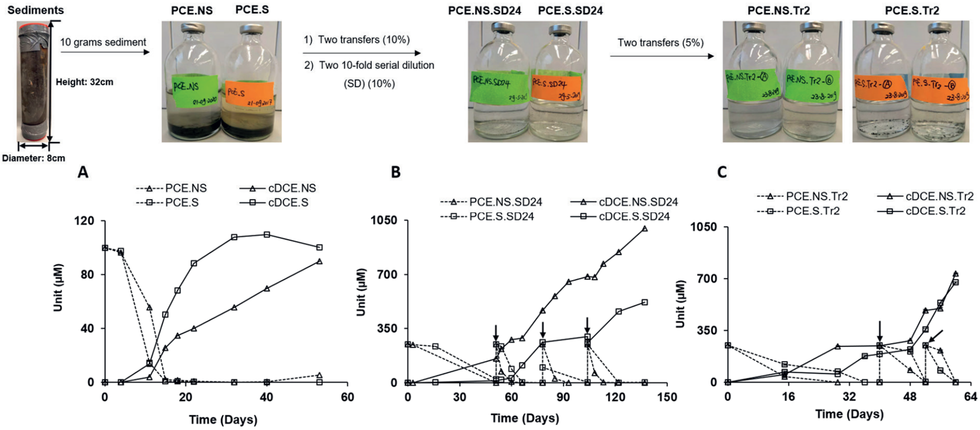

Figure 2.2 PCE dechlorination to cDCE in initial microcosms (A), serial dilutions (B) and further transfers (C) in the presence (S) and absence (NS) of sulfate. SD.24:the fourth (i.e. 10-4 dilution) cultures in the second serial dilution in step 3 (Figure 2.1); Tr2: the second transfers in Step 4 (Figure 2.1). See also Figure 2.1 for a detailed scheme of the experimental set-up and history and relatedness of the different cultures. Vertical arrows indicate spikes of PCE. Data shown are average values, and error bars represent the standard deviation of the duplicates in Tr2. Error bars are not always visible due to small standard deviations.

Detection of known and putative OHRB by quantitative PCR (qPCR) and 16S rRNA gene amplicon sequencing

qPCR analyses revealed the existence of well-known OHRB in the original sample, including Dhc, Dhb, Dsb, Geo and Sul ranging from 1.2 (0.8 SD) × 10^3 of Dhb to 1.5 (0.1 SD) × 10^6 of Geo per gram (Figure 2.3A), which accounted for less than 1 % of the total 16S rRNA gene copy numbers (9.2 (1.6 SD) × 10^8). Based on 16S rRNA gene amplicon sequence data, relative abundances of these OHRB together were less than 2 %, in line with the qPCR results. The 16S rRNA gene copy numbers and relative abundances of these well-characterized OHRB decreased during the enrichment procedure. In particular, Dsb was undetectable after the first serial dilution (Figure 2.3A). For all samples, including original sediment fractions and derived cultures, the 16S rRNA gene of *Dehalogenimonas* (Dhg) and well-characterized RDase genes *vcrA*, *bvcA* and *tceA* were below the detection limit. Apparently, the known OHRB were outcompeteted by other indigenous dehalogenators during PCE dechlorination. In contrast, the microbial community analysis indicated that certain bacteria, including *Halodesulfovibrio* in sulfate-free cultures, and *Desulfovibrio* in sulfate-amended cultures were enriched up to relative abundances of 16.0 (2.3 SD) % and 30.3 (1.7 SD) %, respectively, in Tr2.A/B cultures (Figure 2.3B). Representative strains of both genera were recently shown to debrominate 2,6-DBP to phenol (Liu and Haggblom 2018). We therefore hypothesized that our enrichments might also possess the ability to debrominate 2,6-DBP to phenol, in line with results of the initial screening (Table 2.1).

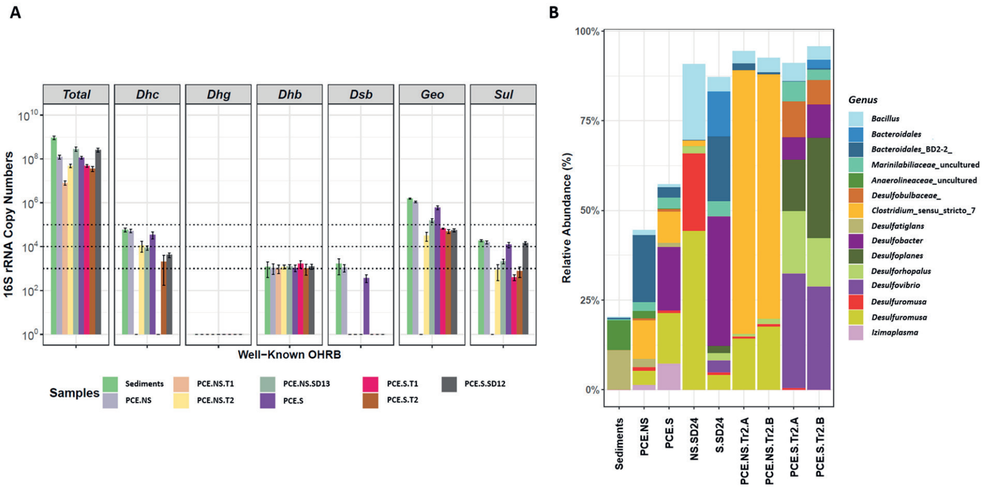

Figure 2.3 Microbial community analysis of PCE-dechlorinating cultures by qPCR (A) and 16S rRNA gene amplicon sequence data at genus level (B). 16S rRNA gene copy numbers per millilitre of the cultures except for the marine sediments (Sediments) that are defined per gram of wet sediment. Total: total bacterial 16S rRNA gene copy numbers; Dhc: *Dehalococcoides*; Dhg: *Dehalogenimonas*; Dhb: *Dehalobacter*; Dsb: *Desulfitobacterium*; Geo: *Geobacter*; Sul: *Sulfurospirillum*. Values and error bars represent the averages and standard deviations of the triplicate qPCRs, respectively. Values below the detection limit are shown as one copy per ml. The added horizontal dotted lines represent 10^3, 10^4 and 10^5 copy numbers, respectively. Only taxa that have a relative abundance > 5 % in at least one of the samples are shown. Duplicate enrichments are indicated by suffixes ‘A’ and ‘B’. T1 and T2: the first and second transfers in step 2 (Figure 2.1); SD12 and SD13: the second (10^{-2}) and third (10^{-3}) dilution cultures in the presence and absence of sulfate, respectively, in the first serial dilution in step 3 (Figure 2.1). See also Figure S2.2.

Switching the electron acceptor from PCE to 2,6-DBP

As mentioned above, debromination of 2,6-DBP was observed in the initial screening of the dehalogenation potential of Aarhus Bay sediment. Moreover, members of enriched genera were previously reported to have debromination potential as outlined above. Thus, we tested whether the PCE dechlorinating enrichments retained the capacity of the original sediment for reductive debromination. Indeed, PCE-dechlorinating enrichments debrominated 2,6-DBP under both sulfate-free and sulfate-amended conditions. In contrast, the cultures failed to dechlorinate 2,6-DCP (Figure 2.1), which was in agreement with the initial screening (Table 2.1). More detailed analyses of duplicate cultures revealed that 2,6-DBP was debrominated to phenol with bromophenol as intermediate (Figure 2.4A). Five spikes of 100 µM 2,6-DBP each were introduced into the cultures. In parallel incubations, PCE dechlorination to cDCE was shown to be maintained as well (Figure 2.4C).

Hydrogen was produced and accumulated up to 29.53 µM after 10 days in sulfate-free cultures after the first spike of 2,6-DBP (Figure 2.4B). Then hydrogen was consumed alongside debromination, while methane accumulated after five spikes of 2,6-DBP up to 1.3 mM. In contrast, hydrogen and methane were not detected under sulfate-amended conditions (Figure 2.4B). Lactate was utilized with the formation of propionate and acetate at an approximate ratio of 3:2.5 in sulfate-free cultures (Figure S2.4A), whereas only acetate was produced and further utilized in sulfate-amended cultures (Figure S2.4B). Similarly, hydrogen and methane were obviously produced in sulfate-free PCE-dechlorinating environments after the first 250 µM PCE spike, with particularly rapid hydrogen formation up to 245.13 µM (Figure 2.4D). Notably, hydrogen and methane were produced in sulfate-amended cultures up to a detectable level after the third PCE spike, but only at concentrations below 30 µM. Lactate degradation followed a similar trend in PCE dechlorinating cultures as in the 2,6-DBP incubations (Figure S2.4C&D). In all cultures where sulfate was added, this was reduced to sulfide.

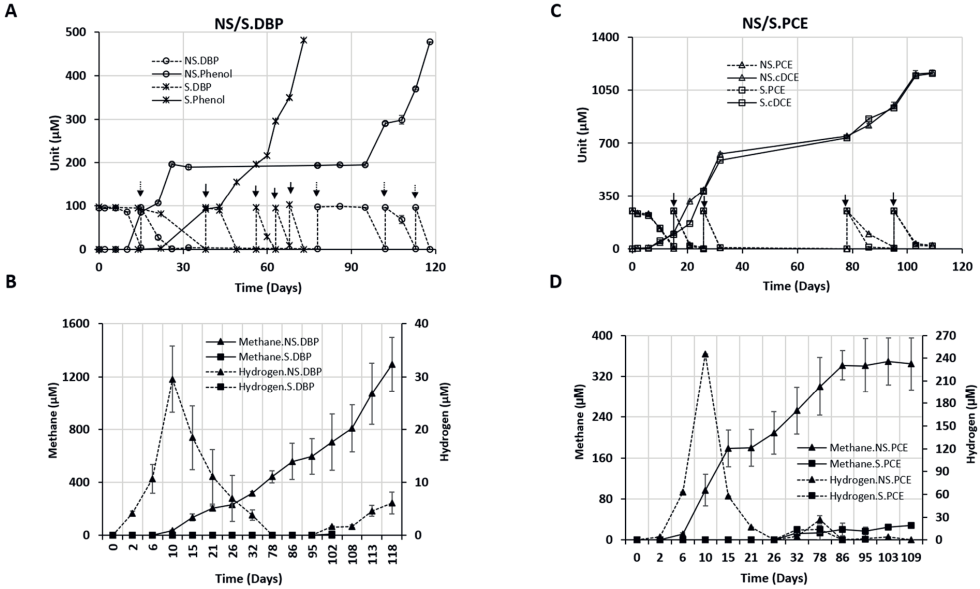

Figure 2.4 Reductive debromination of 2,6-DBP in addition to PCE dechlorination. In parallel cultures, 2,6-DBP and PCE are dehalogenated into phenol (A) and cDCE (C), respectively. Methane and hydrogen (B, D) are measured throughout the experiment in the presence or absence of sulfate. Values and error bars shown in the figure are averages and standard deviation of duplicate cultures. Arrows indicate the spikes of PCE (black) and 2,6-DBP (grey-dotted arrows for sulfate-free cultures, black for sulfate-amended cultures).

Microbial diversity and phylum-level composition of dehalogenating enrichments

To assess the microbial community structure in the different cultures, and particularly to compare PCE- and 2,6-DBP dehalogenating cultures, 16S rRNA gene amplicon sequencing was employed. ASV-based alpha diversity (Shannon index and phylogenetic distances) decreased significantly ($p < 0.01$) in 2,6-DBP debrominating cultures compared to the PCE dechlorinating cultures under the corresponding sulfate-free or sulfate-amended conditions (Figure 2.5A & B). Beta diversity analysis using weighted Unifrac (W-Unifrac) distances revealed that the microbial community structure was clearly reshaped by changing the electron acceptor from PCE to 2,6-DBP, especially in the absence of sulfate (Figure 2.5C). Further NMDS analysis was in agreement with W-Unifrac based ordination and displayed differences of microbial composition during debromination and dechlorination under sulfate-free or sulfate-amended conditions (Figure 2.5D). Among all, sulfate-free debrominating cultures (NS.DBP) showed the biggest distance from the other three types, and the sulfate-amended cultures showed higher similarity regardless of the added organohalide (Figure 2.5C & D). Further microbial composition analysis (Figure 2.5E) showed that *Proteobacteria* was the predominant phylum accounting for 83 (6.6 SD) % and 93 (2.6 SD) % in sulfate-amended dechlorinating (S.PCE) and debrominating (S.DBP) cultures, respectively. *Firmicutes* and *Proteobacteria* were the main phyla in sulfate-free dechlorinating cultures (NS.PCE) accounting for 52 (16 SD) % and 23 (14 SD) %, respectively, whereas *Bacteroidetes* was predominant in sulfate-free debrominating cultures with 83 (5.1 SD) %.

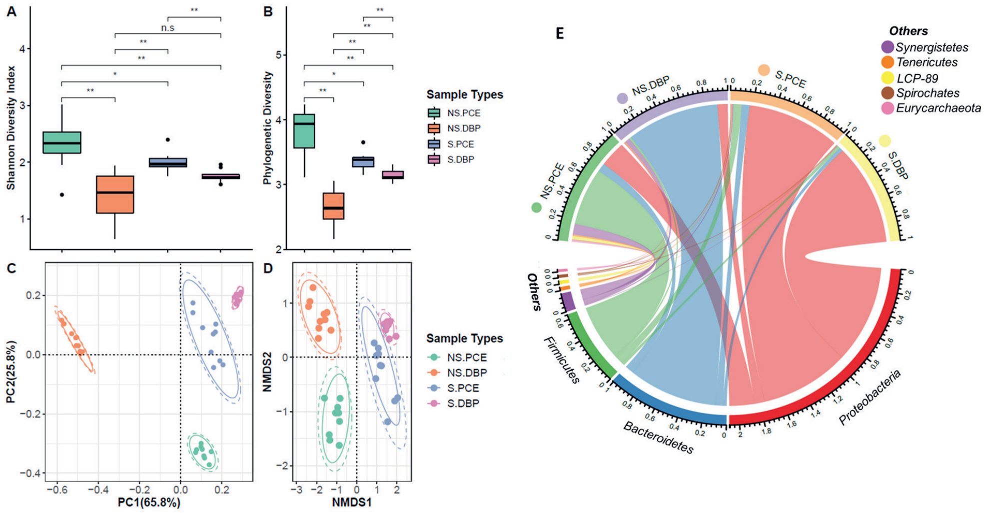

Figure 2.5 Analysis of microbial diversity. Alpha diversity analysis as based on Shannon index (A) and phylogenetic diversity (B); beta diversity analysis including PCoA analysis of Weighted UniFrac distances (C), and non-metric multidimensional scaling (NMDS) analysis of Bray–Curtis dissimilarity (D) with a stress value of 0.08. The average relative abundances at phylum level were calculated for the chord plot corresponding to the four sample types (E). Duplicate cultures were included for each sample type, i.e. sulfate-free PCE dechlorination (NS.PCE, n=9: 5 times sampling, duplicates, 1 failed (B1) as the purified amplicon in low quality), sulfate-free debromination (NS.DBP, n=10: 5 times sampling, duplicates), sulfate-

amended PCE dechlorination (S.PCE, n=10: 5 times sampling, duplicates) and sulfate-amended debromination (S.DBP, n=10: 5 times sampling, duplicates). Ellipses in C and D indicate the samples followed normal (dashed line) and t distribution (solid line) at a confidence level of 0.95. n.s: not significant, $p\text{-value} > 0.05$; "*": $0.01 < p\text{-value} < 0.05$; "**": $p\text{-value} < 0.01$. PC1 and PC2 (C) are the first two principal components, with percentage of variation explained in parentheses.

Microbial community dynamics at genus and ASVs levels

To elaborate in more detail on the microbial community changes associated with the enrichment of dechlorinating and debrominating cultures, comparisons were done at genus- and ASV level (Figure 2.6 & 7). Most notably, we observed the predominance of an unknown genus from Bacteroidetes_BD2_2 in sulfate-free debrominating cultures (NS.DBP) accounting for 83 (5.2 SD) % in relative abundance (Figure 2.6), which included 11 ASVs (Figure 2.7A). Among these, ASV_1808309 accounted for > 50 % of all reads in this genus (Figure 2.7B). This was followed by *Halodesulfovibrio* enriched as the second-most predominant genus up to 6.9 (1.4 SD) %. In contrast, *Bacillus* was the predominant genus with a relative abundance of 31 (18 SD) % in sulfate-free dechlorinating cultures (NS.PCE), with ASV_18083010 and ASV_1808307 accounting for higher proportions than the other three ASVs (Figure 2.7B), and *Halodesulfovibrio* accounted for a relative abundance of 3.7 (1.4 SD) % (Figure 2.6). Notably, *Clostridium_sensu_stricto*_7 decreased in relative abundance from 70.9 to 1.3 % after the 5th addition of PCE in dechlorinating cultures in the absence of sulfate (Figure 2.6), which was mainly caused by the decrease of ASV_1808300 (Figure 2.7B). *Desulforhopalus* increased in relative abundance after the 4th spike and up to 3.9 % after the 5th spike in debrominating cultures (NS.DBP), and was stably maintained in dechlorinating cultures (NS.PCE) at 4.1 (1.8 SD) % without sulfate addition. Similarly, *Desulfuromusa* showed an increasing trend in sulfate-free PCE dechlorinating cultures (NS.PCE) reaching up to 7.8 (2.1 SD) % after 5th spike. Unlike the trend under sulfate-free conditions, *Desulfoplanes* became the major genus and was enriched up to 51 (5.8 SD) % after the 5th PCE spike (S.PCE) in the presence of sulfate. Similarly, in debrominating cultures, *Desulfoplanes* was observed at a stable and high relative abundance of 38 (5.4 SD) % (S.DBP). In addition, *Desulfobacter* and *Bacillus* increased in sulfate-amended dechlorinating cultures (S.PCE) reaching up to 17.8 % and 10.7 % respectively. *Desulfovibrio* accounted for 40 (4.1 SD) % in sulfate-amended debrominating cultures (S.DBP), whereas it represented only a small proportion in sulfate-amended dechlorinating cultures (S.PCE) at 1.1 (0.28 SD) % (Figure 2.6), which was the result of a lower relative abundance of ASV_180830167 (Figure 2.7B). Overall, several *Desulfobacterota* taxa, including *Desulfobacter*, *Desulfobacterium*, *Desulfoplanes* and *Desulfovibrio* were only present in sulfate-amended cultures, whereas *Desulfomicrobium*, *Halodesulfovibrio* and *Methanogenium* were only presented under sulfate-free conditions.

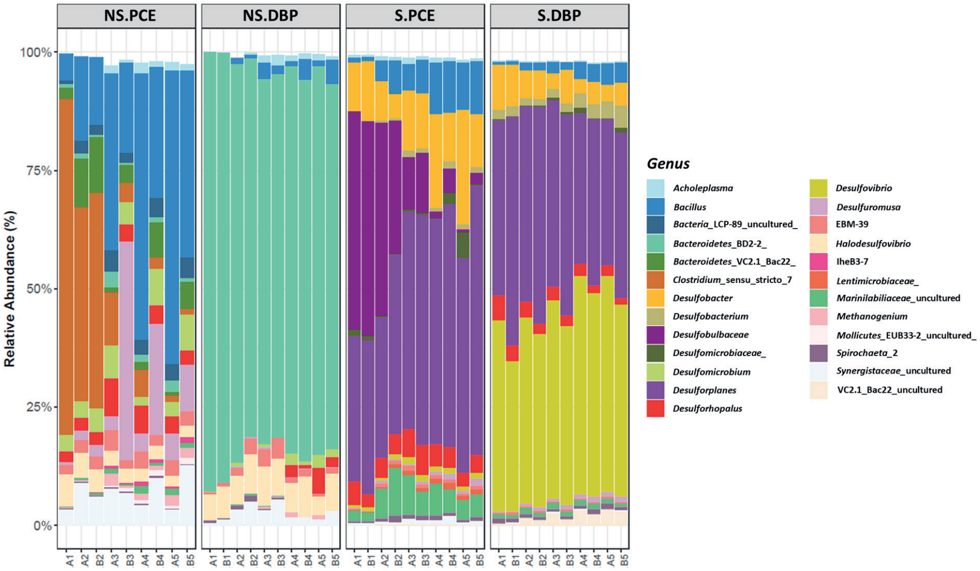

Figure 2.6 Dynamics of microbial community composition during reductive dehalogenation under sulfate-free (NS) and sulfate-amended (S) conditions. Relative abundance of microbial taxa is shown at genus level with a cut-off at 1 % in at least one single sample. Samples are numbered from A1 to A5 and B1 to B5, indicating samples collected after each complete dehalogenation, prior to the spike of PCE or 2,6-DBP, respectively. B1 sampled from the

sulfate-free PCE dechlorinating cultures (NS.PCE) was absent due to the low quality of the PCR product that did not meet the sequencing requirements.

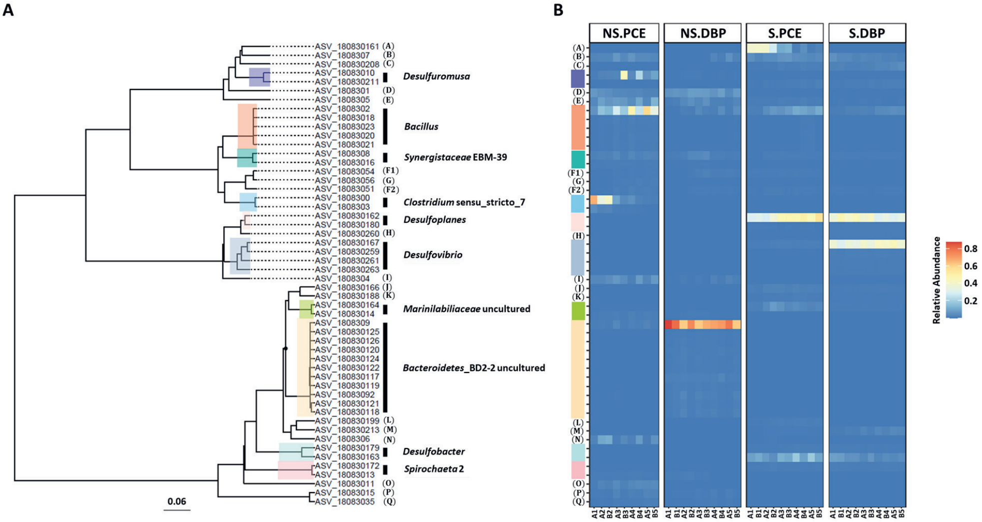

Figure 2.7 Phylogenetic analysis (A) and dynamics of microbial composition (B) at ASVs level. The cut-off relative abundance of ASVs is set at 0.1 % in at least one single sample. ASVs belonging to the same genus are indicated by the same colour (top 10 genera) or letters. Alphabetic letters in Figure 2.6A: A, *Desulfobulbaceae*_; B, *Desulforhopalus*; C, *Desulfobacterium*; D, *Halodesulfovibrio*; E, *Synergistaceae*_uncultured; F, *Acholeplasma*; G, *Mollicutes*_EUB33-2_uncultured_; H, *Desulfovibrionales*_; I, *Desulfomicrobium*; J, *Marinilabiliaceae*_; K, *Bacteroidetes*_vadinHA17_; L, *Lentimicrobiaceae*_; M, VC2.1_Bac22_uncultured_; N, VC2.1_Bac22_; O, Bacteria_LCP-89_; P, *Methanogenium*; Q, *Methanomicrobiaceae*_;

Discussion

Putative RDase genes are being increasingly reported from metagenomic analyses of marine sediments. Considering the global distribution of organohalides in marine environments and their excellent potential as electron acceptors for anaerobic respiration, it is tempting to assume that OHR is occurring in Aarhus Bay sediments contributing to recycling halides, carbon and other nutrients. However, experimental verification of OHR potential in these sediments usually has not been achieved. Recent metagenomic and single-cell genomic analysis revealed presence of putative RDase genes in Aarhus Bay sediments, indicating the possibility for alternative energy conservation through reductive dehalogenation in addition to sulfate reduction at the near-surface sulfate-rich zone (Jochum, et al. 2017, Jochum, et al. 2018). On this basis, we were inspired to investigate OHR potential and the eco-physiology of associated microbial communities.

Reductive dehalogenation of various organohalides by Aarhus Bay marine sediments

Similar to former studies of reductive dehalogenation in marine environments (Ahn, et al. 2003, Futagami, et al. 2009, Futagami, et al. 2013, Kaster, et al. 2014, Matturro, et al. 2016), we could show that pristine marine sediments from Aarhus Bay could reductively dehalogenate a range of organohalides, including PCE, 2,6-DBP, 1,4-DBB, 3-BP and 2,4,6-TIP (Table 2.1), suggesting the presence of multiple reductive dehalogenating microorganisms and corresponding RDase genes. *Firmicutes* were enriched in all dehalogenating cultures (Figure S2.1), with members of the *Clostridiales* being most predominant. These populations may serve as syntrophic partner to dehalogenating populations, for example as hydrogen producer as has been shown previously (Lin, et al. 2020, Merlino, et al. 2015, Yang, et al. 2019). Intriguingly, *Lokiarchaeia* belonging to Asgard archaea (Spang, et al. 2017, Zaremba-Niedzwiedzka, et al. 2017), a recently described group of archaea linked to the origin of eukaryotes (Eme, et al. 2017), were observed in the original sediment and enriched only in 2,4,6-TIP deiodinating cultures regardless of sulfate addition. To this end, it seems promising to employ reductive deiodination to enrich or even isolate strains from *Lokiarchaeota*, previously shown to bear putative RDase genes (Spang, et al. 2019). In addition, *Anaerolineae*, belonging to *Chloroflexota*, were sharply decreased in PCE dehalogenating cultures compared to incubations with other organohalides. Recently, metagenome assembled genomes (MAGs) revealed that *Anaerolineae* have the potential of reductive dehalogenation (Fincker, et al. 2020), however, this has not been experimentally confirmed to date. Finally, members of the *Bacteroidetes* were enriched only in PCE dechlorinating cultures. Considering that to date there are no representative OHRB identified from this phylum, results presented here provide new leads for the isolation and characterization of yet unknown organohalide respiring prokaryotes.

Microbial composition of PCE dechlorination enrichments

Populations of well-characterized OHRB including Dhc, Dhb, Dsb, Geo and Sul (Adrian and Loeffler 2016, Atashgahi, et al. 2016, Atashgahi, et al. 2013, Azizian, et al. 2010a, Fincker and Spormann 2017) were found in the marine sediment studied here, but only at a low abundance below 10^6 16S rRNA gene copies/gram sediment. These microbes further decreased in abundance during transfers and serial dilutions indicating they are unlikely responsible for the PCE dechlorination under the conditions used in this study. We also did not detect known genes encoding the enzymes responsible for reductive dehalogenation of PCE and its metabolites, i.e. *vcrA*-, *bvcA*-, and *tceA* genes (Chen, et al. 2014, Smits, et al. 2004), suggesting the presence of other, variant sequences of RDase genes as previously indicated in subseafloor sediments (Futagami, et al. 2013). The lack of dechlorination beyond cDCE suggests that enzymes required for cDCE and VC dehalogenation were not enriched under the conditions used here as previously observed for other environments (Krajmalnik-Brown, et al. 2004, Scheutz, et al. 2008). This is a common finding indicating likely evolution of VC-respiring *Dehalococcoidia* members due to anthropogenic contaminations in terrestrial environments (McMurdie, et al. 2009). Microbial community analysis revealed that the original Aarhus Bay sediment sample contained two predominant genera with relative abundances over 5 % (Figure 2.3B), including an uncultured genus in the *Anaerolineaceae* belonging to the *Chloroflexota*, and the *Desulfobacterota* genus *Desulfatiglans*. Recent metagenomic data analysis revealed that members of the class *Anaerolineae* encoded putative RDase genes in their genomes, suggesting they might have the potential of reductive dehalogenation (Fincker, et al. 2020). Furthermore, single-cell genomics has shown that *Desulfatiglans*-associated microorganisms contain putative RDase genes in their genomes (Jochum, et al. 2018). However, in contrast to canonical RDases, the encoded putative RDase proteins contain transmembrane domains at the N-terminus but lacked a TAT signal peptide. Also, no accompanying RDase B gene was observed that normally encodes the membrane anchor for the catalytic subunit of RDases (Jochum, et al. 2018). These putative RDases termed as hybrid RDases have not been shown to be functional (Atashgahi 2019). Intriguingly, the relative abundance of *Anaerolineaceae* and *Desulfatiglans* decreased to less than 1 % in our highly enriched cultures regardless of the presence of sulfate suggesting they might not be responsible for the observed dehalogenation. In contrast, *Clostridium_sensu_stricto*_7 belonging to the *Firmicutes*, and the *Desulfobacterota* genus *Halodesulfovibrio* were enriched in sulfate-free cultures, whereas other members of the *Desulfobacterota* including *Desulfovibrio*, *Desulforhopalus*, *Desulfoplanes* and an unknown genus in the *Desulfobulbaceae* became the predominant genera in sulfate-amended cultures (Figure 2.3B & Figure S2.3B). To our knowledge, *Clostridium* members have not been shown to mediate OHR and have been proposed to function as the hydrogen producers facilitating reductive dehalogenation (Lin, et al. 2020, Lo, et al. 2020, Yang, et al. 2019). In contrast, *Desulfobacterota* representatives, including *Halodesulfovibrio marinisediminis* and *Desulfovibrio bizertensis*, have been shown to debrominate 2,4,6-tribromophenol and 2,6-DBP into 4-bromophenol (4-BP) and phenol, respectively (Liu and Haggblom 2018). Furthermore, the genome of *Desulforhopalus singaporensis* was annotated to contain putative RDase genes (GenBank Accession: GCA_900104445.1), but OHR potential in this bacterium has not been experimentally verified (Lie, et al. 1999). Henceforth, we speculated that the well-identified OHRB might be outweighed by other potential dehalogenating microbes in our laboratory microcosms.

Switching organohalides from PCE to 2,6-DBP

The sediments of Aarhus Bay were previously reported to have a high Br/Cl ion ratio, and a variety of brominated organic compounds have been identified, implying the potential for debromination may exist in the seafloor sediments (Christensen and Platz 2001, Jorgensen, et al. 2020, Zinke, et al. 2017). In addition, our initial assessment of dehalogenation capacity corroborated debrominating potential of Aarhus Bay sediments. Further, the genera enriched in PCE-dechlorinating cultures (Figure 2.2), like *Desulfovibrio*, have previously been reported to include strains that were characterized to debrominate 2,4,6-TBP and 2,6-DBP (Liu and Haggblom 2018). Interestingly, a recent study revealed the possibility of dechlorinating cultures to catalyze debromination (Xu, et al. 2022). Indeed, our results are in agreement, as PCE-dechlorinating cultures showed the potential for 2,6-DBP debromination to phenol, whereas 2,6-DCP was not dechlorinated (Figure 2.1). Similarly, Peng et al found marine *Desulfoluna* strains were capable of reductive debromination but not reductive dechlorination (Peng, et al. 2020a). This may indicate niche specialization of marine OHRB for reductive debromination that could gain more energy to support bacterial growth than that of reductive dechlorination (Xu, et al. 2022). The formation and consumption of hydrogen was observed in sulfate-free cultures (Figure 2.4), indicating that hydrogen likely served as the intermediate electron donor for OHR and methanogenesis (Azizian, et al. 2010a, Dolfing and Tiedje 1987) that occurred simultaneously as formerly reported (Aulenta, et al. 2002). On the contrary, methane was not generated in sulfate-amended cultures at first that might be due to the fact that sulfate-reducing bacteria outcompeted methanogens due to higher substrate affinity of sulfate-reducing bacteria to hydrogen than methanogens (Kristjansson and Schönheit 1983, Piché-Choquette and Constant 2019). With the sulfate reduced, methane was detected but at a low concentration below 30 µM (Figure 2.4B&D). Interestingly, reductive dechlorination and debromination were not influenced by the presence of sulfate, which was in line with recent reports of marine OHRB belonging to sulfate-reducing bacteria (SRB) (Liu, et al. 2020, Liu and Haggblom 2018, Peng, et al. 2020a). It is likely that the marine OHRB have developed strategies for concurrent sulfate and organohalide respiration.

Potential OHRB inferred from microbial community analysis

Our results revealed that microorganisms that were previously discovered by metagenome and single-genome assembly as candidate OHRB, such as *Desulfatiglans* and its relatives (Fincker, et al. 2020, Jochum, et al. 2018), were not enriched in PCE dechlorination cultures, which might due to their inability to dechlorinate PCE under the conditions used for the experiments here (Figure 2.3 and Figure S2.3). Furthermore, some of the functionally characterized OHRB, for instance *Dehalococcoides*, that have been observed in Aarhus Bay sediments based on metagenomic analysis (Fincker, et al. 2020), and which strictly depend on hydrogen as electron donor and halogenated compounds as electron acceptor for energy conservation (Maymo-Gatell, et al. 1997), were not enriched in our cultures. Their fastidious and restricted metabolism might have rendered them less competitive, being outcompeted by other, more versatile, OHRB, like RDase-containing sulfate reducers (Peng, et al. 2020a), in the defined mineral marine medium used in this study (Monserrate and Häggblom 1997). Changing the organohalide electron acceptors significantly reshaped the microbial community structure (Figure 2.5 & 2.6), suggesting that different microorganisms might be involved in the dehalogenation of the different chlorinated and brominated compounds tested in our study. Furthermore, the observed decrease in alpha diversity in debrominating cultures suggests that 2,6-DBP or the debrominated phenol might inhibit growth of certain bacteria via the leakage of cellular components, such as K^+ and ATP, or even cell membrane destruction (Cooper, et al. 2015, Escher, et al. 1996, Heipieper, et al. 1991, Stasiuk and Kozubek 2008). Intriguingly, transfers of cultures from the initial screening able to dehalogenate 2,6-DBP were no longer able to debrominate 2,6-DBP. As the microbial community analysis revealed the apparent loss of *Desulfovibrio* in comparison to the transfers from sulfate-amended dechlorinating cultures (Figure 2.1 & S2.5), a likely role of *Desulfovibrio* for reductive debromination can be hypothesized. Interestingly, members of the genus *Bacillus* were strongly enriched in sulfate-free dechlorinating cultures. This genus has to date not been characterized to perform reductive dehalogenation. Interestingly, Lim et al. reported that members of the phylum *Bacteroidetes* were enriched in the presence of natural organohalides (Lim, et al. 2018). Similarly, we observed that members of this phylum were also enriched in sulfate-free debrominating cultures, but OHRB belonging to *Bacteroidetes* remain uncharacterized, providing leads for future attempts to isolate these organisms.

Furthermore, members of several genera recently identified as OHRB were observed, including *Desulfuromusa*, *Halodesulfovibrio* and *Desulfovibrio* (Liu and Haggblom 2018). For each of these genera, several species-level amplicon sequencing variants (ASVs) were observed suggesting that the enriched populations were composed of more than one strain type, such as *Desulfuromusa* with two ASVs (Figure 2.7). To this end, future studies should aim to provide strain-resolved information by meta-omics, such as metagenomics and meta-transcriptomics. Genetic information of new OHRB can be disclosed from genome-resolved binning of metagenome data, providing leads regarding metabolic differences that can guide efforts towards isolation and further characterization of yet unknown dehalogenators.

Conclusions

In conclusion, this work verified the potential for OHR in Aarhus Bay sediments that have previously been shown to be a source of organohalides and putative RDase genes. This is of importance considering the increasing number of studies reporting occurrence of organohalides and putative RDase genes in marine sediments (Fincker, et al. 2020, Jorgensen, et al. 2020, Peng, et al. 2020a, Peng, et al. 2020b). Considering the diversity of organohalides naturally produced in marine environments, OHR should play a key role in recycling halides and organic carbon back to the seawater.

Data availability

The nucleotide sequence data has been deposited in the European Bioinformatics Institute under accession number PRJEB50583.

Acknowledgements

This study was supported by the Dutch Research Council through the UNLOCK project (NRGWI.obrug.2018.005), as well as Wageningen University through its Innovation Program Microbiology. We thank Kasper U. Kjeldsen from Aarhus University for providing sediments from Aarhus Bay for cultivation. We acknowledge the China Scholarship Council (CSC) for the support to Chen Zhang (File No. 201807720048).

Conflict of interest. None declared.

Supplementary information

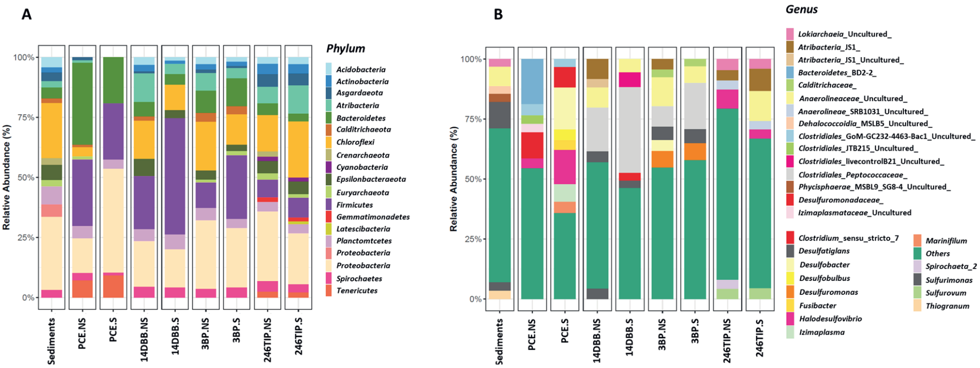

Figure S2.1 Microbial composition of various organohalide-respiring cultures under sulfate-free (NS) and sulfate-amended (S) conditions. Microbial community is analyzed at Phylum (A) and Genus (B) level. The cut-off relative abundance is set at 1 % for phylum and 3 % for genus. “Others” at genus level summarizes all taxa that are below the cut-off threshold (3 %). NS: non-sulfate; S: sulfate-amended; 14DBB: 1,4-dibromobenzene; 3BP: 3-bromophenol; 246TIP: 2,4,6-Triiodophenol.

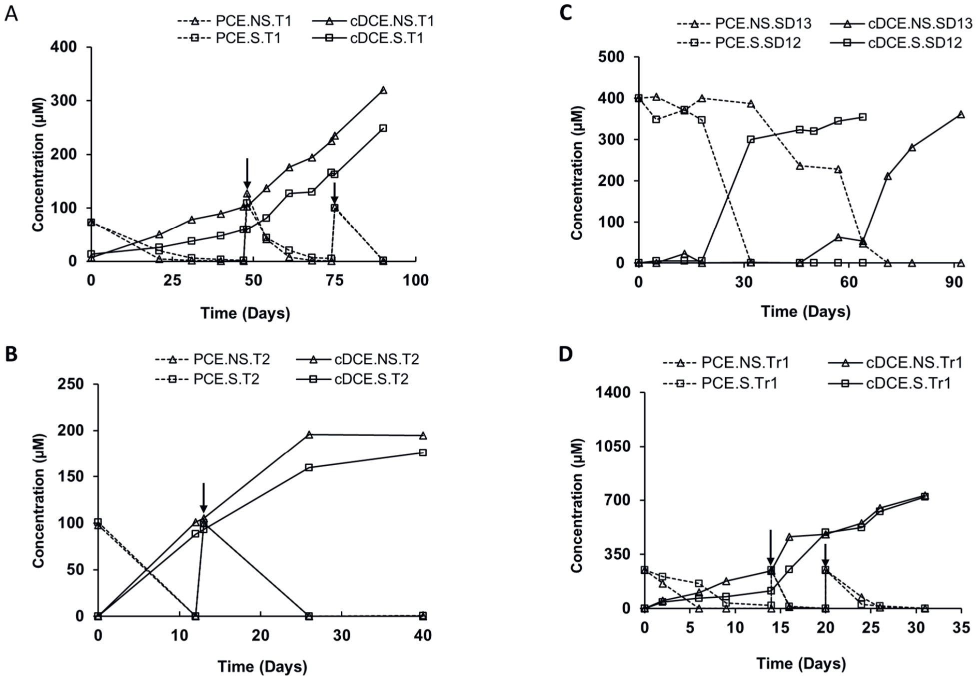

Figure S2.2 PCE dechlorinating cultures of 1st two-time transfers (A: T1 and B: T2), 1st serial dilution (C: SD13 and SD12) and 2nd two-time transfers (D: Tr1). PCE.NS.SD13: the third bottle (10-3) as the highest dilution to maintain PCE dechlorination in the absence of sulfate in the first serial dilution. PCE.S.SD12: second bottle (10-2) as the highest dilution showing PCE dechlorination under sulfate-amended conditions. Tr1: First of the second two-time transfers. The arrows indicate spikes of PCE as well as lactate (NS) or lactate and sulfate (S).

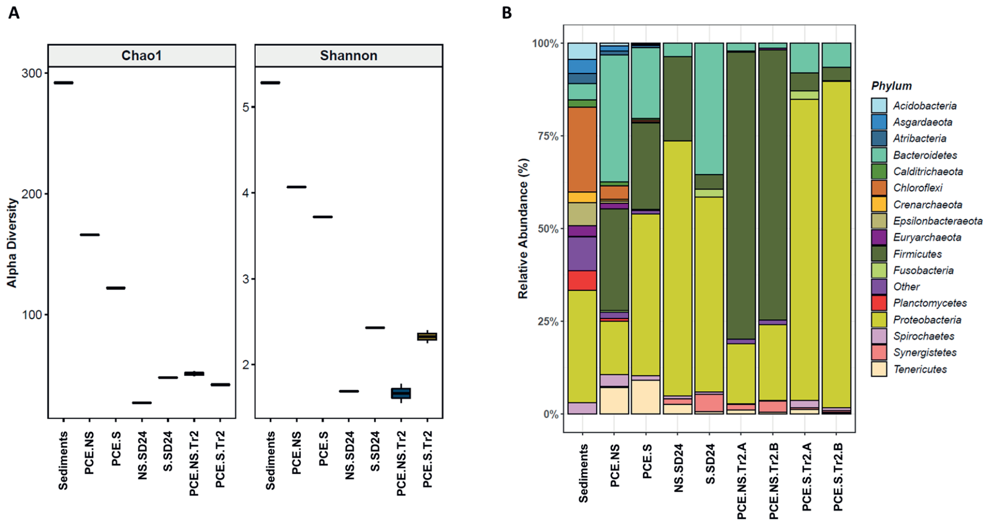

Figure S2.3 Alpha diversity analysis based on Chao1 and Shannon index (A) and microbial composition of PCE dechlorinating cultures at phylum level (B). Top 16 phyla are shown. Remaining phyla are shown as “other”.

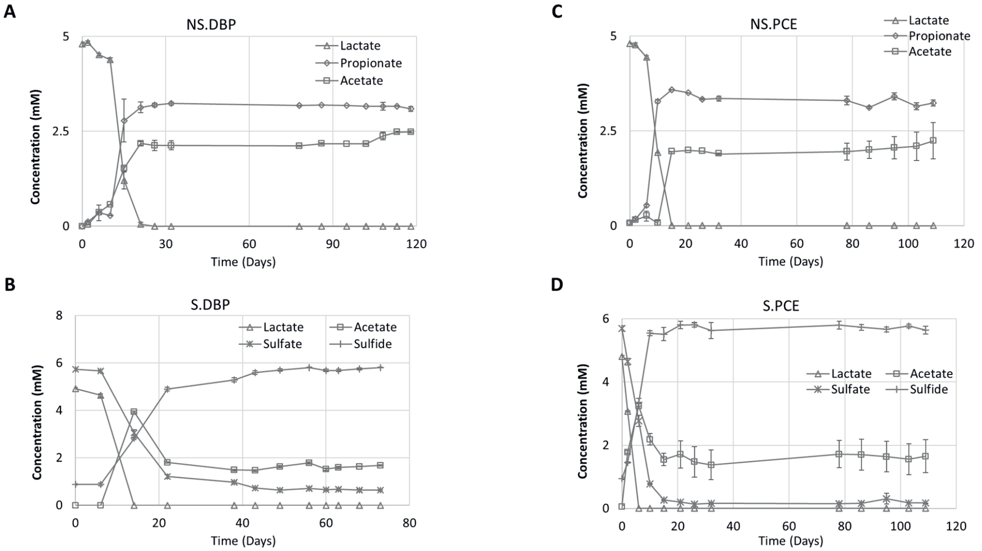

Figure S2.4 Metabolite concentrations in bottles amended with PCE (A,B) and 2,6-DBP (C,D) under sulfate-free (NS) and sulfate-amended (S) conditions. “A” and “B” represent duplicate bottles. Data is shown as average values with standard deviation from duplicate cultures.

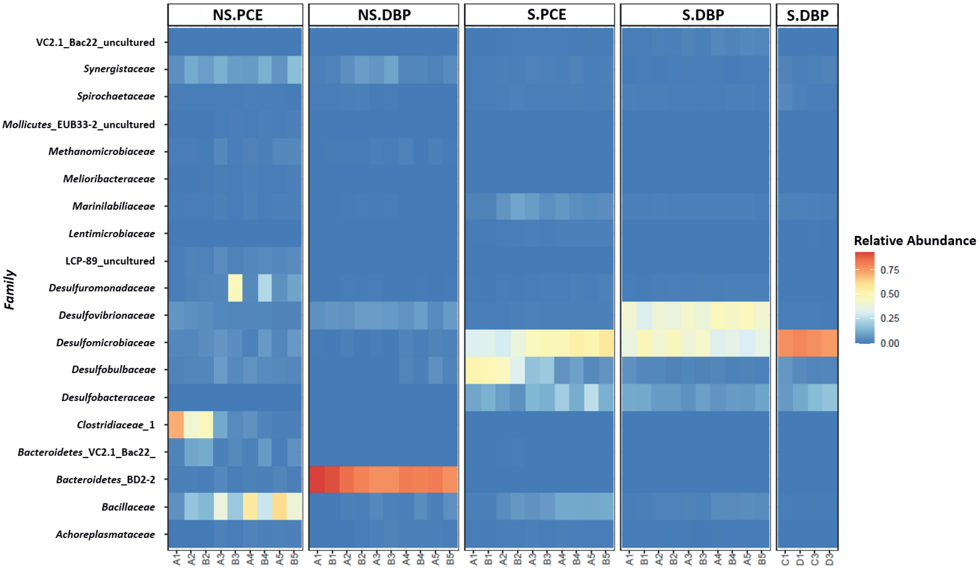

Figure S2.5 Dynamics of microbial composition at family level of four different cultures (NS_PCE, sulfate-free PCE dechlorination; NS_DBP, sulfate-free debromination; S_PCR sulfate-amended PCE dechlorination; S_DBP, sulfate-amended debromination). The cut-off of relative abundance was set at 1%. The duplicate cultures, S.DBP.CD, unable to debrominate 2,6-DBP, were included.

Table S2.1 Primers used in this study. All primers target the 16S rRNA gene, except for *vcrA* and *bvcA* that target reductive dehalogenase genes.

Target	Name	Oligonucleotide sequence (5′–3′)	Reference for primer	Reference for qPCR program
Bacteria	Eub341F	CCTACGGGAGGCAGCAG	(Muyzer, et al. 1993)	(Atashgahi, et al. 2013)
	Eub534R	ATTACCGCGGCTGCTGGC		
Desulfitobacterium	Dsb406F	GTACGACGAAGGCCTTCGGGT	(Smits, et al. 2004)	(Smits, et al. 2004)
	Dsb619R	CCCAGGGTTGAGCCCTAGGT		
Dehalococcoides	Dco728F	AAGGCGGTTTTCTAGGTTGTCAC	(Smits, et al. 2004)	(Atashgahi, et al. 2013)
	Dco944R	CTTCATGCATGTCAAAT		
Dehalobacter	Dre441F	GTTAGGGAAGAACGGCATCTGT	(Smits, et al. 2004)	(Atashgahi, et al. 2013)
	Dre645R	CCTCTCCTGTCCTCAAGCCATA		
Dehalogenimonas	BL-DC-1243F	GGYACAATGGGTTGCCACCGG	(Chen, et al. 2014)	(Chen, et al. 2014)a
	BL-DC-1351R	AACGCGCTATGCTGACACGCGT		
Geobacter	Geo196F	GAATATGCTCCTGATTC	(Amos, et al. 2007)	(Azizian, et al. 2010)
	Geo535R	TAAATCCGAACAACGCTT		
Sulfurospirillum	Sulfuro114F	GCTAACCTGCCCTTTAGTGG	(Sutton, et al. 2015)	(Sutton, et al. 2015)
	Sulfuro421R	GTTTACACACCGAAATGCGT		
tceA	TceA1270F	ATCCAGATTATGACCCTGGTGAA	(Ritalahti, et al. 2006)	(Ritalahti, et al. 2006)
	TceA 1336R	GCGGCATATATTAGGGCATCTT		
vcrA	Vcr1022F	CGGGCGGATGCACTATTTT	(Ritalahti, et al. 2006)	(Ritalahti, et al. 2006)
	Vcr1093R	GAATAGTCCGTGCCCTTCCTC		
bvcA	Bvc925F	AAAAGCACTTGGCTATCAAGGAC	(Ritalahti, et al. 2006)	(Ritalahti, et al. 2006)
	Bvc1017R	CCAAAAGCACCACCAGGTC		

[a] The qPCR program was modified as 98°C for 5 min, followed by 40 cycles of 98°C for 15 s, 68.2°C for 45 s. Melting curves were included from 55°C to 95°C with increments of 0.5°C and 10 s at each step.

References

Adrian L, Loeffler F. *Organohalide-respiring bacteria*. Berlin, Heidelberg: Springer, 2016.

Ahn YB, Rhee SK, Fennell DE *et al.* Reductive dehalogenation of brominated phenolic compounds by microorganisms associated with the marine sponge Aplysina aerophoba. *Appl Environ Microbiol* 2003;69: 4159-66.

Amos BK, Sung Y, Fletcher KE *et al.* Detection and quantification of *Geobacter lovleyi strain* SZ: implications for bioremediation at tetrachloroethene- and uranium-impacted sites. *Appl Environ Microbiol* 2007;73: 6898-904.

Atashgahi S. Discovered by genomics: putative reductive dehalogenases with N-terminus transmembrane helixes. *FEMS Microbiol Ecol* 2019;95: fiz048.

Atashgahi S, Haggblom MM, Smidt H. Organohalide respiration in pristine environments: implications for the natural halogen cycle. *Environ Microbiol* 2018;20: 934-48.

Atashgahi S, Lu Y, Smidt H. Overview of known organohalide-respiring bacteria—phylogenetic diversity and environmental distribution. In: Adrian L, Löffler FE (eds.) *Organohalide-Respiring Bacteria*. Berlin, Heidelberg: Springer Berlin Heidelberg, 2016, 63-105.

Atashgahi S, Maphosa F, Dogan E *et al.* Small-scale oxygen distribution determines the vinyl chloride biodegradation pathway in surficial sediments of riverbed hyporheic zones. *FEMS Microbiol Ecol* 2013;84: 133-42.

Aulenta F, Majone M, Verbo P *et al.* Complete dechlorination of tetrachloroethene to ethene in presence of methanogenesis and acetogenesis by an anaerobic sediment microcosm. *Biodegradation* 2002;13: 411-24.

Azizian MF, Marshall IP, Behrens S *et al.* Comparison of lactate, formate, and propionate as hydrogen donors for the reductive dehalogenation of trichloroethene in a continuous-flow column. *J Contam Hydrol* 2010a;113: 77-92.

Azizian MF, Marshall IP, Behrens S *et al.* Comparison of lactate, formate, and propionate as hydrogen donors for the reductive dehalogenation of trichloroethene in a continuous-flow column. *Journal of Contaminant Hydrology* 2010b;113: 77-92.

Bayer K, Scheuermayer M, Fieseler L *et al.* Genomic mining for novel $FADH_2$-dependent halogenases in marine sponge-associated microbial consortia. *Mar Biotechnol* 2013;15: 63-72.

Caporaso JG, Lauber CL, Walters WA *et al.* Global patterns of 16S rRNA diversity at a depth of millions of sequences per sample. *Proc Natl Acad Sci USA* 2011;108: 4516-22.

Chen J, Bowman KS, Rainey FA *et al.* Reassessment of PCR primers targeting 16S rRNA genes of the organohalide-respiring genus *Dehalogenimonas*. *Biodegradation* 2014;25: 747-56.

Chen K, Huang L, Xu C *et al.* Molecular characterization of the enzymes involved in the degradation of a brominated aromatic herbicide. *Mol Microbiol* 2013;89: 1121-39.

Christensen JH, Platz J. Screening of polybrominated diphenyl ethers in blue mussels, marine and freshwater sediments in Denmark. *J Environ Monit* 2001;3: 543-7.

Cline JD. Spectrophotometric determination of hydrogen sulfide in natural waters. *Limnol Oceanogr* 1969;14: 454-8.

Comba P, Kerscher M, Krause T *et al.* Iron-catalysed oxidation and halogenation of organic matter in nature. *Environ Chem* 2015;12: 381-95.

Cooper M, Wagner A, Wondrousch D *et al.* Anaerobic microbial transformation of halogenated aromatics and fate prediction using electron density modeling. *Environ Sci Technol* 2015;49: 6018-28.

DeWeerd K, Concannon F, Suflita JM. Relationship between hydrogen consumption, dehalogenation, and the reduction of sulfur oxyanions by *Desulfomonile tiedjei*. *Appl Environ Microbiol* 1991;57: 1929-34.

Dolfing J, Tiedje JM. Growth yield increase linked to reductive dechlorination in a defined 3-chlorobenzoate degrading methanogenic coculture. *Arch Microbiol* 1987;149: 102-5.

Edgar RC. Search and clustering orders of magnitude faster than BLAST. *Bioinformatics* 2010;26: 2460-1.

Eme L, Spang A, Lombard J *et al.* Archaea and the origin of eukaryotes. *Nat Rev Microbiol* 2017;15: 711-23.

Escher BI, Snozzi M, Schwarzenbach RP. Uptake, speciation, and uncoupling activity of substituted phenols in energy transducing membranes. *Environ Sci Technol* 1996;30: 3071-9.

Fincker M, Huber JA, Orphan VJ *et al.* Metabolic strategies of marine subseafloor *Chloroflexota* inferred from genome reconstructions. *Environ Microbiol* 2020;22: 3188–204.

Fincker M, Spormann AM. Biochemistry of catabolic reductive dehalogenation. *Annu Rev Biochem* 2017;86: 357-86.

Fung JM, Morris RM, Adrian L *et al.* Expression of reductive dehalogenase genes in *Dehalococcoides ethenogenes* strain 195 growing on tetrachloroethene, trichloroethene, or 2, 3-dichlorophenol. *Appl Environ Microbiol* 2007;73: 4439-45.

Futagami T, Morono Y, Terada T *et al.* Dehalogenation activities and distribution of reductive dehalogenase homologous genes in marine subsurface sediments. *Appl Environ Microbiol* 2009;75: 6905-9.

Futagami T, Morono Y, Terada T *et al.* Distribution of dehalogenation activity in subseafloor sediments of the Nankai Trough subduction zone. *Philos Trans R Soc Lond B Biol Sci* 2013;368: 20120249.

Gribble GW. *Naturally occuring organohalogen compounds—a comprehensive survery*. Prog Chem Org Nat Prod, 1996.

Gribble GW. Recently discovered naturally occurring heterocyclic organohalogen compounds. *Heterocycles* 2012;84: 157-207.

Gribble GW. A recent survey of naturally occurring organohalogen compounds. *Environ Chem* 2015;12: 396-405.

Gutleben J, Koehorst JJ, McPherson K *et al.* Diversity of tryptophan halogenases in sponges of the genus *Aplysina*. *FEMS Microbiol Ecol* 2019;95: fiz108.

Häggblom MM, Ahn YB, Fennell DE *et al.* Anaerobic dehalogenation of organohalide contaminants in the marine environment. *Adv Appl Microbiol* 2003;53: 61-84.

Hashimoto S, Wakimoto T, Tatsukawa R. Possible natural formation of polychlorinated dibenzo-p-dioxins as evidenced by sediment analysis from the Yellow Sea, the East China Sea and the Pacific Ocean. *Mar Pollut Bull* 1995;30: 341-6.

Heipieper H-J, Keweloh H, Rehm H-J. Influence of phenols on growth and membrane permeability of free and immobilized *Escherichia coli*. *Appl Environ Microbiol* 1991;57: 1213-7.

Holscher T, Krajmalnik-Brown R, Ritalahti KM *et al.* Multiple nonidentical reductive-dehalogenase-homologous genes are common in *Dehalococcoides*. *Appl Environ Microbiol* 2004;70: 5290-7.

Jochum LM, Chen X, Lever MA *et al.* Depth distribution and assembly of sulfate-reducing microbial communities in marine sediments of Aarhus Bay. *Appl Environ Microbiol* 2017;83: e01547-17.

Jochum LM, Schreiber L, Marshall IPG *et al.* Single-cell genomics reveals a diverse metabolic potential of uncultivated *Desulfatiglans*-related *Deltaproteobacteria* widely distributed in marine sediment. *Front Microbiol* 2018;9: 2038.

Jorgensen BB, Andren T, Marshall IPG. Sub-seafloor biogeochemical processes and microbial life in the Baltic Sea. *Environ Microbiol* 2020;5: 1688-706.

Kaster AK, Mayer-Blackwell K, Pasarelli B *et al.* Single cell genomic study of *Dehalococcoidetes* species from deep-sea sediments of the Peruvian Margin. *ISME J* 2014;8: 1831-42.

Krajmalnik-Brown R, Hölscher T, Thomson IN *et al.* Genetic identification of a putative vinyl chloride reductase in *Dehalococcoides* sp. strain BAV1. *Appl Environ Microbiol* 2004;70: 6347-51.

Kristjansson J, Schönheit P. Why do sulfate-reducing bacteria outcompete methanogenic bacteria for substrates? *Oecologia* 1983;60: 264-6.

Lahti L, Shetty S. microbiome R package. 2017.

Leloup J, Fossing H, Kohls K *et al.* Sulfate-reducing bacteria in marine sediment (Aarhus Bay, Denmark): abundance and diversity related to geochemical zonation. *Environ Microbiol* 2009;11: 1278-91.

Leri AC, Mayer LM, Thornton KR *et al.* Bromination of marine particulate organic matter through oxidative mechanisms. *Geochim Cosmochim Acta* 2014;142: 53-63.

Lie TJ, Clawson ML, Godchaux W *et al.* Sulfidogenesis from 2-aminoethanesulfonate (taurine) fermentation by a morphologically unusual sulfate-reducing bacterium, *Desulforhopalus singaporensis* sp. nov. *Appl Environ Microbiol* 1999;65: 3328-34.

Lim ML, Brooks MD, Boothe MA *et al.* Novel bacterial diversity is enriched with chloroperoxidase-reacted organic matter under anaerobic conditions. *FEMS Microbiol Ecol* 2018;94: fiy050.

Lin XQ, Li ZL, Zhu YY *et al.* Palladium/iron nanoparticles stimulate tetrabromobisphenol a microbial reductive debromination and further mineralization in sediment. *Environ Int* 2020;135: 105353.

Liu J, Adrian L, Haggblom MM. Transcriptomic and proteomic responses of the organohalide-respiring bacterium *Desulfoluna spongiiphila* to growth with 2, 6-dibromophenol as the electron acceptor. *Appl Environ Microbiol* 2020;86: e02146-19.

Liu J, Haggblom MM. Genome-guided identification of organohalide-respiring *Deltaproteobacteria* from the marine environment. *mBio* 2018;9: e02471-18.

Liu J, Lopez N, Ahn Y *et al.* Novel reductive dehalogenases from the marine sponge associated bacterium *Desulfoluna spongiiphila*. *Environ Microbiol Rep* 2017;9: 537-49.

Lo KH, Lu CW, Lin WH *et al.* Enhanced reductive dechlorination of trichloroethene with immobilized *Clostridium butyricum* in silica gel. *Chemosphere* 2020;238: 124596.

Lozupone C, Knight R. UniFrac: a new phylogenetic method for comparing microbial communities. *Appl Environ Microbiol* 2005;71: 8228-35.

Lozupone C, Lladser ME, Knights D *et al.* UniFrac: an effective distance metric for microbial community comparison. *ISME J* 2011;5: 169-72.

Magnuson J, Stern R, Gossett J *et al.* Reductive dechlorination of tetrachloroethene to ethene by a two-component enzyme pathway. *Appl Environ Microbiol* 1998;64: 1270-5.

Maillard J, Schumacher W, Vazquez F *et al.* Characterization of the corrinoid iron-sulfur protein tetrachloroethene reductive dehalogenase of *Dehalobacter restrictus*. *Appl Environ Microbiol* 2003;69: 4628-38.

Mao X, Polasko A, Alvarez-Cohen L. Effects of sulfate reduction on trichloroethene dechlorination by *Dehalococcoides*-containing microbial communities. *Appl Environ Microbiol* 2017;83.

Maphosa F, De Vos WM, Smidt H. Exploiting the ecogenomics toolbox for environmental diagnostics of organohalide-respiring bacteria. *Trends Biotechnol* 2010;28: 308-16.

Matturro B, Ubaldi C, Rossetti S. Microbiome Dynamics of a Polychlorobiphenyl (PCB) Historically Contaminated Marine Sediment under Conditions Promoting Reductive Dechlorination. *Front Microbiol* 2016;7: 1502.

Maymo-Gatell X, Chien YT, Gossett JM *et al.* Isolation of a bacterium that reductively dechlorinates tetrachloroethene to ethene. *Science* 1997;276: 1568-71.

McMurdie PJ, Behrens SF, Müller JA *et al.* Localized plasticity in the streamlined genomes of vinyl chloride respiring *Dehalococcoides*. *PLoS Genet* 2009;5: e1000714.

McMurdie PJ, Holmes S. Phyloseq: an R package for reproducible interactive analysis and graphics of microbiome census data. *PLoS One* 2013;8: e61217.

Méndez-Díaz JD, Shimabuku KK, Ma J *et al.* Sunlight-driven photochemical halogenation of dissolved organic matter in seawater: a natural abiotic source of organobromine and organoiodine. *Environ Sci Technol* 2014;48: 7418-27.

Merlino G, Balloi A, Marzorati M *et al.* Diverse reductive dehalogenases are associated with *Clostridiales*-enriched microcosms dechlorinating 1, 2-dichloroethane. *BioMed research international* 2015;2015.

Moe WM, Yan J, Nobre MF *et al.* *Dehalogenimonas lykanthroporepellens* gen. nov., sp. nov., a reductively dehalogenating bacterium isolated from chlorinated solvent-contaminated groundwater. *Int J Syst Evol Microbiol* 2009;59: 2692-7.

Mohn WW, Kennedy KJ. Reductive dehalogenation of chlorophenols by *Desulfomonile tiedjei* DCB-1. *Appl Environ Microbiol* 1992;58: 1367-70.

Mohn WW, Tiedje JM. Strain DCB-1 conserves energy for growth from reductive dechlorination coupled to formate oxidation. *Arch Microbiol* 1990;153: 267-71.

Molenda O, Quaile AT, Edwards EA. *Dehalogenimonas* sp. Strain WBC-2 Genome and Identification of Its trans-Dichloroethene Reductive Dehalogenase, TdrA. *Appl Environ Microbiol* 2016;82: 40-50.

Monserrate E, Häggblom MM. Dehalogenation and biodegradation of brominated phenols and benzoic acids under iron-reducing, sulfidogenic, and methanogenic conditions. *Appl Environ Microbiol* 1997;63: 3911-5.

Moon H-B, Kannan K, Choi M *et al.* Polybrominated diphenyl ethers (PBDEs) in marine sediments from industrialized bays of Korea. *Mar Pollut Bull* 2007;54: 1402-12.

Muller JA, Rosner BM, Von Abendroth G *et al.* Molecular identification of the catabolic vinyl chloride reductase from *Dehalococcoides* sp. strain VS and its environmental distribution. *Appl Environ Microbiol* 2004;70: 4880-8.

Muyzer G, De Waal EC, Uitterlinden AG. Profiling of complex microbial populations by denaturing gradient gel electrophoresis analysis or polymerase chain reaction-amplified genes coding for 16S rRNA. *Appl Environ Microbiol* 1993;59: 695-700.

Nelson D, Hozalski R, Clapp L *et al.* Effect of nitrate and sulfate on dechlorination by a mixed hydrogen-fed culture. *Bioremediat J* 2002;6: 225-36.

Oksanen J, Kindt R, Legendre P *et al.* The vegan package. *Community Ecology Package* 2007;10: 719.

Ozturk B, de Jaeger L, Smidt H *et al.* Culture-dependent and independent approaches for identifying novel halogenases encoded by Crambe crambe (marine sponge) microbiota. *Sci Rep* 2013;3: 2780.

Ozuolmez D, Moore EK, Hopmans EC *et al.* Butyrate Conversion by Sulfate-Reducing and Methanogenic Communities from Anoxic Sediments of Aarhus Bay, Denmark. *Microorganisms* 2020;8.

Peng P, Goris T, Lu Y *et al.* Organohalide-respiring *Desulfoluna* species isolated from marine environments. *ISME J* 2020a;14: 815-27.

Peng P, Lu Y, Bosma TNP *et al.* Metagenomic- and cultivation-based exploration of anaerobic chloroform biotransformation in hypersaline sediments as natural source of chloromethanes. *Microorganisms* 2020b;8: 665.

Peng P, Schneidewind U, Haest PJ *et al.* Reductive dechlorination of 1,2-dichloroethane in the presence of chloroethenes and 1,2-dichloropropane as co-contaminants. *Appl Microbiol Biotechnol* 2019;103: 6837-49.

Petro C, Jochum LM, Schreiber L *et al.* Single-cell amplified genomes of two uncultivated members of the deltaproteobacterial SEEP-SRB1 clade, isolated from marine sediment. *Mar Genomics* 2019a;46: 66-9.

Petro C, Zancker B, Starnawski P *et al.* Marine deep biosphere microbial communities assemble in near-surface sediments in Aarhus Bay. *Front Microbiol* 2019b;10: 758.

Piché-Choquette S, Constant P. Molecular hydrogen, a neglected key driver of soil biogeochemical processes. *Appl Environ Microbiol* 2019;85: e02418-18.

Poncheewin W, Hermes GDA, van Dam JCJ *et al.* NG-Tax 2.0: A semantic framework for high-throughput amplicon analysis. *Front Genet* 2019;10: 1366.

Ramiro-Garcia J, Hermes GDA, Giatsis C *et al.* NG-Tax, a highly accurate and validated pipeline for analysis of 16S rRNA amplicons from complex biomes. *F1000Res* 2016;5: 1791.

Ritalahti KM, Amos BK, Sung Y *et al.* Quantitative PCR targeting 16S rRNA and reductive dehalogenase genes simultaneously monitors multiple *Dehalococcoides* strains. *Appl Environ Microbiol* 2006;72: 2765-74.

Scheutz C, Durant ND, Dennis P *et al.* Concurrent ethene generation and growth of *Dehalococcoides* containing vinyl chloride reductive dehalogenase genes during an enhanced reductive dechlorination field demonstration. *Environ Sci Technol* 2008;42: 9302-9.

Smidt H, De Vos WM. Anaerobic microbial dehalogenation. *Annu Rev Microbiol* 2004;58: 43-73.

Smits TH, Devenoges C, Szynalski K *et al.* Development of a real-time PCR method for quantification of the three genera *Dehalobacter*, *Dehalococcoides*, and *Desulfitobacterium* in microbial communities. *J Microbiol Methods* 2004;57: 369-78.

Spang A, Caceres EF, Ettema TJ. Genomic exploration of the diversity, ecology, and evolution of the archaeal domain of life. *Science* 2017;357: eaaf3883.

Spang A, Stairs CW, Dombrowski N *et al.* Proposal of the reverse flow model for the origin of the eukaryotic cell based on comparative analyses of Asgard archaeal metabolism. *Nat Microbiol* 2019;4: 1138-48.

Stasiuk M, Kozubek A. Membrane perturbing properties of natural phenolic and resorcinolic lipids. *FEBS letters* 2008;582: 3607-13.

Sutton NB, Atashgahi S, Saccenti E *et al.* Microbial community response of an organohalide respiring enrichment culture to permanganate oxidation. *PLoS One* 2015;10: e0134615.

Team RDC. *R: A language and environment for statistical computing*. R Found Stat Comput, 2013.

Türkowsky D, Jehmlich N, Diekert G *et al.* An integrative overview of genomic, transcriptomic and proteomic analyses in organohalide respiration research. *FEMS Microbiol Ecol* 2018;94: fiy013.

Wagner C, El Omari M, König G. Biohalogenation: nature's way to synthesize halogenated metabolites. *J Nat Prod* 2009;72: 540-53.

Walters W, Hyde ER, Berg-Lyons D *et al.* Improved bacterial 16S rRNA gene (V4 and V4-5) and fungal internal transcribed spacer marker gene primers for microbial community surveys. *mSystems* 2016;1: e00009-15.

Wever R, van der Horst MA. The role of vanadium haloperoxidases in the formation of volatile brominated compounds and their impact on the environment. *Dalton Trans* 2013;42: 11778-86.

Wiseman SB, Wan Y, Chang H *et al.* Polybrominated diphenyl ethers and their hydroxylated/methoxylated analogs: environmental sources, metabolic relationships, and relative toxicities. *Mar Pollut Bull* 2011;63: 179-88.

Xu G, Zhao S, Chen C *et al.* Dehalogenation of polybrominated diphenyl ethers and polychlorinated biphenyls catalyzed by a reductive dehalogenase in *Dehalococcoides mccartyi* Strain MB. *Environ Sci Technol* 2022.

Yang G, Yin Y, Wang J. Microbial community diversity during fermentative hydrogen production inoculating various pretreated cultures. *Int J Hydrog Energy* 2019;44: 13147-56.

Yilmaz P, Parfrey LW, Yarza P *et al.* The SILVA and “all-species living tree project (LTP)” taxonomic frameworks. *Nucleic Acids Res* 2014;42: D643-8.

Zaremba-Niedzwiedzka K, Caceres EF, Saw JH *et al.* Asgard archaea illuminate the origin of eukaryotic cellular complexity. *Nature* 2017;541: 353-8.

Zinke LA, Mullis MM, Bird JT *et al.* Thriving or surviving? Evaluating active microbial guilds in Baltic Sea sediment. *Environ Microbiol Rep* 2017;9: 528-36.

Chapter 3

Genome-resolved transcriptomics reveals novel organohalide-respiring bacteria from Aarhus Bay sediments

Chen Zhang, Tom N.P. Bosma, Siavash Atashgahi, Hauke Smidt

Manuscript in preparation

Abstract

Organohalide-respiring bacteria (OHRB) are keystone microbes in bioremediation of sites contaminated with organohalides and in natural halogen cycling. Known OHRB belong to distinct genera within the phyla *Chloroflexota*, *Proteobacteria* and *Firmicutes*, whereas information about novel OHRB mediating natural halogen cycling remains scarce. In this study, we applied a genome-resolved transcriptomic approach to characterize the identity and activity of OHRB from PCE-respiring cultures previously enriched from sediments of Aarhus Bay. Combining short- and long-read sequencing approaches, we assembled 37 high quality bins with over 75 % completeness and less than 5 % contamination. Sixteen bins harbored RDase genes, and were affiliated taxonomically to the class of *Bacilli*, and phyla of *Bacteroidota*, *Synergistota*, and *Spirochaetota*, that have not been reported to catalyze reductive dehalogenation. Among the 16 bins, CH3_bin.26, phylogenetically closely related to the genus *Vulcanibacillus*, contained an unprecedented 97 RDase genes. Of these, 84 RDase genes of CH3_bin.26 were transcribed during PCE dechlorination in addition to RDase genes from members of *Synergistales* (CH3_bin.15 and CH3_bin.32) and *Bacteroidales* (CH3_bin.18 and CH3_bin.24). Moreover, metatranscriptome analysis suggested the RDase genes were likely under the regulation of transcriptional regulators not previously associated with OHR, such as HrcA and SigW, which are known to respond to abiotic environmental stresses, such as temperature changes. Combined application of genomic methods enabled us to pinpoint novel OHRB from pristine environments not previously known to mediate reductive dechlorination and to provide evidence towards the diversity, activity and regulation of reductive dehalogenases.

Keywords: Organohalide respiration; Metagenomics; Metatranscriptomics; RDase gene; *Vulcanibacillus*; Transcriptional regulators

Introduction

Organohalide respiring bacteria (OHRB) can derive energy for growth from the use of reductive dehalogenation of halogenated compounds as terminal electron accepting process. They employ reductive dehalogenases (RDases) that catalyze the removal of halide(s) from the carbon backbone via respiratory electron transfer (Mohn and Tiedje, 1992; Adrian and Löffler, 2016). In the process of organohalide respiration (OHR), organohalides serve as the terminal electron acceptor for the electrons derived from, for example, hydrogen or lactate, through a membrane-associated electron transport chain (ETC). In addition to RDases known from OHRB, reductive dehalogenation can also be catalyzed by another type of reductive dehalogenase, thiolytic, glutathione-dependent tetrachloro-P-hydroquinone RDase (TPh-RDase) as previously reported for biodegradation of chlorinated compounds (Xun et al., 1992a,b). In many cases, RDase gene-containing gene clusters in OHRB are composed of genes encoding a transcriptional regulator, the RDase itself, and a potential electron transporter. Thereinto, three regulatory systems of RDase gene clusters have been characterized: CRP (cyclic AMP receptor protein) / FNR (fumarate and nitrate reduction regulator) superfamily, Two-Component Systems (TCS) and MarR (multiple antibiotic resistance regulator) (Gabor et al., 2006; Wagner et al., 2013). The minimum cassette of RDase gene clusters is usually composed of a gene encoding the catalytical subunit, *rdhA*, and a second gene, *rdhB,* coding for a cognate membrane-anchoring protein B (Smidt and De Vos, 2004; Fincker and Spormann, 2017; Wang et al., 2018). Organohalides are present as natural products in marine environments and other high salt environments (Gribble, 2015; Atashgahi et al., 2018; Peng et al., 2020a), which is why it is interesting to study their role in the geochemical carbon and halogen cycles and their potential eco-physiological importance.

OHR exploration in marine sediments has been a long-term topic for several decades, which was mainly based on culture-dependent and molecular detection methods, such as dilution-to-extinction isolation, marker-gene amplicon sequencing and quantification (Smits et al., 2004; Lu et al., 2017; Bokulich et al., 2018). Recent research into the microbial composition of marine sediments, making use of metagenomic techniques and bioinformatics, revealed the presence of microorganisms from various phyla containing genes predicted to code for RDases, including, next to the commonly known phyla, such as *Chloroflexota* and *Firmicutes*, new archaeal phyla, *Lokiarchaeota*, *Thorarchaeota*, and *Heimdallarchaeota* belonging to the proposed *Asgardarchaeota* superphylum (Spang et al., 2019).

Based on single-cell amplified genomes (SAGs) retrieved from sediment of Aarhus Bay, a putative RDase gene was found in the assembled genome DEH-C3, belonging to the *Dehalococcoidia* (Wasmund et al., 2016). Metatranscriptomic data from the surroundings of the initial sampling site revealed a high abundance of *tceA*-like gene transcripts implicating the potential for reductive dehalogenation in this marine sediment from Aarhus Bay (Zinke et al., 2017). Moreover, five *Desulfatiglans*-related SAGs were found bearing putative RDase genes from the sulfate-rich subsurface of Aarhus Bay marine sediments, and it was speculated that OHR might be an alternative energy conservation strategy under sulfate-limiting conditions (Jochum et al., 2018). Nevertheless, although these analyses of extensive DNA and RNA sequence data indicated the existence of potential OHR in marine sediments of Aarhus Bay, unambiguous physiological proof remains pending, and the OHRB involved were not isolated nor unequivocally identified.

In a previous study we have found that marine sediments from Aarhus Bay can dehalogenate a range of halogenated compounds, including tetrachloroethene (PCE), 2,6-dibromophenol (2,6-DBP), 1,4-dibromobenzene (1,4-DBB), 3-bromophenol (3-BP), and 2,4,6-triiodophenol (2,4,6-TIP) (Chapter 2). 16S ribosomal RNA (rRNA) gene amplicon sequencing revealed that members of the phyla *Desulfobacterota*, *Firmicutes* and *Bacteroidota*, such as *Desulfovibrio*, *Desulfuromusa* and *Bacillus*, were enriched in sediment-free PCE dechlorinating cultures.

Desulfovibrio and *Desulfuromusa* were recently shown to be capable of reductive debromination of 2,6-DBP to phenol (Liu and Haggblom, 2018). However, *Bacillus* spp. or members of the *Bacteroidota* have never been reported before to use organohalides as terminal electron acceptors.

Thus, the aim of this study was to identify the OHRB involved in the dehalogenation of PCE aligning to the previously reported study (Chapter 2). To this end, we combined metagenomics and -transcriptomics of sediment-free PCE-dechlorinating enrichment cultures with physiological observations in order to identify the corresponding OHRB and their RDase genes for PCE dechlorination with(out) additional sulfate. This revealed the presence of a large number of genomic bins encoding putative reductive dehalogenases, as well as the expression of many of these genes that appeared to be under the control of transcriptional regulators not previously associated with OHR.

Materials and methods

Chemicals

PCE, TCE, cDCE, VC, and ethene were purchased from Sigma-Aldrich. Stock solutions of lactate (0.5 M) and sulfate (0.5 M) were prepared separately by filter sterilization (syringe filter, 0.2 µm, mdimembrane, Ambala Cantt, India). All other (in)organic chemicals were obtained in analytical grade or higher.

Cultivation

Cultures were incubated in marine medium under sulfate-free (NS) or sulfate-amended (S) conditions as described previously (Chapter 2). These cultures labelled as PCE_NS_Tr2_A/B (PCE.NS.Tr2.A/B, Chapter 2) and PCE_S_Tr2_A/B (PCE.S.Tr2.A/B, Chapter 2), grown in 50 ml per bottle, were the same cultures as indicated in step 4 in the experimental outline of

Chapter 2 (Figure 2.1, Figure 3.1A). The cultures were obtained after three spikes (see below) that were applied when PCE was completely dechlorinated into cDCE. Each spike contained 250 µM PCE and 5 mM lactate (NS and S), and 5 mM sulfate in S cultures. The actively dechlorinating cultures, PCE_NS_Tr3 and PCE_S_Tr3 (50 ml per bottle), respectively, were obtained after 5% transfer of PCE_NS_Tr2_A and PCE_S_Tr2_A. The remainders of PCE_NS_Tr2_A and PCE_S_Tr2_A were sacrificed for metagenome sequencing by Illumina (Novogene Europe, Cambridge, UK). PCE_NS_Tr2_B and PCE_S_Tr2_B cultures were used for metagenome sequencing by Nanopore separately (Novogene Europe). When 80% of the last of three spikes of 250 µM PCE was consumed, PCE_NS_Tr3 and PCE_S_Tr3 were transferred at 5 vol-% to PCE_NS_Tr4 and PCE_S_Tr4, respectively, in three replicates (100 ml per bottle). Similar to the cultures used for metagenome sequencing, three replicate cultures of PCE_NS_Tr4 and PCE_S_Tr4 were collected for metatranscriptome sequencing by Illumina (Novogene Europe) when 80% of PCE was dechlorinated into cDCE after the third spike.

Analytical methods

PCE, TCE, and cDCE were measured by Gas chromatography and mass spectroscopy (GC-MS) installed with an Rt$^{®}$-Q-BOND column (Retek, PA, USA) and a DSQ MS (Thermo Fisher Scientific). Hydrogen and methane were detected by compact GC (Global Analyzer Solutions, Breda, The Netherlands) with a thermal conductivity detector (GC-PDD). Organic acids, including lactate, acetate, and propionate, were measured by SHIMADZU LC2030 PLUS coupled with a Shodex SUGAR Series® SH1821 column. Sulfate was measured by Dionex™ ICS-2100 Ion Chromatography System (Thermo Scientific), and sulfide was analyzed photometrically as previously described (Cline, 1969).

DNA and RNA extraction

Cultures used for DNA and RNA extraction were centrifuged at 10,000 g for 5 min, and then washed three times with 10 mM TE buffer (pH 7.0) to remove residual medium components. Washing of cultures for RNA extraction was done at 4 °C. DNA extraction was done by using the MasterPureTM Gram positive DNA purification Kit (Epicentre, WI, USA) to gain high quality and quantity DNA for metagenomic sequencing, including Illumina for short reads (PE 150, NovaSeq 6000) and Oxford Nanopore for long reads. The RNA extraction was carried out following a bead-beating procedure (Egert et al., 2007). The isolated RNA was purified using RNeasy columns (Qiagen, Venlo, The Netherlands), and residual genomic DNA was subsequently digested by DNase I (Roche, Almere, The Netherlands). The obtained RNA samples were quality-checked by agarose gel electrophoresis and sequenced using Illumina for short reads (PE 150, NovaSeq 6000).

Metagenome data analyses

Metagenome sequence data were generated by Illumina sequencing in paired-end short reads (NovaSeq 6000) and Oxford Nanopore. The pipelines of MetaWRAP, OPERA-MS and Anvi'o were combined to process the raw data as outlined in the following (Figure S3.1) (Uritskiy et al., 2018; Bertrand et al., 2019; Eren et al., 2021). One of the duplicate cultures, PCE_NS/S_Tr2_A, was sent for paired-end Illumina sequencing. Cleaning of short reads was achieved through quality check and trimming using the "read_qc" module of MetaWRAP. Both forward and reverse sequencing of PCE_NS_Tr2_A yielded 33,352,593 reads, respectively, with 33,340,280 read pairs remaining after filtering for human genomic DNA contaminants and quality control. Raw and filtered read pairs of PCE_S_Tr2_A amounted to 26,516,123 and 26,506,140, respectively. Co-assembly of the clean reads from both cultures was done using the "assembly" module of MetaWRAP. PCE_NS/S_Tr2_B cultures were used for Nanopore sequencing. The number of filtered reads of PCE_NS/S_Tr2_B was 1,637,484 and 954,603, respectively. The short-read co-assembly was then combined with the Nanopore long reads using OPERA-MS (Figure S3.1). Subsequently, metatranscriptome sequences (see below for processing details) were introduced to improve the quality of the hybrid assembly by OPERA-MS (Table S3.1). As a next step, the hybrid assembly was used for binning using the "binning" module of MetaWRAP separately with three commonly-used built-in binners: metabat2, maxbin2 and concoct. Further refining of bins was achieved using the "bin_refinement" module, and selection of bins using a cut-off at 50% completeness and 10% contamination. The abundance of the refined bins was determined using the "quant_bins" module in MetaWRAP, which uses Salmon to index the entire metagenomic assembly, and then reads from samples were mapped back to the hybrid assembly. The generated coverage estimates were used to calculate the abundance of each contig in each sample. Length-weighted average of a given bin's contig abundances was used to calculate the bins' abundances. Bin quality was further improved using the "reassemble_bins" module of MetaWRAP. The reassembled bins were then classified using the "classify_wf" module of GTDB-Tk (Rinke et al., 2021), and phylogenomic analysis of bins was performed on the Aanovi'o platform annotated with the "annotate_bins" module of MetaWRAP using the built-in PROKKA. To assess the genomic context of target genes, flanking genes were searched by setting "grep -A 6 -B 5" to fetch the first five upstream genes and first six downstream genes using the translated ".faa" format files. The obtained gene clusters were visualized by "gggenes" (https://github.com/wilkox/gggenes).

Phylogenetic analysis of OHR bins

Thirty-seven bins, also termed Metagenome-Assembled Genomes (MAGs) were retained after filtering using the "Bin_refinement" and "reassemble_bins" modules of MetaWRAP, with settings of > 75 % completeness and < 5 % contamination. These 37 MAGs were then phylogenomically analyzed following the Anvi'o workflow using the "--hmm-source

Bacteria_71", and the output tree file was visualized by ggtree (Yu et al., 2017), which combined the bins' abundance, transcripts, and their genome size. Bins of potentially reductively dehalogenating bacteria were identified using the curated HMM file of RDase genes, which includes reductive dehalogenases of OHRB and tetrachloro-p-hydroquinone (TPh) reductive dehalogenase (Xun et al., 1992b, a; Garber et al., 2020). To establish their evolutionary position, bins were taxonomically classified by "classify_wf" of GTDB (Chaumeil et al., 2020), and bins from the same phylum or class were collected together with selected representative genomes from the respective phylum from the GTDB database (Using GTDB v202) to construct phylogenetic trees using "GToTree" (Lee, 2019) using 74 bacterial single-copy protein-coding genes (SCGs) for concatenated alignment. In addition, RDase entries from the Pfam database (PF13486, https://pfam.xfam.org/) were employed to retrieve all potential OHRB genomes related to bins at the phylum- or class-level. Similarly, 114 RDase protein sequences were collected from 16 bins, and multiple sequence alignments were done using the online Clustal Omega tool to construct a phylogenetic tree (Sievers et al., 2011).

Metatranscriptome data analyses

Similar to the processing of metagenome data, raw Illumina metatranscriptome sequence data was first cleaned through the removal of human genomic contaminants that may be introduced during samples preparation and extraction. Similarly, Salmon as built in the quant_bin module of MetaWRAP was also employed to calculate the abundance of bins based on transcript mapping to the respective contigs. Tuxedo packages (https://github.com/trinityrnaseq) were used for genome-guided RNA-seq analysis, including Tophat, Cufflinks, Cuffmerge and Cuffdiff (Figure S3.1). The hybrid assembly used for the binning (see above) was set as the template for aligning the RNA-seq data by Tophat. Cufflinks was used for assembling transcript structures from read alignments, and transcripts were counted based on Cuffdiff output, which was used for performing differential expression analysis. The abundance of standardized transcripts was taken into account to construct expression profiles of functional genes under NS and S conditions.

Functional analyses of metabolic pathways encoded in the different bins

To evaluate the potential metabolism encoded in the 37 assembled bins, MagicLamp (https://github.com/Arkadiy-Garber/MagicLamp) was employed to search metabolic marker genes according to the established HMM files as described in “hmm-meta.txt” in the “hmms” directory (Garber et al., 2020). In our physiological experiments, we observed, alongside reductive dehalogenation, sulfate reduction as well as hydrogen and methane production, and relevant marker genes were selected. For sulfur metabolism, genes related to sulfide/sulfur/thiosulfate oxidation, sulfite/sulfate reduction, and thiosulfate disproportionation were retrieved. The initial step of sulfate reduction is the reduction of sulfate to sulfite with the formation of adenosine 5’-phosphosulfate (APS) as the intermediate, catalyzed by sulfate adenylyl-transferase (Sat) or adenylyl-sulfate kinase, and adenylyl-sulfate reductase (Apr) reducing APS to sulfite (Muyzer and Stams, 2008; Leloup et al., 2009; Anantharaman et al., 2018). Sulfite reductase is the critical enzyme to catalyze the reduction of sulfite to sulfide, which is the limiting step for sulfate reduction (Bradley et al., 2011; Leavitt et al., 2015). Two types of sulfite reductase genes were taken into consideration, including those encoding dissimilatory sulfite reductase (*dsr* genes) and anaerobic sulfite reductase (*asr* genes) (Peck Jr, 1961; Hallenbeck et al., 1989). Marker genes encoding enzymes involved in the halogen cycle were selected in addition to RDase and TPh-RDase genes, including genes encoding haloacid dehalogenase type II for organohalide breakdown, DMSO reductase type II PcrA/B for perchlorate reduction, and chlorite dismutase for chlorite reduction (Koonin and Tatusov, 1994; Hisano et al., 1996; Coates and Achenbach, 2004; Bender et al., 2005; Peng et al., 2017). Marker genes coding for hydrogenases were divided into three groups according to the metal content at active sites, i.e. [Ni-Fe]-hydrogenase, [Fe-Fe]-hydrogenase, and [Fe]-hydrogenase

(Lubitz et al., 2014; Piché-Choquette and Constant, 2019). For the well-studied [Ni-Fe]-hydrogenases, eight subgroups, group 1, group 2a, group 2b, group 3a, group 3b, group 3c, group 3d, and group 4, and two subgroups of [Fe-Fe]-hydrogenases, group A and group B, were included (Lubitz et al., 2014; Piché-Choquette and Constant, 2019; Schoelmerich and Muller, 2019). Metabolic genes responsible for methane production and oxidation were also searched against the assembled bins, which included *pmoA*, *pmoB*, *pmoC*, *mmoB*, and *mmoD* for methane oxidation, and *mcrA*, *mcrB*, and *mcrG* for methane production (Hakemian and Rosenzweig, 2007; Evans et al., 2019).

Results

PCE dechlorination to cDCE

Stable, sediment-free PCE-dechlorinating cultures enriched from Aarhus Bay marine sediments (Chapter 2) were spiked three times with PCE at 250 µM (black arrows in Figure 3.1B). The cultures were grown with (S) and without (NS) sulfate. The NS/S_Tr2 cultures reductively dechlorinated PCE to cDCE, reaching a final concentration of 734.7 µM and 675.1 µM respectively, after 3 spikes of 250 µM of PCE, with TCE as intermediate (Figure 3.1B). The resulting biomass was collected for DNA isolation for metagenome sequencing after dehalogenation of the third spike of PCE (grey arrows in Figure 3.1B). Similarly, the PCE_NS_Tr4 and PCE_S_Tr4 cultures reductively dechlorinated PCE to final concentrations of 636.8 µM and 528.8 µM cDCE, respectively, after 3 spikes of 250 µM of PCE. Biomass was collected when 80% of the third spike was dehalogenated to cDCE and was used for RNA extraction for metatranscriptome sequencing, thus ensuring that the OHR-associated genes were active, especially the corresponding RDase genes. The cultures from the 4th transfer without sulfate fully dechlorinated the 1st spike of PCE within 14 days, whereas the full dechlorination of the 1st spike of PCE required 30-34 days in all other sulfate-amended cultures.

This is probably due to competition between sulfate and PCE as the final electron acceptor as was also observed in our previous study (Chapter 2). The electron donor and carbon source, lactate, was consumed with the formation of propionate and acetate at a ratio of around 2.5 : 1 in cultures not amended with sulfate, whereas only acetate was produced in cultures where sulfate was added.

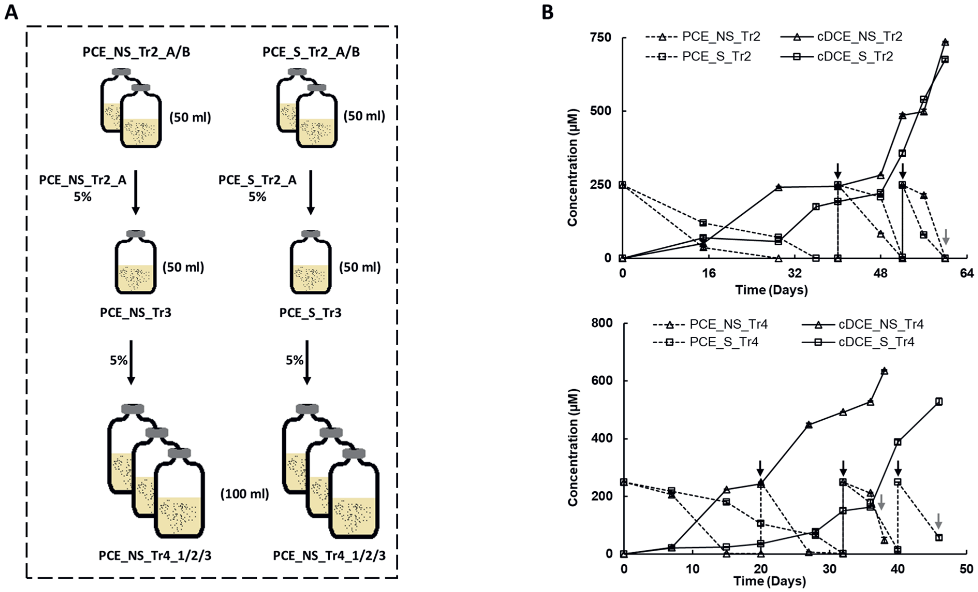

Figure 3.1 Schematic diagram (A) of PCE dechlorinating cultures (B) sampled for metagenome and -transcriptome sequencing. PCE_NS_Tr2_A/B: duplicate PCE dechlorinating sulfate-free cultures; PCE_S_Tr2_A/B: duplicate PCE dechlorinating sulfate-amended cultures; PCE_NS/S_Tr4_1/2/3: triplicate PCE dechlorinating cultures; black arrows in B indicate PCE spikes; grey arrows represent timepoints at which cultures were harvested.

Abundance and expression of bins in PCE dechlorinating cultures

Using the sequence data of both NS and S cultures, 37 assembled bins were retained based on completeness (>75 %) and contamination (<5%) thresholds (Table S3.2). Four of these bins, CH3_bin.15 (classified into genus *Desulforhopalus*), CH3_bin.22 (classified into

Desulfobacter), CH3_bin.34 (classified into *Pseudodesulfovibrio*) and CH3_bin.5 (classified into order *Synergistales*) had 100% completeness and no contamination according to the CheckM output (Parks et al., 2015; Uritskiy et al., 2018). The 37 assembled bins were classified into six bacterial phyla, *Bacteroidota*, *Delongbacteria*, *Desulfobacterota*, *Firmicutes*, *Spirochaetota*, and *Synergistota*, and one archaeal phylum, *Halobacteriota*, according to the taxonomic classification following the workflow of GTDB-Tk (classify_wf) (Figure 3.2). The bins belonging to *Delongbacteria* and *Halobacteriota* did not encode any putative RDase genes, indicating that these organisms were probably not involved in the dechlorination of PCE.

In the NS cultures, CH3_bin.17, classified into *Clostridiaceae*, and CH3_bin.5 classified as a member of *Synergistales* were dominant on average with 12299.6 and 3401.2 genome copies per million reads (reflecting how often a given bin is represented in the sequence data), respectively (Table S3.2), followed by CH3_bin.26 classified as member of *Vulcanibacillus* with 1831.6 genome copies. CH3_bin.21, classified into *Desulfuromusa* was the most highly expressed genome and accounted for 9101.4 genomic transcripts per million reads on average, followed by CH3_bin.15 classified as member of *Desulforhopalus* with 673.9 genomic transcripts per million reads. The genomes of CH3_bin.14 (classified into *Desulfomicrobium*) and CH3_bin.26 were also highly expressed with over 300 genomic transcripts per million reads.

When sulfate was present, CH3_bin.19, belonging to *Desulfoplanes*, was the most abundant and highly expressed, accounting for 6076.2 genome copies and 1145.1 genomic transcripts per million reads, followed by CH3_bin.22 with 3103.4 copies and 106.5 transcripts per million reads. CH3_bin.34, belonging to *Pseudodesulfovibrio* was the third most abundant with 3095.2 genome copies and 19.3 transcripts per million reads. CH3_bin.25, belonging to the same genus, had 333.7 transcripts as the second most highly expressed bin with 666.8 genome copies per million reads (details shown in Table S3.2). CH3_bin.26 belonging to the genus

Vulcanibacillus was annotated with 97 putative RDase genes. Transcriptomics was used to check whether these genes were indeed expressed in the cultures studied. Other genomic bins containing RDase genes, CH3_bin.5, CH3_bin.10 and CH3_bin.32, belonging to *Synergistales*, CH3_bin.15 from *Desulfobacterota*, CH3_bin.28 belonging to *Melioribacteraceae*, and CH3_bin.12, CH3_bin.18, CH3_bin.24 and CH3_bin.31 from *Bacteroidales* were present and expressed in all cultures during PCE dechlorination irrespective of the presence of sulfate, while all their correspondent RDase genes were also expressed (Fig 3.2; Table S3.4). In the sulfate amended cultures, CH3_bin.23 and CH3_bin.6, belonging to the order *Bacteroidales*, and CH3_bin.30, belonging to the *Oceanispirochaeta*, potentially contributed to the sulfate reduction, as evidenced by the detection of their genomic transcripts (Figure. 3.2, Table S3.2, and Table S3.4). In addition, the potential OHRB, CH3_bin.15 belonging to *Desulforhopalus* and CH3_bin.32 belonging to *Synergistales*, were also found to be expressed under sulfate-added condition and their correspondent RDase gene transcripts were observed with on average 65.3 (CH3_bin.15-RDase gene) and 145.5 (CH3_bin.32-RDase gene) transcripts per million reads, respectively (Table S4.4).

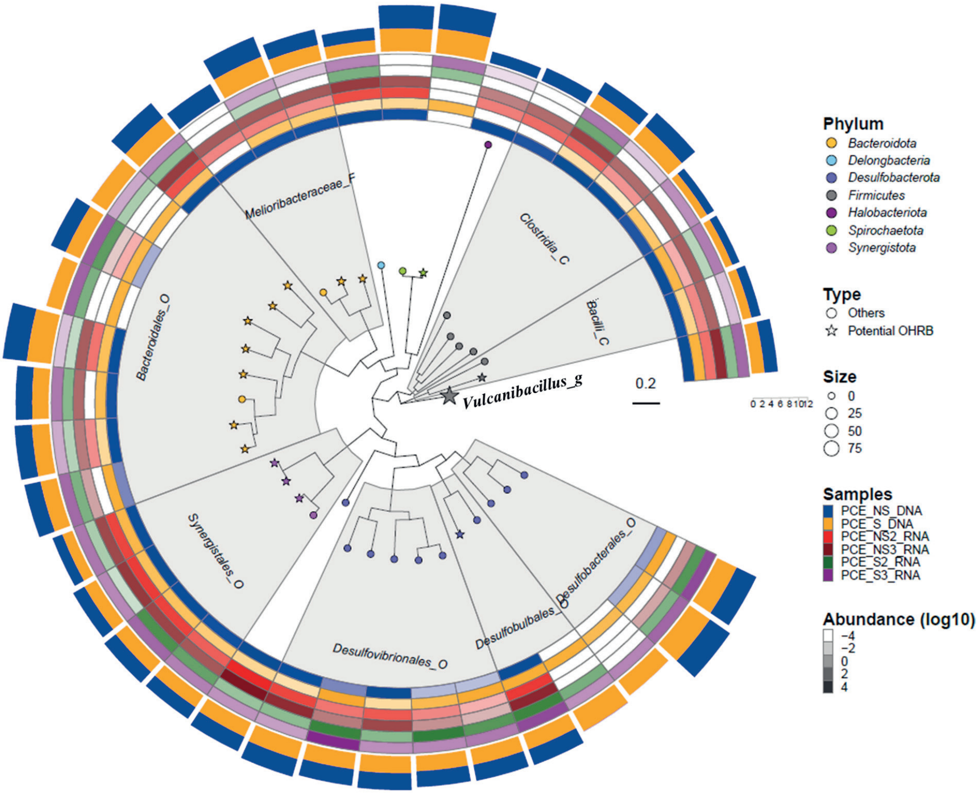

Figure 3.2 Phylogenomic tree of assembled bins constructed on the basis of 71 bacterial marker genes as implemented in Anvi'o. Tips of the tree labelled with the star symbol indicate bins containing RDase genes ("Potential OHRB"), with symbol size representing the number of RDase genes. Colors of tree tips indicate their classification at the phylum level. Areas shaded in grey indicate bins belonging to the same taxon at the level of Order (_O), Class (_C) or Family (_F). The combined heatmap in the outer circles in different colors indicate the presence of bins sourced from metagenomic (PCE_DNA) and meta-transcriptomic (PCE_RNA) data from cultures grown in the absence or presence of sulfate (NS/S). Transparency of the colors in the heatmap represents the abundance of a given bin (Unit: genome copies per million reads) in log10. The two outer circles bearing the same color pattern as the metagenomic samples indicate the presence and bar height represents the bin's genome size as measured by the scaler (0-12 Mbp).

Phylogenomic position of bins representing potential OHRB

To further assess the phylogeny of bins containing RDase genes and thus assumed to bear OHR potential, representative genomes of the different taxa were retrieved from the GTDB database to construct phylogenomic trees. Nine OHR-potential bins, CH3_bin.1, CH3_bin.12, CH3_bin.18, CH3_bin.23, CH3_bin.24, CH3_bin.28, CH3_bin.6, CH3_bin.31, and CH3_bin.35, belonging to *Bacteroidota*, were phylogenetically analyzed with representative genomes (Figure 3.3A). CH3_bin.1 and CH3_bin.12 belong to genus UBA12077, in which three out of six representative genomes were annotated as potential OHRB. CH3_bin.18 belongs to genus SR-FBR-E99, and no RDase was found encoded in the genomes of any of the representatives. CH3_bin.23 was classified into family VadinHA17, which included four potential OHRB representatives from genera UBA9300, JAADHC01, SLNP01 and LD21, of which UBA9300 was most closely related to CH3_bin.23. CH3_bin.31 was phylogenetically close to *Marinifilaceae*, which contained genera *Ancylomarina*, *Marinifilum*, *Ancylomarina*_A, and *Labilibaculum*. Interestingly, we found RDase genes in *Ancylomarina*, *Marinifilum*, and *Ancylomarina*_A. CH3_bin.28 and CH3_bin.35 from family *Melioribacteraceae* were close to the potential OHRB family member, JAADIR01. CH3_bin.24 was classified to genus UBA12170 that has in total two OHRB candidates across the included representatives. CH3_bin.6 was in a close relationship with genus BM520, in which one of three representatives was noted as OHRB candidate. CH3_bin.13 was classified into genus *Izemoplasma*_B in the phylum *Firmicutes*, in which all five representative genomes were potential OHRB (Figure 3.3B). CH3_bin.26 was affiliated with *Vulcanibacillus*, which has one isolate, *V. modesticaldus*, bearing one putative RDase gene. CH3_bin.32, belonging to the *Synergistota*, was close to *Aminiphilus*. In addition, CH3_bin.5 and CH3_bin.10 were phylogenetically close to *Aminobacterium* (Figure 3.3C). Within the *Desulfobacterota*, CH3_bin.15 was closest to

Desulforhopalus that has two OHRB of the ten genome representatives (Figure 3.3D). CH3_bin.30 from *Spirochaeota* was classified into *Oceanispirochaeta* (Figure 3.3E).

Figure 3.3 Phylogenomic trees of phyla including bins containing RDase genes. Representative genomes at phylum level: *Bacteroidota* (A), *Synergistota* (C), *Desulfobacterota* (D), and *Spirochaetota* (E) and class level: *Bacilli* (B). Red circles filled with star indicate potential OHRB, whereas black-solid dots represent non-OHRB .Colored shades indicate branches and nodes containing bins that encode RDase genes, in line with the color patterns used in Figure 3.1.

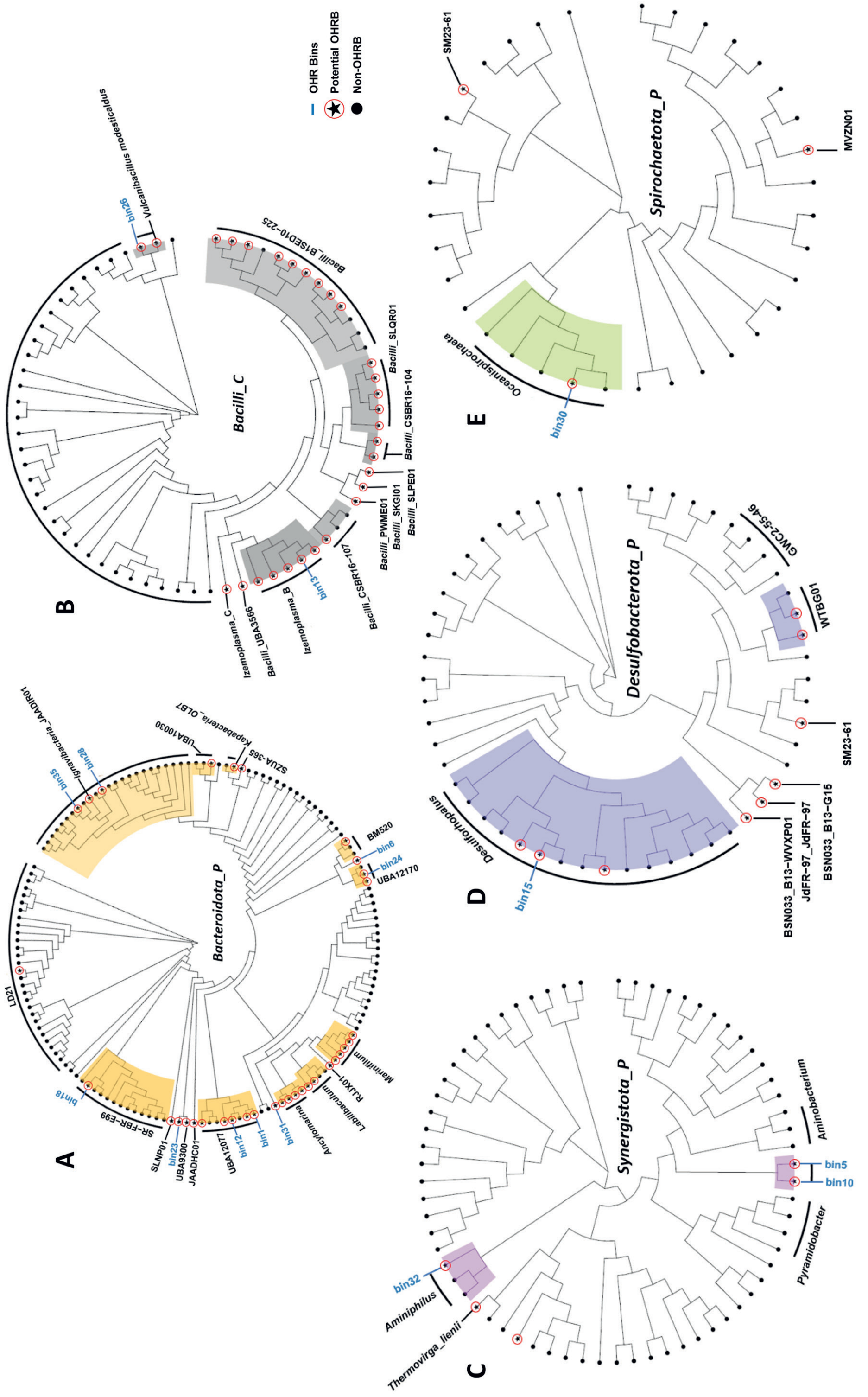

A
Bacteroidota_P
LD21
bin18
SR-FBR-E99
SLNP01
bin23
UBA9300
JAADHC01
UBA12077
bin12
bin1
bin31
Ancylomarina
Labilibaculum
RJJX01
Marinifilum
BM520
bin6
bin24
UBA12170
SZUA-365
Kapabacteria_OLB7
UBA10030
Ignavibacteria_JAADIR01
bin28
bin35
B
Bacilli_C
bin26
Vulcanibacillus modesticaldus
Bacilli_B1SED10-225
Bacilli_SLQR01
Bacilli_CSBR16-104
Bacilli_SLPE01
Bacilli_SKGI01
Bacilli_PWME01
Bacilli_CSBR16-107
bin13
Izemoplasma_B
Bacilli_UBA3566
Izemoplasma_C
– OHR Bins
★ Potential OHRB
● Non-OHRB
C
Synergistota_P
Aminobacterium
bin5
bin10
Pyramidobacter
bin32
Aminiphilus
Thermovirga_lienii
D
Desulfobacterota_P
Desulfohopalus
bin15
BSN033_B13-WVXP01
JdFR-97_JdFR-97
BSN033_B13-G15
SM23-61
WTBG01
GWC2-55-46
E
Spirochaetota_P
Oceanispirochaeta
bin30
SM23-61
MVZN01

Genomic survey of metabolism agreeing to physiological observations during PCE dechlorination

22 bins were found bearing metabolic genes for sulfur metabolism, of which CH3_bin.1, CH3_bin.12, CH3_bin.24, CH3_bin.28, CH3_bin.31, and CH3_bin.35 contained genes encoding both sulfate adenylyl-transferase (S_A_transferase) and adenylyl-sulfate kinase (A_S_kinase) to initiate the reduction of sulfate to sulfite with adenosine 5'-phosphosulfate (APS) as the intermediate. CH3_bin.14, CH3_bin.15, CH3_bin.16, CH3_bin.19, CH3_bin.22, CH3_bin.25, CH3_bin.27, CH3_bin.34, CH3_bin.8 and CH3_bin.9 were annotated with sulfite reductases catalyzing the further reduction of sulfite to sulfide (Figure 3.4D). Interestingly, there was no assembled bin bearing the complete gene set for sulfate reduction to sulfide.

Metabolic marker-gene analyses revealed that there were two types of dehalogenases annotated to utilize organohalides, including RDase and TPh_RDase (Figure 3.4D). We identified 15 bins containing respiratory RDase genes and one TPh-RDase gene from CH3_bin.15 belonging to *Desulforhopalus*. Hydrogen was produced during lactate utilization and PCE dechlorination up to around 70 µM and consumed again after 26 days. Meanwhile, methane was also detected and accumulated to around 240 µM in the absence of added sulfate (Figure 3.4C). Probably, the produced hydrogen provided the electrons for reductive dehalogenation and methanogenesis under these conditions. Further genomic analysis revealed that marker genes encoding group A [Fe-Fe]-hydrogenases were abundant across the bins, for example, CH3_bin.30 and CH3_bin.13 carried five and four genes respectively, and several bins were also found to encode subgroup 1 and 4 type [Ni-Fe]-hydrogenases (Figure 3.4D). The higher numbers found of genes coding for [Fe-Fe]-hydrogenase suggested that they were likely the main contributors to hydrogen oxidation in accordance with previous results that [Fe-Fe]-hydrogenases were more active and had higher turnover frequency than [Ni-Fe]-hydrogenases (Madden et al., 2012). In addition, CH3_bin.23, CH3_bin.31 and CH3_bin.6 had only [Fe-Fe]-

hydrogenases, whereas, CH3_bin.10, CH3_bin.14, CH3_bin.15, CH3_bin.21 and CH3_bin.26 only encoded [Ni-Fe]-hydrogenases. Genes coding for methyl-coenzyme M reductases (*mcr*) contributing to methane production were only found in CH3_bin.33, classified into *Methanogenium*, which contained two genes of each *mcrA*, *mcrB*, and *mcrG*.

Figure 3.4 Metabolite detection and annotation of related marker genes. Utilization of lactate under sulfate-free, NS (A), and sulfate-amended, S (B) conditions. Hydrogen and methane were only detected in NS cultures (C); Marker genes involved in the cycling of sulfur, halogens, hydrogen and methane were searched against the bins and counted (D); Thereinto, specific marker genes were selected corresponding to physiological observations (D). Bars in figures A, B and C represent the standard errors of the duplicate cultures as described in Figure 3.1.

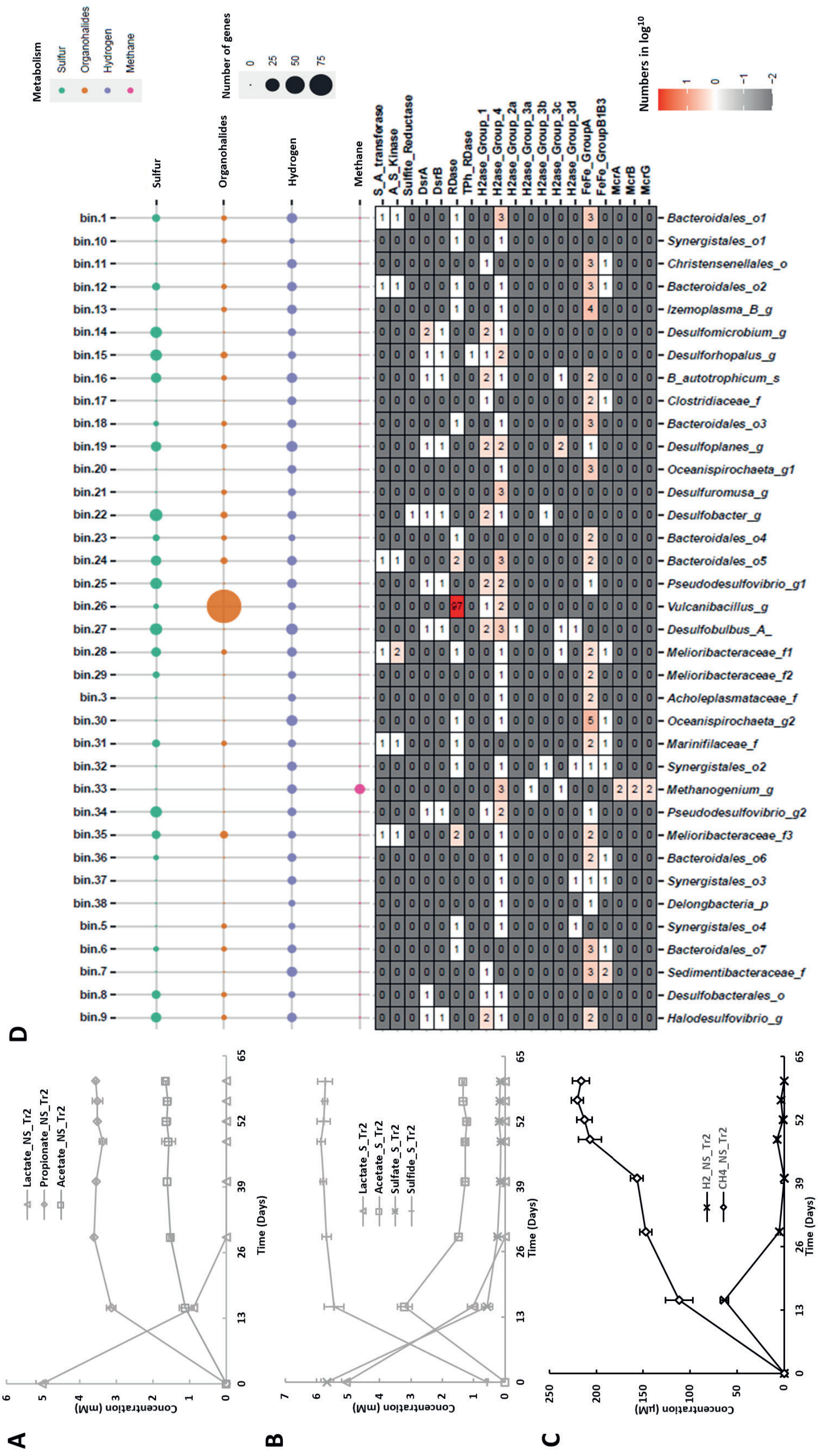

		S_A_transferase	A_S_Kinase	Sulfite_Reductase	DsrA	DsrB	RDase	TPh_RDase	H2ase_Group_1	H2ase_Group_4	H2ase_Group_2a	H2ase_Group_3a	H2ase_Group_3b	H2ase_Group_3c	H2ase_Group_3d	FeFe_GroupA	FeFe_GroupB1B3	McrA	McrB	McrG
bin.1	*Bacteroidales_o1*	1	1	0	0	0	1	0	0	3	0	0	0	0	0	3	0	0	0	0
bin.10	*Synergistales_o1*	0	0	0	0	0	1	0	0	1	0	0	0	0	0	0	0	0	0	0
bin.11	*Christensenellales_o*	0	0	0	0	0	0	0	1	0	0	0	0	0	0	3	1	0	0	0
bin.12	*Bacteroidales_o2*	1	1	0	0	0	1	0	0	1	0	0	0	0	0	3	1	0	0	0
bin.13	*Izemoplasma_B_g*	0	0	0	0	0	1	0	0	1	0	0	0	0	0	4	0	0	0	0
bin.14	*Desulfomicrobium_g*	0	0	0	2	1	0	0	2	1	0	0	0	0	0	0	0	0	0	0
bin.15	*Desulforhopalus_g*	0	0	0	1	1	0	1	1	2	0	0	0	0	0	0	0	0	0	0
bin.16	*B_autotrophicum_s*	0	0	0	1	1	0	0	2	1	0	0	0	1	0	2	0	0	0	0
bin.17	*Clostridiaceae_f*	0	0	0	0	0	0	0	1	0	0	0	0	0	0	2	1	0	0	0
bin.18	*Bacteroidales_o3*	0	0	0	0	0	1	0	0	1	0	0	0	0	0	3	0	0	0	0
bin.19	*Desulfoplanes_g*	0	0	0	1	1	0	0	2	2	0	0	0	2	0	1	0	0	0	0
bin.20	*Oceanispirochaeta_g1*	0	0	0	0	0	0	0	0	1	0	0	0	0	0	3	0	0	0	0
bin.21	*Desulfuromusa_g*	0	0	0	0	0	0	0	0	3	0	0	0	0	0	0	0	0	0	0
bin.22	*Desulfobacter_g*	0	0	1	1	1	0	0	2	1	0	0	1	0	0	0	0	0	0	0
bin.23	*Bacteroidales_o4*	0	0	0	0	0	1	0	0	0	0	0	0	0	0	2	0	0	0	0
bin.24	*Bacteroidales_o5*	1	1	0	0	0	2	0	0	3	0	0	0	0	0	2	0	0	0	0
bin.25	*Pseudodesulfovibrio_g1*	0	0	0	1	1	0	0	2	2	0	0	0	0	0	1	0	0	0	0
bin.26	*Vulcanibacillus_g*	0	0	0	0	0	97	0	1	2	0	0	0	0	0	0	0	0	0	0
bin.27	*Desulfobulbus_A_*	0	0	0	1	1	0	0	2	3	1	0	0	1	1	0	0	0	0	0
bin.28	*Melioribacteraceae_f1*	1	2	0	0	0	1	0	0	1	0	0	0	1	0	2	1	0	0	0
bin.29	*Melioribacteraceae_f2*	0	0	0	0	0	0	0	0	1	0	0	0	0	0	2	0	0	0	0
bin.3	*Acholeplasmataceae_f*	0	0	0	0	0	0	0	0	1	0	0	0	0	0	2	0	0	0	0
bin.30	*Oceanispirochaeta_g2*	0	0	0	0	0	1	0	0	1	0	0	0	0	0	5	1	0	0	0
bin.31	*Marinifilaceae_f*	1	1	0	0	0	1	0	0	0	0	0	0	0	0	2	1	0	0	0
bin.32	*Synergistales_o2*	0	0	0	0	0	1	0	0	1	0	0	1	0	1	1	1	0	0	0
bin.33	*Methanogenium_g*	0	0	0	0	0	0	0	0	3	0	1	0	1	0	0	0	2	2	2
bin.34	*Pseudodesulfovibrio_g2*	0	0	0	1	1	0	0	1	2	0	0	0	0	0	1	0	0	0	0
bin.35	*Melioribacteraceae_f3*	1	1	0	0	0	2	0	0	1	0	0	0	0	0	2	0	0	0	0
bin.36	*Bacteroidales_o6*	0	0	0	0	0	0	0	0	1	0	0	0	0	0	2	1	0	0	0
bin.37	*Synergistales_o3*	0	0	0	0	0	0	0	0	1	0	0	0	0	1	1	1	0	0	0
bin.38	*Delongbacteria_p*	0	0	0	0	0	0	0	0	1	0	0	0	0	0	1	0	0	0	0
bin.5	*Synergistales_o4*	0	0	0	0	0	1	0	0	1	0	0	0	0	1	0	0	0	0	0
bin.6	*Bacteroidales_o7*	0	0	0	0	0	1	0	0	0	0	0	0	0	0	3	1	0	0	0
bin.7	*Sedimentibacteraceae_f*	0	0	0	0	0	0	0	1	0	0	0	0	0	0	3	2	0	0	0
bin.8	*Desulfobacterales_o*	0	0	0	1	0	0	0	1	1	0	0	0	0	0	0	0	0	0	0
bin.9	*Halodesulfovibrio_g*	0	0	0	1	1	0	0	2	1	0	0	0	0	0	2	0	0	0	0

Phylogeny of RDases and their gene expression

Most RDases from CH3_bin.26 were phylogenetically closely related to each other with respect to their amino acid sequences (Table S3.3). RDases from other bins, except CH3_bin.35, CH3_bin.15, CH3_bin.31 and CH3_bin.24, were in a close phylogenetic relationship to each other, but distant to the RDases from CH3_bin.26 (Figure 3.5), suggesting a different origin. RDase gene expression profiles were analyzed to specify their possible contributions to PCE dechlorination. No RDase gene transcripts were observed for CH3_bin.35, CH3_bin.1, CH3_bin.6, CH3_bin.10, CH3_bin.12, bin13, CH3_bin.23, CH3_bin.24, CH3_bin.28, CH3_bin.30, or CH3_bin.31. Hence, it is unlikely that those genes were involved in the dechlorination of PCE. In contrast, transcripts of several RDase genes of CH3_bin.26 were observed regardless of the presence of sulfate, including RDase3, RDase9, RDase21, RDase23, RDase43, RDase54, RDase58, RDase60, RDase61, RDase64, RDase75, RDase79 and RDase96. The RDase gene of CH3_bin.18 was transcribed only in PCE_S3 culture with 508.2 transcripts, whereas, 23 RDase genes of CH3_bin.26 were only found expressed in PCE_NS3 (Table S3.4). All the other RDase genes were expressed to different extents with and without sulfate. The genes from CH3_bin.15, and RDase36, RDase41, RDase42, RDase45, and RDase46 from CH3_bin.26, were expressed in all duplicate cultures (Figure 3.5). Notably, 84 of the 97 RDase genes from CH3_bin.26 were found expressed during PCE dechlorination, which suggests the important role of CH3_bin.26 to dehalogenate PCE in the cultures described here. In addition, most RDase genes in CH3_bin.26 were found clustered together in one assembled contig, with less than five genes interval between every two RDase genes (Table S3.4).

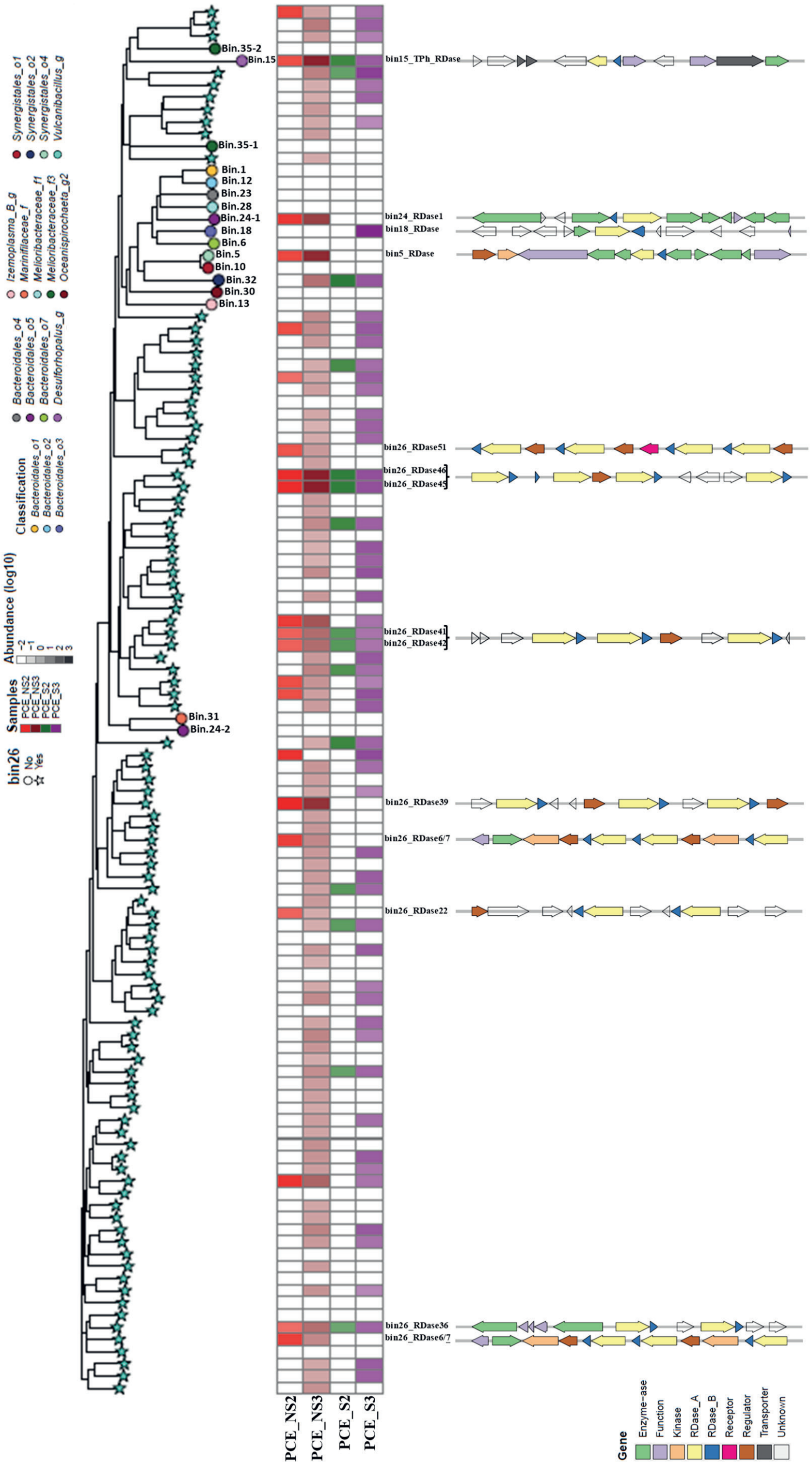
bin26
No
Yes
Samples
PCE_NS2
PCE_NS3
PCE_S2
PCE_S3
Abundance (log10)
-2
-1
0
1
2
3
Classification
Bacteroidales_o1
Bacteroidales_o2
Bacteroidales_o3
Bacteroidales_o4
Bacteroidales_o5
Bacteroidales_o7
Desulforhopalus_g
Izemoplasma_B_g
Marinifilaceae_f
Melioribacteraceae_f1
Melioribacteraceae_f3
Oceanispirochaeta_g2
Synergistales_o1
Synergistales_o2
Synergistales_o4
Vulcanibacillus_g
Bin.35-2
Bin.15
Bin.35-1
Bin.1
Bin.12
Bin.23
Bin.28
Bin.24-1
Bin.18
Bin.6
Bin.5
Bin.10
Bin.32
Bin.30
Bin.13
Bin.31
Bin.24-2
bin15_TPh_RDase
bin24_RDase1
bin18_RDase
bin5_RDase
bin26_RDase51
bin26_RDase46
bin26_RDase45
bin26_RDase41
bin26_RDase42
bin26_RDase39
bin26_RDase6/7
bin26_RDase22
bin26_RDase36
bin26_RDase6/7
PCE_NS2
PCE_NS3
PCE_S2
PCE_S3
Gene
Enzyme-ase
Function
Kinase
RDase_A
RDase_B
Receptor
Regulator
Transporter
Unknown

Figure 3.5 Phylogenetic tree of RDases and their gene transcripts attached with corresponding gene clusters. The protein sequences of RDases were collected and aligned via online Clustal Omega. Stars at the nodes indicate that RDases were encoded on CH3_bin.26. RDases encoded on other bins are depicted by differently colored circles. The extended heatmap corresponding to the RDase node indicates gene transcript abundance (log10 transformed). The depicted gene clusters represent those RDase genes transcribed in both duplicates of NS and S, only in duplicates of NS, or only in S. RDase41/42, RDase45/46, and RDase6/7 are in the same cluster, respectively (Table S3.4).

Diverse regulatory systems flanking RDase genes

Similar to the genes encoding RDases, the neighboring genes coding for transcriptional regulators were subjected to further analysis. CRP / FNR and TCS were the main expressed transcriptional regulators, containing 22 and 9 members, respectively (Figure 3.6A). CRP, the cAMP-activated global transcriptional regulator, was represented by 12 members, divided further into three groups based on sequence similarities (Chandler, 1992). CRP-2 and CRP-3 were represented by a higher number of transcripts compared to CRP-1 (Figure 3.6B). Five members of GlxR (Kim et al., 2004), a CRP-like regulator, were found expressed, with GlxR1-3 exhibiting higher transcription levels compared to the rest.

Nine two-component systems (TCS) were identified, of which NatR2 for regulating sodium ion extrusion (Ogura et al., 2007), WalR2 for cell wall metabolism and virulence, and RpfG for signaling response, were highly expressed (Figure 3.6B). Interestingly, four transcriptional regulators functioning as repressors were also highly expressed, including DtxR for inhibiting Diphtheria toxin production, HrcA for preventing heat-shock induction, SarZ for attenuating virulence, and AcrR for global stresses (Ma et al., 1996; Narberhaus, 1999; Pohl et al., 1999; Kaito et al., 2006). In addition, CysL, belonging to LysR-type regulators related with L-Cysteine biosynthesis (Guillouard et al., 2002), and SigW, an extra-cytoplasmic function (ECF) sigma factor responding to alkaline shock stress (Wiegert et al., 2001), were also induced during PCE dechlorination (Figure 3.6B). To better understand the regulons of these expressed transcriptional regulators, we obtained promoter sequences of RDase genes by defining intergenic regions shorter than 300bp between the RDase gene and the upstream gene (Table S3.5). There were 12 promoter sequences collected and each was found to contain binding sites following the consensus for CRP regulons of *Escherichia coli* (5'-TGTGACAAAATTCA*T-3', MX000093: CRP, PRODORIC) (Dudek and Jahn, 2022) (Figure 3.6C). In a similar way, predicted binding sites of FNR followed the consensus 5'-TT*T*CA**AA**AA-3' according to the two promoters of RDase genes following the consensus for known FNR regulons (MX000004: Fnr, PRODORIC). The binding sites of GlxR, YpdB, and NatR were predicted based on their RDase genes' promoters alignment. Two promoter candidates, RDase4 and RDase70 of CH3_bin.26, were assumed to be under the regulation of NtcA (MX000209: NtcA), of which only the promoter sequence of RDase70 was found to contain the binding site, 5'-GTATAAATATAAAC-3'.

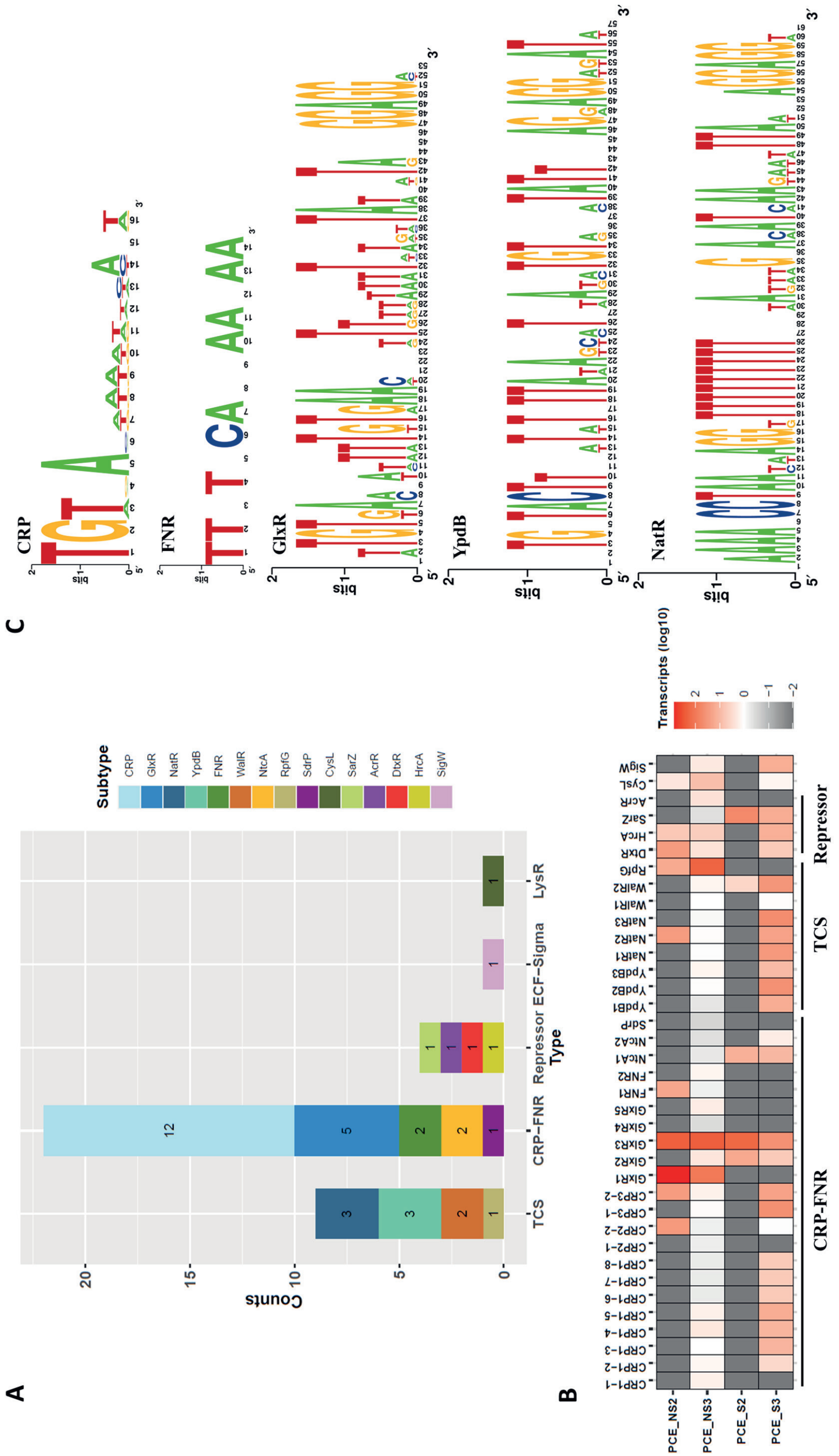
A
Counts
0
5
10
15
20
Type
TCS
CRP–FNR
Repressor
ECF–Sigma
LysR
3
3
2
1
12
5
2
2
1
1
1
1
1
1
1
Subtype
CRP
GlxR
NatR
YpdB
FNR
WalR
NtcA
RpfG
SdrP
CysL
SarZ
AcrR
DtxR
HrcA
SigW
B
PCE_NS2
PCE_NS3
PCE_S2
PCE_S3
CRP1-1
CRP1-2
CRP1-3
CRP1-4
CRP1-5
CRP1-6
CRP1-7
CRP1-8
CRP2-1
CRP2-2
CRP3-1
CRP3-2
GlxR1
GlxR2
GlxR3
GlxR4
GlxR5
FNR1
FNR2
NtcA1
NtcA2
SdrP
YpdB1
YpdB2
YpdB3
NatR1
NatR2
NatR3
WalR1
WalR2
RpfG
DtxR
HrcA
SarZ
AcrR
CysL
SigW
CRP-FNR
TCS
Repressor
Transcripts (log10)
2
1
0
−1
−2
C
CRP
FNR
GlxR
YpdB
NatR
bits
5′
3′

Figure 3.6 Classification and transcript abundance of expressed transcriptional regulators (A,B) and their predicted binding motifs (C). A) groups of transcriptional regulators, TCS, two-component systems; CRP-FNR, CRP (cyclic AMP receptor protein) / FNR (fumarate and nitrate reduction regulator); ECF-Sigma (ECF-σ): Extra-cytoplasmic function sigma factor; PCE_NS2 and PCE_NS3: duplicate PCE dechlorinating cultures without additional sulfate; PCE_S2 and PCE_S3: duplicate PCE dechlorinating cultures with additional sulfate; The potential binding sites were identified on the basis of binding motif in the potential promoter regions and displayed in Weblogo (https://weblogo.berkeley.edu/logo.cgi).

Discussion

Our previous work demonstrated that marine sediments from Aarhus Bay can dehalogenate a broad range of organohalides, such as PCE, under sulfate amended and sulfate free conditions (Chapter 2), which for the first time provided physiological evidence of OHR for marine sediments of Aarhus Bay (Wasmund et al., 2014; Wasmund et al., 2015; Wasmund et al., 2016; Zinke et al., 2017; Jochum et al., 2018). Therefore, further pinpointing OHRB populations residing in Aarhus Bay marine sediments was the logical next step. To this end, we recruited metagenomics and -transcriptomics, yielding 37 assembled bins with high quality, of which 16 bins were predicted to represent OHRB due to their genomic annotation with RDase genes. The taxonomic classification of these OHR bins unveiled a wide distribution of RDase genes among members of *Bacteroidota*, *Snergistota*, and *Spirochaetota* in addition to the well-known phyla, such as *Firmicutes* and *Chloroflexota* (Atashgahi et al., 2016). Gene expression analyses indicated that RDase genes of CH3_bin.26, CH3_bin.15, CH3_bin.24, CH3_bin.18, and CH3_bin.5 played the main role in PCE dechlorination, in which CH3_bin.26 was phylogenetically close to *Vulcanibacillus modesticaldus*, and bore an unprecedently high number of 97 different RDase genes, which is significantly more than the copy numbers in typical OHRB (e.g. *Dehalococcoides mccartyi* CG1 with 36 RDase genes (Molenda et al., 2020)). In addition, most of the induced RDase genes were clustered with genes encoding diverse regulatory systems suggesting their strong flexibility adapting to environmental changes or the availability of different organohalides.

Wide distribution of RDases beyond well-characterized OHRB

Most of the OHRB were isolated from organohalide-contaminated areas, such as soils, rivers and lakes (Wiegel and Wu, 2000; Lee and He, 2010; Chambon et al., 2013). They belong to the phyla *Chloroflexota*, *Firmicutes*, *Desulfobacterota*, and *Proteobacteria* (Atashgahi et al., 2016; Waite et al., 2020). Although pristine marine sediments have been shown to contain OHRB such as *Dehalococcoides* (Fincker et al., 2020), fewer OHRB were isolated from pristine marine environments, which might be due to the limited knowledge of their metabolic potential and limited methods for isolation. The employed integration of metagenomics and metatranscriptomics in this study allowed for the assembly of 15 OHR bins with high quality, some of which belonging to *Bacteroidota*, *Spirochaetota*, and *Synergistota* phyla that have never been reported to catalyze reductive dehalogenation. The average nucleotide identity (ANI) of these OHR bins was below 95% in all cases after running the "classify_wf" of GTDB, indicating they are novel genomes. Our further exploration together with representative genomes of these phyla revealed that 112 genomes of *Bacteroidota*, 15 genomes of *Spirochaetota*, and seven genomes of *Synergistota* are bearing RDase genes, with none of the corresponding isolates being physiologically characterized to perform OHR. To this end, it is noteworthy that our study using genome-resolved strategies discovered that the RDase genes from CH3_bin.18, classified into *Bacteroidota*, and from CH3_bin.5 and CH3_bin.32, classified into *Synergistota*, were expressed in PCE dechlorinating cultures (Table S3.2), and their genome abundances and genomic transcripts were in high numbers, suggesting that OHR potential exists in these phyla. The RDase genes in the other bins from the above phyla were not found expressed in our data, indicating that they were probably not involved in the respiration of PCE in our experiments. We found 32 representative genomes from the class

Bacilli that are annotated with RDase genes. CH3_bin.26 is closely related to *Vulcanibacillus* which has one isolate from a moderately hydrothermal vent containing one RDase gene (l'Haridon et al., 2006). In contrast, CH3_bin.26 was predicted to contain 97 RDase genes, a number that is higher than the maximum number of 36 currently reported for members of *Dehalococcoides* (Kube et al., 2005; Seshadri et al., 2005; Molenda et al., 2020). *Desulfobacterota* is a reclassified phylum from Deltaproteobacteria and well known for catalyzing sulfate reduction (Waite et al., 2020). Eighty-nine of the 939 representative genomes in the *Desulfobacterota* were found to carry RDase genes, similar to previously described strains of *Desulfoluna*, *Desulfuromusa*, and *Desulfovibrio* (Liu and Haggblom, 2018; Peng et al., 2020b). CH3_bin.21, classified into *Desulfuromusa*, had no annotated genes involved in OHR or sulfate reduction and had a high abundance when sulfate was absent as was also found in the preceding study (Chapter 2). CH3_bin.21 only has three group 4 [Ni-Fe]-hydrogenase genes, and could thus act as a potential hydrogen producer in our cultures. Noticeably, the higher numbers found of genes coding for [Fe-Fe]-hydrogenase suggested that they were likely the main contributors to hydrogen production in accordance with previous results that [Fe-Fe]-hydrogenases were more active and had higher turnover frequency than [Ni-Fe]-hydrogenases (Madden et al., 2012). CH3_bin.15 was most closely affiliated with the genus *Desulforhopalus*, of which one putative OHRB is *D. singaporensis* (Lie et al., 1999). Noticeably, the deduced RDase from CH3_bin.15 does not belong to the canonical RDases associated with OHR, such as PceA from *Dehalococcoides* (Magnuson et al., 1998; Fung et al., 2007), and was more similar in sequence and size to TPh-RDase from *Sphingobium chlorophenolicum* (previously named as *Flavobacterium* sp.) that can dehalogenate tetrachlorohydroquinone thiolytically (Xun et al., 1992b, a). Of interest, the TPh-RDase from CH3_bin.15 was not reported for respiratory dehalogenation to conserve energy, however, the transcript data revealed TPh-RDase bears potential biodegrading activity of PCE in the cultures studied here. Moreover, the genomic abundance and transcript of CH3_bin.15 indicated its participation in PCE dechlorination. Thus, further metabolic analysis of CH3_bin.15 is essential. Altogether, marine sediments of Aarhus Bay are home to several new OHRB candidates with diverse RDase genes.

RDase gene clusters

Recently, an extensive genomic survey found that some RDase gene clusters lack genes encoding anchor protein B, or the N-terminus of RDase bears transmembrane domains, which could leave the RDase functioning in the cytoplasm or the C-terminus spanning towards the outer face of the membrane (Low et al., 2015; Atashgahi, 2019). In our study, we also observed some OHR bins without putative RdhB encoding genes, including CH3_bin.12, CH3_bin.1, CH3_bin.28, CH3_bin.32 and CH3_bin.6. Of these, transcripts of the RDase gene in CH3_bin.32 indicated the possible cytoplasmic dehalogenation that awaits further experimental confirmation. In most cases, RDase genes were accompanied by diverse functional gene sets, such as cobamide cofactor biosynthesis pathway genes in *Sulfurospirillum* strains and molecular chaperones in *Desulfitobacterium* (Smidt et al., 2000; Goris et al., 2014; Goris et al., 2017). Similarly, some RDase gene clusters found in the present study contained chaperone genes vicinal to genes encoding RDase3, RDase4, RDase35, RDase93 of CH3_bin.26 that could protect the RDase activity in a manner of maintaining structural integrity when exposed to harsh environments. Besides, there were several genes encoding electron transport complexes accompanying RDase genes, including RDase in CH3_bin.13, CH3_bin.31, RDase2 in CH3_bin.24 and CH3_bin.35, and RDase4, RDase67, RDase69, RDase73, RDase82, and RDase84 in CH3_bin.26, which could form new electron transport chains to promote OHR in addition to the previously identified ones (Kublik et al., 2016; Wang et al., 2018).

Furthermore, RDase genes were frequently flanked by genes coding for transcriptional regulators, which might timely and accurately regulate the expression of vicinal RDase genes in response to the added organohalides. Three regulatory systems were previously characterized, including those of the CRP-FNR family, MarR and TCS (Smidt et al., 2000; Gabor et al., 2006; Mazon et al., 2007; Wagner et al., 2013; Goris et al., 2014). Expressed transcriptional regulators classified into CRP/FNR systems accounted for the largest numbers in our study, whereas, GlxR, as a new regulator, showed different regulons inferred from the promoter alignment as well as YpdB and NatR from the class of TCS. In addition, four negative regulators were found that could follow the modulation reported for MarR-type regulators (Wagner et al., 2013), but their binding sites were unclear and need further demonstration. Noticeably, ECF sigma factor, SigW, was also found transcribed during PCE dechlorination, which was rarely reported to regulate dehalogenation, and its DNA binding motif seems different from that in *Bacillus subtilis* (MX000079: SigW). Taken together, the newly-discovered regulatory systems diversified the known modes of regulation of dehalogenation that could be the result of adaptation to challenging environments, and further molecular identification would substantially build up our understanding on reductive dehalogenation and its regulation in natural systems.

Acknowledgements

This study was supported by the Dutch Research Council through the UNLOCK project (NRGWI.obrug.2018.005), as well as Wageningen University through its Innovation Program Microbiology. We thank Felix Homa and Victor de Jager (Laboratory of Microbiology, Wageningen University) for providing help for the metagenomic and meta-transcriptomic analyses. We furthermore would like to thank Sjoerd Engelbertink for GC-MS measurements. We acknowledge the China Scholarship Council (CSC) for the support to Chen Zhang (File No. 201807720048).

Supplementary Information

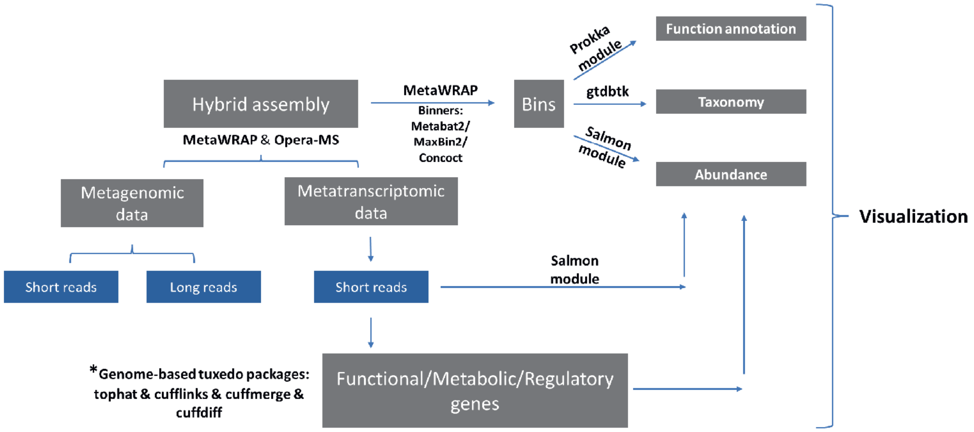

Figure S3.1 Outline of metagenomic and meta-transcriptomic sequence processing and analyses. * Analyses of metatranscriptomic data was performed by tuxedo packages that include tophat (aligning reads), cufflinks (assembling transcripts), cuffmerge (merging transcripts) and cuffdiff (identifying differentially-expressed transcripts) (Trapnell, et al. 2012). Arrows in blue indicate stepwise analyses. Visualization of output data was achieved using R and the required packages, including ggplot2, ggtree, and gggenes.

Data availability of supplementary tables

The supplementary tables for this chapter are reposited at:

https://git.wur.nl/afsg-microbiology/publication-supplementary-materials/2023_chen_thesis_decoding_ohr_aarhus_bay.git).

Table S3.1 Metagenomic assembly, using short and long read DNA sequences as well as short read metatranscriptome sequences

Table S3.2 Metagenome Assembled Genomes (MAGs) with abundance of genomic copies and transcripts in per million reads unit

Table S3.3 Protein sequences of RDases among bins

Table S3.4 Transcriptional profile of RDase genes in OHR bins

Table S3.5 Predicted promoter sequences of RDase genes

References

Anantharaman K, Hausmann B, Jungbluth SP *et al.* Expanded diversity of microbial groups that shape the dissimilatory sulfur cycle. *ISME J* 2018;12: 1715-28.

Atashgahi S. Discovered by genomics: putative reductive dehalogenases with N-terminus transmembrane helixes. *FEMS Microbiol Ecol* 2019;95: fiz048.

Atashgahi S, Haggblom MM, Smidt H. Organohalide respiration in pristine environments: implications for the natural halogen cycle. *Environ Microbiol* 2018;20: 934-48.

Atashgahi S, Lu Y, Smidt H. Overview of known organohalide-respiring bacteria—phylogenetic diversity and environmental distribution. In: Adrian L, Löffler FE (eds.) *Organohalide-Respiring Bacteria*. Berlin, Heidelberg: Springer Berlin Heidelberg, 2016, 63-105.

Bender KS, Shang C, Chakraborty R *et al.* Identification, characterization, and classification of genes encoding perchlorate reductase. *J Bacteriol* 2005;187: 5090-6.

Bertrand D, Shaw J, Kalathiyappan M *et al.* Hybrid metagenomic assembly enables high-resolution analysis of resistance determinants and mobile elements in human microbiomes. *Nat Biotechnol* 2019;37: 937-44.

Bokulich NA, Kaehler BD, Rideout JR *et al.* Optimizing taxonomic classification of marker-gene amplicon sequences with QIIME 2's q2-feature-classifier plugin. *Microbiome* 2018;6: 1-17.

Bradley A, Leavitt W, Johnston D. Revisiting the dissimilatory sulfate reduction pathway. *Geobiology* 2011;9: 446-57.

Cases I, De Lorenzo V. Promoters in the environment: transcriptional regulation in its natural context. *Nat Rev Microbiol* 2005;3: 105-18.

Chambon JC, Bjerg PL, Scheutz C *et al.* Review of reactive kinetic models describing reductive dechlorination of chlorinated ethenes in soil and groundwater. *Biotechnol Bioeng* 2013;110: 1-23.

Chandler MS. The gene encoding cAMP receptor protein is required for competence development in Haemophilus influenzae Rd. *Proc Natl Acad Sci USA* 1992;89: 1626-30.

Chaumeil P-A, Mussig AJ, Hugenholtz P *et al.* GTDB-Tk: a toolkit to classify genomes with the Genome Taxonomy Database. *Bioinformatics* 2020;36: 1925-7.

Chen WJ, Zhu T. Networks of transcription factors with roles in environmental stress response. *Trends Plant Sci* 2004;9: 591-6.

Cline JD. Spectrophotometric determination of hydrogen sulfide in natural waters. *Limnol Oceanogr* 1969;14: 454-8.

Coates JD, Achenbach LA. Microbial perchlorate reduction: rocket-fuelled metabolism. *Nat Rev Microbiol* 2004;2: 569-80.

Dudek C-A, Jahn D. PRODORIC: state-of-the-art database of prokaryotic gene regulation. *Nucleic Acids Res* 2022;50: D295-D302.

Eren AM, Kiefl E, Shaiber A *et al.* Community-led, integrated, reproducible multi-omics with anvi'o. *Nat Microbiol* 2021;6: 3-6.

Evans PN, Boyd JA, Leu AO *et al.* An evolving view of methane metabolism in the Archaea. *Nat Rev Microbiol* 2019;17: 219-32.

Fincker M, Spormann AM. Biochemistry of catabolic reductive dehalogenation. *Annu Rev Biochem* 2017;86: 357-86.

Franzosa EA, Hsu T, Sirota-Madi A *et al.* Sequencing and beyond: integrating molecular'omics' for microbial community profiling. *Nat Rev Microbiol* 2015;13: 360-72.

Fung JM, Morris RM, Adrian L *et al.* Expression of reductive dehalogenase genes in *Dehalococcoides ethenogenes* strain 195 growing on tetrachloroethene, trichloroethene, or 2, 3-dichlorophenol. *Appl Environ Microbiol* 2007;73: 4439-45.

Gabor K, Verissimo CS, Cyran BC *et al.* Characterization of CprK1, a CRP/FNR-type transcriptional regulator of halorespiration from *Desulfitobacterium hafniense*. *J Bacteriol* 2006;188: 2604-13.

Garber A, Ramirez G, Merino N *et al.* MagicLamp: toolkit for annotation of ‘omics datasets using curated HMM sets. *GitHub Repository Available online at https://github com/Arkadiy-Garber/MagicLamp (accessed January, 2022)* 2020.

Goodwin S, McPherson JD, McCombie WR. Coming of age: ten years of next-generation sequencing technologies. *Nat Rev Genet* 2016;17: 333-51.

Goris T, Schenz B, Zimmermann J *et al.* The complete genome of the tetrachloroethene-respiring Epsilonproteobacterium *Sulfurospirillum halorespirans*. *J Biotechnol* 2017;255: 33-6.

Goris T, Schubert T, Gadkari J *et al.* Insights into organohalide respiration and the versatile catabolism of Sulfurospirillum multivorans gained from comparative genomics and physiological studies. *Environ Microbiol* 2014;16: 3562-80.

Gribble GW. Recently discovered naturally occurring heterocyclic organohalogen compounds. *Heterocycles* 2012;84: 157-207.

Gribble GW. A recent survey of naturally occurring organohalogen compounds. *Environ Chem* 2015;12: 396-405.

Guillouard I, Auger S, Hullo M-Fo *et al.* Identification of *Bacillus subtilis* CysL, a regulator of the cysJI operon, which encodes sulfite reductase. *J Bacteriol* 2002;184: 4681-9.

Hakemian AS, Rosenzweig AC. The biochemistry of methane oxidation. *Annu Rev Biochem* 2007;76: 223-41.

Hallenbeck PC, Clark MA, Barrett EL. Characterization of anaerobic sulfite reduction by *Salmonella typhimurium* and purification of the anaerobically induced sulfite reductase. *J Bacteriol* 1989;171: 3008-15.

Hisano T, Hata Y, Fujii T *et al.* Crystal structure of L-2-Haloacid dehalogenase from *Pseudomonas* sp. YL: an α/β hydrolase structure that is different from the α/β hydrolase fold. *J Biol Chem* 1996;271: 20322-30.

Hug LA, Maphosa F, Leys D *et al.* Overview of organohalide-respiring bacteria and a proposal for a classification system for reductive dehalogenases. *Philos Trans R Soc Lond B Biol Sci* 2013;368: 20120322.

Jochum LM, Schreiber L, Marshall IPG *et al.* Single-cell genomics reveals a diverse metabolic potential of uncultivated *Desulfatiglans*-related Deltaproteobacteria widely distributed in marine sediment. *Front Microbiol* 2018;9: 2038.

Kaito C, Morishita D, Matsumoto Y *et al.* Novel DNA binding protein SarZ contributes to virulence in *Staphylococcus aureus*. *mol Microbiol* 2006;62: 1601-17.

Kim H-J, Kim T-H, Kim Y *et al.* Identification and characterization of *glxR*, a gene involved in regulation of glyoxylate bypass in *Corynebacterium glutamicum*. *J Bacteriol* 2004;186: 3453-60.

Koonin EV, Tatusov RL. Computer analysis of bacterial haloacid dehalogenases defines a large superfamily of hydrolases with diverse specificity: application of an iterative approach to database search. *J Mol Biol* 1994;244: 125-32.

Kube M, Beck A, Zinder SH *et al.* Genome sequence of the chlorinated compound–respiring bacterium *Dehalococcoides* species strain CBDB1. *Nat Biotechnol* 2005;23: 1269-73.

Kublik A, Deobald D, Hartwig S *et al.* Identification of a multi-protein reductive dehalogenase complex in *Dehalococcoides mccartyi* strain CBDB1 suggests a protein-dependent respiratory electron transport chain obviating quinone involvement. *Environ Microbiol* 2016;18: 3044-56.

l'Haridon S, Miroshnichenko M, Kostrikina N *et al. Vulcanibacillus modesticaldus* gen. nov., sp. nov., a strictly anaerobic, nitrate-reducing bacterium from deep-sea hydrothermal vents. *Int J Syst Evol Microbiol* 2006;56: 1047-53.

Leavitt WD, Bradley AS, Santos AA *et al.* Sulfur isotope effects of dissimilatory sulfite reductase. *Front Microbiol* 2015;6: 1392.

Lee LK, He J. Reductive debromination of polybrominated diphenyl ethers by anaerobic bacteria from soils and sediments. *Appl Environ Microbiol* 2010;76: 794-802.

Lee MD. GToTree: a user-friendly workflow for phylogenomics. *Bioinformatics* 2019;35: 4162-4.

Leloup J, Fossing H, Kohls K *et al.* Sulfate-reducing bacteria in marine sediment (Aarhus Bay, Denmark): abundance and diversity related to geochemical zonation. *Environ Microbiol* 2009;11: 1278-91.

Lie TJ, Clawson ML, Godchaux W *et al.* Sulfidogenesis from 2-aminoethanesulfonate (taurine) fermentation by a morphologically unusual sulfate-reducing bacterium, *Desulforhopalus singaporensis* sp. nov. *Appl Environ Microbiol* 1999;65: 3328-34.

Liu J, Haggblom MM. Genome-guided identification of organohalide-respiring Deltaproteobacteria from the marine environment. *mBio* 2018;9: e02471-18.

Low A, Shen Z, Cheng D *et al.* A comparative genomics and reductive dehalogenase gene transcription study of two chloroethene-respiring bacteria, *Dehalococcoides mccartyi* strains MB and 11a. *Sci Rep* 2015;5: 1-12.

Lubitz W, Ogata H, Rudiger O *et al.* Hydrogenases. *Chem Rev* 2014;114: 4081-148.

Ma D, Alberti M, Lynch C *et al.* The local repressor AcrR plays a modulating role in the regulation of acrAB genes of *Escherichia coli* by global stress signals. *Mol Microbiol* 1996;19: 101-12.

Madden C, Vaughn MD, Díez-Pérez I *et al.* Catalytic turnover of [FeFe]-hydrogenase based on single-molecule imaging. *J Am Chem Soc* 2012;134: 1577-82.

Magnuson J, Stern R, Gossett J *et al.* Reductive dechlorination of tetrachloroethene to ethene by a two-component enzyme pathway. *Appl Environ Microbiol* 1998;64: 1270-5.

Maillard J, Schumacher W, Vazquez F *et al.* Characterization of the corrinoid iron-sulfur protein tetrachloroethene reductive dehalogenase of *Dehalobacter restrictus*. *Appl Environ Microbiol* 2003;69: 4628-38.

Maillard J, Willemin MS. Regulation of organohalide respiration. *Adv Microb Physiol* 2019;74: 191-238.

Martınez-Antonio A, Collado-Vides J. Identifying global regulators in transcriptional regulatory networks in bacteria. *Curr Opin Microbiol* 2003;6: 482-9.

Mazon H, Gabor K, Leys D *et al.* Transcriptional activation by CprK1 is regulated by protein structural changes induced by effector binding and redox state. *J Biol Chem* 2007;282: 11281-90.

Mohn WW, Tiedje J. Microbial reductive dehalogenation. *Microbiol Mol Biol Rev* 1992;56: 482-507.

Molenda O, Puentes Jacome LA, Cao X *et al.* Insights into origins and function of the unexplored majority of the reductive dehalogenase gene family as a result of genome assembly and ortholog group classification. *Environ Sci Process Impacts* 2020.

Muyzer G, Stams AJ. The ecology and biotechnology of sulphate-reducing bacteria. *Nat Rev Microbiol* 2008;6: 441-54.

Narberhaus F. Negative regulation of bacterial heat shock genes. *Mol Microbiol* 1999;31: 1-8.

Ogura M, Tsukahara K, Hayashi K *et al.* The Bacillus subtilis NatK–NatR two-component system regulates expression of the natAB operon encoding an ABC transporter for sodium ion extrusion. *Microbiology* 2007;153: 667-75.

Parks DH, Imelfort M, Skennerton CT *et al.* CheckM: assessing the quality of microbial genomes recovered from isolates, single cells, and metagenomes. *Genome Res* 2015;25: 1043-55.

Peck Jr H. Enzymatic basis for assimilatory and dissimilatory sulfate reduction. *J Bacteriol* 1961;82: 933-9.

Peng P, Goris T, Lu Y *et al.* Organohalide-respiring *Desulfoluna* species isolated from marine environments. *ISME J* 2020;14: 815-27.

Peng P, Zheng Y, Koehorst J *et al.* Concurrent haloalkanoate degradation and chlorate reduction by *Pseudomonas chloritidismutans* AW-1T. *Appl Environ Microbiol* 2017; 83: e00325-17.

Piché-Choquette S, Constant P. Molecular hydrogen, a neglected key driver of soil biogeochemical processes. *Appl Environ Microbiol* 2019;85: e02418-18.

Pohl E, Holmes RK, Hol WG. Crystal structure of a cobalt-activated diphtheria toxin repressor-DNA complex reveals a metal-binding SH3-like domain. *J Mol Biol* 1999;292: 653-67.

Rinke C, Chuvochina M, Mussig AJ *et al.* A standardized archaeal taxonomy for the Genome Taxonomy Database. *Nat Microbiol* 2021;6: 946-59.

Schoelmerich MC, Muller V. Energy-converting hydrogenases: the link between H2 metabolism and energy conservation. *Cell Mol Life Sci* 2019.

Seshadri R, Adrian L, Fouts DE *et al.* Genome sequence of the PCE-dechlorinating bacterium *Dehalococcoides ethenogenes*. *Science* 2005;307: 105-8.

Sievers F, Wilm A, Dineen D *et al.* Fast, scalable generation of high-quality protein multiple sequence alignments using Clustal Omega. *Mol Syst Biol* 2011;7: 539.

Smidt H, De Vos WM. Anaerobic microbial dehalogenation. *Annu Rev Microbiol* 2004;58: 43-73.

Smidt H, van Leest M, van der Oost J *et al.* Transcriptional regulation of the cpr gene cluster in ortho-chlorophenol-respiring *Desulfitobacterium dehalogenans*. *J Bacteriol* 2000;182: 5683-91.

Smits TH, Devenoges C, Szynalski K *et al.* Development of a real-time PCR method for quantification of the three genera *Dehalobacter*, *Dehalococcoides*, and *Desulfitobacterium* in microbial communities. *J Microbiol Methods* 2004;57: 369-78.

Uritskiy GV, DiRuggiero J, Taylor J. MetaWRAP—a flexible pipeline for genome-resolved metagenomic data analysis. *Microbiome* 2018;6: 1-13.

van de Pas BA, Smidt H, Hagen WR *et al.* Purification and molecular characterization of ortho-chlorophenol reductive dehalogenase, a key enzyme of halorespiration in *Desulfitobacterium dehalogenans*. *J Biol Chem* 1999;274: 20287–92.

Wagner A, Segler L, Kleinsteuber S *et al.* Regulation of reductive dehalogenase gene transcription in *Dehalococcoides mccartyi*. *Philos Trans R Soc Lond B Biol Sci* 2013;368: 20120317.

Waite DW, Chuvochina M, Pelikan C *et al.* Proposal to reclassify the proteobacterial classes Deltaproteobacteria and Oligoflexia, and the phylum Thermodesulfobacteria into four phyla reflecting major functional capabilities. *Int J Syst Evol Microbiol* 2020;70: 5972-6016.

Wang S, Qiu L, Liu X *et al.* Electron transport chains in organohalide-respiring bacteria and bioremediation implications. *Biotechnol Adv* 2018;36: 1194-206.

Wang W, Xu L, Su J *et al.* Transcriptional regulation of antiviral interferon-stimulated genes. *Trends Microbiol* 2017;25: 573-84.

Wasmund K, Algora C, Muller J *et al.* Development and application of primers for the class Dehalococcoidia (phylum *Chloroflexi*) enables deep insights into diversity and stratification of subgroups in the marine subsurface. *Environ Microbiol* 2015;17: 3540-56.

Wasmund K, Cooper M, Schreiber L *et al.* Single-cell genome and group-specific *dsrAB* sequencing implicate marine members of the class Dehalococcoidia (Phylum *Chloroflexi*) in sulfur cycling. *mBio* 2016;7.

Wasmund K, Schreiber L, Lloyd KG *et al.* Genome sequencing of a single cell of the widely distributed marine subsurface Dehalococcoidia, phylum *Chloroflexi*. *ISME J* 2014;8: 383-97.

Wiegel J, Wu Q. Microbial reductive dehalogenation of polychlorinated biphenyls. *FEMS Microbiol Ecol* 2000;32: 1-15.

Wiegert T, Homuth G, Versteeg S *et al.* Alkaline shock induces the *Bacillus subtilis* σ^W regulon. *Mol Microbiol* 2001;41: 59-71.

Xun L, Topp E, Orser C. Glutathione is the reducing agent for the reductive dehalogenation of tetrachloro-p-hydroquinone by extracts from a *Flavobacterium* sp. *Biochem Biophys Res Commun* 1992a;182: 361-6.

Xun L, Topp E, Orser C. Purification and characterization of a tetrachloro-p-hydroquinone reductive dehalogenase from a *Flavobacterium* sp. *J Bacteriol* 1992b;174: 8003-7.

Yu G, Smith DK, Zhu H *et al.* ggtree: an R package for visualization and annotation of phylogenetic trees with their covariates and other associated data. *Methods Ecol Evol* 2017;8: 28-36.

Zinke LA, Mullis MM, Bird JT *et al.* Thriving or surviving? Evaluating active microbial guilds in Baltic Sea sediment. *Environ Microbiol Rep* 2017;9: 528-36.

Chapter 4

Organohalide respiration by a *Desulforhopalus*-dominated community

Chen Zhang, Siavash Atashgahi, Tom N.P Bosma, Hauke Smidt

Manuscript in preparation

Abstract

Despite the fact that several potential organohalide-respiring bacteria (OHRB) were discovered in metagenome-assembled genomes (MAGs) in our previous study of marine sediments from Aarhus Bay, delineation of their roles and interactions are yet to be disentangled. Henceforth, obtaining corresponding pure cultures or more defined consortia would be highly instrumental for more detailed eco-physiological studies. To this end, we isolated a colony from an anaerobic slant tube culture inoculated with a stable PCE dehalogenating enrichment. Intriguingly, the derived culture exhibited debromination only, instead of PCE dechlorination, under sulfate-reducing conditions. The culture was capable of conserving energy for growth via debromination of 2,6-dibromophenol (2,6-DBP). Analysis of 16S rRNA gene sequence data extracted from shot gun metagenome sequences revealed that a strain belonging to *Desulforhopalus* was the predominant member of the consortium at a relative abundance of 29 %. Moreover, five bins (completeness > 85% and contamination < 3%) were assembled and all were identified as potentially new species (average nucleotide identity, ANI < 95%). Two bins from potential OHRB, CH4_bin.3 belonging to *Desulfoplanes*, and CH4_bin.4 belonging to *Marinifilaceae*, were found to encode reductive dehalogenase (RDase) genes, whereas CH4_bin.5 was found to contain a gene coding for thiolytic tetrachloro-p-hydroquinone (TPh-) RDase bearing 23.4 % identity to TPh-RDase of *Sphingobium chlorophenolicum*. The expression of all three RDase genes was strongly-induced after adding 2,6-DBP. Acetylene, a known inhibitor of different redox-active metalloenzymes, was found to inhibit methanogenesis as well as reductive dehalogenation without affecting gene expression, suggesting post-transcriptional inhibition. Phylogenomic analyses revealed the ecological importance of complementary roles of community members, including complete *de novo* vitamin B12 biosynthesis, which agreed with physiological data. Altogether, the findings presented here provided insight into the mutualism of the consortium and provided leads for synthetic OHR community optimization strategies for *in situ* bioremediation.

Keywords: organohalide-respiring bacteria (OHRB), Reductive dehalogenase (RDase), 2,6-dibromophenol debromination, *Desulforhopalus*, acetylene inhibition, phylogenomics

Introduction

Owing to recent technological and conceptual advances particularly regarding DNA and RNA sequence based approaches, an ever increasing number of studies is being conducted where such approaches provide substantial support for understanding the biological activity in underexplored biospheres, also expanding our knowledge on evolutionary aspects across the tree of life (Goodwin, et al. 2016, Schuster 2008, Zaremba-Niedzwiedzka, et al. 2017). Recently, accumulating evidence revealed the presence of RDase genes in marine sediments of Aarhus Bay, and detection of corresponding transcripts suggested the occurrence of organohalide respiration (OHR), further diversifying the spectrum of local energy-conserving mechanisms, especially under low nutrient conditions such as those prevailing in marine sediments (Jochum, et al. 2018, Zinke, et al. 2017). In addition, a high Br^-/Cl^- ratio alongside the depth of sediments suggested the prevalence of reductive debromination (Zinke, et al. 2017). On this basis, experiments described in chapter 2 of this thesis eco-physiologically validated the OHR potential of Aarhus Bay sediments on tetrachloroethane (PCE), 2,6-dibromophenol (2,6-DBP), 3-bromophenol (3-BP), 1,4-dibromobenzene (1,4-DBB), and 2,4,6-triiodophenol (2,4,6-TIP) (Chapter 2). Subsequent metagenomic and -transcriptomic analyses allowed for the assembly of metagenome assembled genomes (MAGs), representing a diverse group of novel, potential organohalide respiring bacteria (OHRB), most of which showed induction of the expression of genes related to OHR in the presence of PCE (Chapter 3).

Reductive dehalogenation is catalyzed by reductive dehalogenases (RDases), which in general are classified into two types due to their differences in catalytic mechanism: 1) RDases in anaerobes, and particularly OHRB (Fincker and Spormann 2017, Mohn and Tiedje 1992); 2) thiolytic tetrachloro-p-hydroquinone (Tph)-RDase in aerobes (Apajalahti and Salkinoja-Salonen 1987, Xun, et al. 1992a, Xun, et al. 1992b). Both enzymes require anoxic conditions for their catalytic activity (Ni, et al. 1995, Vogel and McCarty 1985). Beyond their role in the biotransformation of organohalides, respiratory RDases have been shown to be coupled to energy conservation for bacterial growth, which is not the case for TPh-RDase. Therefore, respiratory RDases have attracted more research interests. In spite of sequence dissimilarities, several functional motifs of respiratory RDases are conserved, including a twin-arginine translocation (Tat domain, RR) signal peptide, and two Iron-Sulfur cluster motifs (Fe-S1: FCXXCXXCXXXCP and Fe-S2: CXXCXXXCP) involved in the electron transfer from the electron donor to the catalytic site of the enzyme (Atashgahi 2019, Fincker and Spormann 2017, Jugder, et al. 2015, Kunze, et al. 2017). In addition, the operon that encodes the respiratory RDase, also named RdhA or RDase A, in most cases also encodes a second protein, RDase B, that acts as an anchor protein to localize RDase A to the outer face of the cytoplasmic membrane (Jugder, et al. 2015). TPh-RDases were classified into the Glutathione-S-Transferase (GST) superfamily, in which cysteine and serine are two conserved catalytic site residues that are critical for the catalytic activity of Tph-RDases that use glutathione as the reducing equivalent (McCarthy, et al. 1996). Interestingly, our previous data reported in chapter 3 revealed the presence of a TPh-RDase gene in CH3_bin.15, which was affiliated with the strictly anaerobic genus *Desulforhopalus* (Isaxons and Teske 1996, Lie, et al. 1999). Moreover, the TPh-RDase gene was also induced during PCE dehalogenation regardless of the additional sulfate. Nevertheless, a role of TPh-RDase under anoxic conditions and its relationship with the respiratory RDases found in other MAGs awaits further study.

The activity of respiratory RDases requires a corrinoid cofactor. Previous work on *Dehalococcoides* has shown that they lack *de novo* corrinoid biosynthesis capacity, and that absence of corrinoids abolished RDase activity (Kube, et al. 2005, Magnuson Jon, et al. 1998, Maymó-Gatell, et al. 2001, Yan, et al. 2016). Thus, members of *Dehalococcoides* require the supplementation of external corrinoids for reductive dehalogenation (Kube, et al. 2005). With more OHRB isolated and characterized, few OHRB, such as *Sulfurospirillum multivorans*, have been shown to not only utilize a range of different electron donors and carbon sources, but also self-supply the necessary corrinoid cofactor via a complete biosynthesis pathway (Goris, et al. 2015). A recent coculture study of *D. mccartyi* strain 195 and *S. multivorans* achieved the complete PCE dehalogenation to ethene over three times faster as compared to a monoculture of *D. mccartyi* strain 195 without adding corrinoids (Kruse, et al. 2021). This was the first synthetic coculture establishment, which successfully showed the conceptual feasibility of synthesizing an OHR community, however, following a bottom-up approach for establishing defined synthetic consortia remains challenging due to the complex ecological and physiological interactions among the members and availability of cultured isolates. Moreover, to what extent such defined consortia can be successfully applied for *in situ* bioremediation remains uncertain (Garber, et al. 2020, Kapoore, et al. 2022). In comparison, a top-down approach that relies on establishing a robust consortium through enrichment appears to have less of these concerning issues (Bernstein 2019, Lawson, et al. 2019).

Acetylene has wide inhibitory effects on microbial processes, i.e. methanogenesis, nitrogen fixation and reductive dehalogenation (Belay and Daniels 1987, Pon et al. 2003). Recent studies revealed that acetylene hydratase and nitrogenase of *Pelobacter* sp. strain SFB93 can ferment and reduce acetylene, respectively, (Akob et al. 2017), abating the inhibition of acetylene on reductive dehalogenation of PCE to ethene when incubated with *Dehalococcoides* (Mao et al. 2017). However, it has not been shown to what extent this inhibitory effect of acetylene acts at transcriptional, translational or enzyme level. In addition, whether the coexisting nitrogenase in OHRB can prevent the inhibition of reductive dehalogenation still remains elusive.

In this study, we isolated a mutualistic consortium that is capable of reductive debromination of 2,6-DBP without adding external cobalamin, vitamin B12 (B12). Further genome-resolved analyses identified five novel bins, of which three were bearing RDase and TPh-RDase genes possibly involved in reductive debromination that was post-transcriptionally inhibited by acetylene. Metabolic pathway analysis confirmed that this consortium contains the complete *de novo* B12 biosynthesis pathway. Interestingly, further phylogenomic analyses suggested *Marinifilum* and *Ancylomarina* as new potential OHRB.

Materials and methods

Chemicals

PCE, 2,6-DBP, 2,4-DBP, 2,4-6-DBP, 1,4-dibromobenzene (1,4-DBB), 1,2-DBB, 1,3-DBB, 1,2,4-tribromobenzene (1,2,4-TBB), 2,6-dichlorophenol (2,6-DCP), 2,4-DCP, 2,4,6-TCP, 1,4-dichlorobenzene (1,4-DCB), 1,2-DCB, 1,3-DCB, 1,2,4-TCB, benzene, 2,4,6-triiodiphenol (2,4,6-TIP), 2,4-DIP, 2,6-DIP, 2-IP, and 4-IP were purchased from Sigma-Aldrich. Stock solutions of sulfate (0.5 M), sulfite (0.5 M), thiosulfate (0.5 M), nitrate (0.5 M), formate (0.5 M), acetate (0.25 M), pyruvate (0.5 M), and lactate (0.5 M) were prepared by filter sterilization (syringe filter, 0.2 μm, mdimembrane, Ambala Cantt, India). All other (in)organic chemicals were of analytical grade.

Isolation and cultivation

Marine medium was prepared for cultivation as previously described (Monserrate and Häggblom 1997, Peng, et al. 2020). The final growth medium was composed of 50 mL anoxic marine medium, $Na_2S \cdot 9H_2O$ (0.48 g/L, 2 mM) serving as the reducing agent, and Resazurin

(0.005 g/L) as the redox indicator. The headspace of culture bottles was exchanged with N_2/CO_2 (80 : 20%, 140KPa), and bottles were sealed with Teflon-coated butyl rubber septa and aluminum crimp caps (GRACE, MD, USA). Slant tubes contained 5 ml marine medium with 0.8% low-melting point agarose (Sigma-Aldrich) and were incubated in the dark at 20 ℃. The isolation was initiated starting from the mother bottle, S.SD23 (third bottle of PCE dechlorination after two-time serial dilution with additional sulfate, details in Figure 2.2 of Chapter 2), and 200 μL was used to inoculate the anaerobic slant tube. Colonies were picked from the slant and transferred into liquid marine medium to check for PCE dechlorination in the presence of additional sulfate. The above-mentioned halogenated compounds were tested as the electron acceptors with lactate as the electron donor and carbon source. To study the growth of the community on 2,6-DBP (200 μM), hydrogen (20 mM) and acetate (5 mM) served as the electron donor and carbon source respectively. Acetylene (≈ 1.8 mM) was injected into the bottles and served as the inhibitor for microbial processes, including reductive dehalogenation. Prior to this growth measurement on H_2/acetate as the sole electron donor and carbon source with 2,6-DBP as the electron acceptor, 2.5 ml actively debrominating culture was transferred three times (10% vol/vol) in a row to 48 ml fresh medium supplemented with H_2/acetate and 2,6-DBP as described above and incubated to rule out the influence of residual medium components, especially lactate and sulfate. The generation of a B12 independent culture followed the same steps, i.e. three consecutive transfers and incubation to exclude residual B12 in the cultures.

Analytical methods

PCE, trichloroethene (TCE), cis-dichloroethene (cDCE), trans-dichloroethene (tDCE), ethene and acetylene were detected by gas chromatography combined with mass spectrometry (GC-MS) with an Rt®-Q-BAND column (Retek, PA, USA) and DSQ-MS (Thermo Fisher Scientific).

Hydrogen gas was detected by Compact GC (Global Analyzer Solutions, Breda, The Netherlands) with a pulsed discharge ionization detector (GC-PDD). Thermo Scientific Accela High-Performance Liquid Chromatography (HPLC) system installed with an Agilent Poroshell 120 EC-C18 column and a UV/Vis detector was used to measure halogenated phenols, and benzenes, benzene, and phenol. Organic acids were measured by SHIMADZU LC2030 PLUS coupled with a Shodex SUGAR Series® SH1821 column, including lactate, propionate, acetate and formate. Sulfate, sulfite, thiosulfate and nitrate were measured by using Thermo Scientific DionexTM ICS-2100 Ion Chromatography System (Dionex ICS-2100). Sulfide was analyzed by photometric method using methylene blue as described previously (Cline 1969).

Scanning Electron Microscopy (SEM)

The culture was sampled for field emission scanning electron microscopy (FE-SEM). Five ml culture was sampled and incubated with glutaraldehyde (2.5%) for 20 min, and then prefixed to the cover slide coated with poly-L-lysine for 2 h. After that, the cover slide was washed three times with 0.1 M sodium cacodylate (pH 7.2) and then 1 h fixed with 1% osmium tetroxyde in the same cacodylate buffer. Finally, the samples were dehydrated with various ethanol concentrations and incubated for 10 min at each step. Imaging of the sample was completed using a Magellan 400 instrument at the Wageningen Electron Microscopy Center (WEMC).

DNA and RNA extraction and reverse-transcriptase quantitative PCR (RT-qPCR)

The consortium cultures were first centrifuged at 10,000 × g for 5 min, the supernatant was discarded and the precipitates were then washed three times with 200 μL TE buffer (pH = 7.0, 4 °C) on ice to remove any residual medium components that might interfere with downstream DNA and RNA extraction. For genomic DNA extraction, MasterPureTM Gram positive DNA purification Kit (Epicentre, WI, USA) was used, following manufacturer's instructions. For RNA isolation, prior to the sample collection, cultures in eighteen bottles were grown with additional lactate (15 mM) and sulfate (20 mM) to exponential phase for 72 h after transfer without any additional 2,6-DBP. Nine bottles were collected as the 0 hour samples. In the remaining nine bottles, three were kept as before without any injection, three replicate cultures were injected with 200 μM 2,6-DBP, and the last three were injected with 200 μM 2,6-DBP and with 1.8 mM acetylene together, and cells were collected and washed as described above. Collected biomass was mixed with 0.4 ml cold TE buffer (4 μl *2*-mercaptoethanol), and 0.5 ml TRIzolTM reagent (Thermo Fisher Scientific) was added, followed by bead-beating for 3 min (3 times, 1 min per time with cooling on ice in between) at speed 5.5 (FastPrep-24 5G, MP biomedicals, Irvine, CA, USA). After bead-beating, UltraPureTM phenol : chloroform : isoamyl alcohol in ratio of 25 : 24 : 1 in 200 μl (Thermo Fisher Scientific) was added and mixed by vortex. Then, the separated aqueous phase containing RNA was transferred to an RNeasy column (Qiagen, Venlo, The Netherlands) for purification followed by DNase I (Roche, Almere, The Netherlands) treatment to remove residual DNA. In order to check for purity of the obtained culture, a near-full length fragment of bacterial 16S ribosomal RNA (rRNA) gene was amplified using universal bacterial primers 27F/1492R (Table 4.1) and subjected to Sanger sequencing as previously described (Suzuki and Giovannoni 1996). Bacterial 16S rRNA gene-targeted qPCR was used for assessing the growth of the microbial community via the increase of 16S rRNA gene copy numbers using the general primers Eub341F/Eub534R (Table 4.1). RT-qPCR was introduced to measure the relative expression of RDase genes by using the One Step PrimeScript™ RT-PCR Kit (Perfect Real Time) (Takara Bio, Saint-Germain-en-Laye, Germany). Primers targeting RDase genes were designed using the NCBI primer design tool with the setting parameters, Expected PCR product sizes ranged from 75bp to 150bp and melting temperatures from 57 to 60 °C (Table 4.1). RT-qPCR targeting the bacterial 16S rRNA was used for normalization of RDase gene expression.

Table 4.1 Primers used in this study for (RT)-quantitative PCR

Target	Name	Oligonucleotide sequence (5´–3´)	Purpose and (RT)-qPCR programs
Bacterial 16S rRNA gene	Eub341F	CCTACGGGAGGCAGCAG	qPCR bacterial abundance; see (Atashgahi, et al. 2013, Muyzer, et al. 1993)
	Eub534R	ATTACCGCGGCTGCTGGC	
Bacterial 16S rRNA gene	27F	AGAGTTTGATCMTGGCTCAG	Universal for Bacteria Sanger Sequencing
	1492R	TACGGYTACCTTGTTACGACTT	
CH4_CH4_bin.3-RDase1	B3RD1-919F	GTCATGTCCGGAATGGGTGA	qPCR RDase genes Stage1: Reverse transcription 42 ℃ 5 min 95 ℃ 10 s Stage2: PCR reaction 95 ℃ 5 s 60 ℃ 20 s 40 Cycles
	B3RD1-1044R	GTCTATGGGCTTGGTCTCGG	
CH4_bin.3-RDase2	B3RD2-479F	CCAACACTGATGCCGCAAAT	
	B3RD2-598R	TGTGCTGGGTTTCGCTGTAT	
CH4_bin.4-RDase	B4RD-734F	CCGACTGGAGCGATTTTCCT	
	B4RD-864R	CATGGCAGAATAACCGGCAC	
CH4_bin.5-TPh-RDase	B5TRD-282F	CGGATCGCTTCGTCCTGAAT	
	B5TRD-430R	CCATCTGCTCAGTTGTTCGC	

Metagenome sequencing and analyses

Metagenome sequence data was generated by Illumina paired-end short reads (PE150, Novaseq6000, Novogene) and PacBio long reads (Sequel, Novogene). The raw paired-end Illumina and PacBio reads were at first examined using the quality check module, “read_qc” of MetaWRAP. (Uritskiy, et al. 2018). Low-quality reads as well as human contaminant reads were removed. The raw PacBio long-read data was combined to improve the quality of assembly following OPERA-MS (Bertrand, et al. 2019). Considering the improved features of the hybrid assembly in comparison to the short-read assembly, including contigs’ N50, maximum contig size and number of contigs, the follow-up analyses were based on the hybrid assembly. “Kraken2” was used to identify the taxonomic composition of the community by mapping the clean Illumina reads against the SILVA database version 138 (Quast, et al. 2013, Yilmaz, et al. 2014) and to calculate the relative abundance of 16S rRNA gene reads of each taxonomy over the total reads of the 16S rRNA gene. The resulting hybrid assembly was binned and refined using the MetaWRAP modules, “Binning module” combining metabat2, maxbin2 and concoct with the cut-off set at > 50 % completeness and < 10 % contamination, and “Bin_refinement” to improve the bin set. The abundance of the refined bins was quantified using the “quant_bins” module, and the relative abundance of each bin was calculated by mapping the Illumina data to a concatenated file of the five bins using default parameters. Bins were reassembled, taxonomically classified and annotated via the “classify_wf” workflow of GTDB-Tk and the “prokka” module of MetaWRAP, respectively (Rinke, et al. 2021). The relative abundance of bins was calculated using CoverM v0.6.1 (https://github.com/wwood/CoverM).

Phylogenetic analysis of bins and inference of metabolic pathways

There were five bins assembled, and their classification by GTDB-Tk revealed that all of them were new species as their average nucleotide identity (ANI) with entries in GTDB (v207) was lower than 95%. Fifty-two representative genomes most closely related to bins were extracted from the GTDB database (v207) and were included for phylogenetic analysis by GToTree (Lee 2019). Metabolic traits associated with reductive dehalogenation were also inferred, including the metabolic genes encoding RDase (*rdh*), TPh-RDase (TPh-*rdh*), haloacid dehalogenase (*hdh*), pathways involved in the metabolism of sulfate, nitrate, hydrogen, nitrogen, acetylene, Wood-Ljundahl pathway (WLP), *de novo* B12 biosynthesis and B12 transporters (Akob, et al. 2017, Arnoux, et al. 2003, Gopinath, et al. 2013, Greening, et al. 2016, Howard and Rees 1996, Jiao, et al. 2021, Jormakka, et al. 2003, Moore and Warren 2012, Ragsdale 2008, Søndergaard, et al. 2016, van Vliet, et al. 2021). To this end, MagicLamp (Garber, et al. 2020) was used with the retrieved COG numbers of metabolic genes from the .gff format of bins and their related representative genomes to infer the metabolic potential of the consortium. The constructed phylogenetic tree was visualized and modified by ggtree (Yu, et al. 2017).

Results

Debrominating potential of the isolated consortium

In order to isolate members of the stable, sediment-free PCE dechlorinating enrichment derived from Aarhus Bay sediment (chapter 2), we inoculated a sample of this culture onto an anaerobic agar slant (Figure 4.1A). We were able to retrieve a single colony that developed after 69 days of incubation. After transfer to liquid medium, the derived culture exhibited debrominating activity of 2,4,6-DBP and 2,6-TBP to 4-BP and phenol, respectively, but was no longer able to dechlorinate PCE (Figure 4.1A). To better understand the physiological traits of the colony-derived culture, different electron donors and carbon sources, such as H_2/acetate and pyruvate, and various electron acceptors, such as sulfate and nitrate, and in particular a range of different halogenated compounds, were tested (Table 4.2). In line with the initial results, the culture only displayed debrominating potential rather than dechlorination or deiodination. While the colony-derived culture was able to utilize sulfate, sulfite, and thiosulfate as electron acceptor, it was not capable of reducing nitrate. The culture was found to completely debrominate 2,6-DBP to phenol after nine days with the formation of bromophenol as the intermediate (Figure 4.1B). Meanwhile, the added sulfate served as a competitive electron acceptor and was reduced to sulfide, in which lactate as the electron donor and carbon source was utilized with the production of acetate (Figure 4.1C). In line with what was observed for the incubation in the presence of sulfate, the reductive debromination also proceeded in the sulfate-free culture (Figure S4.1A), in which lactate was consumed fermentatively with the formation of propionate and acetate in a ratio of roughly 2 : 1 (Figure S4.1B).

In order to check for purity of the colony-derived culture, Sanger sequencing of a PCR product obtained using universal bacterial 16S rRNA gene-targeted primers 27F/1492R was attempted, however, the resulting sequence could not be resolved, indicating that the culture comprises a mixed consortium rather than a pure culture. Further scanning electron microscopy (SEM) analyses confirmed the presence of diverse morphologies in the community (Figure S4.1C), albeit with a rod-shaped cell-type being predominant.

Table 4.2 Physiological properties of the isolated consortium

Compounds as e-donors and e-acceptors	**Utilization**
Compounds used as electron donor and/or carbon source	
H_2[a]	+
Formate[a]	+
Acetate	-
Lactate	+
Pyruvate	+
Fermentative growth on	
Lactate	+
Pyruvate	+
Compounds used as electron acceptor	
Sulfate	+
Sulfite	+
Thiosulfate	+
Nitrate	-
Halogenated compounds used as electron acceptor[b]	
2,6-Dibromophenol (2,6-DBP); 2,4-DBP; 2,4,6-DBP;	+ ; + [c] ; + [c] ;
1,4-Dibromobenzene (1,4-DBB); 1,2-DBB; 1,3-DBB; 1,2,4-TBB	+ [d] ; - ; - ; - ;
2,6-Dichlorophenol (2,6-DCP); 2,4-DCP; 2,4,6-TCP;	- ; - ; -
1,4-Dichlorobenzene (1,4-DCB); 1,2-DCB; 1,3-DCB; 1,2,4-TCB;	- ; - ; - ; - ;
2,4,6-Triiodophenol (2,4,6-TIP); 2,4-DIP; 2,6-DIP; 2-IP; 4-IP;	- ; - ; - ; - ; - ;

[a]used as the electron donor only in the presence of acetate as carbon source; [b]tested with lactate as electron donor and carbon source;

[c]4-bromophenol was formed as the final product rather than phenol; [d]bromobenzene was formed as the final product rather than benzene.

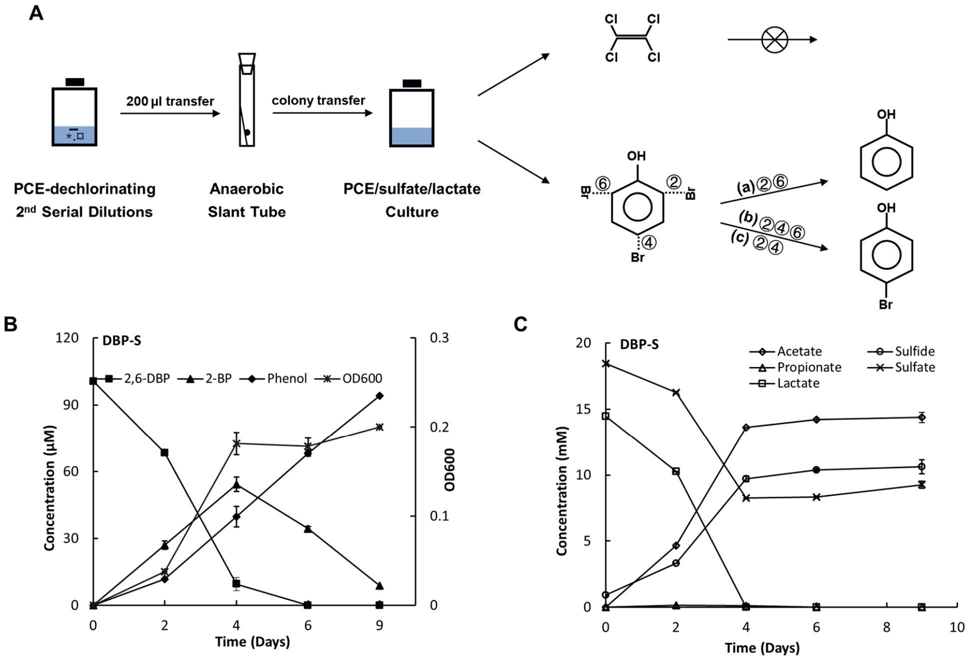

Figure 4.1 Schematic diagram of colony isolation and its reductive debromination of 2,6-dibromophenol (2,6-DBP) in the presence of sulfate. The mother bottle (10^{-3}) was selected from the second serial dilution in the presence of sulfate as previously described (Chapter 2). The colony-derived culture could completely debrominate 2,6-DBP to phenol, whereas 2,4,6- or 2,4- brominated phenols were transformed into 4-bromophenol (4-BP) (A). Debromination of 2,6-DBP to phenol (B) with the formation of 2-bromopenol (2-BP) as the intermediate, together with sulfate reduction to sulfide (C) to support the bacterial growth (OD600). Three replicate bottles were set for the reductive debromination of 2,6-DBP with additional sulfate. Data are presented as mean ± standard deviation (SD). Error bars indicate the SD.

Bacterial growth supported by reductive debromination of 2,6-DBP

Reductive dehalogenation has previously been shown to be either catalyzed by respiratory corrinoid-dependent RDase or non-respiratory glutathione-dependent TPh-RDase (Mohn and Tiedje 1992, Mohn and Tiedje 1990, Xun, et al. 1992a, Xun, et al. 1992b). To this end, reductive dehalogenation enabled by respiratory RDase as the terminal electron accepting process has been characterized to contribute to respiratory energy conservation for bacterial growth (Bosma, et al. 1988, Mohn and Tiedje 1990). Previously, acetylene has been shown to inhibit reductive dehalogenation by *Dehalococcoides* (Pon, et al. 2003). Our experiments validated acetylene can specifically inhibit RDase activity without influencing other metabolic activities, including lactate consumption and sulfate reduction (Figure S4.2). We therefore measured the bacterial growth during 2,6-DBP debromination compared to a culture to which acetylene was added. H_2/acetate was added as the electron donor and carbon source and 2,6-DBP as electron acceptor to the cultures, respectively, in which the bacteria grew from 2.06 (± 0.90) × 10^5 to 1.59 (± 0.16) × 10^7 16S rRNA gene copies / ml after the complete debromination of 200 µM 2,6-DBP in ten days (Figure 4.2). Simultaneously, in cultures to which acetylene was added reductive debromination of 2,6-DBP was completely stopped (Figure 4.2A), and the growth of the consortium was halted (Figure 4.2B). This finding suggested that one or more respiratory RDases were active as reductive debrominase of 2,6-DBP, contributing to the cell growth of the consortium. Intriguingly, cell growth came to a halt after four days with half of the added 2,6-DBP debrominated, suggesting that the non-respiratory RDase, TPh-RDase, might have also contributed to the degradation of 2,6-DBP without bacterial growth as the output. Indeed, additional research is needed to further investigate this observation.

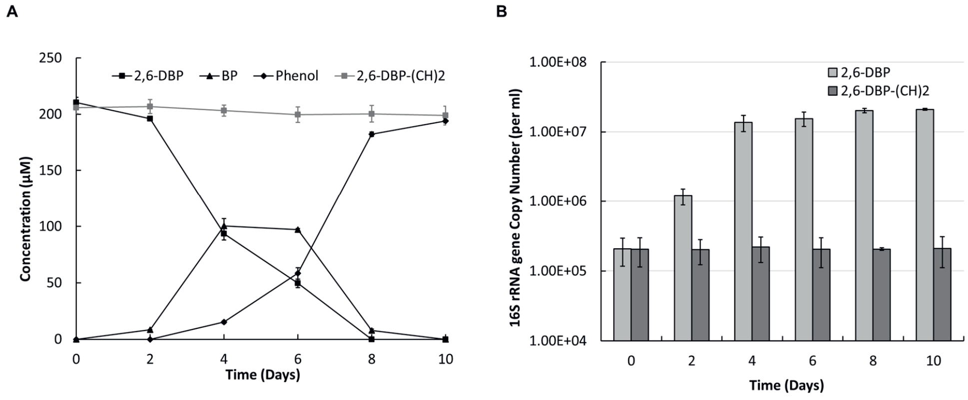

Figure 4.2 Reductive debromination to support the growth of consortium. H_2/acetate served as the electron donor and carbon source for 2,6-DBP debromination, and acetylene added to the

negative control (grey line) inhibited 2,6-DBP debromination (A). Quantitative PCR targeting the bacterial 16S rRNA gene was used to assess the cell growth with and without acetylene added (B). (CH)2: acetylene; three replicate bottles were set for the experiment, and data are presented as mean ± standard deviation (SD). Error bars indicate the SD.

***Desulforhopalus*-dominated consortium for reductive debromination**

In order to further investigate the composition and metabolic potential of the consortium, metagenome sequencing, including short-read and long-read sequencing, was employed. Taxonomic assignment of 16S rRNA gene sequences derived from the metagenome dataset revealed that *Desulforhopalus*, classified into *Desulfobacterota*, accounted for the largest percentage with 29%, followed by populations of *Klebsiella* and *Myroides* with 8% each, and genera *Mycoplasma* (7%) and *Endomicrobium* (7%) (Figure 4.3A). In addition, 11% of the sequences were affiliated with the *Bacterodia,* while 10% belonged to *Desulfobacterota* other than *Desulforhopalus*. This overall aligned well with the community analyses of the original PCE-dechlorinating cultures (Chapter 2). To accurately decipher the taxonomy and genomic information, short and long metagenome sequence reads were assembled and binned into five genomes (MAGs) that were further classified using the GTDB-TK workflow. CH4_bin.1 was found to belong to the genus *Oceanispirochaeta*, CH4_bin.2 and CH4_bin.3 were affiliated to *Desulfoplanes*, CH4_bin.4 to the family *Marinifilaceae*, and CH4_bin.5 was affiliated with the genus *Desulforhopalus* (Table S4.1) . All five MAGs were identified as new species based on ANI values with most closely related species being lower than 95%. The reads of the five MAGs accounted for 95.96% of total reads, with CH4_bin.5 accounting for 65.62%, CH4_bin.3 13.61%, CH4_bin.2 10.56% and CH4_bin.4 for 3.55%, leaving 4.04% of all reads unmapped (Figure 4.3B). Furthermore, CH4_bin.5 was characterized by 100% completeness and 0% contamination according to 120 bacterial single-copy maker genes. In summary, both approaches supported the notion that CH4_bin.5, identified as member of *Desulforhorpalus*, was the most abundant member of the consortium.

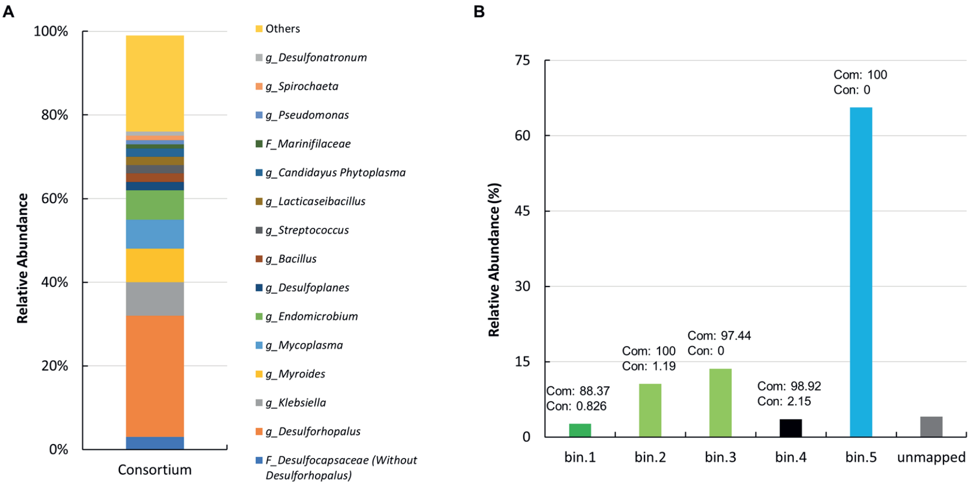

Figure 4.3 Relative abundance of microbial community members and the assembled bins within the colony-derived consortium. Microbial composition was calculated based on the mapping file generated from the clean raw Illumina reads against the SILVA database version 138 (Quast, et al. 2013, Yilmaz, et al. 2014) (A). The hybrid assembly was binned into five novel bins, and the relative abundance of each bin was calculated based on its numbers of reads over the numbers of total reads (B). "Others" represent the assigned taxa with a relative abundance < 1% and unassigned taxa; *F*, family; *g*, genus. Com: completeness (%); Con: contamination (%); unmapped: reads were not binned.

RDase genes and their expression during reductive debromination

To further examine, which of the bins are responsible for the observed reductive debromination, MAGs were annotated, leading to the identification of three genes predicted to encode canonical corrinoid-dependent RDases, two of which were found on CH4_bin.3 and one on CH4_bin.4. A fourth gene, predicted to code for a thiolytic glutathione-dependent RDase was found on CH4_bin.5 (Figure 4.4A). Subsequently, the genomic context, i.e. the two neighboring genes upstream and downstream of each RDase gene, was included in the analysis. All three RDase genes encoding the catalytic subunit of respiratory RDases (RdhA) were accompanied by genes predicted to encode the cognate membrane anchor protein (RdhB) Interestingly, both RDase genes found on CH4_bin.3 were accompanied by a gene predicted to code for a formate hydrogenase transcriptional activator, HyfR (Skibinski David, et al. 2002), suggesting both loci originated from the same ancestor. Another transcriptional regulator, Btr (Gaballa and Helmann 2007), for siderophore bacillibactin production under iron-limiting conditions, was found encoded upstream of RDase in CH4_bin.4. Finally, upstream of the TPh-RDase encoding gene we observed a gene predicted to code for a transcriptional regulator, NoDD2, regulating nodulation factor production (Fellay, et al. 1998). Although these different regulators have been described with divergent functions, their roles are in general closely related with energy conservation and nutrient acquisition. As to the three predicted corrinoid-dependent RDases, three commonly conserved functional motifs were found, including a twin arginine signal peptide (RR), as well as two iron-sulfur cluster motifs, FCXXCXXCXXXCP and CXXCXXXCP, that were conserved in sequence and structural configuration for binding the iron-sulfur clusters to transfer electrons (Figure 4.4B). TPh-RDase was classified into the superfamily of glutathione-S-transferases (GST) that differ from respiratory RDase in sequence and conserved motifs. Sequence alignment of TPh-RDase in CH4_bin.5 to that of *Sphingobium chlorophenolicum* revealed that two catalytic site residues, cysteine (C) and serine (S), were conserved in sequence and simulated structure. All four RDases were predicted to be membrane-spanning enzymes, suggesting direct contact with substrates and dehalogenation in the extracytoplasmic space (Figure S4.3).

As a next step, we analyzed the transcription of RDase genes using RT-qPCR. This analysis revealed that expression of all four RDase genes were induced several orders of magnitude within 30 min after the addition of 2,6-DBP. More specifically, the relative expression of the TPh-RDase gene increased up to 1.30 (± 0.16) × 10^4 fold compared to the control to which no organohalide was added. Similarly, expression of genes encoding the respiratory RDases, i.e. RDase-1 and RDase-2 of CH4_bin.3, and RDase of CH4_bin.4, increased by 3.04 (± 0.29) ×

10^3, 2.63 (± 0.24) × 10^3, and 1.65 (± 0.20) × 10^3 fold, respectively (Figure 4.4C). Interestingly, we found that the inhibitor acetylene did not affect RDase gene expression, suggesting that inhibition acts post-transcriptionally.

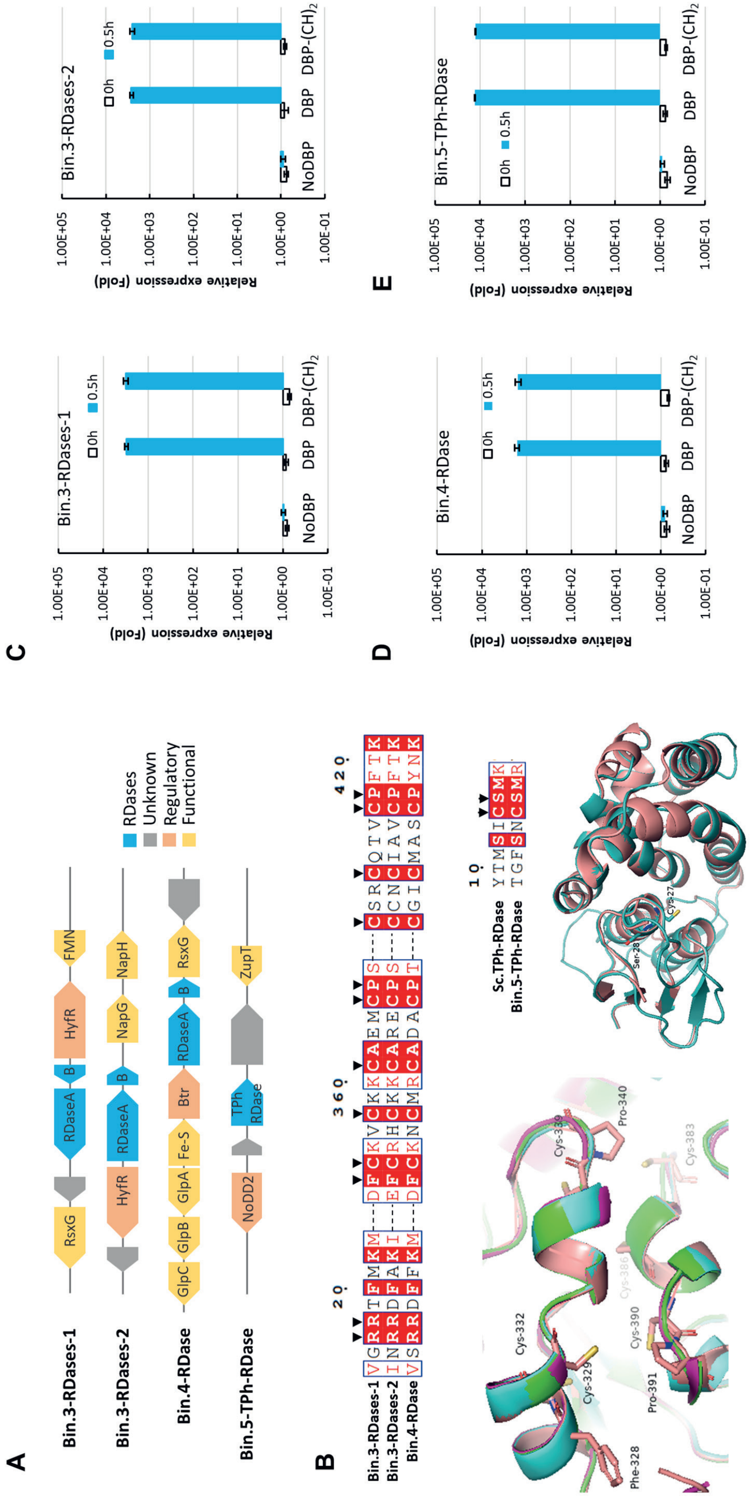
A
Bin.3-RDases-1
RsxG
RDaseA
B
HyfR
FMN
Bin.3-RDases-2
HyfR
RDaseA
B
NapG
NapH
Bin.4-RDase
GlpC
GlpB
GlpA
Fe-S
Btr
RDaseA
B
RsxG
Bin.5-TPh-RDase
NoDD2
TPh RDase
ZupT
RDases
Unknown
Regulatory
Functional
B
20
360
420
Bin.3-RDases-1 VGRRTFMKM---DFCKVCKKCAEMCPS---CSRCQTVCPFTK
Bin.3-RDases-2 INRRDFAKI---EFCRHCKKCARECPS---CCNCIAVCPFTK
Bin.4-RDase VSRRDFFKM---DFCKNCMRCADACPT---CGICMASCPYNK
10
Sc.TPh-RDase YTMSICSMK
Bin.5-TPh-RDase TGFSNCSMR
Phe-328
Cys-329
Cys-332
Pro-391
Cys-390
Cys-386
Cys-339
Pro-340
Cys-383
Ser-28
Cys-27
C
Bin.3-RDases-1
D
Bin.4-RDase
E
Bin.5-TPh-RDase
Bin.3-RDases-2
Relative expression (Fold)
1.00E+05
1.00E+04
1.00E+03
1.00E+02
1.00E+01
1.00E+00
1.00E-01
0h
0.5h
NoDBP
DBP
DBP-(CH)$_2$

Figure 4.4 The genomic context, conserved motifs and structures, and expression of RDase encoding genes identified in the bins. RDase genes with the two neighboring genes located up- and downstream (A). Amino acid sequence alignment of conserved motifs of the respiratory RDases of CH4_bin.3 and CH4_bin.4, and TPh-RDase of CH4_bin.5 and *Sphingobium chlorophenolicum* respectively displayed by EsPript 3.0, and corresponding superimposed structures as generated by PyMol (v.2.3.4) (see below for additional details) (B). Reverse-transcriptase quantitative PCR was used to measure the expression of RDase genes from CH4_bin.3 (C) and CH4_bin.4 (D), and TPh-RDase gene from CH4_bin.5 (E), before (0 h) and 30 min (0.5 h) after addition of 2,6-DBP only, no addition, and addition of 2,6-DBP and acetylene together. Expression values were normalized to 16S rRNA measurements. For the structures shown in B, respiratory RDase (PDB: 5m2g1, in salmon) from *Sulfurospirillum multivorans* was aligned as the best structural template (Kunze, et al. 2017). In the superimposed structure, CH4_bin.3-RDase1 is depicted in green, CH4_bin.3-RDase2 in cyan and CH4_bin.4-RDase in magenta. TPh-RDase (PDB: 7za5.1, in salmon) is shown as dimer as the structural basis for TPh-RDase of CH4_bin.5 in teal. FMN: Flavoprotein that can bind the flavin mononucleotide (FMN) as the prosthetic group; RDases: composed of RDaseA and anchor protein B; HyfR: transcriptional regulator of formate hydrogenase; RsxG: electron transporter; NapGH: electron transporter associated with periplasmic nitrate reductase. GlpABC: Anaerobic glycerol-3-phosphate dehydrogenase complex; Btr: transcriptional regulator; Fe-S: Ferredoxin with iron-sulfur clusters; TPh-RDase: none respiratory RDase; NoDD2: regulator for nodulation; ZupT: zinc transporter. Arrows indicate the conserved sites, in which some were labelled in the superimposed the structure. NoDBP: no 2,6-DBP added; DBP-(CH)2: both 2,6-DBP and acetylene added. Each treatment in C-E was set with three replicates and values represent mean ± standard deviation (SD). Error bars indicate the SD.

Phylogenomic analyses of bins and closely-related representative genomes

To gain a better understanding of the phylogenies and metabolic traits of bins compared to genomes of closely-related organisms, we constructed phylogenetic tree of bins and associated representative genomes, and subsequently investigated encoded metabolic traits related to the above-mentioned physiological data (Figure 4.5). As mentioned above, these MAGs were classified into four taxonomical groups, in which CH4_bin.1 was affiliated with the genus *Oceanispirochaeta*, CH4_bin.2 and CH4_bin.3 were assigned to the genus *Desulfoplanes*, CH4_bin.4 was affiliated to the family *Marinifilaceae*, and CH4_bin.5 was assigned to the genus *Desulforhopalus*. The 15 representative genomes from *Desulforhopalus*, including CH4_bin.5, all bear the conserved metabolic genes for sulfate reduction, *de-novo* corrinoid biosynthesis, H_2 metabolism, and Wood-Ljungdahl pathway (WLP). Interestingly, whereas CH4_bin.5 was predicted to encode a glutathione-dependent TPh-RDase, the genomes of three other *Desulforhopalus* members contained genes predicted to code for corrinoid-dependent respiratory RDases, suggesting that these strains might have OHR potential. Furthermore, whereas most *Desulforhopalus* spp. genomes included in our analysis encoded the complete WLP, two members, *D. vacuolatus* and CH4_bin.5 were found to lack the core genes of the WLP, including *acsA*, *acsB* and *acsCD*, coding for carbon monoxide dehydrogenase, acetyl-CoA synthase and corrinoid iron sulfur protein (CFeSP), respectively (Zhuang, et al. 2014). Interestingly, the genome of one of the isolates, *D. singaporensis,* encodes all genes for the complete WLP indicating the co-occurrence of OHR potential with the assimilation of C1 compounds. In contrast, CH4_bin.1, CH4_bin.2, CH4_bin.3 and CH4_bin.4 and their associated reference genomes were all found to lack the core genes for WLP, suggesting their incapability of one-carbon compound fixation.

B12 is the required cofactor for corrinoid-dependent RDases linked with OHR (Yan, et al. 2016). Based on the analysis of bins, the *de novo* biosynthesis observed for the colony-derived consortium could be achieved by CH4_bin.3 and CH4_bin.5 separately, without the non-essential *cbiJ* gene, in line with what we observed earlier in marine *Desulfoluna* strains capable of OHR (Peng, et al. 2020), or coordinatively achieved with CH4_bin.4 by providing the *cbiJ* gene missing in other bins. Hence, in summary, the genomic inferences in terms of predicted metabolic capacity of the colony-derived consortium sufficiently explain the observed OHR capacity of the consortium in the absence of added B12 (Figure S4.4).

All six genomes affiliated with the genus *Marinifilum*, including CH4_bin.4, were predicted to encode respiratory corrinoid-dependent RDases. Similarly, five out of six genomes affiliated with the closely related genus *Ancylomarina* were predicted to code for corrinoid-dependent RDases. Accordingly, these genera, as a subgroup within the *Marinifilacease* family, are predicted to comprise novel OHRB taxa. In addition, all included genomes of these taxa contained genes encoding type A and type B [Fe-Fe] hydrogenases for catalyzing H_2 metabolism, in contrast to *Desulforhopalus* spp. genomes that were predicted to encode [Ni-Fe] hydrogenases. Interestingly, as outlined above, the critical *cbiH* gene of *de novo* B12 biosynthesis (Moore and Warren 2012), was found conserved among the members of both genera *Ancylomarina* and *Marinifilum* suggesting a symbiotic role in *de novo* B12 biosynthesis. Being closely related to *Ancylomarina* and *Marinifilum*, available genomes of the genus *Labilibaculum* were found to contain similar functional genes, such as genes coding for [Fe-Fe] hydrogenases and CbiH, but only two of the six genomes included here, namely *L. antarcticum* and *L. filiforme*, were predicted to encode corrinoid-dependent RDases.

Physiological characterization of the consortium showed that the community was unable to reduce nitrate as the terminal electron acceptor, most probably due to the lack of genes encoding membrane-bound and periplasmic nitrate reductase (NarAB and NapAB) in these assembled bins. Similarly, the five bins retrieved from the consortium also were found to lack *norAB*, *nosDZ*, and *nrfAH* genes, indicating their inability of denitrification and ammonification, respectively (Simon 2002, Zumft 1997). Intriguingly, most of the reference genomes from the genera *Desulforhopalus* and *Marinifilum* were found to contain *napAB*, suggesting their potential to reduce nitrate to nitrite. Further, genes encoding the complete nitrogenase complex for nitrogen fixation were found in CH4_bin.2 and CH4_bin.5, suggesting their capability of fixing molecular nitrogen to produce ammonia in case of N-shortage.

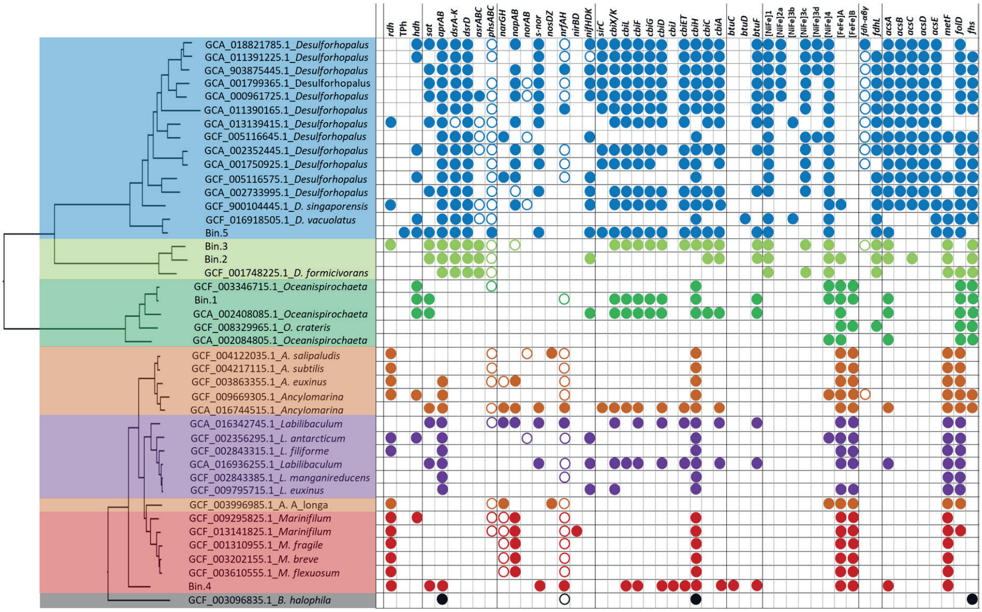

Figure 4.5 Phylogenies of the assembled bins and most closely related reference genomes, and comparison of their metabolic genes. In addition to the five bins, 52 related representative genomes from the GTDB database (v207) were included for tree construction by GToTree following the default parameters (Lee 2019). Filled circles represent encoded functional genes or complete gene clusters. Open circles represent genes for which not the entire cluster was detected. Colors indicate the different phylogenies of bins and their closest relatives. *D. formicivorans*: *Desulfoplanes formicivorans*; *rdh*: RDase gene; TPh: TPh-RDase gene; *hdh*: haloacid dehalogenase gene; *sat*, *aprAB*, *dsrA-K*(*ABCTMK*), *dsrD*, *asrABC*, and *phsABC* for sulfate reduction (van Vliet, et al. 2021); *narGH* and *napAB* for nitrate reduction (Arnoux, et al. 2003); *norAB*, *nirBD*, and *nosDZ* for denitrification (Zumft 1997); *nrfAH* for ammonification (Simon 2002); from *sirC* to *cbiA* for the complete anaerobic *de novo* corrinoid biosynthesis (Moore and Warren 2012). *btuFCD* encodes the ABC-type corrinoid transporter (Rupakula, et al. 2015); Four groups of [Ni-Fe] hydrogenases, 1, 2a, 3b, 3c, 3d, and 4, and two groups of [Fe-Fe] hydrogenases, A and B (Greening, et al. 2016, Schoelmerich and Muller 2019, Søndergaard, et al. 2016); *fdh-αβγ*, or *fdhABG*, codes for formate dehydrogenase (Ferry 1990, Jormakka, et al. 2003); *fdhL* codes for NAD$^+$-dependent formate dehydrogenase (Lu, et al. 2010, Popov and Lamzin 1994); *acsABCDE*, *folD*, *metF* and *fhs* are critical genes for the Wood-Ljungdahl pathway (WLP) (Borrel, et al. 2016, Ragsdale and Pierce 2008).

Discussion

Research described in chapter 2 of this thesis supported the notion that microorganisms inhabiting marine sediments of Aarhus Bay were capable of using a variety of halogenated compounds, such as PCE and 2,6-DBP, as terminal electron acceptors for anaerobic respiration (Chapter 2). Henceforth, we set out to isolate the microorganisms responsible for this activity. This led to the isolation of a highly enriched consortium from an anoxic slant tube culture, which was characterized to dehalogenate brominated compounds rather than the chlorinated and iodinated compounds that the original enrichment was able to dehalogenate. The combination of short- and long-read metagenome sequence data generated in this study revealed that a population most closely affiliated with the genus *Desulforhopalus* was most abundant in this consortium, and five novel high quality MAGs could be assembled with > 85% completeness and < 2.5% contamination. Among these five MAGs, CH4_bin.3 and CH4_bin.4 were affiliated with the genus *Desulforplanes* and family *Marinifilaceae* respectively, and were identified as potential OHRB based on the presence of respiratory RDase-encoding genes, whereas, the *Desulforhopalus* associated CH4_bin.5 was found to encode a non-respiratory TPh-RDase. Intriguingly, the transcription of all RDase genes was strongly induced when 2,6-DBP was added, indicating that multiple strains simultaneously acted on this substrate, rather than outcompeting each other, at least for the duration of our studies that included multiple transfers. In addition, the consortium was found to have the genetic capacity for complete *de novo* B12 biosynthesis suggesting a symbiotic relationship for self-supplementing B12 to OHR.

This consortium was isolated from a stable, sediment-free PCE dechlorinating enrichment culture propagated in the presence sulfate, and which was mainly composed of members of the genera *Desulfoplanes*, *Desulfobacter*, *Bacillus* and *Desulforhopalus*. Of interest, the consortium lost the ability to dechlorinate PCE, but instead retained the capability to debrominate 2,6-DBP concomitant with retaining populations of *Desulfoplanes* and

Desulforhopalus in the consortium, suggesting their role as potential debrominators, rather than being involved in the dechlorination observed in the original culture. This was further supported by the fact that, based on the metagenomic analyses of the consortium, both populations comprised a large proportion within the 2,6-DBP debrominating consortium described in this study (Figure 4.3), in which CH4_bin.3 classified into *Desulfoplanes* encoded two RDase genes, whereas CH4_bin.5 belonging to *Desulforhopalus* coded for a TPh-RDase, which was formerly characterized to catalyze glutathione-dependent thiolytic reductive dehalogenation in strictly aerobic bacteria (Xun, et al. 1992a). In contrast, our data suggest that the thiolytic RDase in CH4_bin.5 might function in anaerobes, and thus in anoxic environments. The sequence alignment and structural simulation of RDases reinforced their membrane-bound property (Figure S4.3), and conservation of catalytical motifs or residues (Figure 4.4). Interestingly, cysteine residues are essential and conserved in both types of enzymes. In corrinoid-dependent RDases a cysteine residue is recruited to bind B12, whereas in TPh-RDases the cysteine residue has been shown to form a covalent intermediate with glutathione during catalysis (Bommer, et al. 2014, McCarthy, et al. 1997). Acetylene was previously reported as a general inhibitor for many biological processes, such as methane production and fermentation, and OHR (DeWeerd, et al. 1991, Pon, et al. 2003). Therefore, we decided to assess whether we can use it in this study for the measurement of bacterial growth from OHR. To this end, our physiological data revealed that acetylene specifically inhibited reductive dehalogenation without inhibitory effects on sulfate reduction and lactate oxidation (Figure S4.2). Interestingly, we found CH4_bin.2 and CH4_bin.5 encode complete nitrogenase complexes (N_2ases), NifHDK, which can reduce acetylene into ethene (Hyman and Daniel 1988). However, there was no ethene conversion from acetylene suggesting that N_2ases were inactive, possibly due to the presence of ammonium in the marine medium (9 mM), which can completely inhibit N_2ase activity (Dixon and Kahn 2004, Hübner, et al. 1993). Interestingly, recent studies revealed acetylene hydratase can allow bacteria to utilize acetylene as carbon source to support OHR (Akob, et al. 2017, Mao, et al. 2017). Nevertheless, we did not find this enzyme being encoded across the genomic assembly of the consortium. Notably, the inhibition by acetylene occurred at post-transcriptional level as the transcription of all RDase genes was highly-induced after adding 2,6-DBP (Figure 4.2). Unfortunately, the exact mechanism of acetylene inhibition still remains unresolved. It was reported that acetylene can target metalloenzymes, especially the metal cofactors Fe, Ni, Mo, and Cu, or bind directly with substrates and/or active sites (Hyman and Daniel 1988). It is thus tempting to speculate that the acetylene could target the iron-sulfur clusters or the catalytic sites of RDases to block the transfer of reducing equivalents, impeding RDase catalysis. Nevertheless, further experiments will be needed to elaborate the mechanism.

Respiratory reductive dehalogenation catalyzed by corrinoid-dependent RDases has been shown to serve as the terminal electron accepting process to complete the electron transfer through a membrane-associated electron transport chain (ETC) coupled to proton motive force formation and ATP production (Kublik, et al. 2016, Kunze, et al. 2017, Wang, et al. 2018). Based on the five MAGs identified in this study, we propose ETCs and related activities in the 2, 6-DBP debrominating consortium studied here (Figure 4.6). CH4_bin.3 harbors two RDases, RDase1 and RDase2 (Figure 4.4), and we assumed that both RDases are part of ETCs that allow usage of hydrogen or lactate as electron donor as observed for *Dehalobacter restrictus* and *Desulfoluna spongiiphila*, respectively (Kruse, et al. 2013, Peng, et al. 2020, Rupakula, et al. 2013). The membrane-bound flavoprotein, binding flavin mononucleotide (FMN) that was found encoded adjacent to RDase1, is predicted to function in a similar way as RdhC in the electron transfer (Buttet, et al. 2018), which was initially hypothesized as transcriptional regulator of OHR in *Desulfitobacterium dehalogenans* (Smidt, et al. 2000). In addition to the FMN encoding gene, the RDase1 encoding gene is also accompanied by a gene coding for RsxG, homologous to RnfG, which has been shown to transfer electrons from the quinol pool to nitrogenase (Koo, et al. 2003). Interestingly, a quinol dehydrogenase complex, NapGH, was predicted to be encoded downstream of RDase2 (Fincker and Spormann 2017, Kern and Simon 2008), acting as electron carrier to pass the electrons from the menaquinol pool to RDase2. The NapGH complex usually transfers electrons to the NapAB complex for nitrate respiration (Kern and Simon 2008). Based on the MAGs identified in this study, the consortium lacks the NapAB complex, in line with the observation that the culture was not able to use nitrate as electron acceptor (Table 4.1). With lactate added as the organic carbon source and electron donor, the fact that OHR and sulfate reduction occurred simultaneously, indicated the electrons were shared (Figure 4.6A). Lactate was consecutively oxidized into pyruvate and acetate by lactate and pyruvate dehydrogenase, respectively, to release the electrons entering the menaquinol pool. It is tempting to speculate that part of the electrons from this pool are transferred to the sulfate reduction pathway. To this end it should be noted that we did not observe genes coding for QmoABC that was previously shown to enable the conversion of APS to sulfite (van Vliet, et al. 2021), and thus an alternative complex is needed to fulfil this role. Dsr proteins subsequently reduce the sulfite to sulfide. In the absence of sulfate, hydrogen was observed as the result of lactate fermentation, which then served as the intermediate electron donor that is oxidized by Ni-Fe hydrogen uptake-type hydrogenases (HupLS) to transfer the electrons to RDases through the above-mentioned electron carrier proteins. The ETC including the RDase encoded on CH4_bin.4 is proposed to function in a similar manner as outlined for CH4_bin.3 to generate and transport electrons for the generation of a proton motive force and ATP synthesis (Figure 4.6B). Intriguingly, an anaerobic glycerol-3-phosphate (G3P) dehydrogenase complex (GPDH), GlpACB, which was previously characterized as the membrane-anchoring enzyme to catalyze G3P conversion into dihydroxyacetone phosphate achieving the electron flow through the cytosol to the membrane (Koekemoer, et al. 1995), was found encoded on CH4_bin.4. We therefore speculated that this GPDH complex transfers electrons to the RDase initiating the ETP for OHR in this organism. Based on the model proposed here, further studies will be needed for the characterization and experimental validation of ETCs in the organisms studied here. In addition to the active respiratory RDases, the gene encoding the non-respiratory TPh-RDase from CH4_bin.5 was also highly expressed, suggesting an active role of this enzyme in the observed debromination of the 2,6-DBP to phenol (Figure 4.4E). The complete inhibition of reductive debromination by acetylene furthermore suggests that acetylene inhibited activity of both types of RDases. Finally, the *Desulforhopalus* population (CH4_bin.5) is proposed to act as the B12 provider for OHRB (CH4_bin.3, CH4_bin.4) due to its nearly-complete gene-set for *de novo* B12 biosynthesis except for *cbiJ* (Figure 4.6C), which was not required for OHR as previous described (Peng, et al. 2020). Moreover, CH4_bin.4 contains a *cbiJ* gene indicating that this might play a role in the complete B12 biosynthesis of the isolated consortium.

In summary, we provide evidence that the debromination potential of the isolated consortium is associated with the respiratory RDases and TPh-RDase encoded on bins that were phylogenetically-affiliated with potentially novel species within the genera *Desulfoplanes*, *Marinifilum* and *Desulforhopalus*. Moreover, phylogenomic analyses inferred for the first time that members of *Marinifilum* and *Ancylomarina* are potential OHRB, reinforcing a yet underestimated diversity of OHRB in marine environments. In addition, acetylene exerted specific inhibition on reductive dehalogenation post-transcriptionally, and could serve as an indicator to clarify the relationship between OHR, nitrogen fixation and acetylene oxidation in ammonium-low or free environments. Furthermore, the distribution of genes encoding a complete *de novo* B12 biosynthesis pathway and physiological data supported the collaborative relationship within the consortium that deserves further study.

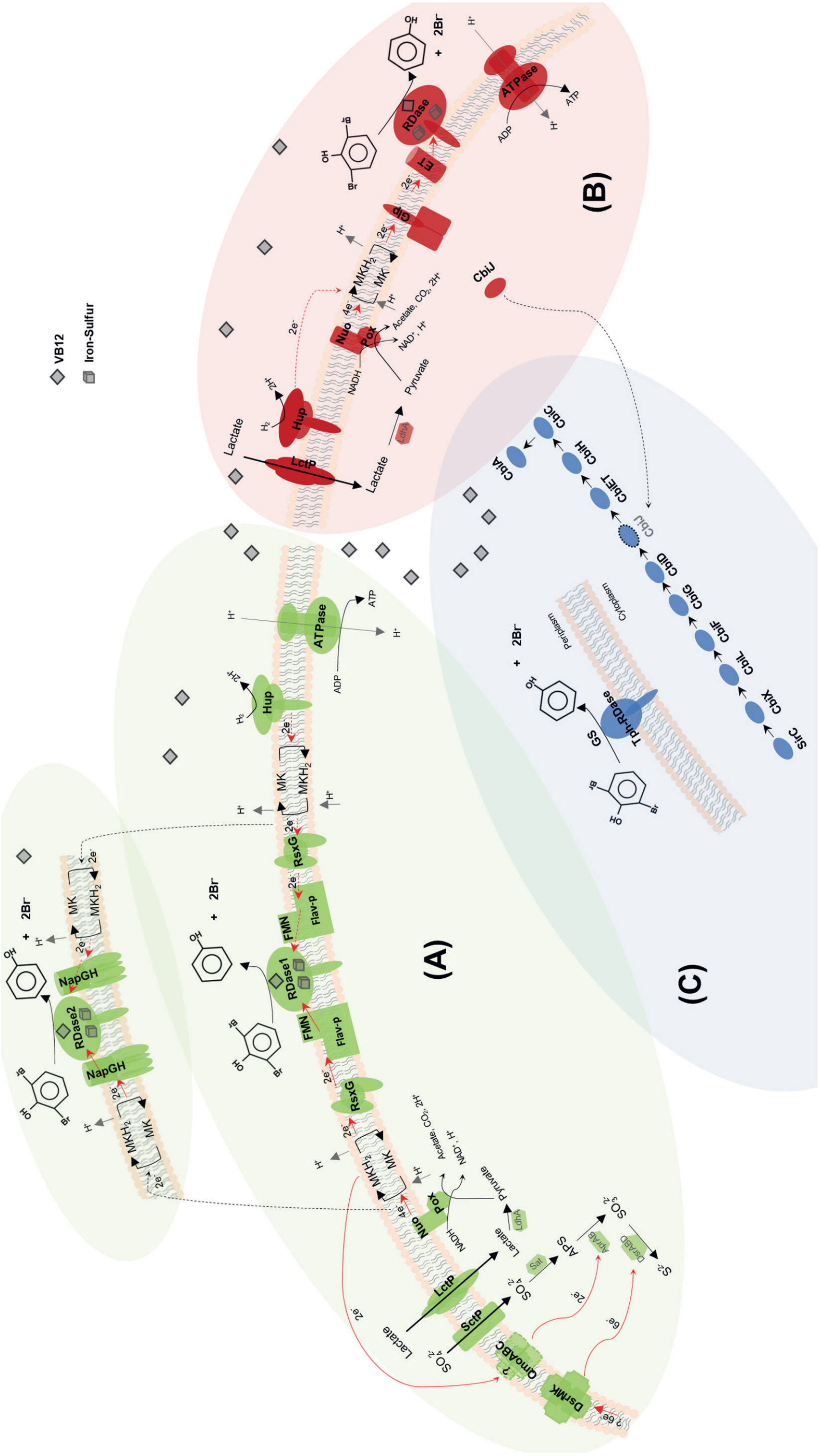
VB12
Iron-Sulfur
(A)
(B)
(C)
LctP
SctP
QmoABC
DsrMK
Nuo
Pox
LdhA
Sat
AprAB
DsrABD
RsxG
Flav-p
FMN
RDase1
RDase2
NapGH
MK
MKH₂
Hup
ATPase
ADP
ATP
Lactate
Pyruvate
NADH
NAD⁺, H⁺
Acetate, CO₂, 2H⁺
SO₄²⁻
APS
SO₃²⁻
S²⁻
H₂
2H⁺
H⁺
2e⁻
4e⁻
6e⁻
? 6e⁻
2Br⁻
RDase
ET
Glp
CbiJ
Tph-RDase
GS
Periplasm
Cytoplasm
SirC
CbiX
CbiL
CbiF
CbiG
CbiD
CbiJ
CbiET
CbiH
CbiC
CbiA
OH
Br
HO

Figure 4.6 Proposed schematic overview of electron transport chains (ETCs) of organohalide respiration associated with sulfate reduction and de novo B12 biosynthesis. Electron transfer from lactate or H_2 to the RDases and other proteins encoded on CH4_bin.3 to catalyze OHR and sulfate reduction (A). RDase of CH4_bin.4 follows a similar ETC pattern without sulfate reduction (B). In contrast, non-respiratory TPh-RDase of CH4_bin.5 transforms 2,6-DBP to phenol and provides the essential B12 for OHR to respiratory RDases (C). Color patterns used in this figure are in line with Figure 4.5. MKH_2/MK: menaquinones; NapGH: periplasmic nitrate reductase; Flav-p: flavoprotein, which can bind with flavin mononucleotides (FMN); RsxG: electron transporter, homologous with RnfG (Koo, et al. 2003); Nuo: NADH dehydrogenase; Pox: Pyruvate dehydrogenase; LctP: lactate permease; LdhA: lactate dehydrogenase; SctP: sulfate permease; Sat: sulfate adenylyltransferase; AprAB: APS reductase; DsrABD: dissimilatory sulfite reductase; DsrMK: electron transport complex function with DsrABD; QmoABC: electron transport complex; Hup: [Ni-Fe] hydrogen uptake-type hydrogenases, includes the large and small subunits; Glp: glycerol-3-phosphate (G3P) dehydrogenase complex; ET: ferredoxin as intermediate electron transporter; SirC-CbiA: complete B12 de novo biosynthesis. Red arrows indicate the assumed electron flow, black dotted arrows indicate parallel electron flow in (A), and CbiJ as the supplementary from CH4_bin.4 (B) to CH4_bin.5 (C) to form a complete B12 biosynthesis pathway; “? 6e-”: unknown source of deprived electrons; “? QmoABC”: not found in genomic annotation, and could be replaced by another functionally similar complex;

Acknowledgements

This study was supported by the Dutch Research Council through the UNLOCK project (NRGWI.obrug.2018.005), as well as Wageningen University through its Innovation Program Microbiology. We thank Peng Peng for giving expert guidance for isolation of anaerobes. We acknowledge the China Scholarship Council (CSC) for the support to Chen Zhang (File No. 201807720048).

Supplementary Information

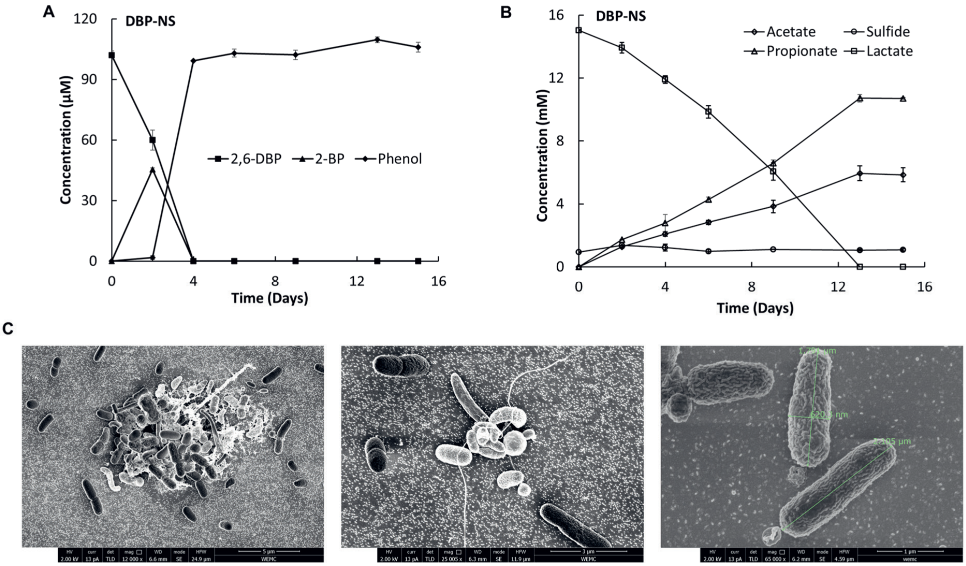

Figure S4.1 Reductive debromination of 2,6-dibromophenol (2,6-DBP) under sulfate-free conditions and scanning electron microscopy (SEM) of the consortium (related to Figure 4.1). 2,6-DBP was debrominated into phenol with the formation of 2-bromophenol as the intermediate (2-BP) (A). Lactate was consumed with the formation of propionate and acetate (B). The consortium was visualized by SEM at various magnifications, 12000 X (left), 25005 X (middle) and 65000 X (right) (C). The rod-shaped bacterium was measured in diameter (620.3 nm) and length (1.791 – 2.105 µm) as shown in green lines and letters.

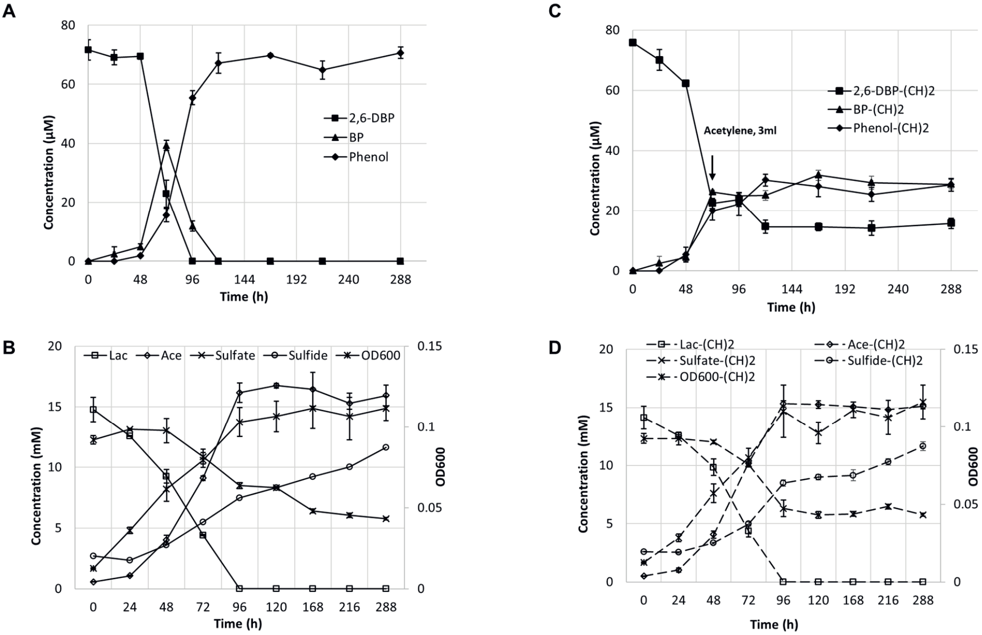

Figure S4.2 Inhibition by acetylene specifically on reductive debromination of 2,6-DBP in the presence of sulfate reduction (related to Figure 4.2). Reductive debromination of 2,6-DBP in addition to sulfate as the electron acceptor, and metabolite measurement with lactate as the electron donor and carbon source in the absence of acetylene (A, B), and presence of acetylene (C, D) respectively. (CH)2: acetylene; downward arrow indicates the injection of acetylene; Dashed lines represent the metabolism of lactate and sulfate after the addition of acetylene. Three replicate bottles were set, and the data indicate the mean ± SD. Error bars represent the SD.

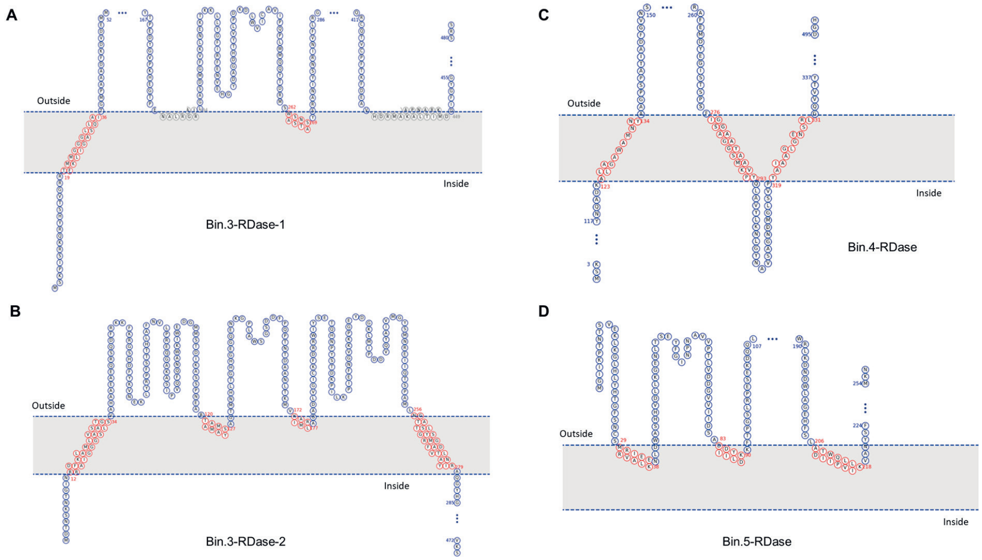

Figure S4.3 Transmembrane configuration prediction of RDases and Tph-RDase of assembled bins (related to Figure 4.4), including two RDases from CH4_bin.3 (A, B); one RDase from CH4_bin.4 (C) and TPh-RDase from CH4_bin.5 (D). The prediction of transmembrane configuration of the (TPh-) RDases was achieved by MemBrain (Feng, et al. 2020).

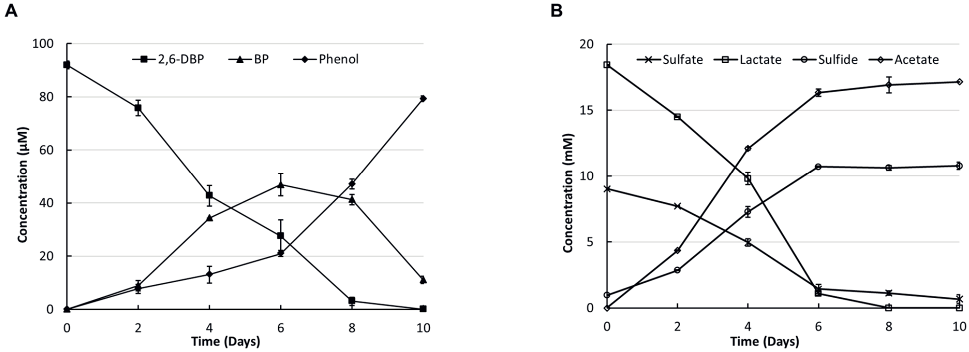

Figure S4.4 Reductive debromination of 2,6-DBP without additional B12 (related to Figure 4.5). Reductive debromination of 2,6-DBP to phenol with bromophenol as the intermediate (A). Lactate served as the electron donor and carbon source and was consumed to form acetate, and sulfate as the electron acceptor was reduced into sulfide (B). 2,6-DBP: 2,6-dibromophenol; BP: bromophenol; The experiment was set with three replicate bottles, and the data indicate the mean ± SD. Error bars represent the SD.

Table S4.1 Information of the assembled bins (MAGs)

Bins	**Classification**	**GC (%)**	**N50 (bp)**	**Size (bp)**	**Abundance**	**ANI [a] (%)**
CH4_bin.1	*g_Oceanispirochaeta*	43.1	10840	5074027	392.735242	93.85
CH4_bin.2	*g_Desulfoplanes*	51.4	199123	3841128	1567.138705	78.11
CH4_bin.3	*g_Desulfoplanes*	50.3	87237	4114339	1983.865769	78.14
CH4_bin.4	*f_Marinifilaceae*	38.6	43215	5488154	523.39148	N/A [b]
CH4_bin.5	*g_Desulforhopalus*	49.3	837424	3685696	9786.929752	76.45

[a] ANI: average nucleotide identity to the closest reference genome;

[b] N/A: indicates novel genus without closely related reference genome;

Reference

Akob DM, Baesman SM, Sutton JM *et al.* Detection of diazotrophy in the acetylene-fermenting anaerobe *Pelobacter* sp. strain SFB93. *Appl Environ Microbiol* 2017;83: e01198-17.

Apajalahti JH, Salkinoja-Salonen MS. Complete dechlorination of tetrachlorohydroquinone by cell extracts of pentachlorophenol-induced *Rhodococcus chlorophenolicus*. *J Bacteriol* 1987;169: 5125-30.

Arnoux P, Sabaty M, Alric J *et al.* Structural and redox plasticity in the heterodimeric periplasmic nitrate reductase. *Nat Struct Mol Biol* 2003;10: 928-34.

Atashgahi S. Discovered by genomics: putative reductive dehalogenases with N-terminus transmembrane helixes. *FEMS Microbiol Ecol* 2019;95: fiz048.

Belay N, Daniels L. Production of ethane, ethylene, and acetylene from halogenated hydrocarbons by methanogenic bacteria. *Appl Environ Microbiol* 1987;53: 1604-10.

Bernstein HC. Reconciling ecological and engineering design principles for building microbiomes. *mSystems* 2019;4: e00106-19.

Bertrand D, Shaw J, Kalathiyappan M *et al.* Hybrid metagenomic assembly enables high-resolution analysis of resistance determinants and mobile elements in human microbiomes. *Nat Biotechnol* 2019;37: 937-44.

Bommer M, Kunze C, Fesseler J *et al.* Structural basis for organohalide respiration. *Science* 2014;346: 455-8.

Bosma TN, van der Meer JR, Schraa G *et al.* Reductive dechlorination of all trichloroand dichlorobenzene isomers. *FEMS Microbiol Ecol* 1988;53: 223-9.

Buttet GF, Willemin MS, Hamelin R *et al.* The membrane-bound c subunit of reductive dehalogenases: topology analysis and reconstitution of the FMN-binding domain of PceC. *Front Microbiol* 2018;9: 755.

Cline JD. Spectrophotometric determination of hydrogen sulfide in natural waters. *Limnol Oceanogr* 1969;14: 454-8.

DeWeerd K, Concannon F, Suflita JM. Relationship between hydrogen consumption, dehalogenation, and the reduction of sulfur oxyanions by *Desulfomonile tiedjei*. *Appl Environ Microbiol* 1991;57: 1929-34.

Dixon R, Kahn D. Genetic regulation of biological nitrogen fixation. *Nat Rev Microbiol* 2004;2: 621-31.

Fellay R, Hanin M, Montorzi G *et al.* nodD2 of *Rhizobium* sp. NGR234 is involved in the repression of the *nodABC* operon. *Mol Microbiol* 1998;27: 1039-50.

Feng S-H, Zhang W-X, Yang J *et al.* Topology prediction improvement of α-helical transmembrane proteins through helix-tail modeling and multiscale deep learning fusion. *J Mol Biol* 2020;432: 1279-96.

Fincker M, Spormann AM. Biochemistry of catabolic reductive dehalogenation. *Annu Rev Biochem* 2017;86: 357-86.

Gaballa A, Helmann JD. Substrate induction of siderophore transport in *Bacillus subtilis* mediated by a novel one-component regulator. *Mol Microbiol* 2007;66: 164-73.

Garber A, Ramirez G, Merino N *et al.* MagicLamp: toolkit for annotation of 'omics datasets using curated HMM sets. *GitHub Repository Available online at https://githubcom/Arkadiy-Garber/MagicLamp (accessed January, 2022)* 2020.

Goodwin S, McPherson JD, McCombie WR. Coming of age: ten years of next-generation sequencing technologies. *Nat Rev Genet* 2016;17: 333-51.

Gopinath K, Venclovas Č, Ioerger TR *et al.* A vitamin B12 transporter in Mycobacterium tuberculosis. *Open Biol* 2013;3: 120175.

Goris T, Schiffmann CL, Gadkari J *et al.* Proteomics of the organohalide-respiring Epsilonproteobacterium *Sulfurospirillum multivorans* adapted to tetrachloroethene and other energy substrates. *Sci Rep* 2015;5.

Greening C, Biswas A, Carere CR *et al.* Genomic and metagenomic surveys of hydrogenase distribution indicate H_2 is a widely utilised energy source for microbial growth and survival. *ISME J* 2016;10: 761-77.

Howard JB, Rees DC. Structural basis of biological nitrogen fixation. *Chem Rev* 1996;96: 2965-82.

Hübner P, Masepohl B, Klipp W *et al.* nif gene expression studies in Rhodobacter capsulatus: nfrC-independent repression by high ammonium concentrations. Mol Microbiol 1993;10: 123-32.

Hyman MR, Daniel A. Acetylene inhibition of metalloenzymes. *Anal Biochem* 1988;173: 207-20.

Isaxons M, Teske A. *Desulforhopalus vacuolatus* gen. nov., sp. nov., a new moderately psychrophilic sulfate-reducing bacterium with gas vacuoles isolated from a temperate estuary. *Arch Microbiol* 1996;166 160-8.

Jiao J-Y, Fu L, Hua Z-S *et al.* Insight into the function and evolution of the Wood-Ljungdahl pathway in Actinobacteria. *ISME J* 2021;15: 3005-18.

Jochum LM, Schreiber L, Marshall IPG *et al.* Single-cell genomics reveals a diverse metabolic potential of uncultivated *Desulfatiglans*-related Deltaproteobacteria widely distributed in marine sediment. *Front Microbiol* 2018;9: 2038.

Jormakka M, Byrne B, Iwata S. Formate dehydrogenase–a versatile enzyme in changing environments. *Curr Opin Struct Biol* 2003;13: 418-23.

Jugder BE, Ertan H, Lee M *et al.* Reductive dehalogenases come of age in biological destruction of organohalides. *Trends Biotechnol* 2015;33: 595-610.

Kapoore RV, Padmaperuma G, Maneein S *et al.* Co-culturing microbial consortia: approaches for applications in biomanufacturing and bioprocessing. *Crit Rev Biotechnol* 2022;42: 46-72.

Kern M, Simon J. Characterization of the NapGH quinol dehydrogenase complex involved in *Wolinella succinogenes* nitrate respiration. *Mol Microbiol* 2008;69: 1137-52.

Koekemoer TC, Litthauer D, Oelofsen W. Isolation and characterization of adipose tissue glycerol-3-phosphate dehydrogenase. *Int J Biochem Cell Biol* 1995;27: 625-32.

Koo M-S, Lee J-H, Rah S-Y *et al.* A reducing system of the superoxide sensor SoxR in *Escherichia coli*. *EMBO J* 2003;22: 2614-22.

Kruse S, Türkowsky D, Birkigt J *et al.* Interspecies metabolite transfer and aggregate formation in a co-culture of *Dehalococcoides* and *Sulfurospirillum* dehalogenating tetrachloroethene to ethene. *ISME J* 2021;15: 1794-809.

Kruse T, Maillard J, Goodwin L *et al.* Complete genome sequence of *Dehalobacter restrictus* PER-K23T. *Stand Genomic Sci* 2013;8: 375-88.

Kube M, Beck A, Zinder SH *et al.* Genome sequence of the chlorinated compound–respiring bacterium *Dehalococcoides* species strain CBDB1. *Nat Biotechnol* 2005;23: 1269-73.

Kublik A, Deobald D, Hartwig S *et al.* Identification of a multi-protein reductive dehalogenase complex in *Dehalococcoides mccartyi* strain CBDB1 suggests a protein-dependent respiratory electron transport chain obviating quinone involvement. *Environ Microbiol* 2016;18: 3044-56.

Kunze C, Bommer M, Hagen WR *et al.* Cobamide-mediated enzymatic reductive dehalogenation via long-range electron transfer. *Nat Commun* 2017;8: 15858.

Lawson CE, Harcombe WR, Hatzenpichler R *et al*. Common principles and best practices for engineering microbiomes. *Nat Rev Microbiol* 2019;17: 725-41.

Lee MD. GToTree: a user-friendly workflow for phylogenomics. *Bioinformatics* 2019;35: 4162-4.

Lie TJ, Clawson ML, Godchaux W *et al.* Sulfidogenesis from 2-aminoethanesulfonate (taurine) fermentation by a morphologically unusual sulfate-reducing bacterium, *Desulforhopalus singaporensis* sp. nov. *Appl Environ Microbiol* 1999;65: 3328-34.

Magnuson Jon K, Stern Robert V, Gossett James M *et al.* Reductive dechlorination of tetrachloroethene to ethene by a two-component enzyme pathway. *Appl Environ Microbiol* 1998;64: 1270-5.

Mao X, Oremland RS, Liu T *et al.* Acetylene fuels TCE reductive dechlorination by defined *Dehalococcoides*/*Pelobacter* consortia. *Environ Sci Technol* 2017;51: 2366-72.

Maymó-Gatell X, Nijenhuis I, Zinder SH. Reductive dechlorination of cis-1,2-dichloroethene and vinyl chloride by "*Dehalococcoides ethenogenes*". *Environ Sci Technol* 2001;35: 516-21.

McCarthy DL, Louie DF, Copley SD. Identification of a covalent intermediate between glutathione and cysteine13 formed during catalysis by tetrachlorohydroquinone dehalogenase. *J Am Chem Soc* 1997;119: 11337-8.

McCarthy DL, Navarrete S, Willett WS *et al.* Exploration of the relationship between tetrachlorohydroquinone dehalogenase and the glutathione S-transferase superfamily. *Biochemistry* 1996;35: 14634-42.

Mohn WW, Tiedje J. Microbial reductive dehalogenation. *Microbiol Mol Biol Rev* 1992;56: 482-507.

Mohn WW, Tiedje JM. Strain DCB-1 conserves energy for growth from reductive dechlorination coupled to formate oxidation. *Arch Microbiol* 1990;153: 267-71.

Monserrate E, Häggblom MM. Dehalogenation and biodegradation of brominated phenols and benzoic acids under iron-reducing, sulfidogenic, and methanogenic conditions. *Appl Environ Microbiol* 1997;63: 3911-5.

Moore SJ, Warren MJ. The anaerobic biosynthesis of vitamin B12. *Biochem Soc Trans* 2012;40: 581-6.

Ni S, Fredrickson JK, Xun L. Purification and characterization of a novel 3-chlorobenzoate-reductive dehalogenase from the cytoplasmic membrane of *Desulfomonile tiedjei* DCB-1. *J Bacteriol* 1995;177: 5135-9.

Peng P, Goris T, Lu Y *et al.* Organohalide-respiring *Desulfoluna* species isolated from marine environments. *ISME J* 2020;14: 815-27.

Pon G, Hyman MR, Semprini L. Acetylene inhibition of trichloroethene and vinyl chloride reductive dechlorination. *Environ Sci Technol* 2003;37: 3181-8.

Quast C, Pruesse E, Yilmaz P *et al.* The SILVA ribosomal RNA gene database project: improved data processing and web-based tools. *Nucleic Acids Res* 2013;41: D590-6.

Ragsdale SW. Enzymology of the Wood–Ljungdahl pathway of acetogenesis. *Ann N Y Acad Sci* 2008;1125: 129-36.

Rinke C, Chuvochina M, Mussig AJ *et al.* A standardized archaeal taxonomy for the Genome Taxonomy Database. *Nat Microbiol* 2021;6: 946-59.

Rupakula A, Kruse T, Boeren S *et al.* The restricted metabolism of the obligate organohalide respiring bacterium *Dehalobacter restrictus*: lessons from tiered functional genomics. *Philos Trans R Soc Lond B Biol Sci* 2013;368: 20120325.

Schuster SC. Next-generation sequencing transforms today's biology. *Nat Methods* 2008;5: 16-8.

Simon J. Enzymology and bioenergetics of respiratory nitrite ammonification. *FEMS Microbiol Rev* 2002;26: 285-309.

Skibinski David AG, Golby P, Chang Y-S *et al.* Regulation of the Hydrogenase-4 Operon of *Escherichia coli* by the σ^{54}-Dependent Transcriptional Activators FhlA and HyfR. *J Bacteriol* 2002;184: 6642-53.

Smidt H, van Leest M, van der Oost J *et al.* Transcriptional regulation of the *cpr* gene cluster inortho-chlorophenol-respiring *Desulfitobacterium dehalogenans*. *J Bacteriol* 2000;182: 5683-91.

Søndergaard D, Pedersen CN, Greening C. HydDB: a web tool for hydrogenase classification and analysis. *Sci Rep* 2016;6: 1-8.

Suzuki MT, Giovannoni SJ. Bias caused by template annealing in the amplification of mixtures of 16S rRNA genes by PCR. *Appl Environ Microbiol* 1996;62: 625-30.

Uritskiy GV, DiRuggiero J, Taylor J. MetaWRAP—a flexible pipeline for genome-resolved metagenomic data analysis. *Microbiome* 2018;6: 1-13.

van Vliet DM, von Meijenfeldt FB, Dutilh BE *et al.* The bacterial sulfur cycle in expanding dysoxic and euxinic marine waters. *Environ Microbiol* 2021;23: 2834-57.

Vogel TM, McCARTY PL. Biotransformation of tetrachloroethylene to trichloroethylene, dichloroethylene, vinyl chloride, and carbon dioxide under methanogenic conditions. *Appl Environ Microbiol* 1985;49: 1080-3.

Wang S, Qiu L, Liu X *et al.* Electron transport chains in organohalide-respiring bacteria and bioremediation implications. *Biotechnol Adv* 2018;36: 1194-206.

Xun L, Topp E, Orser C. Glutathione is the reducing agent for the reductive dehalogenation of tetrachloro-p-hydroquinone by extracts from a *Flavobacterium* sp. *Biochem Biophys Res Commun* 1992a;182: 361-6.

Xun L, Topp E, Orser C. Purification and characterization of a tetrachloro-p-hydroquinone reductive dehalogenase from a *Flavobacterium* sp. *J Bacteriol* 1992b;174: 8003-7.

Yan J, Şimşir B, Farmer AT *et al.* The corrinoid cofactor of reductive dehalogenases affects dechlorination rates and extents in organohalide-respiring *Dehalococcoides mccartyi*. *The ISME J* 2016;10: 1092-101.

Yilmaz P, Parfrey LW, Yarza P *et al.* The SILVA and “all-species living tree project (LTP)” taxonomic frameworks. *Nucleic Acids Res* 2014;42: D643-8.

Yu G, Smith DK, Zhu H *et al.* ggtree: an R package for visualization and annotation of phylogenetic trees with their covariates and other associated data. *Methods Ecol Evol* 2017;8: 28-36.

Zaremba-Niedzwiedzka K, Caceres EF, Saw JH *et al.* Asgard archaea illuminate the origin of eukaryotic cellular complexity. *Nature* 2017;541: 353-8.

Zhuang WQ, Yi S, Bill M *et al.* Ljungdahl pathway facilitates one-carbon metabolism in organohalide-respiring *Dehalococcoides mccartyi*. *Proc Natl Acad Sci U S A* 2014;111: 6419-24.

Zinke LA, Mullis MM, Bird JT *et al.* Thriving or surviving? Evaluating active microbial guilds in Baltic Sea sediment. *Environ Microbiol Rep* 2017;9: 528-36.

Zumft WG. Cell biology and molecular basis of denitrification. *Microbiol Mol Biol Rev* 1997;61: 533-616.

Chapter 5

Organohalide respiration by a sulfate-reducing formatotroph, *Desulforhopalus singaporensis*

Chen Zhang, Siavash Atashgahi, Tom N.P Bosma, Hauke Smidt

Manuscript in preparation

Abstract

Our previous enrichment studies and multi-omic data analyses indicated that members of the genus *Desulforhopalus* are capable of reductive dehalogenation (RD). Here, we studied organohalide respiration (OHR) in *Desulforhopalus singaporensis*, a sulfate reducer, as genome analysis predicted the presence of a respiratory reductive dehalogenase (RDase) gene. Our results revealed that *D. singaporensis* can debrominate 2,6-dibromophenol (2,6-DBP), 2,4-DBP, and 2,4,6-tribromophenol to phenol and 4-bromophenol, respectively, regardless of the presence of vitamin B12 in the medium, due to its complete *de novo* biosynthesis of vitamin B12. Debromination of 2,6-DBP suppressed sulfate reduction in *D. singaporensis*. Interestingly, *D. singaporensis* was identified as a formatotroph using formate as the electron donor instead of H_2 for the Wood-Ljungdahl pathway to conserve energy and fix CO_2 leading to the formation of acetate. In addition, *D. singaporensis* gained more biomass under formatotrophic conditions in the presence of 2,6-DBP compared to the control without additional 2,6-DBP or in the presence of acetylene, previously shown to inhibit reductive debromination, respectively. Furthermore, RDase gene expression profiles showed that the acetylene inhibited RDase activity post-transcriptionally. Altogether, this study experimentally verified the OHR potential of *D. singaporensis* in the presence of formate, which served as the electron donor and was used in carbon assimilation through the Wood-Ljungdahl pathway.

Key words: *Desulforhopalus singaporensis*; sulfate reducers; RDase gene; reductive debromination; Wood-Ljungdahl pathway.

Introduction

With the advancement of DNA sequencing technology, microbiomes residing in a broad range of different pristine and man-made environments are increasingly being explored in order to establish the microbial composition and to discover novel microorganisms and metabolic pathways (Goodwin et al., 2016). Using sequence-based approaches, it has also been shown that reductive dehalogenases (RDases) are widely distributed in pristine marine sediments and that these enzymes are not restricted to the well-identified organohalide-respiring bacteria (OHRB) that belong to the phyla *Chloroflexota*, *Firmicutes* and *Proteobacteria* (among which the class *Deltaproteobacteria*, recently reclassified as *Desulfobacterota* phyl. nov.) (Waite et al., 2020). For example, also Asgard Archaea which have been proposed to have played a role in the evolution of eukaryotic cells, appear to have RDase encoding genes in their genomes (Fincker and Spormann, 2017; Atashgahi et al., 2018a; Spang et al., 2019; Waite et al., 2020). These findings reinforce the ecological importance of dehalogenation for the biogeochemical cycles of halogen and carbon. In our previous study we showed the enrichment of bacterial populations not previously associated with organohalide respiration (OHR) in anaerobic dehalogenating cultures derived from pristine marine sediments from Aarhus Bay illustrating the potential importance of OHR in these sediments (Chapter 2). The subsequent metagenomic analysis allowed the generation of several metagenome assembled genomes (MAGs), some of which were identified as potentially novel species of OHRB bearing RDase genes that were highly expressed as revealed by metatranscriptome sequencing and reverse-transcriptase quantitative PCR analysis of RNA extracted from cultures grown in the presence of halogenated compounds (chapter 4). Unfortunately, only a few isolated strains, close to the MAGs, are available to characterize their metabolic functions, especially their reductive dehalogenation (RD) potential.

OHRB are widely applied for *in situ* bioremediation of sites polluted with organohalides (Nijenhuis and Kuntze, 2016; Atashgahi et al., 2018b). All known OHRB are vitamin B12 (B12)-dependent and require the addition of non-specific electron donors, such as glycerol and lactate (Payne et al., 2011; Zanaroli et al., 2015; Atashgahi et al., 2017). Accordingly, it would be economically interesting to employ versatile OHRB, especially strains that can grow autotrophically by assimilating CO_2 or formate for *in situ* bioremediation (Yishai et al., 2016). Recent culture-independent studies, such as single-cell genomics and metagenomics, revealed a linkage between RD and the Wood-Ljungdahl pathway (WLP) among populations of marine *Chloroflexota* (Fullerton and Moyer, 2016; Sewell et al., 2017; Fincker et al., 2020), suggesting their potential for autotrophic OHR. Furthermore, the obligate OHRB *Dehalococcoides mccartyi*, using H_2 as the electron donor, contains an incomplete WLP lacking four critical genes, *metF* (coding for methylene-tetrahydrofolate reductase, MTHFR), *acsE* (coding for methyltransferase, MeTr), *fdh* (coding for formate dehydrogenase, FDH), and *acsA* (coding for carbon monoxide dehydrogenase, CODH) (Maymo-Gatell et al., 1997; Holliger et al., 1999; Maymo-Gatell et al., 1999; Zhuang et al., 2014). In an experiment to verify potential autotrophic OHR, the lack of *acsA* caused CO accumulation, which inhibited the growth of *D. mccartyi* and attenuated RD, possibly as a result of inactivation of metalloenzymes, such as hydrogenases (Zhuang et al., 2014). Hence, having the complete WLP or, alternatively, the presence of CO oxidizers, could ameliorate side effects of CO accumulation on cell growth of OHRB. In contrast to the obligatory OHRB, some versatile OHRB, such as *Desulfitobacterium hafniense* DCB-2, contain a full set of genes for CO_2-fixing WLP (Kim et al., 2012). However, to our knowledge, the potential for autotrophic OHR has not been experimentally verified.

Newly-assembled RDase gene clusters revealed that RDase-encoding operons are frequently correlated with genes encoding proteins involved in nitrogen metabolism, such as the NtrC-type transcriptional activators (Zimmer et al., 2000; Bush and Dixon, 2012; Liu and Haggblom, 2018), but their association with OHR has not yet been demonstrated.

The aim of this study was to provide evidence that *Desulforhopalus* sp. populations that were enriched in dehalogenating cultures derived from Aarhus Bay marine sediment (chapter 4), are indeed capable of autotrophic RD using the WLP and that they are indeed B12 independent. Since we unfortunately did not obtain pure culture isolates from our cultures, we tested two available isolates, *Desulforhopalus singaporensis* DSM 12130 and *Desulforhopalus vacuolatus* DSM 9700, and tested them for their ability to use organohalides as terminal electron acceptor during OHR. Since only *Desulforhopalus singaporensis* 12130 was capable of OHR, this strain was further used in our study. We were able to demonstrate (i) the reductive debromination of 2,6-DBP with priority over sulfate reduction when the organism was grown with lactate, and (ii) OHR with 2,6-DBP as electron acceptor with formate as the only source of carbon and electrons, under formatotrophic conditions. Finally, (iii) the concurrent respiratory debromination led to an increase in biomass concentration as compared to growth with formate only.

Materials and methods

Chemicals

Chlorinated compounds, including tetrachloroethene (PCE), 2,6-dichlorophenol (2,6-DCP), 2,4-DCP, 2,4,6-TCP, 1,4-dichlorobenze (1,4-DCB), 1,2-DCB, 1,3-DCB, 1,2,4-TCB, benzene, and brominated compounds, including 2,6-DBP, 2,4-DBP, 2,4-6-DBP, 1,4-dibromobenzene (1,4-DBB), 1,2-DBB, 1,3-DBB, and 1,2,4-tribromobenzene (1,2,4-TBB), and iodinated compounds, 2,4,6-triiodiphenol (2,4,6-TIP), 2,4-DIP, 2,6-DIP, 2-IP, and 4-IP, were purchased from Sigma-Aldrich. Stock solutions of sulfate (0.5 M), sulfite (0.5 M), thiosulfate (0.5 M), nitrate (0.5 M), formate (0.5 M), acetate (0.25 M), pyruvate (0.5 M), and lactate (0.5 M) were prepared by filter sterilization (syringe filter, 0.2 μm, mdimembrane, Ambala Cantt, India). All other (in)organic chemicals were of analytical grade.

Cultivation

D. vacuolatus (DSM 9700) and *D. singaporensis* (DSM 12130) were purchased as lyophilized cultures from the Leibniz Institute DSMZ (German Collection of Microorganisms and Cell Cultures GmbH, Braunschweig, Germany). Lyophilized cultures were used taking account their sensitivity to low oxygen concentrations following the instructions "Handling of vacuum-dried anaerobic cultures". Anoxic marine medium was prepared as previously described (Monserrate and Häggblom, 1997; Peng et al., 2020), with minor adjustments for cultivation of *D. vacuolatus* and *D. singaporensis*, respectively. The concentrations of NaCl were adjusted to 10 g/L for *D. vacuolatus* and 5 g/L for *D. singaporensis* respectively (Isaxons and Teske, 1996; Lie et al., 1999; Kuever et al., 2015). In addition, *D. vacuolatus* was grown at 19 ℃ and *D. singaporensis* at 30 °C. Resazurin (0.005 g/L) was added as the redox indicator and $Na_2S{\cdot}9H_2O$ (0.48 g/L, 2 mM) served as the reducing agent for maintaining anoxic conditions. 120 ml serum bottles were filled with 50 ml marine medium and the headspace was replaced with N_2 / CO_2 (80:20 %, 140 Kpa). Bottles were sealed by teflon-coated butyl rubber septa and aluminum crimp caps (GRACE, MD, USA). The above-mentioned halogenated compounds (100 μM) were selected as the electron acceptors in combination with lactate as the electron donor and carbon source to assess the dehalogenating potential of both *D. vacuolatus* and *D. singaporensis*. 2,6-DBP (100 μM) was employed to test for OHR-supported cell growth of *D. singaporensis* with formate (10 mM) added as the electron donor and carbon source. Meanwhile, acetylene (1.8 mM) was tested as the specific inhibitor of reductive debromination and added to validate the role of reductive debromination for bacterial growth and expression of the RDase-encoding gene cluster. In addition, B12 (0.04 mg/L) was checked for its indispensability for reductive debromination. To this end, residual amounts of B12 from mother cultures were removed through three consecutive transfers (10% vol/vol) and incubation.

Analytical methods

Gas chromatography coupled with mass spectrometry (GC-MS), using an Rt®-Q-BAND column (Retek, PA, USA) and DSQ-MS (Thermo Fisher Scientific) was used to measure PCE, trichloroethene (TCE), cis-dichloroethene (cDCE), trans-dichloroethene (tDCE), ethene and acetylene. All remaining chlorinated, brominated and iodinated compounds were measured using a Thermo Scientific Accella High-Performance Liquid Chromatography (HPLC) system installed with Agilent Poroshell 120 EC-C18 column and a UV/Vis detector. Meanwhile, SHIMADZU LC2030 PLUS coupled with a Shodex SUGAR Series® SH1821 column was used to measure the consumption and production of organic acids, including lactate, propionate, acetate and formate. Sulfate, sulfite, thiosulfate, and nitrate were detected using a Thermo Scientific DionexTM ICS-2100 Ion Chromatography System (Dionex ICS-2100). A photometric method using methylene blue was used to determine the accumulation of sulfide as previously described (Cline 1969).

DNA and RNA extraction and reverse transcriptase quantitative PCR

Cultures grown under different conditions were harvested by centrifugation at 10,000 × g for 5 min, and the supernatants were discarded. Subsequently, the collected biomass was washed three times with 200 µL TE buffer (pH=7.0) on ice to remove residual medium components and metabolites that might interfere with downstream DNA and RNA extraction. Total genomic DNA was extracted from cultures of *D. vacuolatus* and *D. singaporensis* using the MasterPureTM Gram positive DNA purification Kit (Epicentre). For RNA extraction from triplicate cultures per condition, the collection of samples followed the same steps as described above for DNA extraction, but collection of biomass was done by centrifugation at 4 °C. Cells were disrupted using combined physical and chemical lysis. Collected biomass was mixed with 0.4 ml cold TE buffer (4 µl *2*-mercaptoethanol), and 0.5 ml TRIzolTM reagent (Thermo Fisher Scientific) was added, followed by bead-beating for 3 min (3 times, 1 min per time with cooling on ice in between) at speed 5.5 (FastPrep-24 5G, MP biomedicals, Irvine, CA, USA). After bead-beating, UltraPureTM phenol : chloroform : isoamyl alcohol in ratio of 25 : 24 : 1 in 200 µl (Thermo Fisher Scientific) was added and mixed by vortex. Then, the separated aqueous phase containing RNA was transferred to an RNeasy column (Qiagen, Venlo, The Netherlands) for purification followed by DNase I (Roche, Almere, The Netherlands) treatment to remove residual DNA. For both DNA and RNA, prewarmed (50 °C) nuclease-free water was added to the membrane as a final step to elute DNA or RNA. The extracted genomic DNA of *D. singaporensis* was used as the template for 16S rRNA gene targeted qPCR with primers Eub341F/Eub534R to determine growth under formatotrophic conditions with 2,6-DBP only and additional acetylene, respectively, compared to cultures without DBP and acetylene. Reverse-transcriptase (RT) qPCR was used to measure expression of RDase genes and other related genes by using the One Step PrimeScript™ RT-PCR Kit (Perfect Real Time) (Takara Bio, Saint-Germain-en-Laye, Germany). RT-qPCR targeting the bacterial 16S rRNA was used for normalization of RDase gene expression. Primers used for the analysis of gene expression were designed using the NCBI Primer-BLAST primer design tool (https://www.ncbi.nlm.nih.gov/tools/primer-blast/), setting the amplicon size range from 75 bp to 150 bp and the optimal temperature at 60 °C. All primers used in this study are listed in Table 5.1.

Table 5.1 Primers used in this study for (RT)-quantitative PCR

Target	Name	Oligonucleotide sequence (5′–3′)	(RT)-qPCR programs
Bacteria	Eub341F	CCTACGGGAGGCAGCAG	See the references (Atashgahi, et al. 2013, Muyzer, et al. 1993).
	Eub534R	ATTACCGCGGCTGCTGGC	
16S rRNA	Ds-16S-F	GGCGTGCTTAACACATGCAA	Stage1: Reverse transcription 42 °C 5 min 95 °C 10 sec
	Ds-16S-R	TAGCACACCTTTCGGTGAGT	
bEBP	Ds-bEBP-F	CCCGGCCATCTGTACTGTTT	Stage2: PCR reaction 95 °C 5 sec 60 °C 20 sec 40 Cycles
	Ds-bEBP-R	GTCAGCGCAGAGAGGACATT	
RDase	Ds-RDase-F	GTCCGGCCATAACCAAGGAA	
	Ds-RDase-R	CTGGGCAAAGGCCATGACTA	
Sigma54	Ds-Sigma54-F	TCTGGGAATGGCGGTAGAGA	
	Ds-Sigma54-R	TCAGCAGGGTGACATCGAAC	

Genome sequencing and analysis of *Desulforhopalus vacuolatus*

D. vacuolatus was isolated in 1996 (Isaxons and Teske 1996), however, its genome had not been elucidated at the time this study was initiated. In order to facilitate understanding of its metabolic potential, we sequenced the genome of *D. vacuolatus* using Illumina (Novaseq6000, PE150, Novogene) shotgun sequencing using paired-end short reads of 150 bp. Recently, however, the genome of *D. vacuolatus* has also been published in the context of studying the sulfur metabolism of this organism (Ward, et al. 2021). Accordingly, we combined the assembled genome as the reference with our data to improve the quality of the assembly by using Unicycler (Wick, et al. 2017a, Wick, et al. 2017b). The raw paired-end sequence reads were first cleaned by the "read_qc" module of MetaWRAP (Uritskiy, et al. 2018), to remove low-quality reads. The clean reads were then used for co-assembly with the available genome of *D. vacuolatus* via Unicycler using default parameters. The final assembly was compared to previous ones by QUAST (Mikheenko, et al. 2018) using default settings, and its completeness and contamination was evaluated by checkM (Parks, et al. 2015). Genome statistics for the *D.*

vacuolatus genome are listed in Table S5.1 along with those of 15 other representative genomes of *Desulforhopalus* spp. isolates and MAGs available in the GTDB database.

Pangenomic and phylogenomic analyses

Fifteen representative genomes of *Desulforhopalus* were included for pangenomic analysis, together with the updated genome of *D. vacuolatus* and the metagenome-assembled genome (MAG) CH4_bin.5 (chapter 4), using Anvi'o (Delmont and Eren 2018, Eren, et al. 2015). In addition, the metabolic genes responsible for RD, sulfate reduction (SR) and WLP were extracted from these genomes and compared following the default parameters of Anvi'o. Phylogenetic trees were constructed by GToTree based on a set 74 bacterial marker genes, and predicted metabolic pathways were analyzed using magicLAMP, prokka annotation, and KEGG retrieval (Garber, et al. 2020, Kanehisa and Goto 2000, Uritskiy, et al. 2018). Due to the limited completeness of the genome of *Desulforhopalus* sp002747825 (GCA_002747825.1), which did not meet the required number of bacterial marker genes, this genome was excluded from phylogenetic tree construction.

Results

Pangenomic analysis of *Desulforhopalus* representatives

Our previous work revealed that several members of the genus *Desulforhopalus* potentially contribute to RD, with some being predicted to be OHRB candidates (chapter 3 and 4). To comprehensively assess the full genomic diversity and common features of currently available *Desulforhopalus* members, pangenomic analysis was carried out on the integrated platform, Anvi'o (Eren et al., 2015; Delmont and Eren, 2018). From the 21 genomes of *Desulforhopalus* available in GTDB at the time of analysis, we took 15 representative genomes into our analysis (https://gtdb.ecogenomic.org/). Furthermore, we included the recently genome-sequenced *D.*

vacuolatus, and CH4_bin.5 that we recently obtained from a highly enriched debrominating consortium (chapter 4) (Figure 5.1). The genome sizes ranged from 1.17 Mb for *Desulforhopalus* sp002747825 to 6.21 Mb for *Desulforhopalus* sp000961725, in which the former has genomic completeness of 66.67 % of the bacterial marker genes used for checkM analysis (Table S5.1). The conserved single-copy core gene (SCG) clusters among the genomes included in our analysis were restricted by the genome with the lowest completeness with only 15 out of a total of 74 gene calls. Based on the phylogenomic analysis, CH4_bin.5 was most closely related to the genome of *D. vacuolatus*, which was isolated from the water-covered coast of Kysing Fjord neighbouring Aarhus Bay. Other genomes, including that of *D. singaporensis* that was isolated from Singapore, were found more distantly related (Isaxons and Teske, 1996; Lie et al., 1999; Kuever et al., 2015). In addition, both CH4_bin.5 and *D. vacuolatus* were found to carry the core genes for sulfate reduction, as the other *Desulforhopalus* members, but lacked most of the genes encoding proteins of the WLP (Isaxons and Teske, 1996), which to some extent also reflects their overall evolutionary conservation and geographic proximity of their isolation source. The pangenomic analysis revealed two OHRB candidates, *D. singaporensis* and De_sp013139415, based on the presence of genes predicted to code for respiratory corrinoid-dependent RDases (Figures 5.1, 5.2, 5.3A). By contrast, the strain represented by CH4_bin.5 was predicted to constitute a non-respiratory dehalogenator, bearing a thiolytic tetrachloro-p-hydroquinone RDase (TPh-RDase) (Xun et al., 1992a, b). Interestingly, the closest relative to CH4_bin.5, *D. vacuolatus*, lacks any RDase gene, suggesting its incapability of RD. To this end, we could indeed confirm the ability of *Desulforhopalus singaporensis* to grow by using organohalides as terminal electron acceptor (see below for the corresponding growth experiments; Table S5.2), whereas *Desulforhopalus vacualotus* was not (Table S5.2). Of the halogenated compounds tested, *Desulforhopalus singaporensis* could only use 2,6-DBP, 2,4-DBP, and 2,4,6-DBP, but not any of the other brominated, chlorinated or iodinated compounds tested (see below, Table S5.2). Finally, based on the genomic analysis and presence of the corresponding functional genes (Figures 5.1, 5.2), we hypothesized that *D. singaporensis* would be able to use organohalides as terminal electron acceptor while using the WLP simultaneously for cell growth and source of electrons.

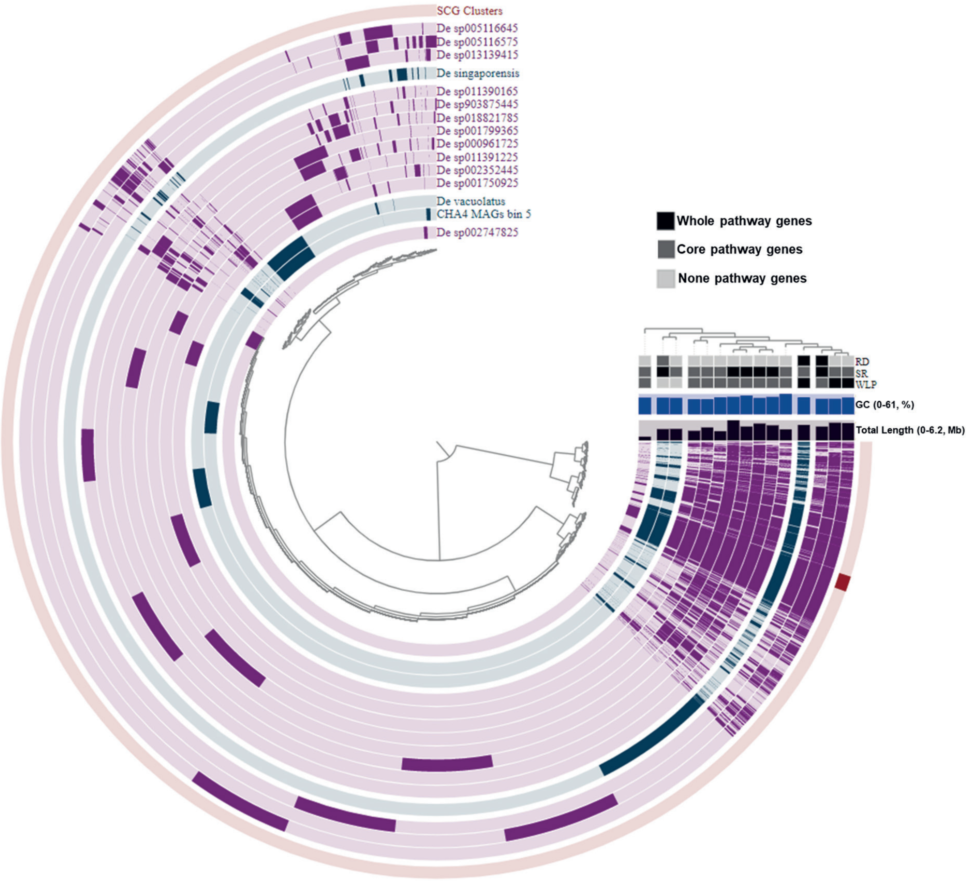

Figure. 5.1 Pangenomic analysis of representative genomes of *Desulforhopalus*. Genes were clustered across the pangenome and layers, including genome size (total length), GC content (%) and the metabolic traits, reductive dehalogenation (RD), sulfate reduction (SR) and Wood-Ljungdahl pathway (WLP) were explicitly considered. Isolated strains, *D. vacuolatus* and *D. singaporensis*, and CH3_bin.5 (chapter 4) are depicted in shades of blue-grey, and all other MAGs available at GTDB are given in shades of magenta. Dark and light color within individual genome rings indicate presence or absence of genes, respectively. The outer ring

(SCG clusters) indicates the 15 single-copy core genes used for phylogenomic tree construction. “Whole” (in black) indicates presence of complete SR/WLP pathway genes or respiratory RDase; “Core” (in dark grey) for essential pathway genes or TPh-RDase; “None” (in light grey) indicates that a given pathway (SR/WLP) is not present; “De”: *Desulforhopalus*; “sp” with 9-digit number is the strain-level taxon identifier taken from GTDB.

Metabolic trait inferences of *Desulforhopalus*

To get a more detailed understanding of potential metabolic traits of *D. singaporensis* and other members of the genus *Desulforhopalus* for which genomes were available, the involved critical genes were further analyzed in detail across all genus members, including the updated genome of *D. vacuolatus* and CH4_bin.5 (Figure 5.2). Most of the *Desulforhopalus* members were found to contain all essential genes for sulfate reduction, with the exception of sp013139415, which lacks *dsrMK*. Similarly, nearly all members carry the core genes for the WLP, except *D. vacuolatus* lacking *acsA*, *acsB*, *acsC* and *acsD*, and CH4_bin.5 which only contains *acsA*. Interestingly, only one genome, sp018821785, contains the genes encoding molybdenum-containing formate dehydrogenases (FDHs), which are composed of three subunits, FdhA, FdhB, and FdhC, to catalyze the reversible conversion between H_2 / CO_2 and formate (Ferry, 1990; Jormakka et al., 2003). By contrast, all other members appeared to lack one or all genes needed to encode functional FDHs, indicating their inability to initiate the WLP in the presence of H_2 only. Instead, genes encoding the NAD^+-dependent formate dehydrogenase (FdhL), which can consume the available formate to provide the electrons and the reducing equivalents in the form of NADH (Berrı et al., 2002), were found in most members except sp018821785 and sp001750925. Further, all genomes investigated here were found to encode group 4 [Ni-Fe] hydrogenases, whereas only the genome of *D. singaporensis* was found to lack the genes encoding group 1 [Ni-Fe] hydrogenases. Instead, the genome of *D. singaporensis* was found to be the only one to contain all genes needed to encode a [Fe-Fe] hydrogenase. Indeed, previous physiological studies revealed that *D. singaporensis* cannot use H_2 as electron donor, whereas

D. vacuolatus has this potential (Isaxons and Teske, 1996; Lie et al., 1999; Kuever et al., 2015) conforming the absence of group 1 [Ni-Fe] hydrogenases in *D. singaporensis*. Therefore, formate, and not H_2, was used as the electron donor in our more detailed physiological studies of *D. singaporensis*, especially targeting the WLP, as described below.

Most of the genomes investigated here contained the complete gene set for *de novo* B12 biosynthesis, *cbi*, including *D. singaporensis* and CH4_bin.5. In contrast, the B12 transporter genes, *btuCDF* (Korkhov et al., 2012), were found to be incomplete among all studied *Desulforhopalus* genomes, suggesting the inability of members of *Desulforhopalus* to import or export B12.

It was reported that *D. singaporensis* can produce poly-β-hydroxybutyrate (PHB), and our genomic analysis confirmed that *D. singaporensis* has the complete biosynthesis gene set, including *phbA* (encoding acetyl-CoA acetyltransferase), *phbB* (encoding acetoacetyl-CoA reductase) and *phbC* (PHB synthase) (Amadu et al., 2021), whereas *D. vacuolatus* and CH4_bin.5 have none of these genes, indicating their inability of biosynthesizing PHB. Furthermore, most of the genomes analyzed here were found to contain the genes encoding transporter proteins for aromatic compounds and long-chain fatty acids, enabling cellular utilization or secretion of these molecules.

Genetic evidence also indicated that *D. singaporensis* contains a periplasmic nitrate reductase (NapAB) that allows to use nitrate as terminal electron acceptor for energy conservation (Gonzalez et al., 2006), in agreement with previous studies (Lie et al., 1999; Kuever et al., 2015). Further, the *D. singaporensis* genome encodes the nitrogenase complex (Burgess and Lowe, 1996), indicating its potential for fixing molecular nitrogen. The other genomes, excluding sp001750925, contain genes encoding an ammonium transporter that can import / export ammonium in the presence / absence of ammonium outside.

In summary, based on genome inferences, *D. singaporensis* as the representative isolate is predicted to bear a versatile metabolism, which could enhance its adaptability to environments with varying nutrient availability, and its metabolites could also synergistically support the growth of other members of microbial communities.

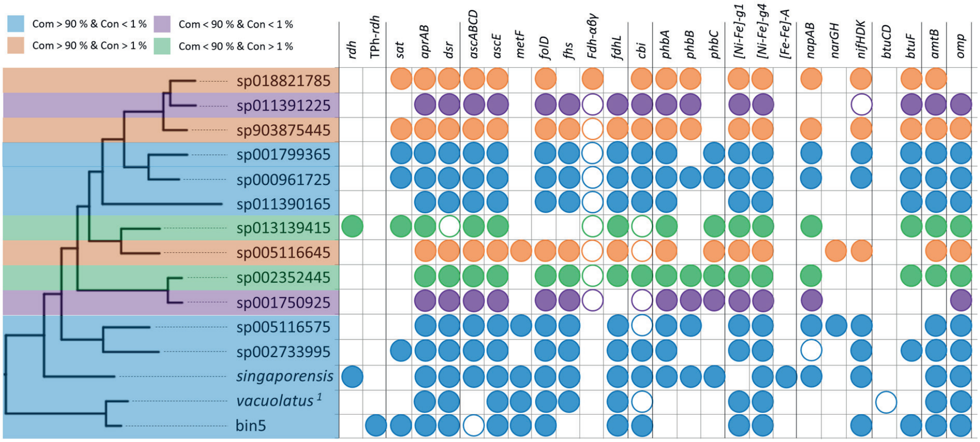

Figure. 5.2 Phylogenetic analysis of *Desulforhopalus* members and their predicted metabolic traits. The representative genomes of *Desulforhopalus* were downloaded from GTDB and their phylogenies were analyzed and constructed by GToTree based on the alignment of 74 concatenated bacterial marker genes (Lee 2019), excluding the sp002747825 automatically due to the low completeness (66.67 %) of marker genes. Color patterns indicate levels of genome completeness (Com) and contamination (Con). Filled circles indicate the presence of all genes needed to encode the complete enzyme complex or the complete metabolic pathway. Open circles and empty cells indicate that only some or none of the required genes are present, respectively. *rdh* encodes reductive dehalogenase; TPh-*rdh* encodes tetrachloro-p-hydroquinone reductive dehalogenase; *sat* encodes sulfate adenylyltransferase; *aprAB*, APS reductase; dsr, dissimilatory sulfite reductase; *fdh-αβγ*, three subunits of formate dehydrogenase; *fdhL* codes for NAD$^+$-dependent formate dehydrogenase; *acsABCDE*, *folD*, *metF* and *fhs* are critical genes for the Wood-Ljungdahl pathway (WLP); *cbi*, de novo vitamin B12 biosynthesis; *phbABC*, for synthesizing polymer poly-β-hydroxybutyrate (PHB); [Ni-Fe]-g1, [Ni-Fe]-g4, and [Fe-Fe]-A, for groups 1 and 4 of [Ni-Fe] hydrogenases, and group A of [Fe-Fe] hydrogenases, respectively; *napAB* and *narGH* for nitrate reduction; *nifHDK*, nitrogenase.

RDase gene operon and reductive dehalogenation potential of *D. singaporensis*

Among the *Desulforhopalus* spp., *D. singaporensis* has the most versatile metabolism among all strains/genomes analyzed here, and was shown to be capable of RD, as confirmed experimentally using a range of chlorinated, brominated, and iodinated compounds (Table S5.2). Therefore, this strain was selected to more extensively verify predicted metabolic traits and to elucidate their potential interconnections. The configuration of the RDase operon suggested that its expression could be regulated by the bacterial enhancing binding protein (bEBP) as the transcriptional activator, in combination with sigma factor 54 (Bush and Dixon, 2012; Liu and Haggblom, 2018), as shown in Fig 5.3A. Further sequence analysis revealed that bEBP contains three domains, the GAF domain (PF13185), the σ^{54}-interacting domain (PF00158), and the HTH domain (PF02954). The GAF domain acts as the sensor to bind small ligands, such as aromatic compounds, and HTH binds to the promoter DNA (Bush and Dixon, 2012). There are two bEBP recognition motifs in the promoter of the RDase gene in analogy to what has been proposed previously for the promoter of an *rdhA* gene in *Desulfoluna spongiiphila* (Liu et al., 2017), 5'-TGGCA-3' and 5'-TTGCT-3', which stabilizes the binding of the bEBP-σ^{54} complex to the promoter and initiates transcription of the downstream genes (Bush and Dixon, 2012). Interestingly, the sequence of the recognition site of bEBP is similar to that of NtrC, a nitrogen regulator protein, which activates the transcription of regulons under nitrogen-limiting conditions (Zimmer et al., 2000). The intergenic region between genes encoding bEBP and the RDase contains also an NtrC-recognition site, 5'-GGTAAAACATGGC-3' (blue highlight in the figure), that partially overlaps with the proposed bEBP recognition motifs (bold black letters). It is tempting to speculate that the intergenic region is not only the promoter of RDase genes, but also the promoter of the bEBP gene itself, which indicates that there could be a trade-off strategy to regulate both genes in response to various conditions. Moreover, the gene adjacent to the RDase encoding *rdhAB* gene cluster, was predicted to encode NapG that was reported to transfer electrons during nitrate respiration (Arnoux et al., 2003; Gonzalez et al., 2006). Altogether, the RDase activity is potentially under the regulation of the σ^{54}-dependent transcriptional activator, bEBP, and might be functionally associated with nitrogen metabolism.

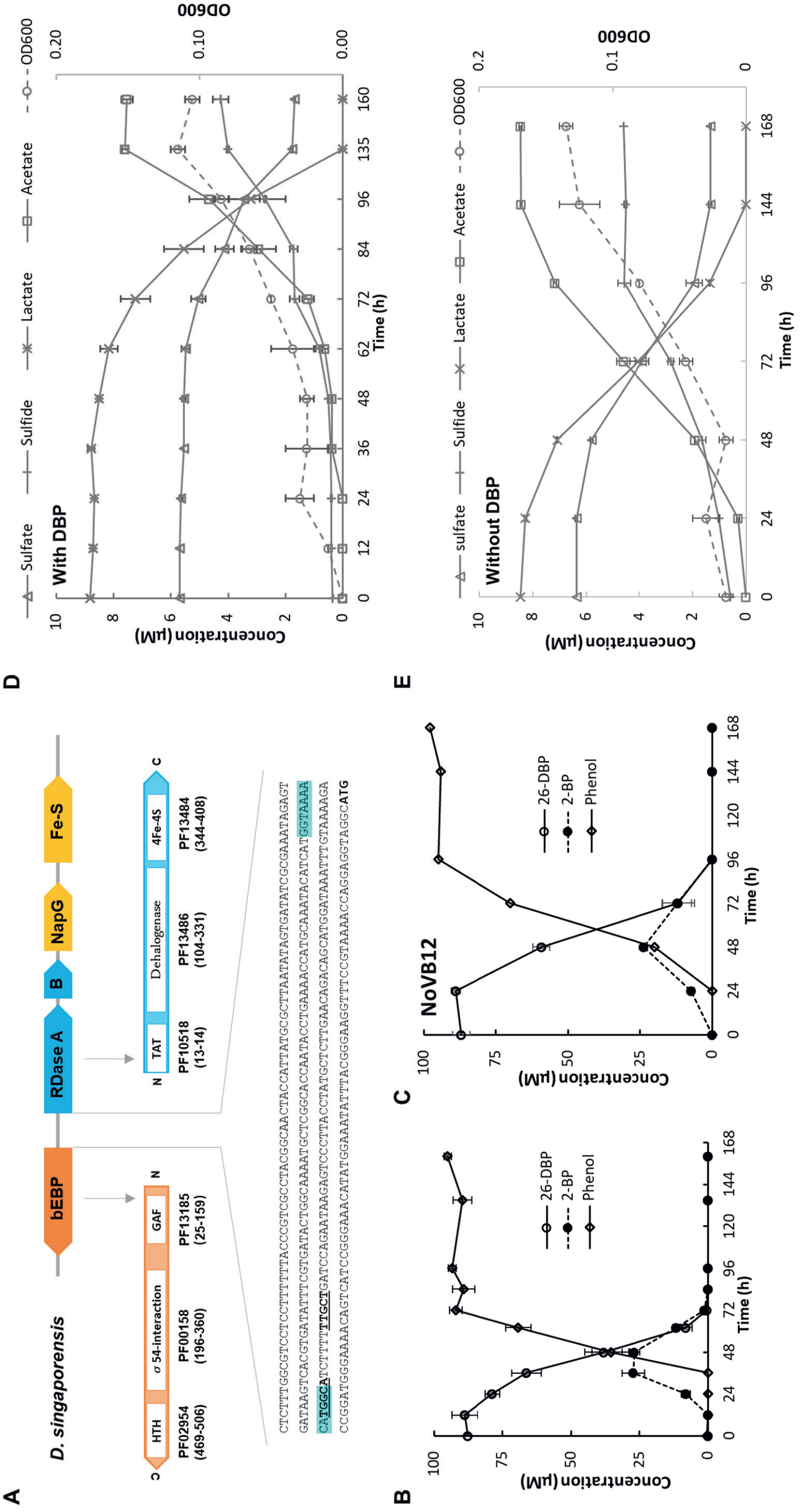
A
D. singaporensis
bEBP
RDase A
B
NapG
Fe-S
C
HTH
σ 54-interaction
GAF
N
PF02954 (469-506)
PF00158 (196-360)
PF13185 (25-159)
N
TAT
Dehalogenase
4Fe-4S
C
PF10518 (13-14)
PF13486 (104-331)
PF13484 (344-408)
CTCTTTGGCGTCCTCCTTTTTTACCCGTCGCCTACGGCAACTACCATTATGCGCTTAATATATAGTGATATCGCGAAATAGAGT
GATAAGTCACGTGATATTTCGTGATACTGGCAAAATGCTCGGCACCAATACCTGAAAACCATGCAAATACATCATGGTAAAA
CATGGCATCTTTTTGCTGATCCAGAATAAGAGTCCCTTACCTATGCTCTTGAACAGACAGCATGGATAAATTTGTAAAAGA
CCGGATGGAAAACAGTCATCCGGGAAACATATGGAAATATTTACGGGAAGGTTTCCGTAAAACCAGGAGGTAGGCATG
B
Concentration (μM)
100
75
50
25
0
0
24
48
72
96
120
144
168
Time (h)
26-DBP
2-BP
Phenol
C
NoVB12
Concentration (μM)
100
75
50
25
0
0
24
48
72
96
120
144
168
Time (h)
26-DBP
2-BP
Phenol
D
Sulfate
Sulfide
Lactate
Acetate
OD600
With DBP
Concentration (μM)
10
8
6
4
2
0
0
12
24
36
48
62
72
84
96
135
160
Time (h)
OD600
0.20
0.10
0.00
E
sulfate
Sulfide
Lactate
Acetate
OD600
Without DBP
Concentration (μM)
10
8
6
4
2
0
0
24
48
72
96
144
168
Time (h)
OD600
0.2
0.1
0

Figure 5.3 Genomic context of RDase genes and reductive debromination of 2,6-DBP in *Desulforhopalus singaporensis*. Genomic context of RDase genes (A), including bacterial enhancing binding protein, bEBP, composed of a GAF domain at N terminus, Sigma54 (σ^{54}) - interacting domain, and helix-turn-helix (HTH) domain at C terminus. The RDase A subunit constitutes an N-terminal twin arginine translocating domain, the dehalogenase core domain, and a C-terminal iron-sulfur cluster domain (4Fe-4S). Corresponding Pfam labels are provided (PF). Below the intergenic region between bEBP and RDase A genes is depicted. The underlined bold black letters represent the binding boxes of Sigma54, and letters highlighted in turquoise indicate the binding sites of bEBP. Reductive debromination was tested in the presence of sulfate as alternative electron acceptor and with lactate as electron donor and carbon source. Metabolites of debromination (2,6-DBP, 2-BP, phenol) are shown for cultures grown in the presence (B) and absence of B12 added with the medium (C). Compounds related to sulfate reduction (sulfate, sulfide) and lactate oxidation (lactate, acetate) are shown for cultures grown in the presence (D) and absence of 2,6-DBP (E). Three replicate bottles were set for the experiment, and data are presented as mean ± standard deviation (SD). Error bars indicate the SD.

Debromination of 2,6-DBP

Our experiments confirmed the ability of *D. singaporensis* to dehalogenate several different organohalides. Within 72 h, 2,6-DBP was completely converted to phenol with bromophenol (BP) as intermediate (Figure 5.3B) upon the consumption of lactate as the electron donor and carbon source (Figure 5.3D). In addition, *D. singaporensis* was able to debrominate 2,6-DBP to phenol without adding B12 (NoB12), which suggests it has complete B12 biosynthesis capacity (Figure 5.3C). Interestingly, the reduction of sulfate, which was added as a competitive electron acceptor, only started after the complete consumption of 2,6-DBP after 72 h, while sulfate reduction required a lag-phase of only 24 h when it was added as the sole terminal electron acceptor (Figure 5.3E). This was surprising because it has been typically observed before that RD is inhibited in the presence of sulfate (e.g., (Liu and Haggblom, 2018; Peng et al., 2020)), although RD has larger redox potentials (210-470 mV) than sulfate reduction (SO_4^{2-} / HS^-, -217 mV) and is therefore energetically more favorable (Adrian and Löffler, 2016).

Acetylene inhibits reductive debromination post-transcriptionally

Acetylene is a general inhibitor of many metabolic pathways, such as methanogenesis and RD (Hyman and Daniel, 1988; Pon et al., 2003) (chapter 4). To clarify the inhibitory effect of acetylene on RD in *D. singaporensis*, we added acetylene to the debrominating cultures. 2,6-DBP debromination stopped immediately after the addition of 3 mL of acetylene (1.8 mM final concentration) (Figure 5.4A). In contrast, lactate utilization and sulfate reduction were not affected in comparison to the actively debrominating cultures where no acetylene was added (Figure 5.4B). Thus, we hypothesized that the acetylene was specifically targeting RD in *D. singaporensis*. To elaborate the inhibitory mechanism, we used RT-qPCR to measure gene expression. The RDase gene was transcribed at low constitutive levels when 2,6-DBP was absent, and expression was induced after the addition of 100 μM 2,6-DBP leading to a 6000-fold increase after 2 h (Figure 4C). Hence, the added acetylene did not prevent the transcription of the RDase gene suggesting that inhibition acts post-transcriptionally. Meanwhile, we also measured the transcription of related genes, namely those encoding bEBP and σ^{54}, in the presence of 2,6-DBP and 2,6-DBP/acetylene, respectively. Interestingly, the expression of genes encoding bEBP and σ^{54} was induced approximately 5-6-fold after 2 h without 2,6-DBP, whereas induction in the presence of 2,6-DBP was less pronounced. Addition of acetylene did not affect transcription of bEBP and σ^{54} encoding genes (Figure 5.4D and 5.4E).

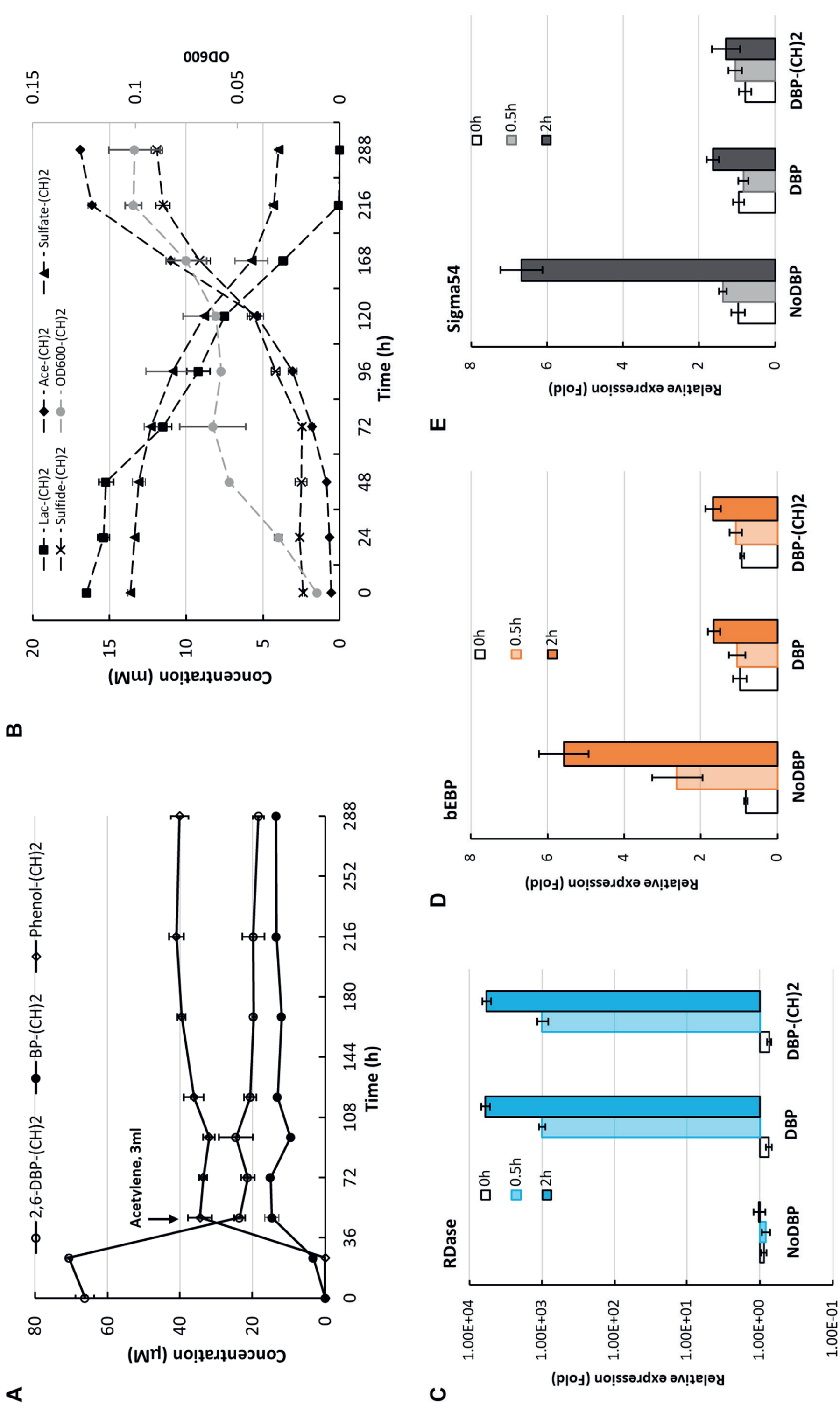
A
2,6-DBP-(CH)2
BP-(CH)2
Phenol-(CH)2
Acetylene, 3ml
Concentration (μM)
Time (h)
B
Lac-(CH)2
Sulfide-(CH)2
Ace-(CH)2
OD600-(CH)2
Sulfate-(CH)2
Concentration (mM)
OD600
Time (h)
C
RDase
0h
0.5h
2h
Relative expression (Fold)
NoDBP
DBP
DBP-(CH)2
D
bEBP
Relative expression (Fold)
NoDBP
DBP
DBP-(CH)2
E
Sigma54
Relative expression (Fold)
NoDBP
DBP
DBP-(CH)2

Figure 5.4 Acetylene inhibition of reductive debromination of 2,6-DBP by *D. singaporensis* and expression of RDase and associated genes encoding potential regulatory proteins. Acetylene ((CH)2) was added after 48 hours (A) and the concomitant lactate oxidation, sulfate reduction and cell growth in OD600 was followed (B). Reverse-transcriptase quantitative PCR (RT-qPCR) of genes encoding RDase A (C), bEBP (D) and Sigma54 (E) at 0, 0.5 and 2 hours after addition of 2,6-DBP compared to cultures to which no 2,6-DBP was added (NoDBP) and cultures with additional acetylene (DBP-(CH)2). RT-qPCR targeting the bacterial 16S rRNA was used for normalization of gene expression. Each treatment in C-E was set with three replicates and values represent mean ± standard deviation (SD). Error bars indicate the SD.

Debromination by *D. singaporensis* in the presence of formate

In the pangenomic analysis, the WLP was discovered as conserved metabolic pathway across most members of *Desulforhopalus*, but there is no experimental confirmation yet of its functionality. Interestingly, all genomes included in this study, except sp018821785, lack one or all genes encoding subunits of formate dehydrogenase (FdhABC) that is required to reduce CO_2 to formate with H_2 as the electron donor, indicating the inability of all but one strain to metabolize H_2 (Jormakka et al., 2003). This corresponds with our finding that *D. singaporensis* cannot use H_2 and acetate as the energy and carbon source (Table S5.2). Alternatively, all but two genomes included in the present study carry a gene predicted to encode an NAD^+-dependent formate dehydrogenase (FdhL), which can oxidize one molecule of formate to generate NADH, and reduce another molecule of formate for further processing in the methyl branch of the WLP (Ragsdale, 2008; Ragsdale and Pierce, 2008). As expected, the added formate supported growth with the final product of acetate (Figure 5.5), conforming with a functional WLP in *D. singaporensis* for bacterial anabolism from formate. In addition, formate also served as the electron donor for 2,6-DBP debromination (Figure 5.5A). In this experiment, acetate was produced in minor amounts towards the end of the incubation . Compared to the experiment where only formate and no 2,6-DBP was added, the reductive debromination generated additional biomass at later time points from 192 h onwards (Figure 5.5B), which suggests that the additional energy was being used for bacterial growth rather than carbon assimilation from formate to PHB as previously described (Lie et al., 1999).

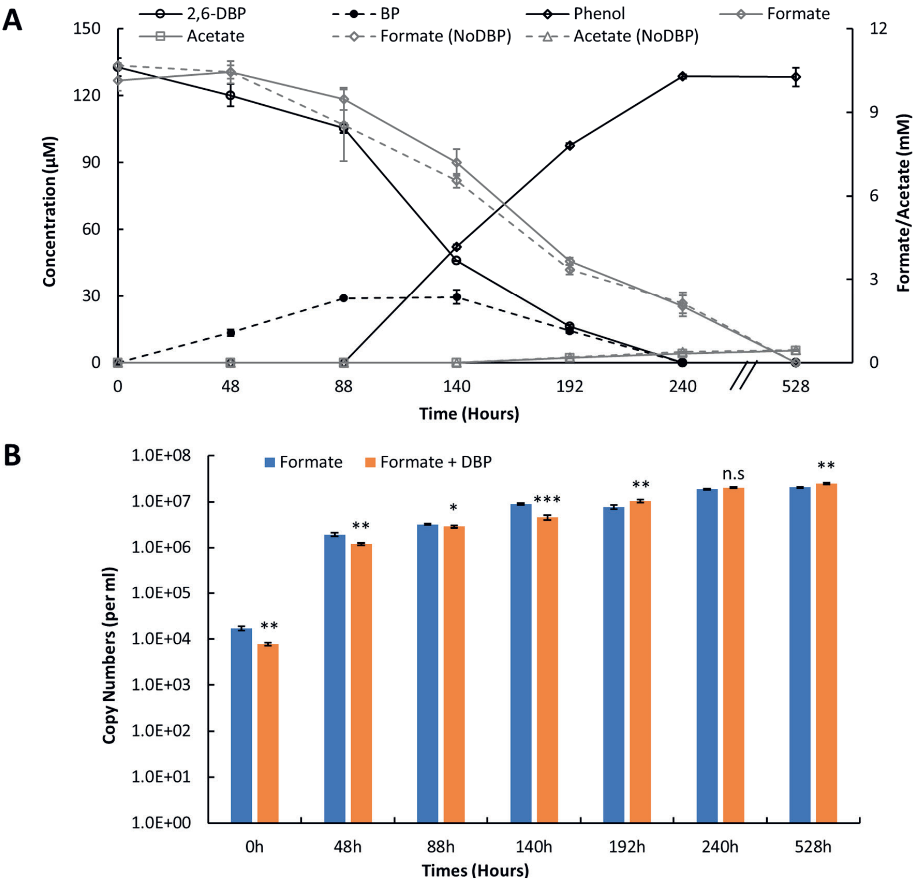

Figure 5.5 Reductive debromination of 2,6-DBP by *D. singaporensis* driven by the Wood-Ljungdahl pathway (WLP) under formatotrophic conditions. Reductive debromination of 2,6-DBP into phenol at the presence of formate serving as the electron donor Also shown is the utilization of formate and production of acetate in the presence or absence of 2,6 DBP (A). 16S rRNA gene-targeted quantitative PCR (qPCR) measuring growth of *D. singaporensis* under formatotrophic conditions in the presence (orange bars) or absence (blue bars) of 2,6-DBP (B). Three replicate bottles were set for the experiment, and data are presented as mean ± standard deviation (SD). Error bars indicate the SD. Statistical significance of differences between cultures grown in the presence or absence of 2,6-DBP was tested using student t'test. "***": p-value < 0.001; "**": 0.001 < p-value < 0.01; "*": 0.01 < p-value < 0.05; "n.s": not significant.

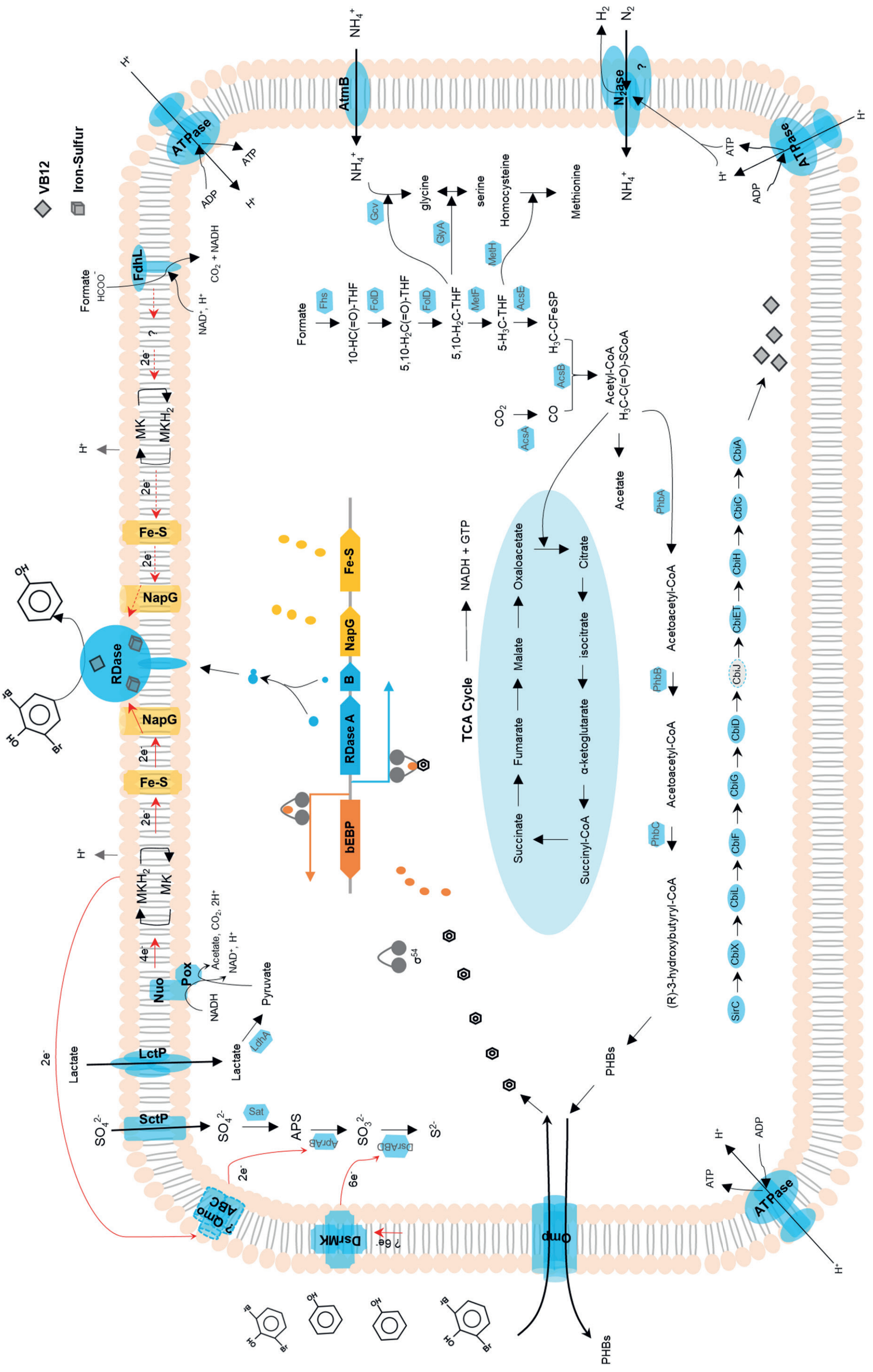
VB12
Iron-Sulfur
ATPase
ADP
ATP
H+
AtmB
NH4+
N2ase
?
H2
N2
FdhL
Formate
HCOO-
NAD+, H+
CO2 + NADH
2e-
?
MK
MKH2
Fe-S
NapG
RDase
B
RDase A
bEBP
σ54
Gcv
glycine
GlyA
serine
Homocysteine
MetH
Methionine
Fhs
10-HC(=O)-THF
FolD
5,10-H2C(=O)-THF
5,10-H2C-THF
MetF
5-H3C-THF
AcsE
H3C-CFeSP
AcsB
Acetyl-CoA
H3C-C(=O)-SCoA
CO2
AcsA
CO
Acetate
PhbA
Acetoacetyl-CoA
PhbB
PhbC
(R)-3-hydroxybutyryl-CoA
PHBs
TCA Cycle
NADH + GTP
Oxaloacetate
Citrate
isocitrate
α-ketoglutarate
Succinyl-CoA
Succinate
Fumarate
Malate
SirC
CbiX
CbiL
CbiF
CbiG
CbiD
CbiJ
CbiET
CbiH
CbiC
CbiA
Nuo
NADH
Pox
Acetate, CO2, 2H+
NAD+, H+
Pyruvate
4e-
LctP
Lactate
LdhA
SctP
SO42-
Sat
APS
AprAB
SO32-
DsrABD
S2-
6e-
? Qmo ABC
DsrMK
? 6e-
Omp
OH
HO
Br

Figure 5.6 Overview of the metabolic pathways of *D. singaporensis*. Genes involved in reductive debromination of 2,6-DBP, sulfate reduction, Wood-Ljungdahl pathway, *de novo* vitamin B12 biosynthesis, nitrogen fixation, poly-β-hydroxybutyrate biosynthesis and secretion, ammonium and large molecules transporters, and other functions are shown. Transfer of electrons obtained from lactate to RDase (solid red line), and transfer of electrons from formate to RDase (dotted red line). Blue arrow indicates the transcription of RDase genes, while the orange arrow indicates the transcription of the bEBP gene. The complete TCA cycle of *D. singaporensis* is shown in the blue-shaded area. CbiJ in grey-filled dashed circle is absent in the genome annotation of *D. singaporensis*. "?" means unknown source for electrons and electron transporter.

Discussion

Our previous study indicated the RD potential of sulfate-reducing *Desulforhopalus* (chapter 3 and 4), but the verification at strain level was not yet carried out. Furthermore, *Desulforhopalus* affiliated bins retrieved from the PCE- and 2,6-DBP dehalogenating cultures, CH3_bin.15 and CH4_bin.5, respectively, only encoded thiolytic, non-respiratory RDases. To this end, our pangenomic analyses revealed that *D. singaporensis* was the only isolate bearing a respiratory RDase gene, concurrent with complete WLP and *de novo* B12 biosynthesis pathways. Accordingly, *D. singaporensis* was selected for more detailed studies towards the validation of genome-based predictions of its metabolic properties. Our results confirmed reductive debromination by *D. singaporensis* regardless of the addition of B12. Sulfate reduction was inhibited during debromination of 2,6-DBP and only started after 2,6-DBP was completely debrominated to phenol.

Acetylene is known to inhibit organohalide respiration, which was confirmed here. In line with what was shown for the 2,6-DBP debrominating consortium studied in Chapter 4 of this thesis, acetylene inhibition of debromination in *D. singaporensis* was also shown to occur post transcriptionally. Interestingly, expression of associated genes predicted to encode regulatory proteins, including bEBP and Sigma54, was inhibited after adding 2,6-DBP (Figure 5.4).

Henceforth, we speculate that the global transcriptional regulating complex, bEBP-Sigma54, switches to upregulate the gene expression of RDase after binding with 2,6-DBP, consequently seizing to induce its own expression (Figure 5.6). Furthermore, we confirmed *D. singaporensis* as a formatotroph, with OHR leading to more biomass production compared to the sole formatotrophic condition.

Pangenomic analysis revealed that CH3_bin.5 is phylogenomically closest to *D. vacuolatus*. and contains a gene encoding thiolytic tetrachloro-p-hydroquinone (TPh) which can act as an RDase (Xun et al., 1992b) and thus is an indication of potential for RD. Intriguingly, no RDase gene was found in the genome of the available isolate of *D. vacuolatus*. Accordingly, no RD was observed with this strain (Table S5.2). In contrast, a respiratory RDase gene was found only in *D. singaporensis* and sp013139415 (Figure 5.1), while all other *Desulforhopalus* genomes included in this study did not contain any RDase-encoding gene (Figure 5.2). It is thus tempting to speculate that the presence of RDase genes in *Desulforhopalus* spp. is likely the result of gene transfer from the surroundings. Unlike the most well-identified OHRB, *D. singaporensis* was unable to utilize H_2 as the electron donor to promote OHR (Table S5.2), whereas *D. vacuolatus* can use H_2 with acetate as energy and carbon sources (Isaxons and Teske, 1996; Lie et al., 1999; Kuever et al., 2015). These observations are in line with the results of our detailed comparative genomic analysis that revealed that the genome of *D. singaporensis* only encodes group 4 [Ni-Fe] and group A [Fe-Fe] hydrogenases but is devoid of the group 1 [Ni-Fe] hydrogenase as opposed to the rest *Desulforhopalus* members, such as *D. vacuolatus* (Figure 5.2). Moreover, *D. singaporensis* recruited an NAD^+-dependent formate dehydrogenase (FDH) to oxidize formate into CO_2 and NADH, instead of H_2, which can be produced by the respiratory FDHs under anoxic conditions (Popov and Lamzin, 1994; Jormakka et al., 2003). Under formatotrophic conditions, the increased reducing power provided by NADH could reinforce the resistance of *D. singaporensis* against oxic stresses (Berrı et al., 2002). Hence, we could show that formate played a dual role in firstly providing electrons for OHR, and secondly promoting the WLP through its methyl branch (Zhuang et al., 2014; Borrel et al., 2016; Adam et al., 2019; Jiao et al., 2021). Of interest, *D. singaporensis* has the complete metabolic pathway for biosynthesizing PHB as extension from the WLP (Figure 5.6), which could be stored as carbon source, and made accessible for other members of a microbial consortium. This feature deserves further studies as it was beyond the scope of analyses described here.

Dissimilar to previously identified marine OHRB (Liu and Haggblom, 2018; Peng et al., 2020), the reductive debromination by *D. singaporensis* inhibits sulfate reduction, which was subsequently initiated after complete debromination of 2,6-DBP (Figure 5.3). As a potential regulator of RDase gene expression, the NtrC-like activator bEBP has a GAF domain (Bush and Dixon, 2012), which can potentially bind with 2,6-DBP and form a complex with Sigma54 to activate the expression of the RDase gene, whereas the transcription of other regulons was temporarily inhibited, including the expression of bEBP and Sigma54 encoding genes (Figure 5.4). In addition to the binding sites of Sigma54 at the promoter of the RDase gene, we also identified NtrC type binding sites of bEBP, which overlapped with the Sigma54 recognition site, indicating their concerted and tight regulation of RDase gene expression. Moreover, the promoter of the RDase gene also overlapped with the promoter of the bEBP gene in the opposite direction, suggesting their competition for transcriptional initiation agreeing to the transcriptional data reported here. Accordingly, we speculate that the added 2,6-DBP preferentially binds with bEBP and Sigma54, forming a tripartite complex that specifically upregulates transcription of the RDase gene, while retarding other metabolic activities, which might also partially explain the inhibition of sulfate reduction after adding 2,6-DBP (Figure 5.3). The decrease in 2,6-DBP concentrations via debromination gradually might have switched the global regulation by the bEBP-Sigma54 complex back to other functional genes. The molecular validation of the role of the bEBP-Sigma54 complex in regulating expression of the

RDase gene and other functions awaits further studies. Interestingly, bEBP, belonging to the NtrC type, was reported to upregulate nitrogen fixation to supplement the shortage of ammonium (Kim and Rees, 1994; Burgess and Lowe, 1996; Howard and Rees, 1996) in response to nitrogen limitation (Zimmer et al., 2000; Desnoues et al., 2003). *D. singaporensis* is predicted to contain a complete nitrogenase (NifHDK, Figure 5.2). However, ammonium limitation did not initiate nitrogen-fixing activity in our experiments, and also acetylene inhibition of RD was not alleviated by N_2ase activity converting acetylene to ethene at low concentrations of ammonium (Hardy et al., 1973). Altogether, these observations pointed towards lack of N_2ase activity, and its induction appears to be fastidious. Furthermore, the gene downstream of the RDase genes, was predicted to encode NapG that was characterized for its role in electron transfer during nitrate respiration (Kern and Simon, 2008). This suggests that OHR of *D. singaporensis* is metabolically associated with nitrogen metabolism, similar to what has been reported for other OHRB such as *Sulfurospirillum multivorans* (Goris et al., 2014; Fincker and Spormann, 2017). Henceforth, the metabolic association of halogen and nitrogen cycles requires further investigation.

In summary, we could show through comparative pangenome analyses that *D. singaporensis* is a metabolically versatile member of the genus *Desulforhopalus*. We demonstrated experimentally that the reductive debromination-associated OHR in *D. singaporensis* is associated with the WLP under formatotrophic conditions for catabolism and anabolism. Furthermore, we hypothesize based on genome analyses and transcriptional data that the global regulator system, bEBP-Sigma54 complex, could preferentially bind with 2,6-DBP, upregulating RDase activity towards 2,6-DBP, giving OHR priority over other metabolic activities, such as sulfate reduction. Further, NapG that is encoded next to the RDase was proposed to transfer electron to RDase for OHR. Altogether, these observations suggest associations of halogen and nitrogen metabolism in *D. singaporensis*.

Acknowledgements

This study was supported by the Dutch Research Council through the UNLOCK project (NRGWI.obrug.2018.005), as well as Wageningen University through its Innovation Program Microbiology. We thank Peng Peng for providing expert advice for anaerobic cultivation and chemical measurements. We acknowledge the China Scholarship Council (CSC) for the support to Chen Zhang (File No. 201807720048).

Supplementary Information

Table S1 Genome sequences of *Desulforhopalus* spp isolates and MAGs included in this study

GTDB Taxonomy	GTDB Accession	Completion (%)	Contamination (%)	Genome Size	GC (%)	Contigs	N50 (bp)	Longest Contig	Isolation Source
Desulforhopalus sp000961725	GCA_000961725.1	99.87	0.89	6515854	51.68	72	136826	404491	Opalinus Clay rock porewater BRC-3 borehole, Switzerland
Desulforhopalus sp001750925	GCA_001750925.1	81.05	0.6	3128497	44.92	319	13985	48982	sample #3730, Pacific Ocean: Hydrate Ridge South
Desulforhopalus sp001799365	GCA_001799365.1	91.91	0.89	4509726	55.56	471	16504	69200	Rifle well CD01 at time point 2 / B, USA
Desulforhopalus sp002352445	GCA_002352445.1	89.47	2.68	4214536	45.03	566	13908	69131	N/A
Desulforhopalus sp002733995	GCA_002733995.1	99.91	0.63	4123694	44.41	52	145887	304794	N/A
Desulforhopalus sp002747825	GCA_002747825.1	66.67	0	1224655	49.48	23	83732	142714	N/A
Desulforhopalus sp011390165	GCA_011390165.1	96.43	0.6	3588576	60.73	108	66955	207228	N/A
Desulforhopalus sp011391225	GCA_011391225.1	84.7	0.89	3002185	50.34	304	14012	50694	N/A
Desulforhopalus sp013139415	GCA_013139415.1	92.54	4.89	4497267	45.93	637	9189	67552	N/A
Desulforhopalus sp018821785	GCA_018821785.1	98.81	2.28	5470697	48.64	315	33866	112261	N/A
Desulforhopalus sp903875445	GCA_903875445.1	99.98	1.03	4894380	51.59	117	94457	199924	N/A
Desulforhopalus sp005116575	GCF_005116575.1	99.91	0.07	5748492	45.99	127	179798	433534	N/A
Desulforhopalus sp005116645	GCF_005116645.1	100	1.19	5633479	49.74	95	345994	894946	N/A
Desulforhopalus singaporensis	GCF_900104445.1	99.7	0.6	5008860	50.57	126	110993	269582	Singapore
Desulforhopalus vacuolatus	GCF_016918505.1	99.4	0.3	3830687	48.7	169	121312	410426	water-covered coast of Kysing Fjord, Denmark
*Desulforhopalus vacuolatus**	N/A	99.4	0	3776880	48.74	212	123826	410115	water-covered coast of Kysing Fjord, Denmark
CHA4_MAGs_bin_5	N/A	100	0	3685696	49.32	5	898401	1030039	Station M5, Aarhus Bay, Denmark

*genome sequenced in this study.

Table S5.2 Physiological properties of *Desulforhopalus* isolates

Compounds as e-donors and e-acceptors	***D. singaporensis***	***D. vacuolatus***
Compounds used as electron donors and carbon sources		
H_2[a]	-	+
Formate[a]	+	+
Acetate	-	-
Lactate	+	+
Pyruvate	+	+
Fermentative growth on		
Lactate	+	+
Pyruvate	+	+
Compounds used as electron acceptors		
Sulfate	+	+
Sulfite	+	+
Thiosulfate	+	+
Nitrate	+	-
Nitrogen Fixation[b]	-	N/A
Halogenated compounds used as electron acceptors[c]		
2,6-Dibromophenol (2,6-DBP); 2,4-DBP; 2,4,6-DBP;	+ ; +[d] ; +[d] ;	-[e]
1,4-Dibromobenzene (1,4-DBB); 1,2-DBB; 1,3-DBB; 1,2,4-TBB	- ; - ; - ; - ;	
2,6-Dichlorophenol (2,6-DCP); 2,4-DCP; 2,4,6-TCP;	- ; - ; - ;	
1,4-Dichlorobenzene (1,4-DCB); 1,2-DCB; 1,3-DCB; 1,2,4-TCB;	- ; - ; - ; -;	
2,4,6-Triiodophenol (2,4,6-TIP); 2,4-DIP; 2,6-DIP; 2-IP; 4-IP;	- ; - ; - ; -;	

[a]used as the electron donor only in the presence of acetate as carbon source; [b]nitrogen fixation activity under decreased gradients of ammonia, no activity detected; [c]tested with the lactate as the electron donor and carbon source; [d]formed 4-bromophenol as the final product rather than phenol; [e]No reductive dehalogenation detected; N/A means not reported;

References

Adam PS, Borrel G, Gribaldo S. An archaeal origin of the Wood-Ljungdahl H4MPT branch and the emergence of bacterial methylotrophy. *Nat Microbiol* 2019.

Adrian L, Löffler FE. *Organohalide-respiring bacteria* volume 85: Springer, 2016.

Amadu AA, Qiu S, Ge S *et al.* A review of biopolymer (Poly-β-hydroxybutyrate) synthesis in microbes cultivated on wastewater. *Sci Total Environ* 2021;756: 143729.

Arnoux P, Sabaty M, Alric J *et al.* Structural and redox plasticity in the heterodimeric periplasmic nitrate reductase. *Nat Struct Mol Biol* 2003;10: 928-34.

Atashgahi S, Haggblom MM, Smidt H. Organohalide respiration in pristine environments: implications for the natural halogen cycle. *Environ Microbiol* 2018a;20: 934-48.

Atashgahi S, Lu Y, Zheng Y *et al.* Geochemical and microbial community determinants of reductive dechlorination at a site biostimulated with glycerol. *Environ Microbiol* 2017;19: 968-81.

Atashgahi S, Maphosa F, Dogan E *et al*. Small-scale oxygen distribution determines the vinyl chloride biodegradation pathway in surficial sediments of riverbed hyporheic zones. *FEMS Microbiol Ecol* 2013;84: 133-42.

Atashgahi S, Sánchez-Andrea I, Heipieper HJ *et al.* Prospects for harnessing biocide resistance for bioremediation and detoxification. *Science* 2018b;360: 743-6.

Berrı, x, os-Rivera SJ *et al.* Metabolic engineering of *Escherichia coli*: increase of NADH availability by overexpressing an NAD^+-dependent formate dehydrogenase. *Metab Eng* 2002;4: 217-29.

Borrel G, Adam PS, Gribaldo S. Methanogenesis and the Wood–Ljungdahl pathway: an ancient, versatile, and fragile association. *Genome Biology and Evolution* 2016;8: 1706-11.

Burgess BK, Lowe DJ. Mechanism of molybdenum nitrogenase. *Chem Rev* 1996;96: 2983-3012.

Bush M, Dixon R. The role of bacterial enhancer binding proteins as specialized activators of σ^{54}-dependent transcription. *Microbiol Mol Biol Rev* 2012;76: 497-529.

Cline JD. Spectrophotometric determination of hydrogen sulfide in natural waters. *Limnol Oceanogr* 1969;14: 454-8.

Delmont TO, Eren AM. Linking pangenomes and metagenomes: the *Prochlorococcus* metapangenome. *PeerJ* 2018;6: e4320.

Desnoues N, Lin M, Guo X *et al.* Nitrogen fixation genetics and regulation in a Pseudomonas stutzeri strain associated with rice. *Microbiology* 2003;149: 2251-62.

Eren AM, Esen ÖC, Quince C *et al.* Anvi'o: an advanced analysis and visualization platform for 'omics data. *PeerJ* 2015;3: e1319.

Ferry JG. Formate dehydrogenase. *FEMS Microbiol Rev* 1990;7: 377-82.

Fincker M, Huber JA, Orphan VJ *et al.* Metabolic strategies of marine subseafloor *Chloroflexi* inferred from genome reconstructions. *Environ Microbiol* 2020;22: 3188–204.

Fincker M, Spormann AM. Biochemistry of catabolic reductive dehalogenation. *Annu Rev Biochem* 2017;86: 357-86.

Fullerton H, Moyer CL. Comparative single-cell genomics of *Chloroflexi* from the Okinawa Trough deep-subsurface biosphere. *Appl Environ Microbiol* 2016;82: 3000-8.

Garber A, Ramirez G, Merino N *et al.* MagicLamp: toolkit for annotation of 'omics datasets using curated HMM sets. *GitHub Repository Available online at https://githubcom/Arkadiy-Garber/MagicLamp (accessed January, 2022)* 2020.

Gonzalez P, Correia C, Moura I *et al.* Bacterial nitrate reductases: molecular and biological aspects of nitrate reduction. *J Inorg Biochem* 2006;100: 1015-23.

Goodwin S, McPherson JD, McCombie WR. Coming of age: ten years of next-generation sequencing technologies. *Nat Rev Genet* 2016;17: 333-51.

Goris T, Schubert T, Gadkari J *et al.* Insights into organohalide respiration and the versatile catabolism of *Sulfurospirillum multivorans* gained from comparative genomics and physiological studies. *Environ Microbiol* 2014;16: 3562-80.

Hardy R, Burns RC, Holsten RD. Applications of the acetylene-ethylene assay for measurement of nitrogen fixation. *Soil Biol Biochem* 1973;5: 47-81.

Holliger C, Wohlfarth G, Diekert G. Reductive dechlorination in the energy metabolism of anaerobic bacteria. *FEMS Microbiol Rev* 1999;22: 383-98.

Howard JB, Rees DC. Structural basis of biological nitrogen fixation. *Chem Rev* 1996;96: 2965-82.

Hyman MR, Daniel A. Acetylene inhibition of metalloenzymes. *Anal Biochem* 1988;173: 207-20.

Isaxons M, Teske A. *Desulforhopalus vacuolatus* gen. nov., sp. nov., a new moderately psychrophilic sulfate-reducing bacterium with gas vacuoles isolated from a temperate estuary. *Arch Microbiol* 1996;166 160-8.

Jiao J-Y, Fu L, Hua Z-S *et al.* Insight into the function and evolution of the Wood–Ljungdahl pathway in Actinobacteria. *ISME J* 2021;15: 3005-18.

Jormakka M, Byrne B, Iwata S. Formate dehydrogenase–a versatile enzyme in changing environments. *Curr Opin Struct Biol* 2003;13: 418-23.

Kanehisa M, Goto S. KEGG: kyoto encyclopedia of genes and genomes. *Nucleic Acids Res* 2000;28: 27-30.

Kern M, Simon J. Characterization of the NapGH quinol dehydrogenase complex involved in *Wolinella succinogenes* nitrate respiration. *Mol Microbiol* 2008;69: 1137-52.

Kim J, Rees DC. Nitrogenase and biological nitrogen fixation. *Biochemistry* 1994;33: 389-97.

Kim S-H, Harzman C, Davis JK *et al.* Genome sequence of *Desulfitobacterium hafniense* DCB-2, a gram-positive anaerobe capable of dehalogenation and metal reduction. *BMC Microbiol* 2012;12: 1-20.

Korkhov VM, Mireku SA, Locher KP. Structure of AMP-PNP-bound vitamin B12 transporter BtuCD–F. *Nature* 2012;490: 367-72.

Kuever J, Rainey FA, Widdel F. *DesulforhopalusBergey's Manual of Systematics of Archaea and Bacteria*, 2015, 1-4.

Lee MD. GToTree: a user-friendly workflow for phylogenomics. *Bioinformatics* 2019;35: 4162-4.

Lie TJ, Clawson ML, Godchaux W *et al.* Sulfidogenesis from 2-aminoethanesulfonate (taurine) fermentation by a morphologically unusual sulfate-reducing bacterium, *Desulforhopalus singaporensis* sp. nov. *Appl Environ Microbiol* 1999;65: 3328-34.

Liu J, Haggblom MM. Genome-guided identification of organohalide-respiring Deltaproteobacteria from the marine environment. *mBio* 2018;9: e02471-18.

Liu J, Lopez N, Ahn Y *et al.* Novel reductive dehalogenases from the marine sponge associated bacterium *Desulfoluna spongiiphila*. *Environ Microbiol Rep* 2017;9: 537-49.

Maymo-Gatell X, Anguish T, Zinder SH. Reductive dechlorination of chlorinated ethenes and 1,2-dichloroethane by "*Dehalococcoides ethenogenes*" 195. *Appl Environ Microbiol* 1999;65: 3108-13.

Maymo-Gatell X, Chien YT, Gossett JM *et al.* Isolation of a bacterium that reductively dechlorinates tetrachloroethene to ethene. *Science* 1997;276: 1568-71.

Mikheenko A, Prjibelski A, Saveliev V *et al.* Versatile genome assembly evaluation with QUAST-LG. *Bioinformatics* 2018;34: i142-i50.

Monserrate E, Häggblom MM. Dehalogenation and biodegradation of brominated phenols and benzoic acids under iron-reducing, sulfidogenic, and methanogenic conditions. *Appl Environ Microbiol* 1997;63: 3911-5.

Muyzer G, De Waal EC, Uitterlinden A. Profiling of complex microbial populations by denaturing gradient gel electrophoresis analysis of polymerase chain reaction-amplified genes coding for 16S rRNA. *Appl Environ Microbiol* 1993;59: 695-700.

Nijenhuis I, Kuntze K. Anaerobic microbial dehalogenation of organohalides-state of the art and remediation strategies. *Curr Opin Biotechnol* 2016;38: 33-8.

Parks DH, Imelfort M, Skennerton CT *et al.* CheckM: assessing the quality of microbial genomes recovered from isolates, single cells, and metagenomes. *Genome Res* 2015;25: 1043-55.

Payne RB, May HD, Sowers KR. Enhanced reductive dechlorination of polychlorinated biphenyl impacted sediment by bioaugmentation with a dehalorespiring Bacterium. *Environ Sci Technol* 2011;45: 8772-9.

Peng P, Goris T, Lu Y *et al.* Organohalide-respiring *Desulfoluna* species isolated from marine environments. *ISME J* 2020;14: 815-27.

Pon G, Hyman MR, Semprini L. Acetylene inhibition of trichloroethene and vinyl chloride reductive dechlorination. *Environ Sci Technol* 2003;37: 3181-8.

Popov VO, Lamzin VS. NAD^+-dependent formate dehydrogenase. *Biochem J* 1994;301: 625.

Ragsdale SW. Enzymology of the Wood–Ljungdahl pathway of acetogenesis. *Ann N Y Acad Sci* 2008;1125: 129-36.

Ragsdale SW, Pierce E. Acetogenesis and the Wood–Ljungdahl pathway of CO_2 fixation. *Biochim Biophys Acta Proteins Proteom* 2008;1784: 1873-98.

Sewell HL, Kaster AK, Spormann AM. Homoacetogenesis in deep-sea *Chloroflexi*, as inferred by single-cell genomics, provides a Link to reductive dehalogenation in terrestrial *Dehalococcoidetes*. *mBio* 2017;8.

Spang A, Stairs CW, Dombrowski N *et al.* Proposal of the reverse flow model for the origin of the eukaryotic cell based on comparative analyses of Asgard archaeal metabolism. *Nat Microbiol* 2019;4: 1138-48.

Uritskiy GV, DiRuggiero J, Taylor J. MetaWRAP—a flexible pipeline for genome-resolved metagenomic data analysis. *Microbiome* 2018;6: 1-13.

Waite DW, Chuvochina M, Pelikan C *et al.* Proposal to reclassify the proteobacterial classes Deltaproteobacteria and Oligoflexia, and the phylum Thermodesulfobacteria into four phyla reflecting major functional capabilities. *Int J Syst Evol Microbiol* 2020;70: 5972-6016.

Ward LM, Bertran E, Johnston DT. Expanded genomic sampling refines current understanding of the distribution and evolution of sulfur metabolisms in the *Desulfobulbales*. *Front Microbiol* 2021;12: 666052.

Wick RR, Judd LM, Gorrie CL *et al.* Completing bacterial genome assemblies with multiplex MinION sequencing. *Microb Genom* 2017a;3.

Wick RR, Judd LM, Gorrie CL *et al.* Unicycler: resolving bacterial genome assemblies from short and long sequencing reads. *PLoS Comput Biol* 2017b;13: e1005595.

Xun L, Topp E, Orser C. Glutathione is the reducing agent for the reductive dehalogenation of tetrachloro-p-hydroquinone by extracts from a *Flavobacterium* sp. *Biochem Biophys Res Commun* 1992a;182: 361-6.

Xun L, Topp E, Orser C. Purification and characterization of a tetrachloro-p-hydroquinone reductive dehalogenase from a *Flavobacterium* sp. *J Bacteriol* 1992b;174: 8003-7.

Yishai O, Lindner SN, Gonzalez de la Cruz J *et al.* The formate bio-economy. *Curr Opin Chem Biol* 2016;35: 1-9.

Zanaroli G, Negroni A, Haggblom MM *et al.* Microbial dehalogenation of organohalides in marine and estuarine environments. *Curr Opin Biotechnol* 2015;33: 287-95.

Zhuang WQ, Yi S, Bill M *et al.* Incomplete - pathway facilitates one-carbon metabolism in organohalide-respiring *Dehalococcoides mccartyi*. *Proc Natl Acad Sci U S A* 2014;111: 6419-24.

Zimmer DP, Soupene E, Lee HL *et al.* Nitrogen regulatory protein C-controlled genes of *Escherichia coli*: scavenging as a defense against nitrogen limitation. *Proc Natl Acad Sci U S A* 2000;97: 14674-9.

Chapter 6

General discussion

With the research described in this thesis, we aimed to provide new insight in the taxonomic, functional and genomic diversity of anaerobic, reductively dehalogenating microorganisms that occur in marine environments. Our research had been inspired by the discovery of a yet undiscovered diversity of organohalide-respiring bacteria (OHRB) in pristine subsurface marine environments (Jochum, et al. 2018, Sewell, et al. 2017, Zinke, et al. 2017), suggesting an important role of these organisms in local and global halogen cycles, and the potential for their recruitment for *in situ* bioremediation towards removing polluted organohalides in the future. This potential was further substantiated by the fact that transcriptome sequence data suggested *in situ* organohalide respiration (OHR) activity in pristine marine sediments (Zinke, et al. 2017). Research described in this thesis therefore started focusing on marine sediments, and more specifically those sampled from Aarhus Bay. Overall, we observed and further characterized a range of phylogenetically and functionally diverse reductively dehalogenating microorganisms, including populations predicted to be true OHRB that possess one or more respiratory, corrinoid dependent, reductive dehalogenases (RDases) as well as populations that bear thiolytic, glutathione dependent, non-respiratory RDases. We validated the predicted OHR potential physiologically on various halogenated compounds, which were found to shape the microbial composition of enrichment cultures differently. As part of the studies described in my thesis, the integrated application of multi-omics data analyses revealed potentially new members of OHRB in marine sediments of Aarhus Bay (Table 6.1), which were distinct from the previously well-identified OHRB (**Chapters, 2 & 3**), and one thiolytic TPh-RDase was also found in CH3_bin.5 affiliated with the anaerobic genus *Desulforhopalus* (**Chapter 3**). In addition, phylogenomic and transcriptional analysis in combination with physiological studies of the isolated consortium pointed towards an intricate relationship to allow for reductive dehalogenation to occur (**Chapter 4**), which can provide novel leads towards optimizing OHR synthetic consortia for future *in situ* bioremediation strategies. Even though we failed to obtain pure culture isolates of reductively dehalogenating populations from the marine sediments of Aarhus Bay, studies of the type strain of *Desulforhopalus*, *D. singaporensis*, provided new insight with respect to interconnecting the versatile metabolism with reductive dehalogenation, including complete *de novo* B12 biosynthesis for OHR, preference of OHR over sulfate reduction, and a complete Wood-Ljungdahl pathway (WLP) for providing electrons to OHR for more biomass production (**Chapter 5**). Moreover, the complete WLP disarmed the CO inhibition on RDase activity as previously-described for *Dehalococcoides mccartyi* that only has an incomplete WLP (Zhuang et al., 2014). In addition, we confirmed the inhibition of RDase activity by acetylene, which was found to act post-transcriptionally. More importantly, the introduced multi-omics disclosed the potential metabolism of the putative OHRB, which can give more substantial guidance and selection for their isolation (Gutleben, et al. 2018).

Table 6.1 Overview of MAGs assembled from marine sediments of Aarhus Bay representing potential OHRB

MAGs[1]	Closest affiliation[2]	Phylum (GTDB)	Numbers[3]
CH3_bin.1	*Bacteroidales*_o1	*Bacteroidota*	1
CH3_bin.12	*Bacteroidales*_o2	*Bacteroidota*	1
CH3_bin.18	*Bacteroidales*_o3	*Bacteroidota*	1
CH3_bin.23	*Bacteroidales*_o4	*Bacteroidota*	1
CH3_bin.24	*Bacteroidales*_o5	*Bacteroidota*	2
CH3_bin.6	*Bacteroidales*_o7	*Bacteroidota*	1
CH3_bin.13	*Izemoplasma*_B_g	*Firmicutes*	1
CH3_bin.31	*Marinifilaceae*_f	*Bacteroidota*	1
CH3_bin.28	*Melioribacteraceae*_f1	*Bacteroidota*	1
CH3_bin.35	*Melioribacteraceae*_f3	*Bacteroidota*	2
CH3_bin.30	Oceanispirochaeta_g2	*Spirochaetota*	1
CH3_bin.10	Synergistales_o1	*Synergistota*	1
CH3_bin.32	Synergistales_o2	*Synergistota*	1
CH3_bin.5	Synergistales_o4	*Synergistota*	1
CH3_bin.26	*Vulcanibacillus*_g	*Firmicutes*	97
CH4_bin.3	*Desulfoplanes*_g	*Desulfobacterota*	2
CH4_bin.4	*Marinifilaceae*_f	*Bacteroidota*	1

[1]MAGs, metagenome-assembled genomes (MAGs) obtained from **chapter 3** and **4**

[2]Closest affiliation, indicates the closest taxonomic affiliation of the MAGs predicted to represent OHRB

[3] Numbers, number of putative RDase genes (as based on counts of *rdhA* genes coding for the catalytic subunit of RDases.

Wide distribution of RDase genes beyond the well-documented OHRB

Advanced nucleic acid sequencing technology and corresponding bioinformatic innovations have strongly contributed to revolutionizing biological research, among which, not in the least, of marine microbiomes, where the taxonomy, metabolism, phylogeny and genetics of the overwhelming majority of yet uncultured microorganisms can be readily inferred from culture-independent genome-resolved sequence data (Sunagawa, et al. 2015). For example, application of metagenomic and -transcriptomic analyses of marine sediments from Aarhus Bay allowed tracking RDase genes and their transcripts (Zinke et al., 2017; Jochum et al., 2018). Nevertheless, additional, dedicated, studies are needed to validate and specify predicted metabolic features, including the potential for OHR. Thus, the collected marine sediment samples were incubated with various organohalides, and physiological observations reinforced predicted versatile OHR activities, including dechlorination, debromination and deiodination (**Chapter 2**). Analysis of microbial composition based on 16S rRNA gene amplicon sequencing revealed that the enriched dehalogenating bacteria were taxonomically distinct from canonical OHRB, such as *Dehalococcoides*, *Dehalogenimonas*, and *Dehalobacter*. Moreover, the microbial composition exhibited significant differences when adding different organohalides. The subsequent metagenomic and -transcriptomic analyses allowed for the assembly of the genomes of potential OHRB and specified the gene expression profile of RDases responsible for tetrachloroethene (PCE) dehalogenation (**Chapter 3**). Thereinto, MAG CH3_bin.26, affiliated with the genus *Vulcanibacillus*, was found to contain 97 RDase genes (Table 6.1), a number that by far exceeds that previously reported for well characterized OHRB, including *Dehalococcoides*. Of these 97 RDases, 84 were expressed at different levels in the presence of PCE, whereas the remaining 13 genes were found inactive, suggesting their activity could be specific for other organohalides. Interestingly, an isolate from this genus, *Vulcanibacillus modesticaldus*, was found having a single putative RDase gene (L'Haridon et al., 2006). Interestingly, most of the MAGs predicted to represent OHRB were classified into phyla that have to date not been considered as important with respect to OHR, including *Bacteroidota*, followed by the *Synergistota* and *Spirochaeota* respectively.Further, we found populations from the class of *Bacilli* as potential OHRB, which agreed to the results of 16S rRNA gene amplicon sequencing (**Chapter 2**). Intriguingly, phylogenetic analysis revealed all the genus representatives of *Marinifilum* and most of the *Ancylomarina* populations that were retrieved carried putative RDase genes (**Chapter 4**). Considering that in the research descibed in this thesis we only studied marine sediments derived from Aarhus Bay, it is safe to assume that there will be more distinct, yet undisclosed OHRB from various phyla in other marine sediments around the globe, which could add new data to further our understanding of the evolution of RDase genes across the bacterial kingdom. Of interest, we found that a group of archaea, *Lokiarchaeota*, belonging to the *Asgardarchaeota* seen as the ancestor of eukaryotes (Spang et al., 2015), was enriched during reductive deiodination of 2,4,6-triodophenol (**Chapter 2**). This is in line with previous reports that MAGs of *Lokiarchaeia* contain putative RDase genes suggesting their potential for OHR (Spang et al., 2019). Intriguingly, searching for the Pfam entry RDase (PF13486) (Fincker and Spormann, 2017) against the most recent version of the GTDB database (release 207) unveiled its even wider distribution among members of the *Asgardarchaeota* (Table 6.2).

Table 6.2 Overview of taxa in the *Asgardarchaeota* containing putative RDase genes

NCBI Accession	*Asgardarchaeota*	Names[1]
GCA_001563335.1	*Thorarchaeota*	archaeon_SMTZ1-45
GCA_001563325.1	*Thorarchaeota*	archaeon_SMTZ1-83
GCA_001940705.1	*Thorarchaeota*	archaeon_AB_25
GCA_002825465.1	*Thorarchaeota*	archaeon_MP8T_1
GCA_002825515.1	*Thorarchaeota*	archaeon_MP11T_1
GCA_003662765.1	*Thorarchaeota*	archaeon1

GCA_004376265.1	*Thorarchaeota*	archaeon2
GCA_004524445.1	*Thorarchaeota*	archaeon3
GCA_004524565.1	*Thorarchaeota*	archaeon4
GCA_004524595.1	*Thorarchaeota*	archaeon5
GCA_008080745.1	*Thorarchaeota*	archaeon6
GCA_011364905.1	*Thorarchaeota*	archaeon7
GCA_016839345.1	*Thorarchaeota*	archaeon8
GCA_016839605.1	*Thorarchaeota*	archaeon9
GCA_016840245.1	*Thorarchaeota*	archaeon10
GCA_016840385.1	*Thorarchaeota*	archaeon11
GCA_016840825.1	*Thorarchaeota*	archaeon12
GCA_016840855.1	*Thorarchaeota*	archaeon13
GCA_016840965.1	*Thorarchaeota*	archaeon14
GCA_016841005.1	*Thorarchaeota*	archaeon15
GCA_016933575.1	*Thorarchaeota*	archaeon16
GCA_018238205.1	*Thorarchaeota*	archaeon17
GCA_018238375.1	*Thorarchaeota*	archaeon18
GCA_018238545.1	*Thorarchaeota*	archaeon19
GCA_018238825.1	*Thorarchaeota*	archaeon20
GCA_018335335.1	*Thorarchaeota*	archaeon21
GCA_001940645.1	*Heimdallarchaeota*	archaeon_LC_3
GCA_001940725.1	*Heimdallarchaeota*	archaeon_LC_2
GCA_001940755.1	*Heimdallarchaeota*	archaeon_AB_125
GCA_003144275.1	*Heimdallarchaeota*	archaeon_B3_Heim
GCA_015523565.1	*Heimdallarchaeota*	archaeon1
GCA_016839875.1	*Heimdallarchaeota*	archaeon2
GCA_016839945.1	*Heimdallarchaeota*	archaeon3
GCA_016839985.1	*Heimdallarchaeota*	archaeon4
GCA_016840095.1	*Heimdallarchaeota*	archaeon5
GCA_018238155.1	*Heimdallarchaeota*	archaeon6
GCA_018238545.1	*Heimdallarchaeota*	archaeon7
GCA_019056785.1	*Heimdallarchaeota*	archaeon8
GCA_019057375.1	*Heimdallarchaeota*	archaeon9
GCA_019057635.1	*Heimdallarchaeota*	archaeon10
GCA_019057815.1	*Heimdallarchaeota*	archaeon11
GCA_019058165.1	*Heimdallarchaeota*	archaeon12
GCA_004375715.1	*Lokiarchaeota*	archaeon1
GCA_004524365.1	*Lokiarchaeota*	archaeon2
GCA_004524545.1	*Lokiarchaeota*	archaeon3
GCA_004524725.1	*Lokiarchaeota*	archaeon4
GCA_005222975.1	*Lokiarchaeota*	archaeon5
GCA_005223125.1	*Lokiarchaeota*	archaeon6
GCA_008000775.1	*Lokiarchaeota*	archaeon7
GCA_008080735.1	*Lokiarchaeota*	archaeon8
GCA_011364925.1	*Lokiarchaeota*	archaeon9
GCA_011364975.1	*Lokiarchaeota*	archaeon10
GCA_013375475.1	*Lokiarchaeota*	archaeon11
GCA_013375485.1	*Lokiarchaeota*	archaeon12

GCA_013375495.1	*Lokiarchaeota*	archaeon13
GCA_014728035.1	*Lokiarchaeota*	archaeon14
GCA_014729315.1	*Lokiarchaeota*	archaeon15
GCA_014730165.1	*Lokiarchaeota*	archaeon16
GCA_014730275.1	*Lokiarchaeota*	archaeon17
GCA_014730295.1	*Lokiarchaeota*	archaeon18
GCA_016839385.1	*Lokiarchaeota*	archaeon19
GCA_016839585.1	*Lokiarchaeota*	archaeon20
GCA_016839635.1	*Lokiarchaeota*	archaeon21
GCA_016839745.1	*Lokiarchaeota*	archaeon22
GCA_016839765.1	*Lokiarchaeota*	archaeon23
GCA_016839845.1	*Lokiarchaeota*	archaeon24
GCA_016839915.1	*Lokiarchaeota*	archaeon25
GCA_016840085.1	*Lokiarchaeota*	archaeon26
GCA_016840165.1	*Lokiarchaeota*	archaeon27
GCA_016840545.1	*Lokiarchaeota*	archaeon28
GCA_016840695.1	*Lokiarchaeota*	archaeon29
GCA_019057355.1	*Lokiarchaeota*	archaeon30
GCA_019057735.1	*Lokiarchaeota*	archaeon31
GCA_019057775.1	*Lokiarchaeota*	archaeon32
GCA_019057795.1	*Lokiarchaeota*	archaeon33
GCA_018238625.1	*Lokiarchaeota*	archaeon34
GCA_019057865.1	*Lokiarchaeota*	archaeon35
GCA_019057975.1	*Lokiarchaeota*	archaeon36
GCA_019058015.1	*Lokiarchaeota*	archaeon37
GCA_019058135.1	*Lokiarchaeota*	archaeon38
GCA_019058365.1	*Lokiarchaeota*	archaeon39
GCA_019058425.1	*Lokiarchaeota*	archaeon40
GCA_019058515.1	*Lokiarchaeota*	archaeon41
GCA_016839365.1	*Hermodarchaeota*	archaeon1
GCA_016839805.1	*Hermodarchaeota*	archaeon2
GCA_016839995.1	*Hermodarchaeota*	archaeon3
GCA_016840065.1	*Hermodarchaeota*	archaeon4
GCA_016840135.1	*Hermodarchaeota*	archaeon5
GCA_016840185.1	*Hermodarchaeota*	archaeon6
GCA_016840405.1	*Hermodarchaeota*	archaeon7
GCA_016840595.1	*Hermodarchaeota*	archaeon8
GCA_016839405.1	*Gerdarchaeota*	archaeon1
GCA_016840945.1	*Gerdarchaeota*	archaeon2
GCA_016840465.1	*Baldrarchaeota*	*Baldrarchaeum yapensis*

[1] archaeon, without specified names follow by the number as the suffix.

Interestingly, RDase genes were found in 41 of a total of 89 *Lokiarchaeota* available in GTDB, 26/53 members of the *Thorarchaeota*, 16/49 MAGs within the *Heimdallarchaeota*, 8/17 members of the *Hermodarchaeota*, 2/3 members of the *Gerdarchaeota*, and 1/3 members of the *Baldrarchaeota*. In total, 94 out of 229 *Asgardarchaeota* members were annotated bearing at least one RDase gene, which suggests their potential for OHR to conserve energy for growth. In addition, by widening the search to other archaeal phyla in GTDB, we also found putative RDase genes distributed in *Euryarchaeota*, *Bathyarchaeota*, *Thermoplasmatota*, *Crenarchaeota*, *Verstraetearchaeota*, *Helarchaeota*, *Thaumarchaeota*, *Hodarchaeota*, and *Borrarchaeota* (Table S6.1). It could become interesting to analyze the difference of RDase sequences from bacteria and archaea, in combination with detailed knowledge of their isolation source, which might provide further insight in phylogeny, evolution and biogeography of RDases and the corresponding microorganisms. Altogether, research described here has contributed to the notion that OHR is not restricted to the well-identified OHRB, but rather expands to a much broader diversity of bacterial and archaeal taxa, reinforcing its essential role in biological processes in a broad range of different pristine and polluted environments.

Diverse transcriptional factors for OHR regulation

RDase gene expression is largely regulated by transcriptional factors encoded in their vicinity (Gabor et al., 2006; Joyce et al., 2006; Mazon et al., 2007; Levy et al., 2008; Maucourt et al., 2020). Normally, transcriptional factors are composed of at least two domains, a sensor domain, to receive ligands or signals, such as organohalides, and a DNA-binding domain binding to the specific DNA sequences upstream of target genes' promoters. More specifically, upon the binding of the sensor domain to its cognate signal, the structure of transcriptional factors is allosterically rearranged, which subsequently leads to an active transcriptional factor that (in)activates the expression of the target genes. For the transcriptional regulation of OHR, currently two well-documented regulatory modes have been characterized that can be distinguished according to their different mode of regulation. To this end, CRP-FNR type regulators act as positive regulators, such as CprK in *Desulfitobacterium* spp. strains (Gabor et al., 2006; Joyce et al., 2006; Mazon et al., 2007; Levy et al., 2008), wheras MarR type regulators act as negative regulators, such as RdhR in *Dehalococcoides mccartyi* (Krasper et al., 2016). Both types have been shown to be involved in the regulation of RDases for dehalogenating organohalides. Intriguingly, there exists a third mode for regulating reductive dehalogenation in OHRB, namely two-component systems (TCS) as proposed for *Sulfurospirillum halorespirans*, where the signal of binding PCE is transduced to phosphorylation of the transcriptional regulator that in turn regulations expression of the downstream RDase genes (Türkowsky et al., 2018).

Our studies in **Chapter 3** provided evidence suggesting that PCE dechlorinating bacteria employed these three main regulatory modes to activate the expression of RDase genes in our enrichment cultures. Thereinto, over half of the transcriptional factors we found associated with RDase genes belonged to different subtypes within the CRP-FNR type family of transcriptional regulators, including CRP, GlxR, FNR, NtcA and SdrP. The second most frequently observed group of regulators found in our data were TCS, including YpdB, NatR, WalR and RpfG. In addition, we observed four repressor-like regulators, DtxR, HrcA, SarZ and AcrR, which have been described to act in response to general stimuli caused by changing environments (Maucourt, et al. 2020). Interestingly, an extra-cytoplasmic function (ECF) sigma factor was predicted to be involved in regulation of RDase gene expression. Contrary to the primary sigma factor, Sigma70, ECF sigma factors were shown to only have retained the two DNA-binding domains, being wrapped by the cognate anti-sigma factor to inhibit its DNA binding activity (Helmann, 2002). We hypothesize that upon environmental stimuli, the ECF sigma factors will be released and become active to regulate the expression of target RDase genes. All these different transcriptional factors mentioned above were co-expressed differentially with their vicinal RDase gene induced by the PCE dechlorination. Although our metagenome- and transcriptome data provided evidence for the involvement of diverse regulatory mechanisms, additional molecular work is needed for unequivocal characterization of the proposed regulons.

In the case of *Desulforhopalus singaporensis* (**Chapter 5**), the transcriptional activator, named bacterial enhancing binding protein (bBEP) (Liu and Haggblom, 2018), is composed of three domains, GAF domain potentially binding with organohalides, HTH domain with DNA-binding potential, and Sigma54-interacting domain, indicating a role for bEBP-Sigma54 complex formation to initiate RDase gene transcription. Intriguingly, our data suggest that bEBP and Sigma54 act as self-repressor of their own gene expression during 2,6-DBP debromination. Nevertheless, also in this case, although we bioinformatically identified the putative DNA-binding sites of bEBP, further molecular demonstration is required also in this case to clarify the bEBP-mediated regulatory mode.

Future perspectives

In **Chapter 2**, we confirmed the predicted ability of Aarhus Bay marine sediments to use a variety of organohalides as terminal electron acceptor for OHR, and then focused on PCE dechlorinating and 2,6-DBP debrominating enrichments, respectively. As the results revealed, the different organohalides shaped the microbial structure differently, which led us to speculate that the different types of organohalides could likely enrich different dehalogenating consortia. A good example is that we observed the dehalogenation of 2,4,6-TIP can increase the growth of *Lokiarchaeota*, which were reported to contain RDase genes (Spang et al., 2019). Recently, accumulative evidence corroborate the *Asgardarchaeota* are ancestral to the Eukaryotes, however, availability of cultured representatives is still limited (Imachi et al., 2020). According to our study, a set of organohalides could be added into the medium as a selective electron acceptor to maintain the growth of organohalide respiring *Asgardarchaeota* members. Furthermore, OHR in *Asgardarchaeota* would certainly be worth further investigation as there might be extensive differences in terms of regulation and with respect to associated electron transport chains (ETCs), to just name two aspects.

In **Chapter 3** and **Chapter 4**, we assembled MAGs representating potential OHRB belong to tax not previously associated with OHR. Some of these taxa have representative isolates, including e.g. *Vulcanibacillus*, *Marinifilum* and *Ancytomarina*. Thus, physiological and molecular characterization of OHR for these isolates could add substantially to our understanding of OHR, its regulation and interaction with other aspects of metabolism, in analogy to the studies described in this thesis for *Desulforhopalus singaporensis* (**Chapter 5**). Phylogenomic analysis of *D. singaporensis* revealed its versatile metabolism, integrating OHR with sulfate reduction, Wood-Ljungdahl pathway and nitrogen fixation, pointing towards its flexibility to adapt to environments with changing nutrient limitations. It might therefore be interesting to investigate the potential of *D. singaporensis* as a candidate member of defined OHR consortia for bioremediating organohalide-polluted marine environments.

Supplementary table

Table S6.1 RDases in Archaea

The supplementary tables for this chapter are reposited at:

(https://git.wur.nl/zhang268/2023_chen_thesis_decoding_ohr_aarhus_bay/-/blob/main/PF13486_Archaea.xlsx)

References

Fincker M, Spormann AM. Biochemistry of catabolic reductive dehalogenation. *Annu Rev Biochem* 2017;86: 357-86.

Gabor K, Verissimo CS, Cyran BC *et al.* Characterization of CprK1, a CRP/FNR-type transcriptional regulator of halorespiration from *Desulfitobacterium hafniense*. *J Bacteriol* 2006;188: 2604-13.

Hayes RP, Moural TW, Lewis KM *et al.* Structures of the inducer-binding domain of pentachlorophenol-degrading gene regulator PcpR from *Sphingobium chlorophenolicum*. *Int J Mol Sci* 2014;15: 20736-52.

Helmann JD. The extracytoplasmic function (ECF) sigma factors. 2002.

Imachi H, Nobu MK, Nakahara N *et al.* Isolation of an archaeon at the prokaryote-eukaryote interface. *Nature* 2020;577: 519-25.

Jochum LM, Schreiber L, Marshall IPG *et al.* Single-cell genomics reveals a diverse metabolic potential of uncultivated *Desulfatiglans*-related Deltaproteobacteria widely distributed in marine sediment. *Front Microbiol* 2018;9: 2038.

Joyce MG, Levy C, Gabor K *et al.* CprK crystal structures reveal mechanism for transcriptional control of halorespiration. *J Biol Chem* 2006;281: 28318-25.

Krasper L, Lilie H, Kublik A *et al.* The MarR-type regulator Rdh2R regulates *rdh* gene transcription in *Dehalococcoides mccartyi* strain CBDB1. *J Bacteriol* 2016;198: 3130-41.

L'Haridon S, Miroshnichenko M, Kostrikina N *et al.* *Vulcanibacillus modesticaldus* gen. nov., sp. nov., a strictly anaerobic, nitrate-reducing bacterium from deep-sea hydrothermal vents. *Int J Syst Evol Microbiol* 2006;56: 1047-53.

Levy C, Pike K, Heyes DJ *et al.* Molecular basis of halorespiration control by CprK, a CRP-FNR type transcriptional regulator. *Mol Microbiol* 2008;70: 151-67.

Liu J, Haggblom MM. Genome-guided identification of organohalide-respiring Deltaproteobacteria from the marine environment. *mBio* 2018;9: e02471-18.

Maucourt B, Vuilleumier S, Bringel F. Transcriptional regulation of organohalide pollutant utilisation in bacteria. *FEMS Microbiol Rev* 2020;44: 189-207.

Mazon H, Gabor K, Leys D *et al.* Transcriptional activation by CprK1 is regulated by protein structural changes induced by effector binding and redox state. *J Biol Chem* 2007;282: 11281-90.

Miyauchi K, Lee H-S, Fukuda M *et al.* Cloning and characterization of *linR*, involved in regulation of the downstream pathway for γ-hexachlorocyclohexane degradation in *Sphingomonas paucimobilis* UT26. *Appl Environ Microbiol* 2002;68: 1803-7.

Molenda O, Tang S, Lomheim L *et al.* Extrachromosomal circular elements targeted by CRISPR-Cas in *Dehalococcoides mccartyi* are linked to mobilization of reductive dehalogenase genes. *ISME J* 2019;13: 24-38.

Nunes-Alves C. Deep sequencing of the global oceans. *Nat Rev Microbiol* 2015;13: 397-.

Ray S, Gunzburg MJ, Wilce M *et al.* Structural basis of selective aromatic pollutant sensing by the effector binding domain of MopR, an NtrC family transcriptional regulator. *ACS Chem Biol* 2016;11: 2357-65.

Sewell HL, Kaster AK, Spormann AM. Homoacetogenesis in deep-sea *Chloroflexi*, as inferred by single-cell genomics, provides a Link to reductive dehalogenation in terrestrial *Dehalococcoidetes*. *mBio* 2017;8.

Spang A, Saw JH, Jorgensen SL *et al.* Complex archaea that bridge the gap between prokaryotes and eukaryotes. *Nature* 2015;521: 173-9.

Spang A, Stairs CW, Dombrowski N *et al.* Proposal of the reverse flow model for the origin of the eukaryotic cell based on comparative analyses of Asgard archaeal metabolism. *Nat Microbiol* 2019;4: 1138-48.

Sunagawa S, Coelho LP, Chaffron S *et al.* Structure and function of the global ocean microbiome. *Science* 2015;348: 1261359.

Türkowsky D, Jehmlich N, Diekert G *et al.* An integrative overview of genomic, transcriptomic and proteomic analyses in organohalide respiration research. *FEMS Microbiol Ecol* 2018;94: fiy013.

Zhuang WQ, Yi S, Bill M *et al.* Incomplete -pathway facilitates one-carbon metabolism in organohalide-respiring *Dehalococcoides mccartyi*. *Proc Natl Acad Sci U S A* 2014;111: 6419-24.

Zinke LA, Mullis MM, Bird JT *et al.* Thriving or surviving? Evaluating active microbial guilds in Baltic Sea sediment. *Environ Microbiol Rep* 2017;9: 528-36.

Summary

Summary

Pristine marine environments have been reported to contain microorganisms capable of organohalide respiration (OHR). In addition, over 5000 natural halogenated compounds were discovered recently in marine sediments, indicating the importance of the marine environment to local and global halogen cycles. We therefore started the exploration of marine sediments from Aarhus Bay for their OHR potential. To this end, sediments were incubated with a variety of halogenated compounds, followed by eco-physiological characterization of potential organohalide respiring bacteria (OHRB) through enrichment, dilution-to-extinction, phylogenomic and transcriptomic analyses.

Chapter 1 gave an overview of the current knowledge of OHR, including a summary of diversity and distribution of reductive dehalogenases (RDase), RDase-containing gene clusters, and RDase-based electron transfer chains.

Chapter 2 verified the OHR potential of marine sediments of Aarhus Bay for chlorinated, brominated and iodinated compounds. The obtained tetrachloroethene (PCE) dechlorinating enrichment was found to be composed of bacteria distinct from the well-documented OHRB. Moreover, a switch in organohalides from PCE to 2,6-dibromophenol (2,6-DBP) significantly affected microbial composition. Of interest, we found that the reductive deiodination of 2,4,6-triiodophenol (2,4,6-TIP) increased the relative abundance of *Lokiarchaeota* belonging to *Asgardarchaeota*, which are seen as the origin of eukaryotes.

Chapter 3 introduced metagenomic and -transcriptomic analyses to pinpoint the dehalogenators responsible for PCE dechlorination under both sulfate-free and sulfate-amended conditions. Metagenome-assembled genomes (MAGs) bearing RDase genes were found to belong to phyla not previously associated with OHR, including *Bacteroidota*, *Synergistota*, and *Spirochaetota*. Furthermore, a MAG classified into *Vulcanibacillus* (CH3_bin.26) carried an

unprecedent number of 97 RDase genes, 84 of which were found to be expressed during PCE dechlorination. Noticeably, many transcriptional regulators were found encoded in the vicinity of RDase genes, such as extra-cytoplasmic factor (ECF-σ), SigW, and co-expressed with the adjacent RDase genes indicating the involvement of diverse regulatory systems in OHR.

Chapter 4 reported the isolation of a consortium that is capable of reductive debromination of 2,6-DBP to phenol. Thereinto, bins (MAGs) belonging to *Desulfoplanes* (CH4_bin.3) and *Marinifilaceae* (CH4_bin.4) were shown to contain respiratory RDase genes, the expression of which was induced in the presence of 2,6-DBP. Interestingly, the pangenomic analysis revealed most of the *Marinifilum* representatives are potential OHRB. Moreover, CH4_bin.5 belonging to *Desulforhopalus* was found predominant with a relative abundance of up to 29%. This bin contained a gene coding for a thiolytic, non-respiratory reductive dehalogenase, TPh-RDase, which was also highly-induced upon addition of 2,6-DBP. This constitutes the first report of a thiolytic RDase being active in an anaerobic microorganism. Further, CH4_bin.5 was predicted to encode a complete de novo vitamin B12 (B12) biosynthesis pathway, which was likely functioning as the B12 supplier for reductive dehalogenation of CH4_bin.3 and CH4_bin.4 in the consortium. This suggests that this isolated consortium executed reductive dehalogenation in a syntrophic manner.

Chapter 5 describes studies of a representative strain, *Desulforhopalus singaporensis*, which was previously identified as a sulfate reducer that is unable to utilize H_2 as the electron donor. We found that *D. singaporensis* bears the potential of reductive debromination of 2,6-DBP to phenol without adding B12. Interestingly, *D. singaporensis* has the complete Wood-Ljungdahl pathway (WLP), utilizing formate as electron donor for growth. In addition, OHR by *D. singaporensis* supported growth supplied with formate compared to the control without adding 2,6-DBP. Notably, as CH4_bin.5, also *D. singaporensis* has a complete *de novo* B12 biosynthesis, and was shown to carry all genes necessary to synthesize poly-β-hydroxybutyrate. This metabolic versatility might qualify *D. singaporensis* as a new candidate for bioremediation of marine environments polluted with brominated compounds.

Chapter 6 discussed the results as described in the thesis. Updated knowledge, remaining questions, and future perspectives with respect to OHR were also mentioned. In summary, this thesis provides new insights that contribute to our understanding of OHR and corresponding microorganisms in pristine marine environments.

Acknowledgements

As my PhD defense is around the corner, enormous memories poured out of my mind over the past five years in Microbiology. Undoubtedly, this PhD thesis would not be completed without help from many people. Here I would like to take this opportunity to thank all these great people I have met during my PhD journey.

First, I would like to thank **Hauke** for giving me the opportunity to start my PhD in MolEco group that extended my understanding of microbiology in ecology and physiology. I have learned a lot from you. On top of that is your integrity, which set up a good example for me to build up my life and career. Your patience and support created more scientific freedom that enabled me to explore more (out) of my research combining multidisciplinary aspects. Accordingly, my academic pursuing is stewed. When I experienced ups and downs during this journey, you always not hesitate to give hands for applause and help. There is no exaggeration to say that your characters do much more influences on me surpassing the research itself.

Siavash, thank you for being my supervisor, especially in the first two years of my PhD. You encouraged me to learn cutting-edge methods which as a reward fundamentally supported the frame of my thesis. Your strictness on research made me up to the right track and transformed me in a proactive attitude towards difficulties in research and life. Moreover, your advice on choosing academy or industry helped me to clarify my interests. **Tom**, thank you for being my supervisor, especially in the last two years of my PhD. Your smiles with wisdom always melted my complaints more easily, which stopped me from depression during the pandemic. Your patience to debug technical problems gave me more favor to the research.

Peng, thank you very much for the collaboration to complete my first paper in Wageningen and skills to grow anaerobes in slant and roll tubes. Most importantly, you are so kind to share invaluable experience and advice to help me sharpening my research. Actually, I cannot quickly

adapt to the anaerobic study without you. **Ton**, your professionals and dedication to the technician position deserve more credits from my respect. I clearly remembered you helped me to create and optimize the detection method and came together with me to find the reporting errors many times. **Felix**, you really provided a helping hand to me for analyzing sequencing data and share your experience of becoming a bioinformatician, distinct to scientist. **Jinsong**, very nice of you to let me join your research and refreshed my mind that small microbes have super power in drinking water system.

I am really thankful to my paranymphs, **Maryse** and **Marina** (**M&M**). With you both, my PhD defense ceremony will be filled with sweetness and happiness. We have many big moments together and you both make me feel so warm and supported, especially during the lockdown. We freely shared our perspectives on global issues that broadened my minds and our common values are strongly interconnected. Your earnestness towards life encouraged me to rethink what is the meaning of life. I also would like to thank my dear other office mates, **Taojun**, **Marjet, Sharon**, **Valentina** and **Tatsuro**, we had lot of happy and fun activities outside office. To **Taojun**, we have more office hours together, which gave me long-lasting memories when we were arguing, laughing, swimming, drinking and bragging. **Steven**, **Ineke, Bart**, and **Victor**, thank you for your assistance in preparing sequencing samples, storing sequencing data and analyzing the sequencing transcriptomes. **Philippe**, thanks for your important introduction tutorial that reminds me safety is on top of wet-lab experiments. **Sudarshan** and **Gerben**, thank you both for developing the workflow to analyze microbiome data. Thanks to my colleagues in MIB. **Diana**, thank you very much to allow me to join the weekly meeting of MicFys that substantially increased my understanding of microbial physiology. **Raymond**, you are so kind and warm to provide good solutions for issues in my molecular work and gave chance to my wife to learn the knowledge of bacterial genetics in BacGen. **Nico**, thank you very much to let me in one-carbon conference hosted at Wageningen.

Menia, **Patricia**, **Jolanda**, **Peter**, **Michelle**, and **Anastasia**, thanks for your kind help to share me with very useful tutorials and advice for learning metagenomic analysis. **Erwin**, **Detmer**, **Clara**, **Burak**, **Anna**, **Janneke**, **Martha**, **Valentina**, **Prokopis**, **Lot**, **Daan**, **Ruth**, **Jannie**, **Emmy**, **Carrie**, **Nancy**, **Joan**, **Sara**, **Reinier**, **Iame**, **Paul**, **Nabeel** and **Yehor**, thanks for your kind help and good advice to improve the quality of my research.

Thanks to my Chinese Colleagues in Wageningen. **Yifan (Zhu)**, you were not only a good scientist, but also a good cook showing me the amazing ingredients and dishes all over the world. **Caifang**, **Ying**, **Zhuang**, **Yangwenshan**, **Ran**, **Jie**, **Kejia**, thanks for organizing the wonderful lunch/dinner parties to make my leisure time more comfortable, and hosting the virtual talks during pandemic period that made me feel not alone. **Zhan**, **Lintianxiang**, **and Dengke**, **Zhe**, **Xiulu**, **Bin**, **Xuchuan**, **Xilong**, **Siyuan**, **Hongwei**, **Dan Lei**, **Cheng**, **Li**, **Xiaoqian**, **Quihong**, **Yifan (Huang)**, **Luzhao** and **Ze**, thanks for your invitation to join your parties that gave me lot of fun and relax. **Wendy** (**Yumeng)**, thanks for your kind help and patience to design and polish the cover of my thesis. **Xikun**, thank you for your advice and encouragements since we were in middle school. It is crazy that we keep contacting with each other until now, and your efforts make our friendship green. **Jingyi**, thanks for your kindness to help me get out of the dilemma of life, and your sweetness deserves good fortune. **Fanrong**, thank you very much for helping me to apply for the scholarship and invited me more times to visit your big house hospitably to enjoy the weekends and these memories were never forgot in my mind. **Claudius**, thanks for introducing me into Sino-WUR joint program and your encouragements helped me to get out of culture shock in my first six months in the Netherlands. Thanks to **Min (Lin)** and **Mingjun**, your efforts increased the chances of CAAS students to know Wageningen.

Ed and **Margreet**, thank you very much sincerely for holding Chinese fellowship to act and spread the love following God’s leading. Your decades’ devotion shocked and empowered me spiritually. Great thanks to my family. **Ge**, you are my younger brother, but your excellence and enthusiasm in chemistry set a good example for me. Your deep thoughts on society gave me more idea to plan the future life. **Mom** and **Dad**, thank you as you are actually the unique parent, who put all eggs in one basket investing on children's education at that hard situation. Against the odds, you never closed the cage, so no limitation to me as the bird to fly as high as what I can. The greatest thanks to my wife, **Yingying**, you are my closest one to commit with me when all were in uncertainty. We have seven years in marriage and ten years in love since 2013. Our unity as one is not as even as we planned, but we tried our best to complete each other over the past. I am nothing without your support. Now, the right time to be united physically and mentally. Last but not least, I want to thank a bit to the past whatever it was fruit or flaw by citing a Chinese poem in part with English translated,

竹杖芒鞋轻胜马，(Better than saddled horse I like sandals and cane)
谁怕？(Oh, I would fain)
一蓑烟雨任平生。(Spend a straw-cloaked life in mist and rain)

回首向来萧瑟处，(Turning my head, I see the dreary beaten track)
归去，(Let me go back!)
也无风雨也无晴。(Impervious to wind, rain or shine, I'll have my will)

苏轼 (Sushi),《定风波》(Calming the Waves), 宋神宗元丰五年三月七日, (7th March 1082).
译，许渊冲先生。(translated by Prof. Dr Yuanchong Xu)

Helix, Wageningen
31st May, 2023

About the author

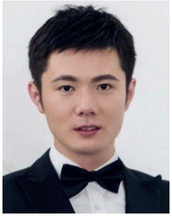

Chen Zhang was born on 5th August, 1992 in Anhui, China. After graduation from Anhui Agricultural university in 2013, he continued his study as a master student in Chinese Academy of Agricultural Science (CAAS) supervised by Prof. Dr. Min Lin. He joined Sino-WUR program from 2016 to 2018 at the laboratory of microbiology (MIB), Wageningen University, supervised by Prof. Dr Hauke Smidt. In October 2018, he started PhD project (described in this thesis) in Molecular Ecology group of MIB under the supervision of Prof. Dr. Hauke Smidt, Dr. Siavash Atashgahi and Dr. Tom N.P. Bosma.

List of Publications

Microbial Ecology and Physiology

1. **Chen Zhang**, Atashgahi Siavash, Bosma NP Tom; Smidt Hauke. “Genome-resolved transcriptomics reveals novel organohalide-respiring bacteria from Aarhus Bay sediments”. (bioRxiv: https://doi.org/10.1101/2023.04.17.537210) Preparation for submission (2023).
2. **Chen Zhang**, Atashgahi Siavash, Bosma NP Tom, Smidt Hauke. “Organohalide respiration by a *Desulforhopalus*-dominated community”. (bioRxiv: https://doi.org/10.1101/2023.04.18.537297) and Preparation for submission (2023).
3. **Chen Zhang**, Atashgahi Siavash, Bosma NP Tom, Smidt Hauke. “Organohalide respiration by a sulfate-reducing formatotroph, *Desulforhopalus singaporensis*”. Preparation for submission (2023).
4. Jing Jin, **Chen Zhang**, Xiaoxu Ren, Bowen Tai, Fuguo Xing. Metagenome analysis identifies microbial shifts upon deoxynivalenol exposure and post-exposure recovery in the mouse gut. *Toxins* 15, no. 4 (2023): 243.
5. **Chen Zhang,** Atashgahi Siavash, Bosma NP Tom, Peng Peng, and Smidt Hauke. "Organohalide respiration potential in marine sediments from Aarhus Bay." *FEMS Microbiology Ecology* 98, no. 8 (2022): fiac073.
6. Jinsong Wang, Baptiste AJ Poursat, Jiahao Feng, David de Ridder, **Chen Zhang,** Albert van der Wal, and Nora B. Sutton. "Exploring organic micropollutant biodegradation under dynamic substrate loading in rapid sand filters." *Water Research* 221 (2022): 118832.
7. Jinsong Wang#, **Chen Zhang#**, Baptiste AJ Poursat, David de Ridder, Hauke Smidt, Albert van der Wal, and Nora B. Sutton. "Unravelling the contribution of nitrifying and methanotrophic bacteria to micropollutant co-metabolism in rapid sand filters." *Journal of Hazardous Materials* (2021): 127760. (**#shared first author**)
8. Qiannan Guo, Zhengfu Zhou, Lijuan Zhang, **Chen Zhang**, Ming Chen, Bo Wang, Min Lin, Wei Wang, Wei Zhang, and Xufeng Li. "*Skermanella pratensis* sp. nov., isolated from meadow soil, and emended description of the genus *Skermanella*." *International Journal of Systematic and Evolutionary Microbiology* 70, no. 3 (2020): 1605-1609.
9. Shiyou Su, Ming Chen, Chao Teng, Shijie Jiang, **Chen Zhang**, Min Lin, and Wei Zhang. "*Hymenobacter kanuolensis* sp. nov., a novel radiation-resistant bacterium." *International Journal of Systematic and Evolutionary Microbiology* 64, no. Pt_6 (2014): 2108-2112.
10. Shijie Jiang, Ming Chen, Shiyou Su, Mingkun Yang, Aihua Li, **Chen Zhang**, Min Lin, Wei Zhang, and Xuegang Luo. "*Sphingobacterium arenae* sp. nov., isolated from sandy soil." *International Journal of Systematic and Evolutionary Microbiology* 64, no. Pt_1 (2014): 248-253.

Molecular Microbiology

11. Yingying Liu[#], **Chen Zhang**[#], Nelli Khudaverdyan, Junyi Wang, Lei Zhang, Mikhail Y Golovko, Svetlana A Golovko, Ang Guo, Jikui Song, Min Wu, and Colin Combs. “TPR domain assigns versatility of BcTir/Tpr system against viral infection”. (https://www.biorxiv.org/content/10.1101/2023.05.26.542521v1). ([#]**shared first author**)
12. Yingying[#] Liu, **Chen Zhang**[#*], Min Wu[*]. “Prokaryotic gasdermins: ancestors of eukaryotic counterparts direct the pyroptosis and cell fates.” *Signal Transduction and Targeted Therapy* 7, 152 (2022). **(**[#*]**shared first and corresponding author**)
13. Yingying Liu[#], **Chen Zhang**[#*], Zhihan Wang, Min Lin, Jin Wang, and Min Wu[*]. "Pleiotropic Roles of Late Embryogenesis Abundant Proteins of *Deinococcus radiodurans* against Oxidation and Desiccation." *Computational and Structural Biotechnology Journal* 19 (2021): 3407-3415. ([#*]**shared first and corresponding author**)
14. Yingying, Liu, Heng Zhang, Jiahui Han, Shijie Jiang, Xiuxiu Geng, Dong Xue, Yun Chen, **Chen Zhang**, Zhengfu Zhou, Wei Zhang, Ming Chen, Min Lin and Jing Wang. "Functional assessment of hydrophilic domains of late embryogenesis abundant proteins from distant organisms." *Microbial Biotechnology* 12, no. 4 (2019): 752-762.
15. Gomaa, Ahmed E, **Chen Zhang**, Zhimin Yang, Liguo Shang, Shijie Jiang, Zhiping Deng, Yuhua Zhan, Wei Lu, Min Lin, and Yongliang Yan. "An enhanced vector-free allele exchange (VFAE) mutagenesis protocol for genome editing in a wide range of bacterial species." *AMB Express* 7, no. 1 (2017): 1-7.
16. **Chen Zhang**, Zhengfu Zhou, Wei Zhang, Zhen Chen, Yuan Song, Wei Lu, Min Lin, and Ming Chen. "The site-directed A184S mutation in the HTH domain of the global regulator IrrE enhances *Deinococcus radiodurans* R1 tolerance to UV radiation and MMC shock." *Journal of Microbiology and Biotechnology* 25, no. 12 (2015): 2125-2134.

Netherlands Research School for the
Socio-Economic and Natural Sciences of the Environment

DIPLOMA

for specialised PhD training

The Netherlands research school for the
Socio-Economic and Natural Sciences of the Environment
(SENSE) declares that

Chen Zhang

born on 5 August 1992 in Anhui, China

has successfully fulfilled all requirements of the
educational PhD programme of SENSE.

Wageningen, 5 July 2023

Chair of the SENSE board
Prof. dr. Martin Wassen

The SENSE Director
Prof. Philipp Pattberg

The SENSE Research School has been accredited by the Royal Netherlands Academy of Arts and Sciences (KNAW)

KONINKLIJKE NEDERLANDSE
AKADEMIE VAN WETENSCHAPPEN

The SENSE Research School declares that **Chen Zhang** has successfully fulfilled all requirements of the educational PhD programme of SENSE with a work load of 46.9 EC, including the following activities:

SENSE PhD Courses

- Environmental research in context (2019)
- Research in context activity: 'Organisation of ETE-MIB workshop and dinner' (2022)

Other PhD and Advanced MSc Courses

- Guide to writing scientific papers, The university of Liège (2016)
- Applied multivariate analysis: data mining and chemometrics, The university of Liège (2016)
- Efficient and Effective Academic Development, Wageningen Graduate Schools (2016)
- Academic Writing and Presenting in English, Wageningen Graduate Schools (2016)
- Academic English for PhD candidates, Wageningen Graduate Schools (2017)
- Introduction to R for Statistical Analysis, PE&RC graduate School (2017)
- Dynamic Models in R: Programming, parameter estimation and model selection, PE&RC graduate School (2019)
- Electron Microscopy course: The Basics: from A to W, EPS graduate school (2019)
- Exploration on Bacterial and Eukaryotic immunity mechanisms, University of North Dakota (2022)

Management and Didactic Skills Training

- Teaching in the MSc course 'Research Methods Microbiology (2019 & 2021)

Oral Presentations

- *Reductive dehalogenation driven by wood-ljungdahl pathway*. Biocon-CO2 workshop 21-22 January 2020, Wageningen, The Netherlands

SENSE coordinator PhD education

Dr. ir. Peter Vermeulen

Colophon

Research described in this thesis was performed at the laboratory of microbiology, Wageningen University, The Netherlands, and financially supported by the Dutch Research Council through the UNLOCK project (NRGWI.obrug.2018.005), as well as Wageningen University through its Innovation Program Microbiology. Chen Zhang was sponsored by a fellowship from the China Scholarship Council (CSC).

Cover design: Yumeng Liu

Printed by: proefschriftmaken

Financial support from the Laboratory of Microbiology, Wageningen University, for printing of this thesis is gratefully acknowledged.